THE EFFECT OF INFLAMMATORY CYTOKINES ON FUNCTIONAL NERVE RECOVERY FOLLOWING PERIPHERAL NERVE INJURY AND REPAIR

By

Hisham A. Shembesh

Academic Unit of Oral and Maxillofacial Medicine, Pathology and Surgery

School of Clinical Dentistry

Claremont Crescent

Sheffield, S10 2TA

A thesis submitted to the Faculty of Dentistry of the University of Sheffield for the degree for Doctor of Philosophy

March 2018

SUMMARY

The aim of this research was to investigate the effect of novel cytokine antagonists, tumour necrosis factor-alpha antagonist (Etanercept) and interleukin-1 antagonist (Anakinra), and interleukin-10 anti-inflammatory cytokine on the inflammatory response at the site of peripheral nerve injury, in order to establish their potential contribution on nerve regeneration and determine their potential effect on the reduction or prevention of neuropathic pain.

The outcome measures of functional nerve recovery were assessed using a combination of electrophysiology to determine the rate of axon regeneration, immunohistochemistry to study immune cell immunoreactivity and their related pain markers expression, and analysis of gait coordination to determine nerve function. In addition, axonal tracing was used to quantity regenerated nerve fibres following nerve conduit repair. The results showed that the peripheral application of interleukin-1 antagonist and combination treatment of interleukin-10 and tumour necrosis factor-alpha antagonist at the time of nerve repair was significantly effective in downregulating macrophage immunoreactivity at the site of nerve injury and repair. Application also decreased expression of GFAP and IBA-1 positive glial cells in the spinal cord. Results showed that interleukin-1 antagonist or tumour necrosis factor-alpha antagonist, as single therapies did not appear to significantly improve the regenerative potential of injured axons after nerve repair. However, application of a combined therapy of tumour necrosis factor-alpha antagonist and interleukin-10 greatly improved recovery, possibly due to reduced immune response and scar tissue formation. Following poly-caprolactone nerve conduit repair, axonal tracing revealed that regenerating axons took a more uniform path in the regeneration process, following treatment with tumour necrosis factor-alpha antagonist, when compared with the sterile water treatment, where many axons displayed a disorganized pattern of regeneration. However, no significant difference in nerve function recovery was observed between the two groups. The findings contained in this work provide new insights into the role of inflammatory cytokines on functional nerve recovery and the development of neuropathic pain after peripheral nerve injury. These agents demonstrate potential as therapeutic strategies for the treatment of peripheral nerve injures.

ACKNOWLEDGEMENTS

To begin with, I would like to acknowledge my sincere thankfulness to my supervisors, Dr. Simon Atkins and Dr. Emma V. Bird. I am really grateful for the support and dedicated involvement from my supervisors in every step throughout the process of preparing this thesis. I am certain that without their continued support and invaluable guidance and encouragement over the last four years, this thesis would have never been accomplished in the right time. I would also like to record my sincere gratefulness to Professor Fiona M. Boissonade for her supervision, valuable guidance and encouragement to complete this work. I truly enjoyed working in the research environment under dedicated supervision of all my supervisors.

I would like to express my sincere thanks to my colleague Emad Albadawi for his collaboration in nerve conduit repair experiment. I would like also to thank Jonathan Field and Dr. Fred Claeyssens for their contribution by providing poly-caprolactone conduit which was used in nerve conduit repair experiment. I wish to express my thankfulness to Dr. Adam Harding for his kind assistance during experiments to help keep the work track. Also, it is my pleasure to acknowledge the valuable input of Dr. Milena De Felice, who contributed to my research by giving her sincere expertise in gait functional analysis using the Catwalk system. I would like to acknowledge the kind endless help of Dr. Matthew Worsley for his technical support and providing essential materials for my research experiments. I would like also to acknowledge my sincere thanks to all staff of the Academic Unit of Oral and Maxillofacial Medicine, Pathology and Surgery at the Charles Clifford dental school. I would like to thank John Wiley and Sons, Elsevier, Neurosurgical focus, Springer and Copyright Clearance Centre for permission to use figures in this thesis. I also appreciate the financial support of the Ministry of Higher Education and Scientific Research during my PhD study.

I would like to express my love and thankfulness to my wife Samira Gurji who has stood by me all through my research and who encouraged me and helped me through hard times. My love and gratitude also go out to my children Adam, Amin and Zakaria, and Marya.

Hisham A. Shembesh, March 2018.

Poster presentations

- The effect of local administration of TNF-α antagonist (Etanercept) on nerve regeneration following Poly-caprolactone conduits repair. Emad Albadawi, Hisham Shembesh, Adam Harding, Jonathan Field, Simon Atkins, Emma Bird, Frederik Claeyssens, John Haycock and Fiona Boissonade. Poster presentation at the 3rd Annual Neuroscience R&D Technologies Conference, London, UK, September 2017 (presented by Emad Albadawi).
- Effect of an interleukin-1 cytokine antagonist on functional regeneration and neuropathic pain following peripheral nerve injury. Hisham Shembesh, Emma Bird, Fiona Boissonade, Simon Atkins. Poster presentation at The Challenge of Chronic Pain, Wellcome Genome Campus, Cambridge, UK, 1-3 March 2017.
- Role of peripheral Interleukin-1 cytokine in peripheral nerve injury. H Shembesh, SJ Atkins, F Boissonade, E Bird. Poster presentation at The Academic Oral and Maxillofacial Surgery conference, Sheffield, UK, 19th November 2015.
- Peripheral targeting of Interleukin-1 cytokine signalling pathway in peripheral nerve injury. H Shembesh, EV Bird, FM Boissonade and SJ Atkins. Poster presentation at British Society of Dental Research Annual Conference, Cardiff, UK,14-16 September 2015.

Table of Contents

List of Figures

List of Tables

Abbreviations

BDNF	Brain-derived neurotrophic factor
CAP	Compound action potential
CCI	Chronic constriction injury
CNS	Central nervous system
CMAK2	Calcium/ calmodulin-dependent kinase 2
COX2	Cyclooxygenase enzyme 2
CVs	Conduction velocities
DRG	Dorsal root ganglia
GAP-43	Growth associated protein- 43
GFAP	Glial fibrillary acidic protein (astrocytes marker)
ELISA	Enzyme-linked immunoassay
IAN	Inferior alveolar nerve
IBA-1	Ionized calcium-binding adapter molecule (microglial marker)
IHC	Immunohistochemistry
IL-1, 6, 8 &10	Interleukine- cytokines
IL-1ra	Interleukine -1 receptor antagonist
1L-10R1	Interleukine -10 receptor-1
Ip	Intraperitoneal
JNK	Jun N-terminal kinase
c-Jun	c- Jun N-terminal kinase
K+	Potassium ions
K v9.1	Potassium ion channel
LAP	Latency Associated Peptide
LIF	Leukaemia inhibitory factor
LPS	Lipopolysaccharides, bacterial endotoxins
MAPK	Mitogen-activated protein kinase
MCP1	Monocyte chemoattractant protein 1
M6P	Mannose-6-phosphate oligosaccharides
MHC	Major histocompatibility
mV	Millivolt

Na+	Sodium ions
Na v1.8	Sodium ion channel
NDS	Normal donkey serum
NGS	Normal goat serum
NGF	Nerve growth factor
NCG	Nerve conduit guidance
NGF–TrkA	Nerve growth factor Tropomyosin receptor kinase A
O.C.T	Optimum cutting temperature medium
PBS	Phosphate Buffered Saline
PBST	Phosphate Buffered Saline plus 0.2% Triton
PCL	Poly-caprolactone
PDL	Poly-D-lycine hydrobromide
PEG	Polyethylene glycol
PGA	Poly-glycolic acid
PKA, PKC	Protein kinase
PNI	Peripheral nerve injury
SNE	Sciatic nerve entrapment
SNL	Spinal nerve ligation
SI	Sprouting Index
TGF-β	Transforming growth factor beta
TNF-α	Tumour necrosis factor alpha
TNFRs	Tumour necrosis factor-α receptors
TLRs	Toll-like receptors
Th2	Type II T helper cells

CHAPTER 1

Literature review

1.1 Introduction

Injury to the peripheral nerves is a major health problem worldwide (Kouyoumdjian, 2006). It is associated with significant functional loss as a result of sensory and/ or motor impairment (Fawcett and Keynes, 1990; Wojtkiewicz et al., 2015). These injuries can also lead to the development of neuropathic pain. Common aetiologies of peripheral nerve damage include; penetrating injury, crush, stretch or ischaemic injuries (Campbell, 2008). Development of neuropathic pain following a nerve injury may also have social consequences and cause longstanding disability (Wojtkiewicz et al., 2015). The incidence of peripheral nerve injury is estimated as 300,000 persons per year in the developed countries (Mohanna et al., 2003). According to the Health and Social Care Information Centre of England, 72783 operations involving release and/ or repair of different peripheral nerves were reported in March 2015 (Health episode statistics for England, 2014 and 2015).

The functional recovery of injured neuronal axons is dependent on the type of injury, site, and distance over which the axons must regenerate to cross the gap between the nerve segments (Rodríguez et al., 2004). The understanding of the complex sequence of events that commences within the axons in response to peripheral nerve injury has increased significantly, promoting the clinician with knowledge of the role of neurobiology to enhance axonal regeneration after repair. The response of peripheral nerves to traumatic injury starts with degradation of the myelin sheath within the distal segment. This is followed by axonal regeneration at the proximal segment (Navarro et al., 2007). Sometimes the proximal segment continues to regrow resulting in a disorganized mass composed of neuronal fibres and fibrous connective tissue which is typically known as a traumatic neuroma. These neuromas are often associated with paraesthesia or chronic neuropathic pain (Foltán et al., 2008).

Despite the potential capability of peripheral nerves to regenerate, the functional outcome is often poor because of the formation of scar tissue in the injured nerve, which impedes the growth of regenerated nerve even after meticulous repair (Atkins et al., 2007).

Over the past hundred years, the outcome following the management of peripheral nerve injury has been of concern, and significant research has been undertaken into the repair methods to improve functional recovery, and attenuate the development of neuropathic pain. Several techniques exist within the literature to repair injured peripheral nerves. These techniques include; direct anastomosis of the cut ends with sutures, or by the use of nerve grafting materials to bridge the gap distance between the segments (Navarro et al., 2007). Despite these advances in surgical repair the outcome is often unpredictable and many patients are left with permanent disability. There are several factors such as age, length of the gap, and time of repair which may influence the outcome after nerve repair. Therefore, future modification in surgical repair solely, is unlikely to considerably improve the outcome after peripheral nerve injury and the return to normal function.

At present, there is invaluable data and ongoing research focusing on the modulation of neurobiology during neuronal regeneration. The investigations in this thesis were undertaken to elucidate the effect of cytokines or their antagonists on neuronal regeneration and the potential development of neuropathic pain (Atkins et al., 2007; Ngeow et al., 2011).

1.2 Biological features of the spinal nerves, cranial nerves and the spinal cord

In response to nerve injury, a cascade of events happens in the central and peripheral nervous systems which affects nerve regeneration and recovery. Therefore, to increase the understanding and clarity of this thesis the biological features of the spinal nerves, spinal cord, glial cells and the cranial nerves will be briefly described in this section.

1.2.1 The functional unit of the nervous system

The neurone is the basic cellular and functional unit of the nervous system (Fitzgerald et al., 2012). The neurone is responsible for the transmission and conduction of electrical changes as nerve impulses (Figure 1.1). Neurones consist of an axon, and a single cell body (soma) (Crossman and Neary, 2015). The axon is a protracted process of the neurone whose cell body (soma) is located in the dorsal root ganglion (DRG) and carries the impulses away from the soma to the axon end terminals (Kerns, 2008). The size of the cell body varies in location and function, and is found to correlate with length of the axon proportionally (Crossman and Neary, 2015). The cell body exhibits short branching processes known as dendrites which conduct nerve impulses from adjacent nerve cells inward toward the cell body. The components of the cytoplasm (axoplasm) of the neurone cell body are similar to most other cells and include a centrally located nucleus and other surrounding structures. The Golgi apparatus and mitochondria are microscopically marked cellular organelles within the cell body. Other distinctive cellular inclusions are known as Nissl bodies or substance which represents an endoplasmic reticulum and its related ribosomes (Crossman and Neary, 2015). The axoplasm also contains intracellular organelles such as microtubules and neurofilaments which play an important part during the process of

nerve regeneration by promoting the axoplasmic transport mechanism (Topp and Boyd, 2012).

A synapse is the site of communication between terminal axons of one neurone and dendrites of another (Crossman and Neary, 2015). “There are synaptic connections between neurones in the central nervous system and in the autonomic ganglia, but not in the DRG” (Kerns, 2008). Transmission of information or electrical changes are processed by the release of specific chemical mediators from the presynaptic membrane of the nerve cell, which then act on postsynaptic membrane receptors (Crossman and Neary, 2015).

Most peripheral nerve axons are myelinated and surrounded by a concentric myelin sheath layer, produced by a Schwann cell (Kerns, 2008). The thickness of the myelin sheath is directly related to the axon diameter. The span of axonal membrane that is covered by each Schwann cell is called an internode (Topp and Boyd, 2012). These sheath layers are lipid rich plasma membranes and confer increased rates of transmission and conduction of nerve impulses. The space between the Schwann cells is known as node of Ranvier, where ion channels are present, and are responsible for continuous propagation of electrical impulses at the subsequent node of Ranvier (Kerns, 2008; Topp and Boyd, 2012).

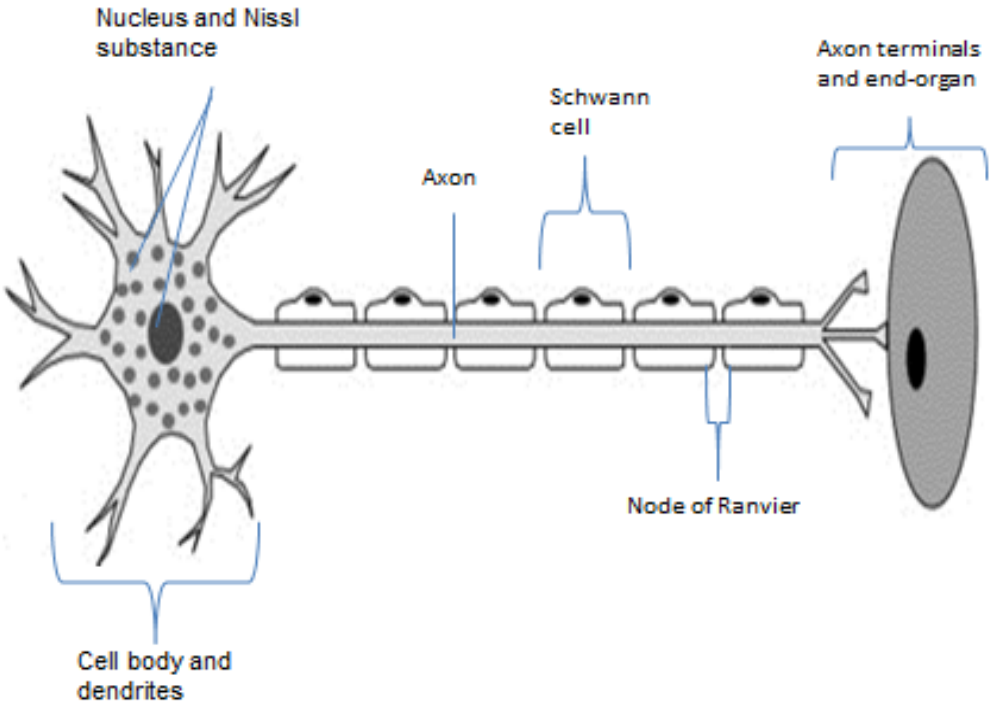

Figure 1.1: Diagram illustrates the anatomy of the neurone cell. (Figure reproduced with permission from John Wiley and Sons and Copyright Clearance Centre).

1.2.2 Anatomical and physiological features of the nerve cell

Anatomical features of the nerve cell

The peripheral nervous system is comprised of nerves and their root and branches, that allow communication with the brain and spinal cord, with the body parts, including the extremities, skeletal muscles and the viscera (Crossman and Neary, 2015). These nerves branch out from the brain and spinal cord and are directed towards targeted receptor or effector cells.

The nerve cell contains bundles of fibres; sensory, motor or mixed, which are surrounded by a specialized connective tissue layers; including the epineurium, endoneurium and perineurium (Figure 1.2). Each bundle of nerve cell fibres is known as a fascicle. Within a fascicle each single axon is surrounded by endoneurium connective tissue which contains fibroblasts their collagen fibres and extracellular matrix (Kerns, 2008). A fascicle is surrounded by the perineurium. The perineurium consist of multiple epithelial-like perineurial cell layers that encircle the nerve axons into fascicles which provide additional mechanical strength to the nerve trunk (Topp and Boyd, 2012). In addition, this connective tissue layer acts as a diffusion barrier which prevents the passage of irritant substances to the exposed axons within the endoneurium (Flores et al., 2000; Kerns, 2008). The epineurium encloses the fascicles together and represents approximately 50 % of the thickness of the peripheral nerves trunk (Flores et al., 2000). This connective tissue layer protects and maintains continuity of the fascicles and their accompanying blood vessels (Flores et al., 2000).

A peripheral nerve is infiltrated by a complex network of external and internal blood supply within the epineurium and the endoneurium connective tissue layer to ensure

uninterrupted blood flow along the course of the nerve trunk. The blood vessels are relatively permeable and capillaries exist only in the endoneurium (Flores et al., 2000). The capillaries form a continuous endoneurial-capillary pattern that possess tight junctions, regulating the endoneurial environment by maintaining the endoneurial fluid pressure at 2-3mmHg, which counter balances the endoneurial oncotic pressure (Topp and Boyd, 2012).

Nerve fibres primarily come in three different diameters which reflects their conduction velocity, and target receptors (Osbourne, 2007). Type A fibres and their subtypes (α, β, γ and δ) are heavily myelinated, the largest in diameter (up to 20 μm), and have the highest conduction rate of electrical impulses. Type B fibres are less myelinated and have a diameter up to 3 μm, and these are autonomic fibres. Type C fibres (nociceptive fibres) are unmyelinated and have the smallest diameter of all nerve fibres (less than 2 μm) (Osbourne, 2007).

Myelination of the nerve fibres enhances the electrical impulse conduction during an action potential (Topp and Boyd, 2012). In large myelinated nerve fibres the conduction velocity is fast in comparison to less myelinated fibres which conduct at a slower rate (Topp and Boyd, 2012). Heavily myelinated fibres are associated with the transmission of motor and proprioceptive impulses whereas less myelinated and unmyelinated fibres convey sensory signals.

Physiology of the nerve cell

In the peripheral nervous system, the neurones create, amplify and propagate electrical impulses along their axon terminals These impulses are called action potentials (Topp and Boyd, 2012).

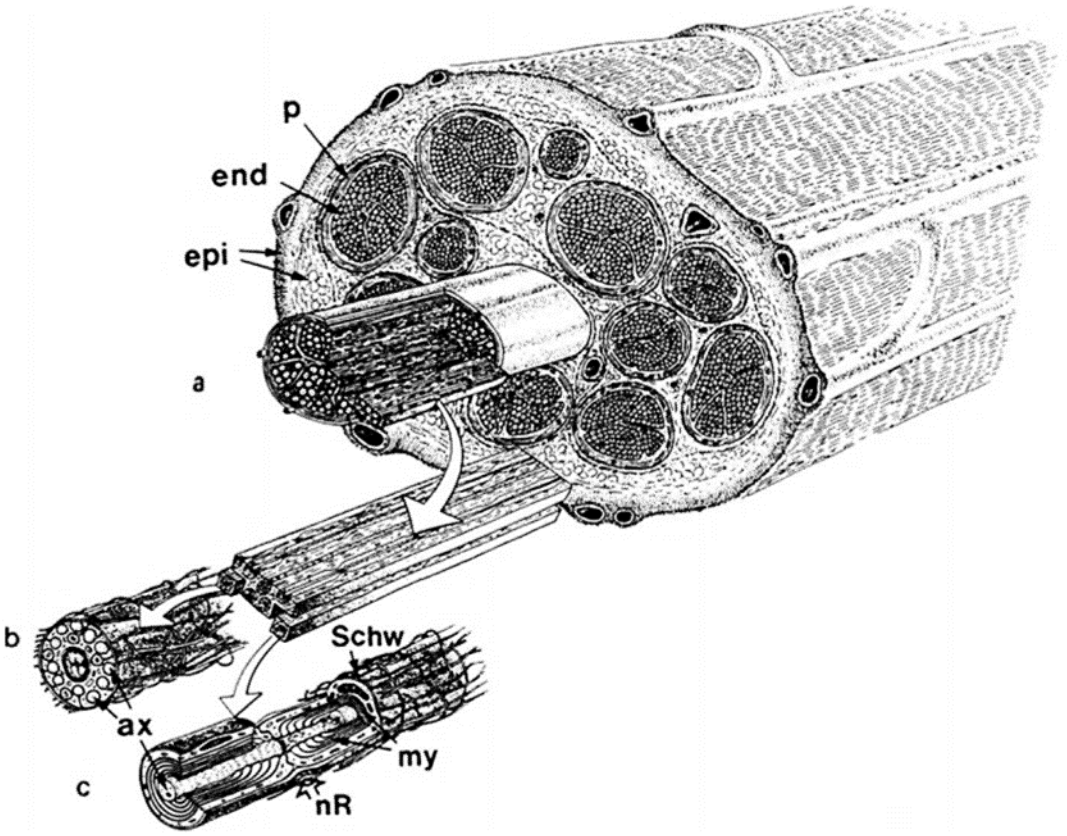

Figure 1.2: Diagram illustrates the organization of connective tissues surrounding nerve fibres. a) Fascicles surrounded by perineurium (p) which embedded in a loose connective tissue, the epineurium (epi) - the outer layers of the epineurium are condensed into a sheath. b) and c) illustrate the appearance of unmyelinated and myelinated fibres respectively. Schw: Schwann cell; my: myelin sheath; ax: axon; nR: node of Ranvier. (Figure reproduced with permission from Elsevier and Copyright Clearance Centre).

An action potential in the nerve cell largely occurs in response to alterations in potassium and sodium ion gradients across the cell membrane in response to tissue damage or mechanical stimulation in the nociceptive fibres and proprioceptive fibres, respectively. At rest the neurone's cell body maintains its intracellular membrane potential at -70 mV by retaining higher concentration of potassium (K+) ions as opposed to low concentration of sodium ions (Na+) (Topp and Boyd, 2012). During excitation, sodium channels open and allow an influx of Na+ ions to produce an action potential by raising the membrane potential to a threshold potential of -50 mV causing membrane depolarization. Afterwards, previously opened sodium channels become inactive and potassium channels open to repolarize the membrane to its resting potential state and generate a new action potential at another site (Topp and Boyd, 2012).

In addition to the electric impulse conduction along the axons of peripheral nerves, there is also the continuous movement of intracellular organelles and neurotrophic substances that are crucial for neurone regeneration and growth. This movement is known as bidirectional axoplasmic flow and may flow in a forward direction (anterograde) away from the cell body to the dendrites, using kinesin molecules (ATPase) (Topp and Boyd, 2012), or in a backward direction (retrograde), from the dendrites towards the cell body, utilizing dynein/dynactine complexs (Lloyd, 2012). The axon cytoskeleton is made up of microtubules, neurofilaments and microfilament proteins, play a role in axonal transport, and also movement of mediators and provision of neurotrophic factors is necessary for nerve cell survival (Lloyd, 2012). Disruption of the cytoskeletal proteins, necessary for axoplasmic transport, has a

detrimental effect on neurone cell integrity, this affecting the growth and maintenance of nerve fibres.

1.2.3 The spinal nerves

There are 31 pairs of spinal nerves that emerge from the dorsal and ventral spinal roots. These nerves comprise motor and sensory nerve fibres to and from all parts of the body (Decosterd and Woolf, 2000; Köbbert and Thanos, 2000; Rigaud et al., 2008; Watson et al., 2009). Spinal nerves exit the vertebral column through the intervertebral foramina. Each spinal nerve comprises somatic and visceral fibres. The somatosensory fibres are peripheral processes of the dorsal root ganglion (DRG) neurons that carry sensory information from the subcutaneous tissues, skin and joints. In addition, the somatomotor fibres are axons of ventral horn neurons which carry motor impulses to the skeletal muscles. The visceral afferent fibres are composed of peripheral processes of DRG neurons which convey sensation from the visceral organs of the body.

Of importance to this work, sciatic nerve will only be described in this section. Equally, mouse and rat sciatic nerve was used as model of peripheral nerve injury in this research work. Currently, the use of sciatic nerve as model of peripheral neuropathy is gaining a greater interest (Decosterd and Woolf, 2000; Köbbert and Thanos, 2000; Rigaud et al., 2008). From anatomical point of view the sciatic nerve crosses lower limb at level of mid-thigh and carry mixed nerve fibres (sensory, somatic a and autonomic motor fibres) that originates from the lumbar segments at regions 4-6 of the spinal cord and its associated DRG cells (Figure 1.3). Although, several injury models were descried, sciatic nerve transection model is considered reliable due to its relevance to human peripheral neuropathy (Decosterd and Woolf, 2000; Köbbert and

Thanos, 2000; Rigaud et al., 2008). In addition, other important factors that were considered for the selection of sciatic nerve because of its larges size and relative ease of access which facilitate the nerve dissection and exposure. Moreover, the mouse model offers some advantages which include availability of several transgenic stains, relative ease of handling, and cost-effectiveness in domiciliary care.

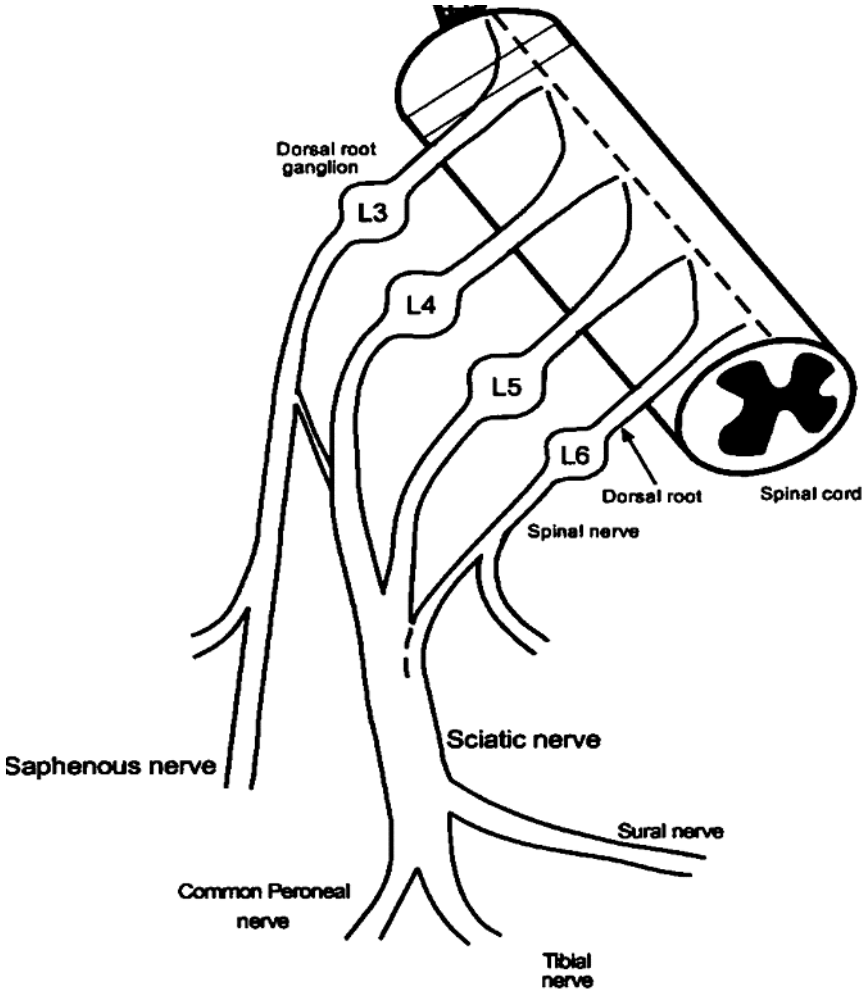

Figure 1.3: Diagram of the sciatic nerve and corresponding dorsal root ganglions projection in the lumbar regions 4-6. Figure reproduced with permission from Wolters Kluwer Health, Inc and Copyright Clearance Centre.

1.2.4 The spinal cord

The spinal cord is an important structure that link the brain with the body which process the motor and sensory signals from the body to the brain (Watson et al., 2009). The spinal cord divided into four regions; cervical, thoracic, lumbar and sacral, each of which is comprised of several segments. Of importance to this work, Lumbar segment-4 (L4) of the spinal cord will only be described. Transversely, L-4 region of the spinal cord resembles a “butterfly” shape and contains the white matter which surround the central gray matter where most of spinal neuronal cell bodies with sensory and motor neurons are located (Watson et al., 2009) (Figure 1.4). The mid region of the butterfly represents intermediate gray commissure which crosses the midline below the white commissure. The gray matter mainly contains the cell bodies of neurons and glia and is divided into four main horns; dorsal, lateral and ventral horns. The horns of gray matter divide the white matter into three columns (funiculi): dorsal, lateral and ventral (Watson et al., 2009). The boundary between the lateral and ventral columns is not distinct.

The dorsal horn is found at all spinal cord levels and contains the sensory nuclei that receive and process incoming somatosensory information toward the midbrain and diencephalon. The intermediate and the lateral horns comprise autonomic neurons innervating visceral and pelvic organs (Watson et al., 2009). The ventral horn comprises motor neurons that innervate skeletal muscle. The ventral root axons join with the peripheral processes of DRG cells to form mixed afferent and efferent spinal nerves, which merge to form peripheral nerves. A large group of axons that are in these areas called a funiculus. Smaller bundles of axons, which share common features within a funiculus are called fasciculus (Watson et al., 2009).

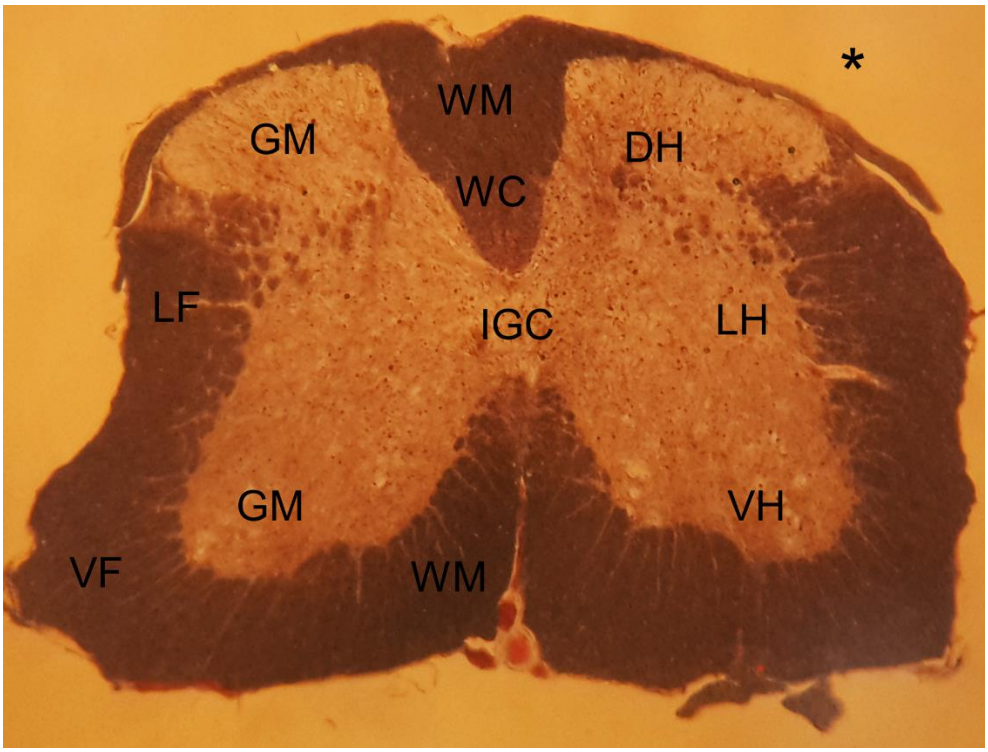

Figure 1.4: Transverse section of the spinal cord under light microscope illustrates anatomical organization of the Lumbar region (L4) of the spinal cord. DH: dorsal horn, GM: gray matter, IGC: intermediate gray commissure, LF: lateral funiculi, LH: lateral horn, VF: ventral funiculi, VH: ventral horn, WC: white commissure, WM: white matter, *: image background.

Spinal gray matter reveals microscopic layers of nuclei that are distributed within the spinal cord which exhibits a pattern of lamination (Figure 1.5). Cytoarchitecture of each lamina is composed of various sizes or shapes of neurons which is related the function of the corresponding nuclear groups (Watson et al., 2009). Briefly, laminae I to IV are concerned with nociceptive sensation which comprise the dorsal horn, whereas laminae V and VI are concerned primarily with proprioceptive sensations. Lamina VII is equivalent to the intermediate zone and acts as a relay between muscle

spindle to midbrain and cerebellum, and laminae VIII and IX comprise the ventral horn and contain mainly motor neurons that innervates skeletal muscle. Lamina X surrounds the central canal and contains neuroglia cells (Watson et al., 2009).

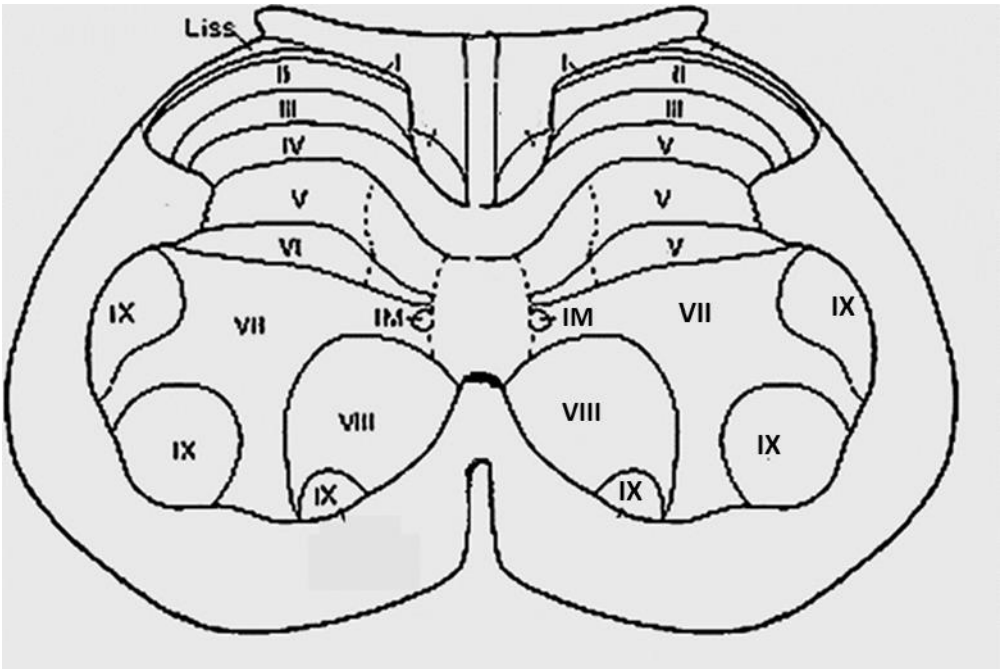

Figure 1.5: Diagram illustrates cytoarchitectonic organization of lamina in the spinal cord sections of lumbar region-4 in the rodents. Lamina I: fine rim of posteromarginal nucleus of dorsal horn; Lamina II: substantia gelatinosa proper; Laminae III and IV: nucleus proprius; Lamina V: Neck of the dorsal horn; Lamina VI: Base of the dorsal horn; Lamina VII: intermediomedial nucleus Lamina VIII: motor interneurons; Lamina IX: mediolateral part of the ventral horn; motor neurons; IM: intermedio-medial nucleus; Liss: Lissauer's tract. (Figure reproduced with permission from John Wiley and Sons and Copyright Clearance Centre).

The human spinal cord is a tubular structure that comprises a bundle of fibre that corresponds to the spinal dorsal and ventral nerve roots on each side (Decosterd and Woolf, 2000; Köbbert and Thanos, 2000; Rigaud et al., 2008; Watson et al., 2009). The dorsal root of a spinal nerve contains sensory fibres whereas, the ventral root which comprise the motor fibres. Each dorsal root exhibit an ovoid swelling known as the dorsal root ganglion (DRG) located close to the junction of the dorsal and ventral roots. The cells of DRG are primary sensory neurons being described as pseudo-unipolar neurons with a single axon (Decosterd and Woolf, 2000; Köbbert and Thanos, 2000; Rigaud et al., 2008; Watson et al., 2009). The sympathetic fibres entering the DRG and regulate the sympathetic outflow to the corresponding DRG. It has been suggested that disruption of the DRG cells function resulting from peripheral nerve injury play important role in neuropathic pain development (Navarro et al., 2007).

1.2.5 Glial cells

In the central nervous system (CNS) glial cells is play supportive role by surrounding neurons and maintain haemostasis and provide insulation between them (De Bock et al., 1843; Aldskogius and Kozlova,1998; Kurosinski and Götz, 2002; Crossman and Neary, 2015) (Figure 1.6). Glial cells are the most abundant cell types in the central nervous system and spinal cord. There are three types of glial cells, namely, astrocytes, oligodendrocytes, and microglial cells. Following peripheral nerve injury microglia and astrocytes activation were considered to play a role in development of neuropathic pain (De Bock et al. 1843; Aldskogius and Kozlova,1998; Kurosinski and Götz, 2002; Crossman and Neary, 2015).

Astrocytes, represent 40-50 % of all glial cells which are restricted to synaptic terminals, have elaborate local processes that give these cells a star-like shape (De Bock et al., 1843; Aldskogius and Kozlova,1998; Kurosinski and Götz,2002; Crossman and Neary, 2015). Their major function is to maintain neuron synaptic junction haemostasis that provide an appropriate chemical environment for neuronal signaling. In close association with neurons, astrocytes enwrap synaptic terminals and make extensive contacts with endothelial cells from the capillaries. Moreover, astrocytes are interconnected with one another by gap junctions (De Bock et al., 1843; Aldskogius and Kozlova,1998; Kurosinski and Götz, 2002).

Oligodendrocytes, which are also restricted to the central nervous system, lay down a laminated, lipid-rich wrapping called myelin around some, but not all, axons. Myelin has important effects on the speed of action potential conduction (De Bock et al., 1843; Aldskogius and Kozlova,1998; Kurosinski and Götz, 2002).

In the central nervous system, microglia are macrophage-like cells that serve a phagocytic function and primarily acts as scavenger cells that remove cellular debris in normal and pathological state. Microglia make up about 5-10 % of the total glial cell in the CNS and spinal cord and primarily derived from resident microglia or macrophage infiltrates the injured area from the circulation (De Bock et al., 1843; Aldskogius and Kozlova,1998; Kurosinski and Götz, 2002; Crossman and Neary, 2015).

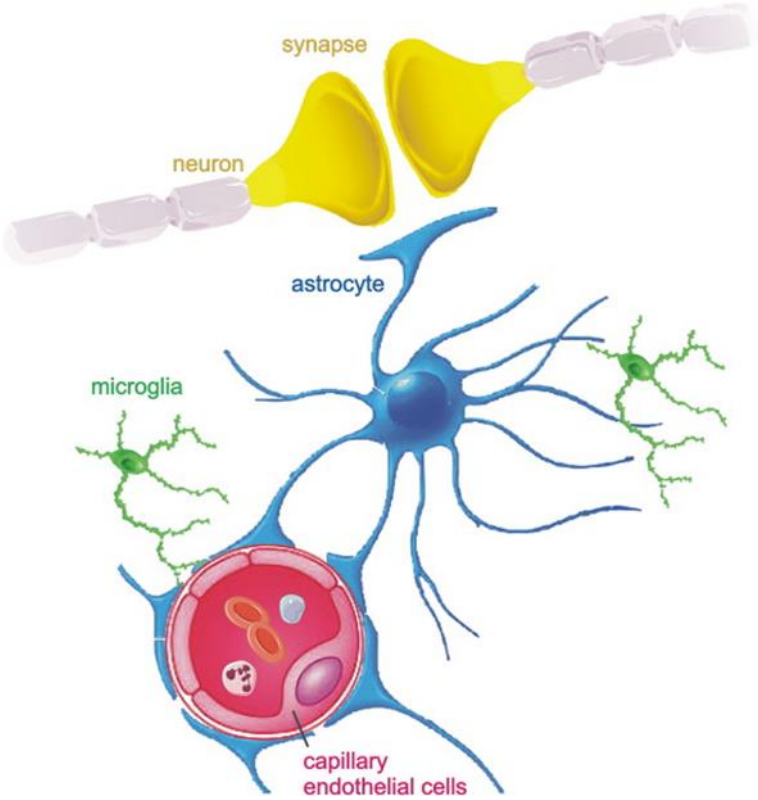

Figure 1.6: Diagram illustrates Glial cells under physiologic make contacts with neurons and capillaries and exchanges nutrients between the blood supply and the active neuron. Glial cells, astrocyte, regulate neuron haemostasis by encircling presynaptic and postsynaptic terminals which help integrate neurotransmitter inputs and release their own transmitters that act on adjacent neurons. (Figure reproduced with Elsevier and Copyright Clearance Centre).

1.2.6 The cranial nerves

Cranial nerves emerge directly from the anterior aspect of the brain stem and process different aspects of the body function that are important for daily activities such as motor functions including chewing and swallowing, and, in addition, responsible for sensation of the skin of face, teeth and intraoral mucous membranes (Craven, 2010; Crossman and Neary, 2015). These functions are of great importance in relation to the dentistry and in providing care for patients with dental problems.

There are 12 pairs of cranial nerves which leave the cranial cavity through foramina or fissures towards their intended target or tissues (Craven, 2010; Crossman and Neary, 2015) (Figure 1.7). These nerves are designated in roman numbers as follows; I (olfactory), II (optic), III (oculomotor), IV (trochlear), V (trigeminal), VI (abducens), VII (facial), VIII (vestibulo-cochlear), IX (glossopharyngeal), X (vagus), XI (accessory) and XII (hypoglossal). The trigeminal nerve will only be described in relevance to this work.

The trigeminal nerve (fifth cranial nerve) comprise three divisions; the ophthalmic, maxillary and mandibular. It is the largest cranial nerve, and made up of mixed nerve fibres, comprising sensory and motor fibres (Craven, 2010; Crossman and Neary, 2015) (Figure 1.8).

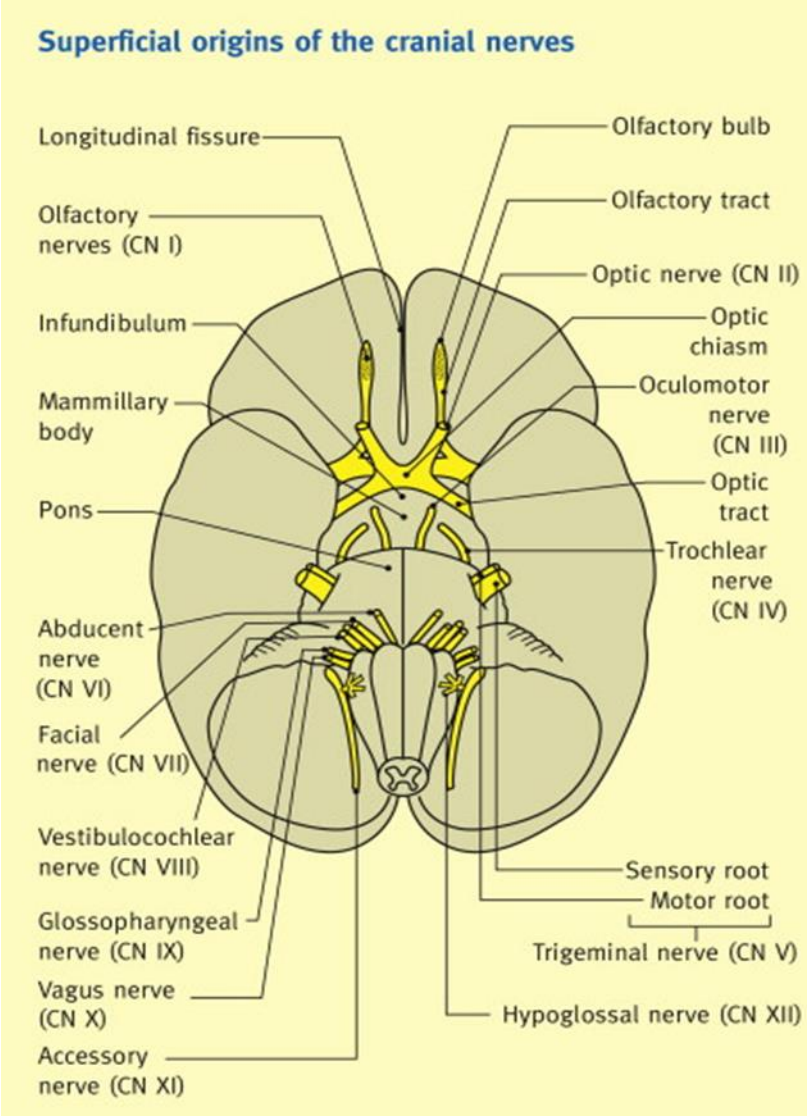

Figure 1.7. Superficial origins of the cranial nerves (Figure reproduced with Elsevier and Copyright Clearance Centre).

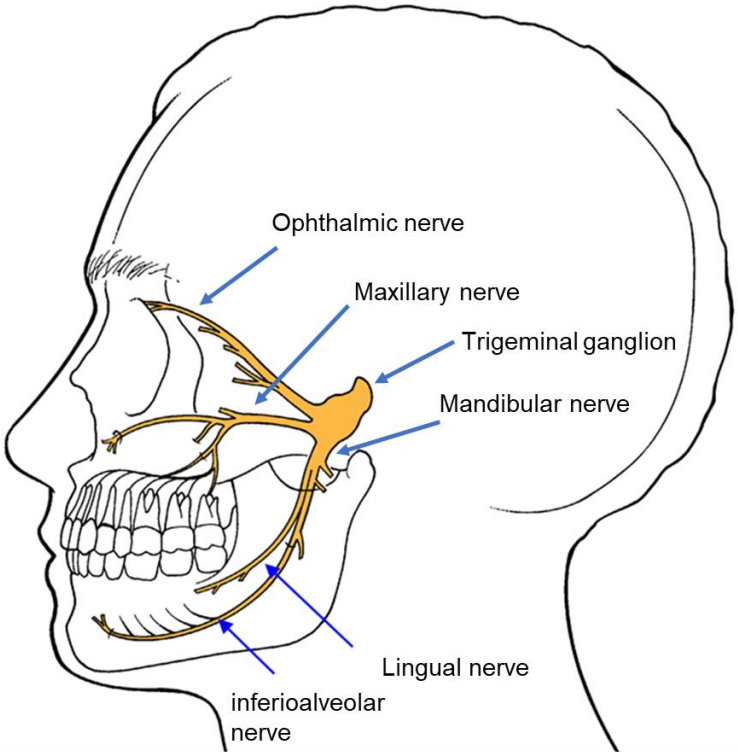

Figure 1.8: Illustration of the trigeminal nerve branches; ophthalmic, maxillary and mandibular nerve branches in face and mouth.

The nerve emerges from the anterolateral aspect of the pons as two roots; sensory and motor root which crosses the upper border of the petrous temporal bone just lateral to the petrous apex, where they enter the middle cranial fossa and expands into the trigeminal ganglion from where the three divisions emerge (Craven, 2010; Crossman and Neary, 2015). The ophthalmic nerve being the most medial while, the largest division, the mandibular nerve being the most lateral. The motor branch runs separately, beneath the ganglion, before joining the mandibular nerve within the foramen ovale. The motor nerve fibres only present in the mandibular division

whereas, the ophthalmic or maxillary nerves are exclusively carries sensory fibres to the oral and facial region (Craven, 2010; Crossman and Neary, 2015).

In the lateral wall of the cavernous sinus, the ophthalmic nerve gives three branches (frontal, lacrimal and nasociliary), all of which cross the superior orbital fissure to enter the orbit cavity (Craven, 2010; Crossman and Neary, 2015). However, the maxillary nerve exit through the foramen rotundum to enter the pterygopalatine fossa and gives three branches (anterior, middle and posterior superior nerves). Moreover, the sensory fibres of the maxillary nerve are distributed to the skin of the upper part of the face, the mucous lining of the nasal cavity and paranasal sinuses, the meninges within the cranial cavity, the anterior and lateral aspects of the scalp, the roots of all the maxillary and mandibular teeth and their gum (Craven, 2010; Crossman and Neary, 2015).

The mandibular nerve exit through the foramen ovale to enter the infratemporal fossa. The motor fibres in the mandibular nerve are distributed to the muscles of mastication, tensor tympani, mylohyoid and tensor veli palatine. The sensory fibres of the mandibular nerve are distributed to the skin of the lower part of face, floor of the oral cavity including the anterior two-thirds of the tongue, the roots of all mandibular teeth, and their gum (Craven, 2010; Crossman and Neary, 2015).

The terminal branches of the trigeminal nerve divisions are at greater risk of damage during various dental treatment or intraoral surgical procedures or as consequence to orofacial traumatic injuries. Injuries to the trigeminal nerve branches usually present as loss or disturbance in taste and/or sensation (Craven, 2010; Crossman and Neary, 2015).

1.3 Peripheral nerve injuries

1.3.1 Epidemiology of peripheral nerve injuries

A peripheral nerve injury is described as damage to the motor and sensory nerves that lie outside the brain or spinal cord (Navarro et al., 2007). Peripheral nerves can be damaged by various mechanism such as neurodegenerative diseases, chemical toxins or mechanical trauma. Only nerve injuries caused by mechanical and iatrogenic trauma are considered here.

1.3.1.1 Traumatic injury to peripheral nerves- *aetiology, incidence and recovery in different extremities and nerves*

Peripheral nerve injury is a global problem and can result in significant disability and incapacity and affect general wellbeing (Eser et al., 2009; Wojtkiewicz et al., 2015). Peripheral nerve injuries encompass a large spectrum of neurological deficits and its symptoms can include weakness, altered sensation, loss of function and chronic pain (Martins et al., 2013). "Neuropathic pain is characterized in humans by spontaneous pain, and/ or evoked pain resulting from hypersensitivity to normally painful stimuli (hyperalgesia) or non-painful stimuli (allodynia)" (Djouhri et al., 2012).

The incidence and aetiological factors of traumatic peripheral nerve injuries reported in the literature are varied according to periods of peacetime or conflict (Martins et al., 2013). In general, most of the knowledge and experience about peripheral nerve injuries was developed during times of war (Seiler and Payne, 1999; Rodríguez et al., 2004; Campbell, 2008). The first report of the causalgia syndrome of the extremities was described in the American Civil War. This syndrome characterized by a burning pain and sensation, was caused by partial nerve injury (Seiler and Payne, 1999; Evans,

2001). The treatment approach of limb injuries at that time was based on the severity of the injury, where a simple suture was advocated for mild injury but amputation reserved for more severe injuries.

During peacetime the incidence and the aetiological spectrum of peripheral nerve injuries reflects the country's development (Eser et al., 2009). In developed countries, peripheral nerve injury frequently results from sports, occupational accidents and road traffic accidents (Robinson, 2000; Campbell, 2008).

Peripheral nerve injuries may result in significant physical and psychological morbidity and economic burden if not managed efficiently, particularly in an individual of working age (Martins et al., 2013). In spite of differences across the study population, there are consistent reports of a higher incidence of peripheral nerve injuries associated with the upper limbs (more than 70 %), and the most affected nerves are the ulnar, radial and brachial plexus (Robinson, 2000; Kouyoumdjian, 2006; Eser et al., 2009). For lower limbs the most frequently injured peripheral nerves are the peroneal or sciatic nerves (Robinson, 2000; Kouyoumdjian, 2006; Eser et al., 2009; Ciaramitaro et al., 2010).

Nerves of the upper and lower extremities can be damaged in various ways, including nerve compression, laceration or complete transection (Dahlin, 2008; Campbell, 2008). In addition, stretch-related damage is the most common type of injury of peripheral nerves of upper and lower extremities, especially in motor vehicle accidents, whereas laceration by sharp objects represents about 30 % of severe nerve injuries. Compression related damage of the extremities, is another type of nerve injury which may involve structural deformation as well as ischemia (insufficient blood supply) (Campbell, 2008). In general, compression related damage shows better regeneration

capacity than a transection injury due to the nature of the transection insult and the significant anatomical disruption of axons or nerve trunk (Seiler and Payne, 1999). Therefore, early management of these transection injuries can result in improved recovery, to some extent, of the lost function, and as a result, it is crucial the pathophysiological consequences of these injuries are understood in order to define an acceptable management strategy to improve the functional recovery of this disabling condition (Martins et al., 2013; Wojtkiewicz et al., 2015).

1.3.1.2 Traumatic injury to cranial nerves- aetiology, incidence and recovery with different nerves

Injury to the nerves of the jaws and face in relation to dentistry has only been appreciated in the last three centuries (Pogrel et al., 2011). However, the consequences of damage to the peripheral branches of trigeminal nerve on patient wellbeing is well documented.

The mechanism of recovery following trigeminal nerve injury is complex, in part due to it being the largest cranial sensory nerve, representing approximately 40 % of the sensory cortex of the human brain (Renton and Yilmaz, 2012). The most commonly injured nerve branches are the inferior alveolar and lingual nerves. The sensory dysfunction of these nerves is more likely to be permanent when the injury is severe and if there is delay between the time of injury and assessment of the patient (Renton and Yilmaz, 2012).

It is well established that damage to the mandibular branch of the trigeminal nerve is amongst the most debilitating injuries in the field of oral surgery. Altered sensation and pain in the oral and maxillofacial region may interfere with eating, drinking, speaking, tooth brushing, and shaving (Renton and Yilmaz, 2012). Subsequently,

injury to the mandibular nerve, may lead to the patient experiencing a reduced quality of life, psychological distress, and social disabilities.

1.3.1.3 Sequelae following different major surgical interventions- trauma, fractures, orthognathic surgery

Damage to the mandibular nerve branches, the inferior-alveolar and lingual nerves, may also follow orthognathic surgery, as well as a result from maxillofacial traumatic injuries and/or their surgical interventions (Bagheri et al., 2009).

Facial fractures often run in lines of weakness, which include sites in close approximation with nerve foraminae such as the mandibular parasymphysis and maxillary fracture sites (i.e., mental, infraorbital), or can cross the line of weakness, such as in the third molar region, directly involving the inferior-alveolar nerve trunk (Bagheri et al., 2009). However, the precise mechanism of trigeminal nerve damage is often uncertain, and injury may result from nerve compression either by displaced bone fragments or soft tissue oedema, or from traction of a displaced fracture, and crushing, avulsion, or even partial or total nerve transection from fractured bone edges (Bagheri et al., 2009). The overall prevalence of neurosensory disturbances associated with the inferior-alveolar nerve before surgical interventions in post-traumatic injuries ranges from 46 % to 58.5 % for fracture lines involving the angle and body of the mandible (Bagheri et al., 2009). However, exaggeration of pre-existing neurosensory disturbances is often observed after surgical repair especially in these fractures. In the majority of cases, the sensory deficit is temporary, but sometimes it is persistent (7.7%) (Bagheri et al., 2009). At the time of fracture repair, the nerve fibres may undergo further damage by additional traction and/or compression while the fracture sites are being reduced and stabilised. Moreover, unintentional and

misapplication of surgical technique, such as placement of fixation screws near or through the mandibular canal can cause nerve injury (Bagheri et al., 2009).

Facial deformity due to abnormal growth or discrepancies in jaw alignment is a well-known concern among young adult patient across the world. Corrections of discrepancies in jaw relationships involve either single or two jaw surgery. The sagittal split ramus osteotomy is the operation of choice for correction of abnormalities in body and ramus of the mandible. The procedure is versatile and reliable but neurosensory disturbances are common due to close approximation of osteotomy lines with lingual and inferior-alveolar nerves (Bagheri et al., 2010). Majority of postoperative neurosensory disturbances reported are transient and resolve without need for intervention. The incidence of persistent neurosensory disturbances of the inferior-alveolar nerve after orthognathic surgery is approximately 12.8 % (Colella et al., 2007), whereas the reported incidence of lingual neurosensory dysfunction ranges from 9.3 % to 19.4 % (Bagheri et al., 2010). Potential recovery of the inferior-alveolar sensory function has been documented to be improved within the first 3 months when compared to the lingual nerve and this may be due to natural protection offered by the mandibular bony canal (Bagheri et al., 2010).

1.3.1.4 Sequelae following different minor surgical interventions- lower wisdom teeth removal, local anaesthesia injection injuries, implants and root canal treatment

Injury to the peripheral branches of the trigeminal nerve can result from minor surgical procedure or even mandibular block anaesthesia in the oral and maxillofacial region (Bagheri et al., 2009). The surgical removal of wisdom teeth (lower third molars) is a commonly performed procedures undertaken to treat pathology related to the

impacted teeth such as pericoronitis, caries, and odontogenic cysts (Renton and Yilmaz, 2012). The overall complication rate relating neurosensory dysfunction of the lingual and inferior-alveolar nerves after lower third molar surgery varies widely from 0.2 % –22 %, depending to a certain extent, on the surgical technique used (Robinson et al., 2000).

Injury of inferior-alveolar nerve following endodontic treatment is rare complication but may lead to longstanding altered sensation which adversely affect the patient's quality of life (Grötz et al.,1998; Rosen, 2014; Rosen,2017). It has been suggested that the possible mechanism of injury of inferior-alveolar nerve when performing endodontic treatments occurs due to either mechanical compression, or chemical neurotoxicity following mechanical tooth preparation, and/or overextension of filling material and irrigants solutions into the mandibular nerve canal (Grötz et al.1998; Rosen, 2014; Rosen,2017). Also, it been suggested that injury of inferior-alveolar nerve following endodontic surgical procedures is a rare but considered a serious complication due to direct injury to the nerve during surgery and may lead to long-term sensory disturbance (Grötz et al.1998; Rosen, 2014; Rosen,2017).

Nerve injury following implant placement in the mandible especially posterior region is serious complications (Alhassani and AlGhamdi, 2010; Juodzbalys et al. 2013). The prevalence of injury to the inferior-alveolar nerve (IAN) or the lingual nerve has been reported range between 3-40 % with an average of 13 % during dental implant placement or bone drilling (Alhassani and AlGhamdi, 2010; Juodzbalys et al., 2013). Other less frequent causes that has been reported such as flap retraction and compression of the mental nerve which could resulting in altered sensation of lower lip (Alhassani and AlGhamdi, 2010; Juodzbalys et al., 2013).

Trigeminal nerve injury also is a rare complication of regional anaesthesia especially in dentistry (Hillerup and Jensen, 2006). As neurosensory dysfunction after mandibular nerve blocks are so uncommon, it is difficult to attain consistent figures about their incidence. Furthermore, it is difficult to identify nerve injury that is caused by trauma to the nerve during injection when compared with those related to the neurotoxicity of the local anaesthetic solutions (Hillerup and Jensen, 2006).

Local anaesthetic agents are the most commonly used drugs for pain control in clinical dentistry (Yapp et al., 2011). It is commonly known that all local anaesthetic agents after injections are followed by complete recovery and return to normal nerve function and activity within a few hours. Local anaesthetic agents, like other medicines, have the potential to be unsafe, with adverse effects that can range from mild dizziness to serious reactions such as cardiac and respiratory depression. Amide local anaesthetic agents are commonly used in dentistry, and are considered as the safest local anaesthetic agent due to their rapid metabolism into inactive metabolites which in turn decreases the risk of systemic toxicity and over dosage (Yapp et al., 2011). However, in relation to local effects a few studies have reported a persistent deficit in sensation (paraesthesia) when articaine has been used as opposed to lidocaine (Hogan, 2008; Haas, 2006; Hillerup and Jensen, 2006). The estimated prevalence of temporary inferior-alveolar and lingual nerve neurosensory dysfunction after mandibular block anaesthesia ranged from 0.15–0.54 % whereas permanent impairment has been reported between 0.0001– 0.01 % in USA (Hillerup and Jensen, 2006). In contrast to this observation other studies on articaine safety had compared articaine to other local anaesthetic (lidocaine) agents and have shown low numbers of adverse or toxic reactions associated with this agent. Furthermore, there is much controversy about the mechanism or theories of persistent sensation deficit related to the site of injection.

Firstly, hydrostatic pressure from injection of the solution (Hogan, 2008), direct mechanical injury from the anaesthetic needle and lastly chemical injury from the local anaesthetic agent (Haas, 2006). An investigation of possible mechanisms of chemical injury or neurotoxicity has been directly related to the duration as well as the increased concentrations of the local anaesthetic solutions (Hogan, 2008). Furthermore, in an animal study model, different solution concentrations (2% versus 4%) of articaine injected into rat sciatic nerves resulted in a concentration dependent reduction of sciatic nerve conduction. Whilst numbers of myelinated axons were not affected, myelin sheath thickness as well as the mean cross-sectional axonal area was significantly reduced (Hillerup et al., 2011).

1.3.1.5 The effect of nerve injury on patient quality of life- peripheral and cranial nerves

Injuries to peripheral and cranial nerves are of significance as they hinder recovery of normal daily functions and carry a high risk of the developing neuropathic pain. Most of damage-induced pain is most probably related to severe nerve injuries (neurotmesis or axonotmesis), whilst neuropraxia as a result of peripheral nerve injury (Ciaramitaro et al., 2010). These consequences of nerve injury have brought to the surgeon's attention the need for a greater understanding of the patients' perception due to this damage, especially when they suffer permanent disability (Sandstedt and Sörensen, 1995).

A long-term adaptation of the neurosensory dysfunction associated with these injuries will have direct effects on the patient physical and psychological wellbeing (Pogrel et al., 2011). It is generally understood that the majority of patients with long term oral neurosensory disturbance (paraesthesia or dysaesthesia) tend to have severe

symptoms and greater socio-psychological consequences (Sandstedt and Sörensen, 1995). Therefore, when defining treatment approaches often results in total recovery with permanent problem for patients with peripheral nerve injury it is vital to determine the extent of nerve tissue damage by thorough assessment of nerve function.

1.3.2 Classification of peripheral nerve injuries

An accurate description and understanding of the types of nerve injury are essential to determine the underlying condition of the damaged nerve at the time of nerve repair. As a result, an introduction to a classification of the degree and mechanism of injury following nerve damage to predict the clinical outcomes after surgical exploration is needed. The most widely accepted classification systems of nerve injuries were first introduced by Seddon in 1942 and later modified by Sunderland in 1951 (Figure 1.9).

1.3.2.1 Seddon's classification system

Seddon divided nerve injuries into three categories namely; neuropraxia, axonotmesis and neurotmesis (Figure 1.9). Seddon's proposed classification system detected the degree of severity, and the capacity of spontaneous recovery of the injured nerve fibres (Zuniga and Radwan, 2013).

Neuropraxia

This is the mildest grade of nerve injury which involves transient and reversible conduction block of electrical nerve impulses (Zuniga and Radwan, 2013). Neuropraxia usually occurs due to either local ischemia or focal demyelination of the myelin layer of the axon (Kerns, 2008) and causes transient functional loss (Burnett and Zager, 2004). The axon membrane is intact, although the action potential is blocked temporarily at the region of damage. The likelihood of full recovery after neuropraxia is good and usually occurs within weeks to months (Robinson, 2000).

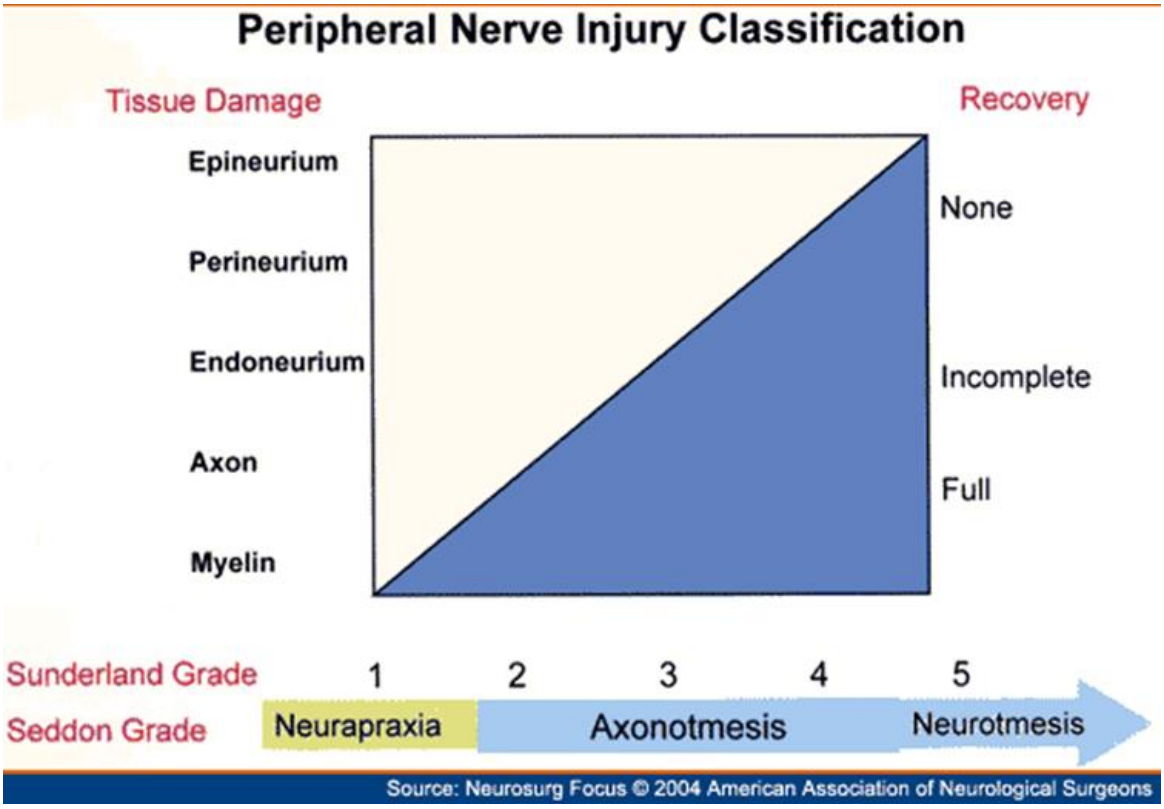

Figure 1.9: Classifications of peripheral nerve injury. (Figure reproduced with permission from Neurosurgical focus).

Axonotmesis

Axonotmesis includes a moderate degree of severity in which there is disruption of the myelin sheath and axon membrane. This degree of nerve injury is most commonly caused by crush injuries or severe compression (Kerns, 2008; Zuniga and Radwan, 2013). The axon still has some continuity retained as both perineurium and epineurium are still intact. At this stage, Wallerian degeneration arises within the degenerated part of the axon distal to injury. The prognosis following axonotmesis is variable, and recovery may take several months (Kerns, 2008; Zuniga and Radwan, 2013).

Neurotmesis

This is the severe type of nerve injury in which the whole nerve trunk is completely sectioned (Zuniga and Radwan, 2013). This degree of nerve damage is commonly seen after lacerations especially following surgical procedures. In neurotmesis, the axon membrane, myelin sheath layer, endoneurium, perineurium and epineurium are disrupted. As a result, Wallerian degeneration begins, but the prognosis for functional recovery is poor and requires surgical intervention (Zuniga and Radwan, 2013).

1.3.2.2 Sunderland's classification system

Sunderland modified the classification system described by Seddon into five degrees of injury according to severity (Figure 1.10). This system is based on the histological changes, and the extent of tissue damage within nerve trunk occurring after the injury (Zuniga and Radwan, 2013). Additional Grade of nerve injury to Sunderland grading scheme has been described as sixth grade of nerve injury (Chhabra et al.2014).

First-Degree Injury

The first-degree injury of Sunderland corresponds to Seddon's neuropraxia in which there is transient disruption of transmission of nerve signals at the injured site (Sunderland, 1990). Similar, to neurapraxia this degree of injury is commonly caused by compression or ischemia. The axon membrane integrity is preserved and has relatively rapid degree of functional recovery. The cell body (soma) of the axon is intact (Robinson, 2000). Although minor changes within the myelin sheath layer occur, there is no Wallerian degeneration, and any histopathological changes are mild (Burnett and Zager, 2004).

Second -Degree Injury

A second-degree injury corresponds to axonotmesis category of Seddon's classification in which there is complete disruption of axon membrane continuity and myelin layer (Kerns, 2008). Subsequently, Wallerian reaction occurs distal to the site of the injury (Sunderland, 1990). In pathological terms, conduction of electrical nerve signals distal to the injury site reduces within 24-72 hours after the injury. Despite the loss of axon continuity, the endoneurial connective tissue layer remain intact to maintain the regenerating fibres within its original sheath. This however, ensures undisturbed regeneration and full recovery (Sunderland, 1990; Burnett and Zager, 2004). Although rate of axonal growth is approximately 1 mm per day, full recovery of function usually takes several months longer than the first degree (Kerns, 2008).

Third-Degree Injury

Nerve injury of the third degree of Sunderland classification ensues when there is complete axon membrane disruption (similar to axonotmesis) but damage involves the endoneurium layer only (Sunderland, 1990; Zuniga and Radwan, 2013). The extent

of damage of endoneurium (intra-fascicular) could be either partial or complete (Sunderland, 1990). In this type of injury, the perineurium which maintains the fascicular structure of the whole nerve trunk is preserved. Here, the degree of Wallerian degeneration distally is severe and as a result some neuronal cell bodies are lost which decrease the number of sprouting fibres (Kerns, 2008). At the site of injury and distally, the axon membrane and its myelin sheath degrades within hours to days in a response to the injury (Wallerian degeneration). At the proximal stump, the cell body response exhibits a series of histomorphological changes known as chromatolysis which reflects a shift in axon function, from being neurotransmission to synthesis for regeneration (Kerns, 2008). Lastly, intraneural fibrosis (scar tissue) can result from the consequent inflammatory reaction, haemorrhage, oedema, and ischemia, impede the axonal regeneration. Recovery usually is possible, but substantially delayed.

Fourth-Degree Injury

In this type of nerve injury, all connective tissue layers of the nerve are destroyed except the epineurium (Sunderland, 1990; Zuniga and Radwan, 2013). This type of nerve injury involves disruption of the fascicular structure of the nerve fibres and causes functional loss. At this stage the nerve trunk is still in continuity, except at the injury site where intraneural scar and neuroma are formed. The neuroma consists of a disorganized mass of regenerating axons contained within fibrous tissue. The degree of damage proximal to the site of injury is more severe than in third-degree injuries resulting in the death of a significant proportion of nerve cells and as a result fewer misdirected axons survive to regenerate (Sunderland, 1990). Functional recovery is not possible without surgical interventions (Robinson, 2000). This type of

injury requires surgical dissection of the involved segment and an appropriate nerve repair.

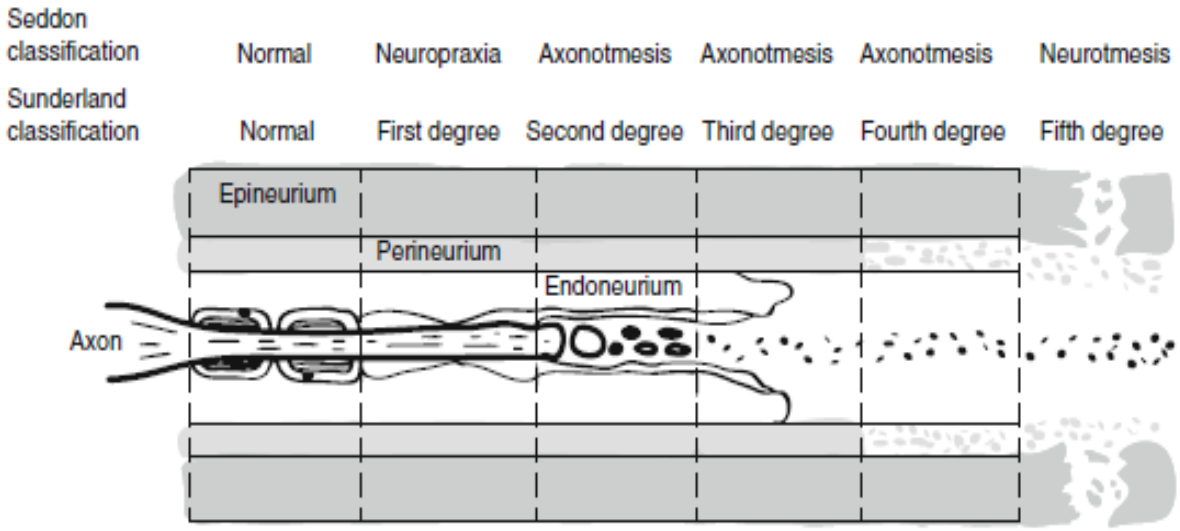

Figure 1.10: Classification of nerve injury based on the extent of histological changes within the neurone. (Figure reproduced with permission from Springer and Copyright Clearance Centre).

Fifth-Degree Injury

This is a severe nerve injury which has the greatest nerve tissue damage and complete loss of function due to transection of the entire nerve trunk (Robinson, 2000; Zuniga and Radwan, 2013). Similar to Seddon's, neurotmesis, the transected ends of the nerve fibre may remain disconnected, or may be joined by scar-tissue or neuroma. Spontaneous regeneration to cross the gap is limited, and full functional recovery remains restricted due to retrograde effects of the injury, and misdirected axons. The likelihoods of beneficial recovery are significantly enhanced by an appropriate surgical repair (Robinson, 2000; Zuniga and Radwan, 2013).

It is well established from the previous classifications, that the capacity of damaged neurones to regenerate to its pre-injury condition is likely dependent upon the extent of tissue damage and amount of continuity remaining within the nerve trunk following injury. In general, neurapraxia have the greatest chance of spontaneous regeneration than axonotmesis or neurotmesis. In the milder injury the prognosis is more favourable because Schwann cells and supporting structures that surround the nerve fibres are intact.

Sixth-Degree Injury

This is a mixed type of nerve injury which represent a complex pattern of tissue damage (Chhabra et al.2014). In this degree of the injury involve various layers across the nerve and usually follow the penetrating trauma of the nerves. The recovery potential is variable and depends upon the degree of tissue damage. The treatment of this type of injury usually range from a simple nerve repair to a complex nerve graft, or transfer (Chhabra et al.2014).

1.3.3 Pathophysiology of peripheral nerve injury

Injury to a peripheral nerve provokes a reaction that incorporates a sequence of biological alterations in the neurone cell body and its associated axon which responds in a distinct way to the damage process. The effects of injury involve the constituents of the neurone cell (Figure 1.11).

1.3.3.1 Wallerian degeneration of injured neurone cell

Investigation of the degeneration process of peripheral nerve fibres in response to injury is still evolving since its first description by 'Waller in 1850' (Navarro et al., 2007). Once nerve damage occurs, degeneration is initially detected within 24 hours, and lasts approximately two weeks following separation of the nerve segments from the cell body (Navarro et al., 2007).

Response of distal Schwann cells-axons to injury

In the peripheral nervous system, almost 90 % of nucleated neural cells present either as 'myelinating and non-myelinating Schwann cells' (Gaudet et al., 2011). Myelinating Schwann cells produce a myelin sheath membrane which surrounds either motor or sensory single large diameter nerve fibres. While the small-diameter unmyelinated axons are loosely enclosed by non-myelinating' Schwann cells (Gaudet et al., 2011).

Soon after injury, Schwann cells respond to the damage process first by division, then proliferation followed by subsequent cessation of myelin sheath formation (Gaudet et al., 2011). Both forms of reactive Schwann cells, reach peak proliferation around 4 days after injury and then there is a decreasing rate of division for up to 2 or 3 weeks (Navarro et al., 2007; Gaudet et al., 2011). Schwann cells respond to the damage process by rapidly dividing into daughter cells and subsequently up-regulating gene expression for molecules to support the degeneration and regeneration processes

(Osbourne, 2007). After injury Schwann cells are rapidly denervated by detachment of myelin sheaths, as a result of activation of ErbB2, tyrosine kinase receptor (Navarro et al., 2007). After division of Schwann cells and initial degradation of myelin sheaths, Schwann cells migrate to form strands within the tube of the basal lamina and these are termed bands of Büngner, to help guide the path of sprouting axons (Stoll and Müller, 1999).

During Wallerian degeneration, Schwann cell proliferation primarily occurs following loss of contact between the Schwann cell-axonal union, and later by a production of interleukin-1, cytokine (IL-1) and Tumour necrosis factor-alpha (TNF-α) that are released from infiltrating macrophages to induce axon disintegration (Ide, 1996). The reaction of the distal nerve segment to injury has been investigated in preclinical studies of peripheral nerve injury, and the axons initially swell, followed by the disintegration of its myelin sheath, until complete degeneration of the axon terminals occurs, with the clearance of the cytoplasmic debris taking place (Johnson et al., 2005). This process is known as anterograde degeneration of Wallerian type that occurs distal to the site of nerve injury and is facilitated by the activation of the 'axonal proteases system' (Myers et al., 2006). Following injury to a peripheral nerve, distally degenerated materials are removed by the reciprocal activity of denervated Schwann cells and recruited macrophages, which serve to create a local environment that favours neuronal axonal regeneration (Rodríguez et al., 2004).

It has been recognized that, following nerve injury the degeneration process is a slow process and severed axon segments that remain intact can conduct action potentials for a few days following a peripheral nerve injury (lag phase; approximately 24-48 hours) (Gaudet et al., 2011).

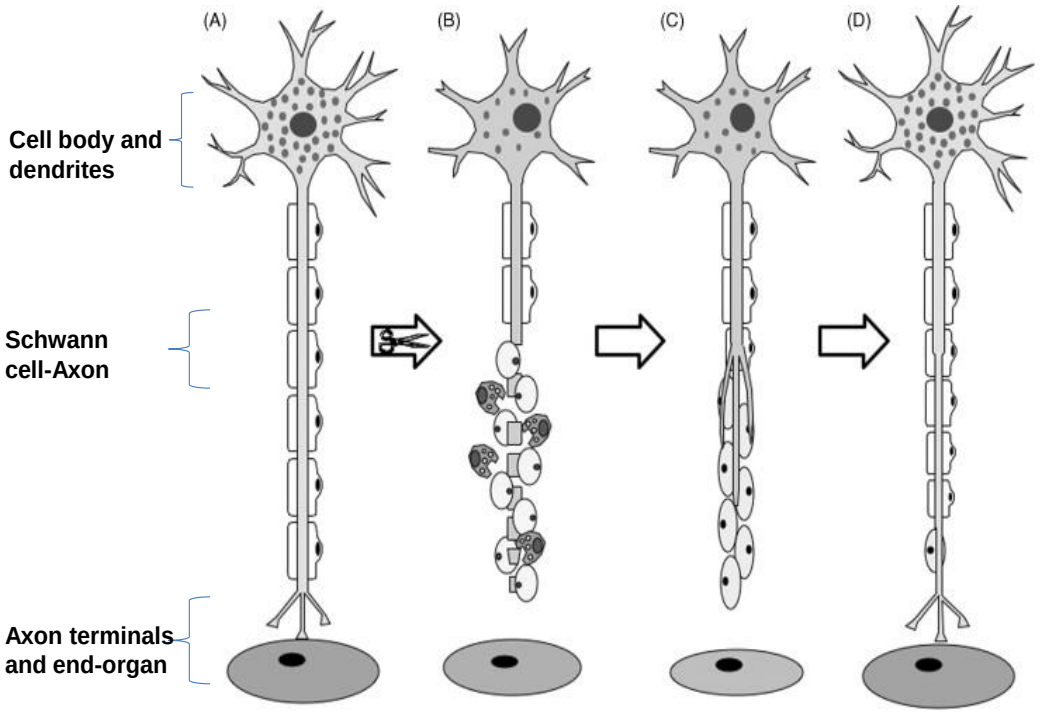

Figure 1.11: Diagram illustrates the degenerative and regenerative events of the neurone cell after peripheral nerve injury. A: normal neurone cell, B: nerve injury and Wallerian degeneration, C: axonal regeneration, D: reconnection of axon and end-targets organ. (Figure reproduced with permission from John Wiley and Sons and Copyright Clearance Centre).

Response of the cell body and proximal segment to injury

As previously mentioned the most detectable early changes are associated with distal segment degeneration, with the destruction of the axon and its myelin sheath, and subsequent clearance by macrophages (Kerns, 2008). Furthermore, it is well recognized that extensive damage also occurs in the proximal portion of the injured axon, which could extend backwards from the site of injury to the first node of Ranvier (Johnson et al., 2005). Proximal changes (retrograde) may occur immediately at the first node of Ranvier next to the site of injury and show a considerable structural change within the soma (Johnson et al., 2005). Changes within the neurone cell body involve the removal of protein synthesizing organelles by action of the lysosomes and are associated with a subsequent increases in the production of cytoplasmic RNA (Johnson et al., 2005).

After axon injury, the soma usually exhibits profound alterations in structure, metabolism, and its physiological activity (phenotypic) (Grafstein, 1975). Typically, the phenotypic changes are first recognized by hypertrophy of the cell body, movement of the nucleus to the periphery of the body, and finally the dissolution of basophilic Nissl substance (ribosome clusters) from the cytoplasm “chromatolysis” (Grafstein, 1975). Collectively, chromatolysis of the soma and disorganization of the ribosome clusters are associated with an anabolic reaction which incorporates various metabolic alterations and appear soon after injury, corresponding with the initial stage of Wallerian degeneration (Fu and Gordon, 1997; Navarro et al., 2007). Metabolic changes include increased cytoplasmic RNA synthesis and increased cellular protein content while neurotransmitters and cytoskeleton proteins production is reduced (Navarro et al., 2007). A shift in the neuronal state from transmission to synthesis is essential for regeneration and survival (Kerns, 2008). Axonal transport plays a pivotal

role in intracellular movement of cellular contents such as proteins, RNA, and organelles from the axon to the soma and vice versa. One to 2 days after injury, there is a reduction in transport of transmitter-associated proteins in the neurone, but following axonal outgrowth initiation, there may be an increase in the amount and/or the rate of axonal transported protein materials (Grafstein, 1975). Meanwhile, re-establishing axonal transport does occur when changes in RNA and protein metabolism take place in response to an increased demand of the cell body to supply materials necessary for support and maintenance of the sprouting axons (Grafstein, 1975). The proximal segment response to injury has been assessed in animal based studies and histologically reveal a reduction in the diameter and the count of nerve fibres, demyelination and reduction of nerve conduction velocity in electrophysiological studies (Gunasekera et al., 2011). Furthermore, there may be a reduced expression of transcription molecules essential for regeneration such as *Jun* N-terminal kinase (JNK, c-Jun), and growth associated pretient-43 (GAP-43), and in some cases, neurone cells may undergo apoptosis and death as a consequence of the injury (Kerns, 2008).

Degenerative changes at the site of injury

Two to 3 days following injury, recruitment of haematogenous macrophages into the degenerating axon segment are thought to be directed by cytokines that are secreted by reactive Schwann cells such as monocyte chemoattractant protein 1 (MCP1) (Tofaris et al., 2002). In Wallerian degeneration, recruitment of non-neural cells such as macrophages is considered imperative in the process of regeneration in injured nerves (Gaudet et al., 2011). During the early phase of Wallerian degeneration, resident macrophages within the endoneurium, are considered prime responders to injury before the infiltration of circulating macrophages. The macrophages express

major histocompatibility molecules and complement receptor 3 and their recruitment is enhanced by the production of immune triggering substances such as antibodies and disruption of the blood-nerve barrier, within 48 hours of the injury (Gaudet et al., 2011).

It has been suggested that Schwann cells express toll-like receptors (TLRs) that act as a first line defence mechanism in the host immune response by activating different signalling cascades including transcription factors and cytokine expression both of which are important in the regeneration process of damaged peripheral nerves. TLR1 is highly upregulated after injury, and degenerated axons release endogenous TLR ligands which bind to TLRs expressed on the surface of Schwann cells, provoking an inflammatory reaction, essential for stimulating axon regeneration (Gaudet et al., 2011). Furthermore, Schwann cells produce essential trophic factors that support the progress of axon growth as well as cytokines and chemokines production to recruit other immune cells into the injured neurone to intensify the inflammatory reaction (Gaudet et al., 2011).

TNF-α, a pro-inflammatory cytokine, is also implicated in the regulation of macrophage infiltration at sites of peripheral nerve injury (Liefner et al., 2000). Liefner et al. (2000) explored the function of TNF-α during Wallerian degeneration by tracking the course of macrophages after nerve injury in control and TNF-α deficient mice. Their results revealed Wallerian degeneration and macrophage infiltration was not affected in the control group, while in TNF-α deficient mice macrophage, recruitment was impaired but without disruption of their myelin phagocytic activity.

Circulating macrophages enter the distal nerve stump between days 4 to 7 after injury and clear the axon and myelin debris within two weeks (Stoll and Müller, 1999). The

final stages of Wallerian degeneration exhibit distinct changes which include reduction of nerve fibre diameter and atrophy of the fascicles with subsequent shrinkage of the nerve trunk. This amount to a reduction of between 50 % to 60 % of the cross-sectional fascicular area (Sunderland, 1990). In third-degree injuries, the retraction of the separated nerve ends causes intra-fascicular damage proceeded by significant local reaction because of the elastic nature of the endoneurium connective tissue layer (Burnett and Zager, 2004). These injuries also lead to vascular damage which is followed by haemorrhage and oedema, which cause a severe inflammatory response. This reaction is followed by a proliferation of fibroblasts, and the formation of fibrous scar tissue which forms a disorganized growth (neuroma) of the injured segment. By 5 to 8 weeks, the process of Wallerian degeneration is usually completed, and only fragments of Schwann cells remain inside the endoneurial tube (Burnett and Zager, 2004).

1.3.3.2 Regeneration and healing of damaged neurone cell

Following peripheral nerve injury, nerve cell state switches from synthesis and transmitting to regeneration, inducing a differential regulation of various cell constituents which regulate pathways that are responsible for either neurone survival or death (Figure 1.12) (Navarro et al., 2007).

Regenerative changes of the cell body and proximal segment

Regeneration and sprouting of severed axons involves the production and supply of trophic factors that are provided by infiltrating macrophages and reactive Schwann cells, and from the local environment within the degenerated distal nerve segment (Rodríguez et al., 2004). Following peripheral nerve injury, myelin sheet removal by

Schwann cells and macrophages help down-regulate regeneration-inhibiting factors including glycoprotein (Navarro et al., 2007).

In severe types of peripheral nerve injury, axonal regeneration begins when Wallerian degeneration has regressed, but in mild nerve injuries the degeneration and regeneration processes occurs simultaneously (Burnett and Zager, 2004). The period of nerve regeneration and healing may persist for several months following injury. However, the earliest signs of regeneration observed in the nerve cell body is the reversal of chromatolysis, centralisation of the nucleus and subsequent restoration of the metabolic functions towards transmission state (Burnett and Zager, 2004).

It has been reported that between approximately 10-30 % of sensory neurone fibres of DRG undergo apoptosis after injury of the sciatic nerve (Navarro et al., 2007). Neuronal cell death has been attributed to several factors including age, severity, and proximity of injury to the neurone's cell body (Navarro et al., 2007). It has been well recognized that after injury the reactive Schwann cells and infiltrating macrophages reciprocally release nerve growth factor (NGF). This trophic factor is conveyed to the neurone cell body by means of fast active transport to support the regeneration of the neurone (Myers et al., 2006).

In peripheral nerve injury, the presence of an intact endoneurium of the axon on either side of the injury region is imperative for successful reconnection of the nerve segments (Johnson et al., 2005). This state of regeneration is complemented by the division, proliferation and arrangement of Schwann cells which will seal the gap within the existing basal lamina-endoneurial tube (Johnson et al., 2005). In the peripheral nervous system, the endoneurium of both myelinated and non-myelinated nerve fibres is continuously covered by basal lamina which act as a natural nerve conduit following

denervation of Schwann cells (Ide, 1996). In this respect, the role of Schwann cell-basal lamina in axon regeneration aids the healing process after moderate type of nerve injury when compared to neurotmesis by acting as a ˝pseudo-conduit˝. (Johnson et al., 2005).

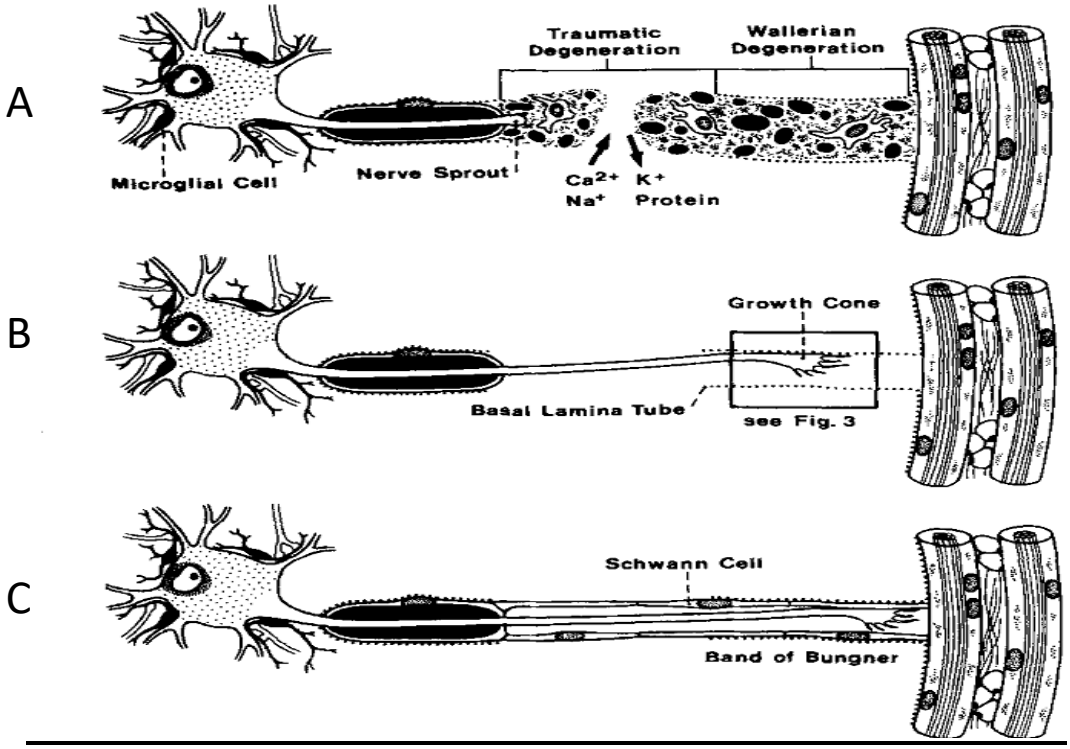

Figure 1.12: Diagram illustrates the regeneration process of severed axons. A: initial axon sprouting, B: growth cone and basal lamina-endoneurial tube formation, C: successful neurone cell regeneration and reconnection of end-targets organ. (Figure reproduced with permission from John Wiley and Sons and Copyright Clearance Centre).

Axon regrowth is initiated at the first node of Ranvier where the bands of Büngner of Schwann cells extend from the proximal axon segment into the distal stump to reach its target organs (Ide, 1996). The rate of axon growth initially is slow, but 2 to 3 days following injury, a length of about 2-3 mm per day can be achieved (Navarro et al., 2007). Schwann cells and basal lamina have been considered to play an important role in axonal regeneration by providing an essential source of trophic factors. Additionally, Schwann cell-basal lamina tubes also provides a favourable growth environment by serving as platforms for regenerating axons (Ide, 1996).

Upon successful regrowth, the regenerating axon and its associated Schwann cells form the growth cone within the endoneurial tube which extend toward the distal degenerated segment (Johnson et al., 2005). The tip of the axon growth cone exhibits specialized guiding actin filaments (filo-podia) that adhere to the Schwann cell-basal lamina and are responsible for regulating the sprouts pathways (Burnett and Zager, 2004).

The growth process sometimes continues over a prolonged period of time even if functional recovery is unlikely and form abnormal growth (Johnson et al., 2005). The lack of appropriate guidance during regeneration, causes sprouting axons to make a tortuous path, with the formation of an abnormal mass or neuroma that is composed of a mixture of immature axons and fibrous connective tissue (Navarro et al., 2007). Myelination by Schwann cells will resume when the axon successfully establishes reinnervation of its intended targets (Johnson et al., 2005). It has been shown that Schwann cells also express laminin, cell adhesion molecule, on the plasma membrane surface, to enhance axon regeneration within the growth cone (Ide 1996; Gaudet et al., 2011). Laminin is upregulated after injury and acts directly on the Schwann cell basal lamina and its associated axon by binding integrin receptors to promote

adhesion to the actin cytoskeleton network within the growth cone (Gaudet et al., 2011). In peripheral nerve injury, however, the blockage of laminin subunit has been shown to inhibit the regeneration of the axons (Gaudet et al., 2011).

Regenerative changes of the injury site and distal segment

It has been postulated that intracellular signals that are responsible for initiation of the regeneration process act at differential time periods which follows a sequence of actions to support and maintain the sprouting and healing of the severed axons (Navarro et al., 2007). In acute states, reactive Schwann cells upregulate gene expression of the trophic factors, and GAP-43, which are delivered to the axon growth cone over a period of several days after injury to promote axonal ingrowth (Fawcett and Keynes, 1990; Hall, 2001). However, expression of these factors is reduced upon successful reinnervation and Schwann cells revert their interaction with the axon (Hall, 2001).

Following peripheral nerve injury, opening of the voltage-gated ions channels with a rapid influx of calcium and sodium ions within the axoplasm causes a hyper-excitability state, and this generates action potentials that are transmitted to reach the cell body. As a result, this electrical response promotes inflow of calcium ions which activates mitogen-activated protein kinase (MAPK) and subsequent release of glutamate and brain-derived neurotrophic factor (BDNF) centrally (Navarro et al., 2007). These protein kinase cascades participate in the retrograde axoplasmic transport which help support and maintain the regeneration process.

Schwann cells express NGF and NGF receptors on their surfaces which guide sprouting axons within the basal lamina tubes. However, upregulation of NGF–TrkA signalling has been linked with the development of neuropathic pain (Myers et al.,

2006). In addition, macrophages release IL-1, a cytokine that promotes expression of NGF in Schwann cells to stimulate the process of regeneration (Brown et al., 1991).

It has long been recognized that abnormal regeneration and subsequent impairment of functional recovery may occur due to failed selectivity of sensory and motor sprouting axons to establish appropriate target reinnervation (Navarro et al., 2007). As a result, this impaired maturation leads to reduction of the axon diameter, and ultimately neuron atrophy.

Successful regeneration of the severed axons depends on the intrinsic capacity of neurone cells to withstand the effect of injury and ability to change from transmitter to regenerative state (Navarro et al., 2007). In severe nerve injury however, the intense inflammatory reaction, fibroblast proliferation and subsequent fibrous scar formation complicate the regeneration process of severed axons, resulting in the formation of neuroma (Osbourne, 2007).

1.3.3.3 Expression of cell-signalling molecules and factors

It is generally agreed that axon damage after nerve injury creates intracellular signals that are responsible for the activation of a number of signalling cascades of several gene expressions within the neurone that may lead to either cell body death or survival and subsequent regeneration (Navarro et al., 2007). In response to injury, the neurone also relies on neurotrophic support for survival and maintenance of its regeneration. As previously mentioned, degeneration of the distal nerve segment is considered to act as a suitable permissive environment for growth of severed axons by providing essential neurotrophic factors (Ide, 1996). Among these neurotrophic factors are neurotrophins (BDNF and NGF), and pro-inflammatory cytokines (TGF-β, IL, IL6, LIF).

Expression of neurotrophic factors in peripheral nerve injury

In uninjured neurones, trophic factors are produced in the end-target organs, and carried to the cell body by way of retrograde axonal transport (Ide, 1996). It has been proposed that interruption of such established harmonious interactions of axons with the cell body by injury causes Schwann cell activation, and subsequently, the production of NGF and BDNF which spread diffusely in a gradient manner around sprouting axons (Ide, 1996). Therefore, a reduced expression of trophic factors reaching the cell body due to axonal disruption is considered a molecular signal which triggers the regeneration process in peripheral nerve injury (Burnett and Zager, 2004).

NGF is considered a key neurotrophic factor which play a major role in peripheral nerve regeneration and the growth process (Burnett and Zager, 2004). NGF's role in promoting sensory axons regeneration has been of great interest for many years (Kelleher et al., 2016). NGF produced locally by Schwann cells and fibroblasts at an injury site, binds to receptors on the Schwann cell surface. Following peripheral nerve injury levels of NGF mRNA and protein increase, whereas in an intact nerve, Schwann cells expression of NGF-mRNA is low in comparison. The up-regulation of NGF by Schwann cells after injury is thought to be regulated by IL-1 released from macrophages infiltrating the nerve injury site (Ide, 1996). Subsequently if macrophage recruitment fails, myelin sheath clearance will be considerably delayed, along with a reduction of levels of NGF synthesis by Schwann cells, resulting in compromised sensory axon regeneration (Ide, 1996). A study by Brown et al. (1991) using the delayed axonal breakdown C57B1/OIa mice model, linked with slow recruitment of macrophages, reported low levels of mRNA for both NGF and its receptor that impaired the regeneration of sensory, but not motor fibres. These data provide

evidence that macrophage recruitment in peripheral nerve injury is essential for NGF synthesis and promoting axon regeneration (Brown et al., 1991).

BDNF and NGF regulate sensory neurone functions in both the central and peripheral nervous system (Meyer et al., 1992). Under normal physiological conditions NGF is produced by end-target tissues, whereas BDNF is synthesized in the CNS by glial cells and peripheral nerves. NGF and BDNF are expressed at low levels in the Schwann cells of normal intact peripheral nerves. However, several days after a peripheral nerve injury, expression levels of BDNF mRNA increase above the normal, reaching a maximum after several weeks (Meyer et al., 1992). In contrast the level of NGF mRNA, shows a biphasic expression, increasing rapidly after 6 hours and reaching a maximum 3-4 days after injury (Ide, 1996). These observations support the work of Brown et al. (1991) that suggest prolonged NGF mRNA upregulation is related to IL-1 release from macrophages at site of injury.

Expression of neuroinflammatory cytokines in peripheral nerve injury

Transforming growth factor beta (TGF-β) is a protein molecule that belongs to the complex cytokine family that are involved in regulating several physiological functions in embryogenesis, angiogenesis and wound healing (O'Kane and Ferguson, 1997). TGF-β subgroups comprises 5 isoforms (TGF-β1-5) of which, TGF-β-1, -2 and -3 are expressed in mammals and exert differential cellular effects. The diverse levels of expression of TGF-β during the wound healing process reflects different biological effects. Serin-threonine kinase is considered to be the transducing signal that activates TGF-β which binds to specific receptors R1 and R2 (O'Kane and Ferguson, 1997).

TGF-β1 has been recognised to play an important role in the wound healing process by regulating collagen production, fibroplasia and downregulation of protease enzyme (O'Kane and Ferguson, 1997). TGF-β1 is also a strong chemotactic molecule for many inflammatory cells such as fibroblasts and is also responsible for mediating expression of other TGF-β types (O'Kane and Ferguson, 1997). TGF-β1 is expressed in all tissues and cells while TGF-β2 is found mostly in saliva, amniotic fluid, and breast milk. However, TGF-β3 is scarce in both body fluids and tissues (O'Kane and Ferguson, 1997).

Fibrosis and scar formation, both of which hinder the healing process, have been attributed to the upregulated levels of TGF-β-1 and -2, while the expression of TGF-β-3 associated with reduced scar formation at the site of nerve injury (Ferguson and O'Kane, 2004; Atkins et al., 2006). Moreover, TGF-β-1 upregulation has been implicated in scarring of the epineurium due to collagen type-1 deposition that is produced by infiltration of fibroblasts at the site of injury (Nath et al., 1998; Atkins et al., 2006). In injured sciatic nerves, exogenous application of anti-TGF-β antibodies was associated with a reduction of fibroblast recruitment and, subsequently a reduction in overall transduction signals for collagen deposition and this reduces scar tissue formation (Nath et al., 1998).

IL-1 protein is a pro-inflammatory cytokine expressed by macrophages in the peripheral nervous system (Thacker et al., 2007). Immediately after nerve injury mRNA levels of IL-1 are elevated and persists at higher levels for several days (Thacker et al., 2007). In addition, IL-1 is considered to play important role in nerve regeneration, by stimulating the synthesis of NGF by activating Schwann cell production (Ide, 1996).

LIF and IL-6 are two other important pro-inflammatory cytokines, that are upregulated following nerve injury (Tofaris et al., 2002). The source of LIF is still not known but “autocrine circuits” regulated by Schwann cells have been attributed to play a part in macrophage recruitment. After injury, Schwann cell and microglial cells play a role in orchestration of the cellular responses and regeneration of damaged neurons by producing IL-6 (Galiano, M et al. 2001; Tofaris, G.K et al.2002). IL-6 indirectly regulate LIF, and MCP-1 pathways, which regulate entry of macrophages and lymphocytes to the injured nerves (Galiano, M et al. 2001; Tofaris, G.K et al.2002).

1.3.4 Neuropathic pain development in response to peripheral nerve injury

The expression patterns of specific regulatory factors such as pro-inflammatory cytokines or alteration of ion channels and glial activation have been implicated in the increased nociception of neurones following peripheral nerve injury and associated neuropathic pain. (Navarro et al., 2007, Mika et al., 2008).

Role of sodium and potassium ion channels in the development of neuropathic pain

Nerve injury can alter the excitation patterns of sodium and potassium ion channels following an increase in their density along the axoplasm, by focal accumulation of vesicles containing ion channel proteins which are predominately found in neuroma tissues (Rasband et al. 2001; Navarro et al., 2007; Theile and Cummins, 2011). It has been proposed that the DRG of primary sensory neurones potentiate the development of neuropathic pain by upregulation of some ion channels (Na v1.3, K v1.1, K v1.3) while the expression of other channels (Na v1.1, Na v1.2, K v1.2, K v2.1) are reduced (Navarro et al., 2007). Following nerve injury, the altered electrical excitation of DRG and maintenance of hyper excitable severed afferent fibres has been attributed to

changes in the expression pattern of sodium and potassium ion channels (Rasband et al. 2001; Navarro et al., 2007; Theile and Cummins, 2011) (Table 1.1).

Table 1.1: Ion channels implicated in neuropathic pain following peripheral nerve injury

Ion channels	subtype	Tissue expression	Role in pain
Sodium ion channels	Na v1.1	CNS, PNS	Neuropathic pain
	Na v1.2	CNS, embryonic PNS	Neuropathic and inflammatory pain
	Na v1.3	CNS, embryonic PNS	Neuropathic and inflammatory pain
	Na v1.7	PNS; sympathetic and sensory neurones	Neuropathic; inflammatory pain
	Na v1.8	PNS; small diameters peripheral neurones	Neuropathic; inflammatory pain; mediate tingling sensation
	Na v1.9	PNS	inflammatory pain
Potassium ion channels	K v1.1 and 1.4	PNS; small diameter neurones	Acute nociception
	K v1.2 and 1.3	PNS; Large diameter neurones	Mechanoreception and proprioception
	K v9.1	Large diameter myelinated spinal neurones	Initiate ectopic electrical activity
CNS: central nervous system; PNS: peripheral nervous system			

Sodium ion channels play a key role in the propagation of noxious signals along nerve fibres towards CNS, and recent research has implicated some sodium ion channels with specific types of neuropathic pain in human and transgenic mice (Liu and Wood, 2011; Bird et al., 2013). Increased expression of Na v1.8 channels have been described in human lingual nerve neuromas and correlated significantly with tingling sensation following iatrogenic trauma of the lingual nerve during the surgical extraction of lower wisdom teeth (Bird et al., 2013). Moreover, neurones excitability which enhance neuropathic pain state following peripheral nerve injury has been reduced by blockage of these channels (Liu and Wood, 2011). In humans, the expression of sodium ion channels is variable. Sodium channels that are preferentially expressed in the peripheral nervous system include Na v1.7, 1.8 and 1.9. Na v1.7 channels are expressed in sympathetic and sensory neurones, whereas Nav1.8 presents only in small diameter peripheral sensory neurones (Navarro et al., 2007; Liu and Wood, 2011). It has been shown that Na v1.8 channels have the ability to retain and transmit nociception of cold temperature while Na v1.9 channels are implicated in the increased sensitivity of inflammatory pain. In damaged neurones expression of Na v1.8 mRNA and protein is reduced following peripheral nerve injury (Liu and Wood, 2011). This may be in response to the production of neuro-inflammatory cytokines during the degeneration process (Dib-Hajj et al., 2010).

Ruangsri et al. (2011) studied the expression of Na v1.8 mRNA in the sciatic nerve entrapment (SNE) model of painful neuropathy in rats. Na v1.8 shRNA vector (cationized gelatine/plasmid DNA polyplex) was injected subcutaneously into the rat hind paw. After 3–4 days Na v1.8 shRNA attenuated the SNE-induced pain behaviour and continued over 4–6 days before returning to its basic levels. In pain behavioural testing knockdown of Na v1.8 mRNA showed alleviation only in the injured nerve, but

not in the DRG, possibly due to unaffected transcription of the Scn10a gene encoding Na v1.8 (Ruangsri et al., 2011). Based on these results it would appear peripheral inhibition of Na v1.8 expression decreases mechanical allodynia and thermal hyperalgesia. The authors concluded that painful neuropathy is caused by the upregulation of Na v1.8 and axonal accumulation of Na v1.8 mRNA protein following nerve injury (Ruangsri et al., 2011).

The nociceptive pathway contributing to the hyper excitability state in myelinated sensory neurones still remains unknown (Tsantoulas et al., 2012). K v9.1 a potassium channel is selectively expressed in large-diameter myelinated sensory neurones following spinal nerve transection (L5), and its down regulation after injury has been correlated with the initiation of ectopic electrical activity and neuropathic pain development (Tsantoulas et al., 2012).

Role of immune mediators and immune cells in development of neuropathic pain

After disruption of the neurone membrane, the local environments in Wallerian degeneration, and release of inflammatory cytokines are believed to alter the neurone cell function which can sensitise nociceptive fibres to noxious stimuli (Zuo et al., 2003). Resident endoneurial mast cells are considered the prime initiator of natural immunity following peripheral nerve injury (Thacker et al., 2007). However, infiltration of mast cells at the site of nerve injury is usually followed by their degranulation and subsequent production of histamine and protease enzymes (Thacker et al., 2007). It has been shown that neural histamine receptors are expressed at high levels in sciatic nerve crush injury models where histamine mediators induce pain by sensitising

nociceptive nerve fibres to non-noxious stimuli thus initiating the development of neuropathic pain (Thacker et al., 2007). Hence, the activation of mast cells in injured peripheral nerves to play a key in initiating an inflammatory response which later leads to the development of neuropathic pain (Zuo et al., 2003). However, mast cell stabilisation with sodium cromoglycate has been shown to reduce infiltration of neutrophils and monocyte to the injury region, and suppressed the development of hyperalgesia. Moreover, blocking of histamine action by application of anti-histamine receptors drugs has been shown to alleviate pain-related behaviours (Zuo et al., 2003).

Neutrophils are the second dominant immune cells in innate immunity that invade nerve tissue within a short period of time after injury where they exert their phagocytic activity and release inflammatory mediators after degranulation (Thacker et al., 2007). Neutrophils are considered to be another major source for various pro-inflammatory cytokines (IL-1 and TNF-α) and chemokine (IL-8) production which enhance neutrophils to express endothelial adhesion molecules, and subsequently enhance degranulation of themselves and produce cytotoxic substance (Thacker et al., 2007).

Intact nerves normally are devoid of neutrophils but, after injury a significant number of neutrophils invade the site of damage in the endoneurium (Perkins and Tracey, 2000). Perkins and Tracey (2000) investigated neutrophil distribution and their contribution to hyperalgesia in a ligation injury model of a rat's sciatic nerve. The study involved administration of a neutrophil cytotoxic antibody, and their results indicated that a greater number of neutrophils infiltrated the endoneurium at the site of injury when compared to the sham-nerve, which coincided with the development of acute hyperalgesia up to 7 days post-injury. Neutrophil depletion at the time of nerve damage was associated with significant attenuation of hyperalgesia but, late depletion of the cells did not relieve chronic hyperalgesia. Authors advocated that neutrophil

recruitment at the site of nerve injury plays a significant part in the development of neuropathic pain in peripheral nerve injury (Perkins and Tracey, 2000).

Lymphocytes; T cells and natural killer cells play role in the development of neuropathic pain following peripheral nerve injury (Moalem and Yu, 2004; Thacker et al., 2007). They infiltrate the site of nerve injury and their upregulation has been shown to associated to be with thermal and mechanical allodynia/ hyperalgesia in several rodent models of nerve injury (Moalem and Yu, 2004; Thacker et al., 2007). The T-Lymphocytes cell divided into Type 1 and Type 2 according to its cytokine expression profile. Type 1 helper T cells produce proinflammatory cytokines (IFN-γ and TNF-α) which increases nociception while, Type 2 helper T cells produce anti-inflammatory cytokines (IL-10) associated with a modest reduction of pain sensitivity following nerve injury (Moalem and Yu, 2004; Thacker et al., 2007).

Role of glial cells in development of neuropathic pain

It has been generally agreed that peripheral nerve injury is associated with an increased density and infiltration of microglial cells in the sensory regions of the superficial and deep laminae I and II of the spinal dorsal horn region (Eriksson et al.,1993; Taves et al., 2013) (see chapter 1; section 1.2.4; Figure 1.5). Several immunohistochemical studies using specific microglial markers to investigate cellular immunoreactivity in different sensory territories in response to peripheral nerve injuries have been undertaken. These studies highlight the specific response of microglial cells in the dorsal horn after nerve injury which are characterized by their proliferation and upregulation of OX-42 pan- microglial markers. In addition, signals responsible for microglial cells reaction are suggested to act quickly, which convey sensory information to the corresponding sensory ganglionic cell bodies and then onward to central projection neurones (Eriksson et al.,1993; Taves et al., 2013). It is also

proposed that the time course for the response of microglial reaction in sensory projection zones is similar in damaged axons that travel either in sensory or motor pathways.

Within the CNS microglia represents approximately 10–20 % of all resident cells and their distribution largely homogenous in different regions, including the spinal cord (Taves et al., 2013). In their typical resting state microglia exhibit a ramified shape with fine radiating processes (Figure 1.13). However, after nerve injury their morphology changes and is described as an amoeboid shape in which the cells stoma becomes large and their projecting processes prolonged and less ramified (Eriksson et al., 1993).

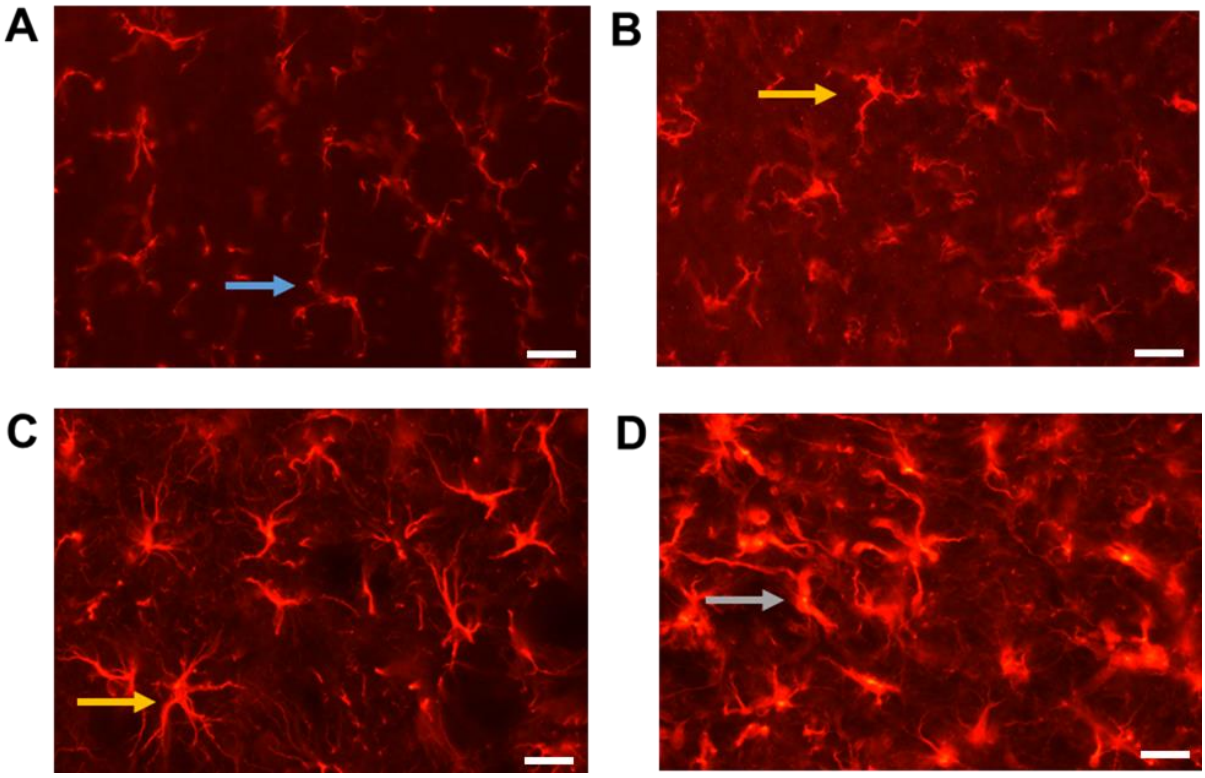

Figure 1.13: Sections of spinal cord after immunohistocal staining with antibody Iba-1 microglial marker showing three different morphological phenotypes of microglial cells. A: The ramified microglia: normal-appearing body with long, thin and radially projecting processes (Blue arrow). B and C: Spinal cords following peripheral nerve injury and repair showing hypertrophied microglia: enlarged body with shorter, thicker processes (Yellow arrows), D: Showing amoeboid microglia: bigger and densely stained body with much fewer processes (Grey arrow). Scale bar = 25 µm.

Neural plasticity and pain hypersensitivity in spinal neurones due to peripheral and central sensitization is widely believed to be mediated by the activity of glial cells (Scholz and Woolf, 2007; Mika et al., 2013).

The sensory input that contributes to the chronic pain state in the spinal cord dorsal horn largely rely on lamina I and II neurones which receive input from primary afferents neurons and convey nociceptive information to projection neurons that ascend to the brain (Mika et al., 2013; Taves et al., 2013). It is believed that following peripheral nerve injury, spinal neurons undergo marked plasticity, and as a result leads to hyper excitability of the projections neurons within the dorsal horn which then induce chronic pain states (Scholz and Woolf, 2007; Mika et al., 2013).

In several preclinical models of peripheral neuropathies microglial cell activation in the dorsal horn after nerve injury, is typically marked by increased proliferation, increased infiltration, and alterations of their morphology (amoeboid active state) (Scholz and Woolf, 2007; Mika et al., 2013; Taves et al., 2013). Furthermore, microglial reaction is also characterized by the production and secretion of a range of pro-inflammatory cytokines that potentially trigger initiation of excitability of injured and non-injured nerves and result in maintenance of increased pain hypersensitivity. Beggs and Salter (2007) investigated the distribution pattern of spinal microglial activation in response to peripheral nerve injury. Their analysis showed a significant increase in microglial counts and the majority of sensory zones mapped to peripherally damaged primary afferent nerve fibres. However, some microglial cell reactivity was also seen in the sensory projections of the intact nerve within the spinal cord. Consequently, the authors proposed that this contributes to neuronal excitability and enhance nociceptive transmission which underlie neuropathic pain behaviours following nerve injury (Beggs and Salter, 2007).

Immunohistochemical studies by Eriksson et al. (1993) examined the microglial response in sensory areas of the spinal dorsal horn after sectioning of the sciatic nerve. Both the qualitative and quantitative analysis of images showed high microglial immunoreactivity with upregulation of OX-42 marker after 24 hours of sciatic nerve injury in the deep laminae of the dorsal horn with less activity of microglia in the superficial laminae in the L4 region. Thereafter, expression levels of OX-42 peaked at day seven, which then declined slowly over different survival periods when animals were culled. Qualitative image analysis in L1 and L4 regions showed similar patterns of distribution of small cells with extensive branching throughout the spinal cord immediately after injury which indicates rapid microglial cell response to sciatic nerve injury (Eriksson et al., 1993).

There is also growing evidence that Mitogen activated protein kinases (MAPKs), a protein kinase, play an essential role in chronic pain processing by acting through a variety of coordinated intracellular signal transduction mechanism which mediate cellular responses that allow cells to respond to multiple and divergent inputs. (White et al., 2011; Hansen and Malcangio, 2013). Therefore, the process of activation of the JNK. c-JNK (JNK) pathway is the major pathway via spinal astrocytes has the potential to contribute to chronic pain states through phosphorylation of several substrates, including transcription factors, and proteins, and thus directly affects a broad range of cellular responses (White et al., 2011; Hansen and Malcangio, 2013). However, it is acknowledged that the JNK pathway in included in a large number of cellular activities including that relating to pain.

Given the findings from the peripheral nerve injury models reviewed, clearly, targeting immune inflammatory profile would be logical approaches to prevent neuropathic pain development (Sommer et al., 1999; Schäfers et al., 2001; Nadeau et al., 2011). Early

evidence from preclinical trials also suggests that some of the agents used to reduce inflammation on the basis of its potent anti-inflammatory action show promising results, but the necessary use of special equipment or implantation of pumps subcutaneously for continuous drug delivery showed no advantage over single administration (Sommer and Kress, 2004, George et al., 2004). Moreover, these agents also raised concerns in relation to the suppression of the immune-inflammation process at the site of nerve injury which may impair regeneration following repair in the peripheral nerve or spinal cord.

Role of inflammatory cytokines in in development of neuropathic pain

Pro-inflammatory cytokines (TNF-α, IL-1, and IL-6) and anti-inflammatory IL-10 that are produced and released by the different immune cells following peripheral nerve injury are considered the key regulatory molecules of initiation and maintenance of neuropathic pain (Thacker et al., 2007). However, the mechanism of action of these cytokine molecules in peripheral nerve injury is still not fully understood and it has been proposed that cytokines alter the physiological coordination's of neurone cells either by direct action on primary sensory fibres, or indirectly by activation of signalling cascades in neuro-immune pathways (Thacker et al., 2007).

IL-1 is a potent pro-inflammatory cytokine that is released from macrophages and Schwann cells following peripheral nerve injury (Dinarello, 1988). IL-1 mRNA is significantly upregulated following nerve injury and is recognised to be strongly associated with pain-related behaviours in peripheral neuropathy (Marchand et al., 2005). The mechanism of action of IL-1 is not fully understood but postulated to be linked to the complex signalling pathways that cause direct excitation of nociceptive nerve fibres and increase their response to painful stimuli following release of

inflammatory mediators (nitric oxide, COX2 and prostaglandins) in peripheral nerve injury (Marchand et al., 2005). Furthermore, peripheral administration of IL-1 has been acknowledged to play a vital role in sensitization of polymodal receptors to painful stimuli which contribute to the development of cutaneous hyperalgesia (Fukuoka et al., 1994). Moreover, in vivo studies have demonstrated a reduction of pain-associated behaviours and attenuation of hyperalgesia following application of IL-1 receptor antagonist (IL-1ra) in neuropathy model of rodent sciatic nerves (Sommer et al., 1999; Schäfers et al., 2001).

It has been suggested that injury-induced neuropathic pain attributed to changes in TNF-α protein levels may be related to the local inflammatory reaction induced by injury around the nerve (George et al., 2004). George et al. (2004) used enzyme-linked immunoassay and immunohistochemistry to monitor changes of TNF-α protein level in a crush injury model. Data from their study showed a rapid rise in TNF-α levels with a two-fold increase after 12 hours, which remained elevated on day 3 and then returned to a baseline value 14 day after injury. Immunohistochemistry studies revealed, after 3 days, strong TNF-α -immunoreactivity in all epineurial macrophages and fewer endoneurium macrophages. Pain behavioural analysis revealed transient by reduced sensitivity to painful stimuli such as heat (hypoalgesia) and mechanical stimuli (hypoesthesia) followed by development of heat hyperalgesia and mechanical allodynia by day 10 after injury. However, they assumed that, the early and transient increase of TNF-α protein level may correspond with the onset of pain-associated behaviour in nerve injury (George et al., 2004).

Following peripheral nerve injury, TNF-α is rapidly upregulated and is believed to promote axonal degeneration, macrophage recruitment, and induce ectopic neuronal activity during Wallerian degeneration by binding and triggering two tumour necrosis

factor-α receptors TNFRs (George et al., 2005). Immunohistochemistry studies have reported the expression of TNFR1 and TNFR2 on normal Schwann cells, and along nerve axons and in DRG neurones following injury. The TNFR1 binds favourably to soluble TNF-α whereas TNFR2 binds to membrane-bound TNF-α molecules, and both elicit different effects (George et al., 2005). George et al. (2005) studied the differential level of TNFR1 and TNFR2 protein using ELISA following chronic constriction or crush injury of mice sciatic nerves. TNF-α protein levels peaked early and transiently after injury. However, TNF-α receptors were detected at a low level in uninjured nerves or sham-controls. TNFR1 level increased 2-fold on days 3 and 7 after injury whereas, TNFR2 was expressed at high levels from day 1 and increased 7- fold on days 3 and 7 after injury. These data indicate that endoneurial TNF-α receptors proteins are differentially regulated during peripheral nerve injury. The authors speculated that the increased TNFR1 level paralleled to the development of pain-related behaviour at early stage of nerve injury. In addition, TNFR2 levels remained elevated for 4 weeks after injury which corresponds to the period of nerve regeneration, and it is proposed that TNFR2 could act as an endogenous TNF antagonist (George et al., 2005).

IL-10 is a major anti-inflammatory cytokine that is produced by a variety of immune cells including T-lymphocytes, macrophages and natural killer cells (de Waal Malefyt et al., 1992; Wagner et al., 1998). In humans, IL-10 is produced by type II T helper cells (Th2) (de Waal Malefyt et al., 1992). It is considered to be a strong inhibitory cytokine molecule that has auto regulatory effects by down regulating the class II major histocompatibility (MHC) antigens reaction, which inhibit macrophage antigen presentation that are mediated by Interferon-γ, TNF-α and IL-1 (de Waal Malefyt et al., 1992).

Immediately after nerve injury, expression of IL-10 increases rapidly and remains elevated for up to 4 weeks, which may reduce inflammatory cytokine release by immune cells (Taskinen et al., 2000). However, Wagner et al. (1998) proposed that IL-10 may be implicated in suppression of intracellular signalling involved in the pro-inflammatory cytokine production pathway by macrophages, and moreover, its peripheral administration at the site of injury would potentially reduce endogenous TNF-α protein expression and subsequently prevent development of neuropathic pain. Their experiment involved intraneurial injection of IL-10 (250 ng) in a CCI model of neuropathy in rat sciatic nerves and shown to exert significant anti-inflammatory and analgesic effects by attenuating thermal hyperalgesia and reducing macrophage immune reactivity, thus suggesting IL-10 diminishes the inflammatory response and nociception of sensory neurones by interfering with TNF-α expression after nerve injury.

It has been suggested that ectopic electrical activity contributes to the onset of neuropathic pain through upregulation of sodium ion channels and TNF-α protein in DRG neurones in peripheral nerve injuries (Shen et al., 2013). Shen et al (2013) identified expression of IL-10 receptor 1 (IL-10R1) in DRG neurones and proposed its role in blocking sodium channels activity could prevent neurone excitation and alleviate neuropathic pain. The experiment involved spinal ligation (L5) model of nerve injury and intrathecal injection of recombinant rat IL-10 (500 ng). Their results showed diminished excitation of DRG neurones and subsequent relief of mechanical allodynia seven days after spinal ligation. In vitro study using recombinant rat IL-10 (200 pg/ml), applied to cultured neurone tissues demonstrated reduction of levels of Nav1.6 and Na v1.8, while TNF-α application up-regulated level of Na v1.6 and Na v1.8 in DRG neurones.

Immune modulation and the targeting of pro-inflammatory cytokines by the application of neutralized antibodies and receptor blockers at time of nerve repair may influence signalling regulatory molecules that are responsible for development of neuropathic pain.

1.4 Therapeutic approaches to enhance regeneration and functional recovery of peripheral nerves after injury

Over the past decade, scientific research has provided substantial knowledge regarding the degeneration and consequent regeneration process of peripheral nerves in response to injury, but much still remains unknown about the complex interaction between the immune and neuronal systems. Recent research has focussed on promoting the regeneration of severed nerves by targeting specific signalling cascades without compromising other important stages of the healing process, critical for nerve repair (Vidal et al., 2013). After injury, the intrinsic capacity of damaged axons to regrow and attain functional recovery is completely dependent on the site and type of injury, and distance over which the axon must regenerate to cross the injury site (Rodríguez et al., 2004). Once nerve damage is established, the severity and type of injury will determine the necessity for surgical nerve repair, and the outcome of recovery of nerve function. In severe types of injury (neurotmesis), axons have a restricted ability to grow and cross the distance of the injury site. Furthermore, if the damaged nerve is left untreated or its repair delayed, neuroma formation will occur (Rodríguez et al., 2004).

Numerous emerging strategies have been proposed to enhance functional regeneration and recovery of severed axons (Rodríguez et al., 2004). These strategies include; surgical repair and nerve grafting procedures, biologically engineered materials (conduits), and more recently locally applied therapeutic agents (Rodríguez et al., 2004). The principal objective of surgical procedures is to achieve reinnervation of intended targets by guiding regenerating axons into the distal segment without further damage to the residual intact fibres at the site of nerve injury (De Albornoz et al., 2011). The success of surgical repair of damaged nerve tissue has been attributed to the type of injury and the proper alignments of nerve fibres at the time of repair (Stefano et al., 2013). Epineurial suturing is the most widely preferred method and permits axon regeneration by approximating individual fascicle of nerve fibres. This method involves direct end to end repair when there is a short gap and both segments of severed nerve can be approximated without undue tension (Rodríguez et al., 2004). If the nerve defect is too long and does not permit tissue repair, an autologous nerve graft can be used. This type of nerve grafting procedure is infrequently used due to the restricted availability and morbidity associated with donor nerve tissue (Stefano et al., 2013). Over the last decade, due to the inherent complications that are associated with nerve grafts, research has focussed on developing novel biologically engineered tissues or materials that could functionally substitute autogenous nerve (Johnson et al., 2005). Conduits are synthetic tube-like channels designed to guide sprouting axons from the regenerating proximal segment to their intended targets and prevent infiltration of fibrous tissue which impedes nerve regeneration (Johnson et al., 2005). Advances in tissue engineering research has been dedicated to produce conduits with biological properties that are similar to natural healing environments, without compromising the regeneration process of axons

(Stefano et al., 2013). A conduit should act as a suitable environment for regeneration by combining biocompatibility and appropriate scaffolding for axon extension and promotion of Schwann cell adhesion and proliferation. It has been documented that nerve regeneration through non-degradable conduit materials elicit chronic inflammatory reaction, but recent tissue engineering introducing a biodegradable conduit based materials such as collagen, poly-glycolic acid, poly-lactic acid, or polyesters which would degrade within reasonable time along with the regeneration process (Li et al., 2014).

As previously discussed, peripheral nerve injury that produces retrograde degeneration extending backwards to involve the corresponding cell body are usually associated with a delayed regeneration process, and recovery may be slow and often incomplete (De Albornoz et al., 2011). Therefore, various conservative treatment modalities have been advocated in addition to the surgical repair, such as electrical nerve stimulation and laser phototherapy to promote the functional recovery. Applications of low frequency electrical stimulation at the time of nerve repair have the potential to stimulate rapid nerve regeneration, and preliminary data have shown that improvements in muscle innervation and increased axonal sprouting occur when this therapy is combined with physical exercise in animal models (De Albornoz et al., 2011). Recently, laser phototherapy application of low intensity has been proposed to enhance recovery of repaired nerves and reduce muscle atrophy. Considered a non-invasive approach with few side effects, this treatment approach is still evolving and its role in promoting nerve regeneration is undetermined due to a variation in reported outcomes, and the lack of high quality clinical trials (De Albornoz et al., 2011).

After an injury the success of functional nerve regeneration is complex and depends on the local environments that surround the regenerating axons (Vidal et al., 2013).

Axon growth may be prevented due to the presence of inhibiting factors or due to scar formation that arises secondary to the intense inflammatory reaction after injury. Consequently, the immune-inflammatory reaction initiates the production of inflammatory cytokines that exert inhibitory and stimulatory effects mediated through several intracellular signalling pathways which permits them to regulate various cellular activities during the healing process of regenerating axons (Vidal et al., 2013). Therefore, one therapeutic strategy involves different experimental modes of drug delivery after nerve repair to enhance the functional regeneration and accelerate recovery of nerve function.

1.4.1 The role of artificially engineered materials (conduit) implantation in peripheral nerve injury

Over the past few years, the interest of nerve conduit guidance (NCG) has increased as an alternative procedure to the standard nerve repair which obviates the need for nerve graft in many cases of nerve injury, with promising results (Wood and Mackinnon, 2015). During nerve repair, tensionless reconstructing of the defect due to tissue loss is not always possible (Johnson et al., 2005; Wood and Mackinnon 2015). Hence, conduit bridging material provides structural support to guide axonal regeneration. An ideal NCG will bridge the gap and simulate nerve architecture as naturally as possible. In addition, these new replacement materials could be utilised to carry therapeutic agents to increase neuron survival and improve nerve growth (Allodi et al., 2012; Wood and Mackinnon, 2015). NCG can provide tubular guidance which help nerve tissue regeneration within the gap between proximal and distal nerve stumps. Within this tubular structure the fibrin clots also act as the initial intrinsic platform that supports the surface ingrowth of the Schwann cells (Allodi et al., 2012).

Regeneration of damaged nerve fibres is often incomplete whether using autograft or conduits (Johnson et al., 2005). This suboptimal outcome has been attributed to cell body apoptosis, fibrosis, or inherent delay in growth of axons to the distal segment. Therefore, to enhance axonal regeneration several experiments have investigated the application of anti-inflammatory cytokines to overcome this problem with the use of synthetic or natural repair in peripheral nerve injury (Johnson et al., 2005; Allodi et al., 2012).

Currently, the technology relating to nerve tissue engineering aims to produce a novel NCG that can promote neural regrowth and protect regenerating axons (Johnson et al., 2005; Nan et al., 2012; Wood and Mackinnon 2015). In addition, the biological and physiochemical properties have been experimentally investigated to support cells adhesions and preserve the viability of neuronal cells.

There are several types of NCG materials that have been globally licenced for repair of peripheral nerve injury including biological and synthetic nerve guidance (Johnson and Soucacos, 2008; Nan et al., 2012). The synthetic NCG is based on polymer substances and this type include lactate polymer, polyethylene and silicone polymer whereas the biological alternatives included arterial and, veins grafts and autologous collagen. These options for peripheral nerve repair are based on their ability to support direct axon growth from the regenerating segment and provide an essential permissive growth environment and prevent fibrous tissue invasion (Johnson et al., 2005; Wood and Mackinnon, 2015). As a result, several studies on nerve conduit materials have addressed several important factors such as biocompatibility (degradation rate and cells viability), mechanical properties, (thickness wall and intraluminal support), flexibility and ease of manipulation (Nan et al., 2012). NCG based- biodegradable polymer also provides the advantage of slow degradation rate and, this avoid removal

once functional regeneration and recovery has been established (Deumens et al., 2010).

The following section will review poly-glycolic acid (PGA), poly-ethylene glycol (PEG) and poly-caprolactone (PCL) use as NCG in field of peripheral nerve repair.

Several preclinical studies have been conducted investigating synthetic biodegradable polymer materials in animal models of peripheral nerve injury. More recently, researchers have been focusing on the manipulation of the internal environment of NCG which is believed to have a profound effect on the neuronal regeneration process (Johnson and Soucacos, 2008; Wood and Mackinnon, 2015). Pateman et al. (2015) assessed poly-acrylate ethylene glycol (PEG) biocompatibility when produced as a 3-dimensional structure by microstereolithography. In their study, thy-1-YFP transgenic mice were used for expression of fluorescent proteins that can enable axon labelling and assessment of axons regeneration across the site of nerve injury and repair. In mice the right common fibular nerves were cut to create a 3 mm gap and then repaired with either PEG conduit (diameter 1 mm, length 5 mmm and wall thickness 250 μm) or nerve graft. The animals were then allowed to recover for three weeks (Pateman et al., 2015).

In both repair groups, axons had frequent disorganised pattern of growth at the join of the proximal segment with the graft or PEG conduit when compared to the distal edge. Furthermore, their result did not show any differences in axonal sprouting between the repair groups, and low values of axonal sprouting at distal end in the PEG conduit repair group was reported. Consequently, the authors proposed this method was associated with reduced disruption and similar recovery in function to the graft repair group (Pateman et al., 2015). Although no formal testing of nerve function (electrophysiology or gait assessment) or pain behavioural assessment was

performed due to difficulties related to the size and position of the common fibular nerve.

Biodegradability of PCL material provides the advantage of acting as a temporary bridging scaffold which gradual degrade and prevents fibrosis and is less likely to cause chronic inflammatory reaction (Johnson and Soucacos, 2008; Wood and Mackinnon, 2015). For repair of short defects, biodegradable NCG are considered more advantageous on this effect to be better recovery of nerve function with less morbidity those associated with standard repair techniques. Bertleff et al. (2005) conducted a multicentre randomized trial to compare the recovery of sensory function following traumatic hand injuries using a biodegradable PCL and direct suturing of hand nerves in patients with different nerve injury (mainly ulnar or radial digital nerves). Seventeen patients received PCL conduits to repair gaps of 8 mm or more and both nerve endings were sutured into the conduit. In addition, 13 patients had undergone direct end-to-end repair. Assessment of sensory function was undertaken at 3, 6, 9, and 12 months after repair by using a computer-assisted force transducer (non-invasive static measures) and 2-point discrimination methods. Recovery of sensation in the nerve guide group was considered at least as good as in the control group and, thus PCL conduit were considered suitable for the repair of nerve defects up to 20 mm without tension during implantation.

Another randomised laboratory study conducted by Shin et al. (2009) evaluated the functional and histomorphological outcome following implantation of 1.5 mm conduit consisting of three synthetic materials (collagen, PCL and PGA) and nerve autograft in repairing a 10 mm defect of the sciatic nerve in a rodent model. After nerve injury a recovery period of 12 weeks electromyographic measurements did not show a significant difference in compound muscle action potentials, or the percentage of axon

count measurements between the autograft and PCL conduit repairs as compared to another conduits repair. In addition, there were no differences in the mean internal nerve fibre area, or mean myelin thickness of all experimental groups. At 12-weeks their result showed that PCL and collagen conduits remained structurally stable with optimum results, whereas PGA conduits had the lowest compound muscle action and degraded quickly. They established that PCL conduits can be used to repair 10mm sciatic nerve defects with improved functional outcome similar to the autograft repair, when compared to the other synthetic conduit guidance materials (Shin et al., 2009). They also, observed that thick walled-conduit impedes regeneration due to compression on regenerating fibres while thin walled conduit had tendency to collapse due to weak internal structures (Johnson and Soucacos, 2008; Shin et al., 2009; Pateman et al., 2015). Therefore, it has been suggested that NCG needs to be thin as feasibly permit but requires some form of mechanical structural support.

Several studies have shown that PCL conduits had improved biological and mechanical properties that would support neuronal axon regeneration and could replace the standard autograft methods for nerve defect repair following nerve injury. Den Dunnen et al. (1996) evaluated nerve regeneration following repair of a 10 mm gap either using a biodegradable PCL conduit (12 mm length) or an autologous nerve graft. Nerve regeneration was assessed using light microscopy, and morphometric analysis. In the PCL group recovery of sensation was determined by performing reflex withdrawal stimulation at week four and six stimulation of the proximal and distal part of the operated paw as compared to autograft repair and was shown to be improved and recovered further. After 10 weeks, their result revealed that average number of myelinated nerve fibres in the PCL repair were twice as large when compared with autograft repair group. In addition, the recovery pattern of the myelinated nerve fibres

was faster in the PCL repair group across short gap defect. The authors proposed that nerve regeneration across gap of 10 mm inside the nerve conduit using a biodegradable PCL was faster and qualitatively better than autologous nerve grafts.

It is important to choose a conduit with optimal internal diameter that does not compromise regeneration of nerve fibres. The internal diameter should provide enough space to facilitate insertion of the nerve segments without compression, but not too large which could stimulate fibrous tissue formation (Bertleff et al., 2005; Johnson and Soucacos, 2008; Shin et al., 2009; Reid et al., 2013; Pateman et al., 2015). Reid et al. (2013) conducted histomorphological and immunohistochemical assessment of long-term nerve regeneration in 10 mm gap model of rat sciatic nerve injury repaired with PCL conduits (diameter 1.6 mm & length14 mm) and autologous nerve graft. After eighteen weeks of recovery, there were no adverse reactions observed. The histological evaluation did not show a significant difference in the pattern or distribution of myelinated fibres between the repair groups and in addition, results revealed similar numbers of axons in the distal stumps and equivalent re-innervation rate of end organ muscle and skin. Based on their findings the authors support the potential use of synthetic biodegradable PCL nerve conduit in clinical nerve repair practice.

1.4.2 Novel targeting of pro-inflammatory cytokines in peripheral nerve injury

Pro-inflammatory cytokines that are produced after injury may act on sensory nerve fibres to generate central sensitization through increased ectopic neuronal activity by the interaction of peripheral injury environment and glial cells, which will lead to an increase in neurones excitability and subsequent initiation of neuropathic pain (Ren and Torres, 2009). The following section will focus on the targeting of pro-inflammatory cytokines (IL-1, TGF-β, and TNF-α) by the application of neutralising

anti-bodies and receptor blockers after nerve repair. In addition, this section will also consider the effect of IL-10, anti-inflammatory cytokine, on nerve regeneration following injury.

1.4.2.1 Application of antibodies to IL-1 cytokine in peripheral nerve injury

IL-1 is a potent pro-inflammatory cytokine that is upregulated during the inflammatory stage of Wallerian degeneration (Ren and Torres, 2009). There is substantial evidence that IL-1 is implicated in the development of neuropathic pain following peripheral nerve injury (Sommer et al., 2001; Ren and Torres, 2009). In addition, IL-1 is thought to be the main inflammatory cytokine in the interaction between glia and neurones following nerve injury and blocking the action of its IL-1 receptor 1 has been associated with a reduction in the development of pain-related behaviours (Sommer et al., 2001; Ren and Torres, 2009). In a chronic constriction injury of the sciatic nerve, Schäfers et al. (2001) investigated the effect of combined epineurial application of neutralized antibodies to TNF receptor and IL-1R1 and compared that with single antibody therapy to TNF and IL-1R1, on attenuating the pain related behaviours in an animal model. Data from their study showed that application of combined regime significantly reduced the thermal hyperalgesia and withdrawal reflexes of the animals when compared to anti-TNF single therapy which were injected once intraoperatively, at day 4 and 7 post-injury. In contrast, daily application of anti-IL-1R1 showed continuous effect on attenuating thermal threshold when observed during the experiment. Additionally, immunohistochemical analysis showed comparable levels of expression of TNF and IL-1 protein at day 10 postoperatively across the groups. The authors proposed that the combined therapeutic approach acted synergistically in reducing pain related behaviour (Schäfers et al., 2001).

Sommer et al. (1999) in a chronic constriction injury model on the sciatic nerve in rats investigated the effect of epineurial application of anti-IL-1R1 on thermal and mechanical hyperalgesia. Pain behavioural analysis revealed that although they were treated at moderate and high doses showed significant reduction of both pain behavioural compared to sham mice groups. In contrast, thresholds of paw withdrawal reflexes to mechanical stimuli was not different to the sham groups at low daily dose of anti-IL-1R1. Immunohistochemical analysis also found that this dose-dependent reduction of neuropathic pain was associated with reduced TNF-α immune reactivity and low infiltration of macrophages at the site of injury across all the experimental groups. The authors speculated that IL-1 induces neuropathic pain by an alternate pathway through activation of bradykinin receptors and prostaglandins, or mediated hyperalgesia through the production of NGF (Sommer et al., 1999).

Sweitzer et al. (2001) investigated the effects of intrathecal administration of IL-1 receptor antagonist and TNF-α antagonist on attenuating mechanical allodynia in the spinal nerve (L5) transection injury model. Preoperative injection of TNF-α antagonist was found to attenuate mechanical allodynia when compared to the IL-1 receptor antagonist. However, a combination of both therapies significantly reduced mechanical allodynia even at low doses. Immunohistochemical analysis and ELISA did not reveal any significant differences in protein expression of IL-1 and TNF-α in any of the experimental groups. Furthermore, treatment did not have any effect on glia or astrocyte activity. The findings of the previous studies were consistent with those of Winkelstein et al. (2001) on exploring the effects of intrathecal administration of IL-1 receptor antagonist and TNF-α antagonist on neuropathic pain. Their pain behavioural analysis demonstrated similar findings in both central and peripheral nerve injury models. The levels of various cytokines expressed and degree of

microglia activity were identical across all the groups investigated. In peripheral spinal section model, the treatment protocol had a significant effect on mechanical allodynia when compared to spinal (L5) nerve root ligation injury. From these observations central blocked of IL-1 mediates its anti-allodynic effects believed to be related to down regulation of pro-inflammatory cytokines rather than inhibiting glial excitation (Sweitzer et al., 2001).

The introduction and development of transgenic and knockout mice models has provided an alternative approach to study regeneration of injured peripheral nerves (Rodríguez et al., 2004). It has been shown that knockout IL-1R1 and TNFR1 mice are associated with reduced invasion of neutrophils and macrophages as well as reduced mechanical hyperalgesia and impaired regeneration of peripheral nerves after injury, when compared to wild mice (Nadeau et al., 2011). Nociception (hyperalgesia) to mechanical stimuli was reinstated, however, after peripheral injection of either recombinant IL-1 or TNF at the site of sciatic nerve ligation. Furthermore, depletion of neutrophils with anti-LY6G significantly decreased hyperalgesia after nerve injury but axon regeneration and recovery was unaffected, which may introduce new insight of only targeting inflammatory cells that mediate initiation of neuropathic pain rather than blocking the entire pro-inflammatory cytokine profile which might be critical for axonal regeneration (Nadeau et al., 2011).

1.4.2.2 Application of antibodies to TNF-α cytokine in peripheral nerve injury

TNF-α is the second most important pro-inflammatory cytokine upregulated following peripheral nerve injury (George et al., 2005). It is believed that TNF-α expression induces ectopic neuronal activity following axon damage and subsequently initiates neuropathic pain by triggering specific receptors TNFR1 and TNFR2 (George et al.,

2005). Tumour necrosis factor antagonist (Etanercept) has been extensively studied in other medical fields and used in the treatment of autoimmune conditions such as rheumatoid arthritis (Kato et al., 2009).

It has been postulated that local application of Etanercept might be associated with the suppression of pro-inflammatory cytokines that mediate the initiation of neuropathic pain by binding to transmembrane TNF isoforms within the endoneurium after sciatic nerve injury (Kato et al., 2009). Kato et al. (2009) examined the distribution and binding specificity of locally administered Etanercept in the crush sciatic model of nerve injury. Immunohistochemical analysis using TNF specific antibody (Anti-IgG) showed Etanercept-IgG immunoreactivity in the endoneurium of damaged nerves after 1 hour and TNF was highly expressed in Schwann cells and macrophages. Pain behavioural analysis following the peripheral application of Etanercept showed reduced mechanical hyperalgesia and withdrawal threshold, leading the authors to speculate that Etanercept had great potential as a targeted therapy in treating neuropathic pain following nerve injury (Kato et al., 2009). In another study, Kato et al. (2010) used the crush sciatic model of nerve injury to investigate the effect of central (intraperitoneal) and peripheral (epineurial) application of Etanercept on axonal regeneration and expression of growth–related proteins. They observed that immediate Etanercept injection enhanced the rate of sensory axon regeneration and expression of GAP-43 detected in ipsilateral DRG of sensory and motor neurones. Histological quantification of axons by light microscope also showed a significant increase the number of regenerating axons within the distal segment and an increased accumulation of Etanercept was also detected in GAP-43-positive immunoreactivity nerve fibres in the proximal nerve segments. They concluded that the immediate

application of Etanercept helps to maintain and support the rate of growth, and regeneration process in crushed axons (Kato et al., 2010).

Sommer et al. (2001) explored the effects of systemic administration of Etanercept with different dose regime on reducing hyperalgesia following peripheral nerve injury. Their study revealed that Etanercept can reduce thermal and mechanical hyperalgesia following constriction injury of mice sciatic nerves (Sommer et al., 2001). Immunohistochemical and histomorphological examination of the sciatic nerve tissues did not reveal any diverse changes within the groups during the degeneration and regeneration processes or in the magnitude of macrophage invasion, which rule out impairments of nerve regeneration by Etanercept therapy. However, pain behavioural analysis showed significant effect following the local application of Etanercept on mechanical hyperalgesia when compared to intraperitoneal treatment. The findings of Sommer et al. (2001) are support the previous studies by Kato et al., 2009; Kato et al., 2010, and suggest that Etanercept has the potential to reduce hyperalgesia and neuropathic pain through inhibition of TNF-α activity either prophylactically or therapeutically.

1.4.2.3 Application of scar-reducing agents in peripheral nerve injury

Scar formation following a severe type of nerve injury (neurotmesis) is common and acts as a mechanical obstacle that impedes axonal regeneration and promotes the development of neuroma formation at the site of injury (Atkins et al., 2007). Experimental manipulation of fibrous tissue formation throughout the process of wound healing at the site of peripheral nerve injury in rodents has led to the proposal of an alternate therapeutic approach to enhance the functional regeneration by

exogenous application of scar reducing agents such as the potent anti-inflammatory mediator (IL-10) or antibodies to TGF-β.

TGF-β isoforms are pro-peptide molecules that contain amino acid chains and a pro-protein region termed the Latency Associated Peptide (LAP) which has “asparagine linked mannose-6-phosphate oligosaccharides” (M6P receptor) (O’Kane and Ferguson, 1997). TGF- β1 and TGF- β2 isoforms specifically bind to M6P receptors on corboxyhydate chain of TGF-β. As a result, exogenous administration of M6P has been suggested as a novel approach in reducing scar formation by competitive inhibition of TGF-β isoforms at the M-6-P receptor (O’Kane and Ferguson, 1997). Moreover, peripheral administration of combined anti-TGF-β antibodies has been shown to reduce scar formation at the site of injury (Nath et al., 1998).

Atkins and colleagues (2006) investigated the outcome of applying antibodies to both TGF- β1 and TGF- β2 at the time of sciatic nerve repair in rats. However, after 7 weeks’ recovery results revealed that animals that had received antibodies to TGF- β at the time of sciatic nerve repair demonstrated reduced levels of collagen which was not significantly different to controls. Electrophysiological testing in the M6P treated group revealed slow conduction velocities and significantly lower compound action potential ratio when compared to repair alone, suggesting a lower proportion of regenerating axon had traversed the repair site. Quantification of myelinated and non-myelinated nerve fibres demonstrated considerably higher fibres count on either side of nerve repair group and those with antibodies to TGF- β, but this was not statistically significant between the groups when compared to controls. The authors reported that neutralization of TGF- β at the time of nerve repair reduced intraneural fibrosis but this approach proved neither to promote axon regeneration or reduced increase of

neuronal sprouting (Atkins et al., 2006). However, they did propose that the optimum stage for administration of this therapeutic agent is either at or shortly after nerve repair.

An additional study by Ngeow et al. (2011a) conducted histomorphometric quantification of neuronal structures, in order to detect any variations at the site of nerve repair after the application of M6P. Together electron and light microscopic analysis did not show any significant difference in myelinated axons diameter across the repair site in repair groups when compared to sham animals. In contrast, axonal density and the cross-sectional area of myelinated axons were reduced distal to the repair site in the repair groups when compared to controls. Moreover, the proportion of non-myelinated to myelinated axons was comparable in both repair and sham groups, and the authors proposed that M6P did not interrupt the myelination process by Schwann cells. Furthermore, Schwann cell proliferation was associated with increased remak bundle counts and axonal density distal to the repaired site (Ngeow et al., 2011a). Another study Ngeow et al. (2011b) explored the effects of M6P, triamcinolone and IL-10 application, at the time of nerve repair. After administration of 600 mM of M6P, electrophysiological analysis showed that sprouting axons attained higher compound action potential modulus ratios and faster conduction velocities, suggesting higher percentages of nerve fibres had regenerated successfully, particularly lager diameter fibres. Gait testing also displayed larger paw print area in the M6P treated group at 3 weeks, indicating better early functional recovery, which plateaued 12 weeks after repair. In addition, collagen levels were significantly higher in all repair group, but not in sham controls. Their results indicated that intraneural scar levels after M6P application were lower than controls, but this was not statistically significant. They proposed that the M6P increased rate of axon regeneration at the

early stage of regeneration is attributed to scar remodelling at the site of nerve repair (Ngeow et al., 2011b).

Another study, Harding et al. (2014) investigated the effect of M6P application on the rate of axonal regeneration following a nerve graft procedure. They developed a technique of visually quantifying the number of individual regenerating axons across a repair site using a strain of transgenic thy-1-YFP-H mice. The image analysis data revealed more sprouting with M6P and vehicle treated groups when compared to controls, which was clear to see as the axons entered the proximal part of the tissue graft. The authors illustrated that approximately 75 % of axons present at 3.5 mm intervals were accurately followed back to the reference line (start point of axon regeneration). Furthermore, visual quantification shown that the M6P treated group had a lower sprouting index when compared to vehicle treated graft, but there was no significant difference between the groups. In repair groups, however, the sprouting index rates were stable at 0.5 mm and 1 mm distance from the reference line, and then continued to decline at an equivalent rate between the remaining intervals. This study revealed that M6P had influenced the early response of regeneration which was specified by an increased sprouting index and the way axons quickly crossed the repair site (Harding et al., 2014).

Wound healing is considered a complex process which involves a sequence of events including haemostasis, inflammation and granulation tissue proliferation and subsequent fibrosis and scar formation (Morris et al., 2014). In wound healing, the production of pro-inflammatory cytokines by immune cells such as macrophages have been implicated in the recruitment of inflammatory cells. In turn, these produce more pro-inflammatory cytokines and as a consequence intensify the inflammatory reaction and stimulate scar formation (Morris et al., 2014). IL-10 is highly expressed in amniotic

fluids and fetal tissue and has been postulated to play an important part in the decrease of pro-inflammatory cytokines production and the inflammatory response and as a result in a healing with minimum scar formation (Morris et al., 2014).

Atkins et al. (2007) studied the effect of exogenous administration of IL-10 and TGF-β3 on functional regeneration after sectioning of the sciatic nerve in C57 black mice. After 6 weeks' post-injury mice which received TGF-β3 showed elevated collagen levels and did not enhance the regeneration of repaired nerves in comparison to sham groups. Conversely, mice groups received low doses of IL-10 revealed higher compound action potential as in control groups proposing that many sprouting myelinated axons had successfully spanned the injury site. Moreover, the level of collagen types I and III were also reduced in IL-10 treated mice (low dose) and controls. They clarified that low doses of IL-10 could be effective in reducing the fibrous tissue formation and improve regeneration of severed nerve fibres, but long-term evaluation of outcome is required. Furthermore, adjusting and implementing an appropriate therapeutic regimes and mode of drug delivery is an important aspect for the regeneration of nerve fibres (Atkins et al., 2007).

Another study by Sakalidou et al. (2011) investigated the effect of IL-10 application on intraneural scar reduction and functional nerve regeneration after end to side anastomosis of peroneal nerve and the tibial nerve in rats. After eight weeks' of recovery the peroneal functional index and electrophysiological testing did not reveal any differences between the groups. Moreover, histomorphological analysis of nerve sections of IL-10 treated groups showed significant higher myelination, reduced scar formation and reduced collagen levels when compared to repair alone. In support of previous work by Atkins et al. (2007), they also predicted that unsuccessful functional

recovery might be attributed to the short term follow up of the experiment protocol (Sakalidou et al., 2011).

1.5 Research hypothesis

Modulating cytokine signalling pathways peripherally either by anti-inflammatory cytokines or anti-scaring agents at the time of nerve repair will decrease macrophage immunoreactivity and glial cells activation, reduce neuropathic pain, and improve functional recovery.

1.6 Aims and objectives

Aims

The overall aims of these studies were to investigate the effects of peripherally applied novel cytokine antagonists and anti-scarring agents on inflammation, and establish their contribution to the reduction or prevention of neuropathic pain, and effect on nerve regeneration. In addition; the study aims to investigate the effect of poly-carprolactone conduit implantations on enhancing the functional nerve regeneration.

Objectives: The main objectives of these studies were to:

1. Determine the effect of anti-inflammatory cytokine on macrophage infiltration at the site of nerve injury and repair, and on glial cells activation in the dorsal and ventral horns of the spinal cord using immunohistochemical techniques and image analysis.
2. To study the effect of novel anti-inflammatory cytokine or anti-scaring agents on axonal regeneration following peripheral nerve injury and repair by conducting electrophysiology recording and analysis of gait movement.
3. Utilise transgenic YFP-H mouse strain to investigate the effect of poly-carprolactone conduit on nerve regeneration following artificial nerve repair by axon tracing technique.

CHAPTER 2

Materials and methods

2.1 Introduction

All procedures were carried out at the University of Sheffield, in accordance with the UK Home Office Animals (Scientific Procedure) Act 1986. All experimental protocols were approved by the University of Sheffield Biological Services and performed in accordance with Project Licence 70/8194.

2.2 Research methodology

2.2.1 Animal husbandry and surgical set up

Experimental animals

Animals used in this research were bred and supplied by an approved UK Home Office facility (Charles River, UK). All animals were housed in plastic cages with unlimited access to water and food. The room temperature was maintained between 19-21 °C with a twelve-hour light/dark cycle. Animals were allowed to acclimatise for one week before undergoing any surgery. Immediately following surgery, during the postoperative recovery period, animals were housed in single cages to reduce any incidents or injury from cage mates.

Surgical procedures were performed under aseptic conditions, all instruments autoclaved and hibitane (5 %) used to disinfect the surgical area. In the first experiment (Chapter 3) Sprague Dawley rats (males) were used to attain the primary result of the research. However, in the other experiments (Chapter 4 and 5) C57-black/ 6 mice were used.

In this work additional sham group from previous work in the Oral neuroscience group is included to explain difference between treatment groups under the investigation. Sterile water is considered as negative control and sham not included initially due to

the ethical issue in accordance with the UK Home Office Animals (Scientific Procedure) Act 1986.

2.2.2 Anti-inflammatory agent preparation and delivery

Preparation of anti-inflammatory cytokine agents used in this research is presented in table 2.1. For the preparation of cytokines antagonist agents, sterile water is used and as a negative control. Normal saline was not used because it is a hypotonic solution and can be painful on injection. Also, it can cause tissue damage and cells lysis if injected into the tissue (Svendsen et al. 2005).

For drug administration, a micro-dialysis needle gauge 34 (outer diameter 0.164 mm and internal diameter 0.1 mm, World Precision Instruments [Microfill]) attached to a length of polyethylene tube (outer diameter 0.60 mm and internal diameter 0.28 mm, INSTECH) connected to a 0.5 ml insulin syringe and needle was used to deliver the agent at specified increments described below (Figure 2.1). All treatments received by animals were randomised and investigators performing the experiments and analysis were blinded.

Table 2.1: Anti-inflammatory cytokines agents applied in sciatic nerve injury and repair experiments.

Drug name	Source	Formulation	Reconstitution	Dose given per 100µl	Total volume
IL-1 receptor antagonist (Kineret ® [Anakinra])	Sobi	100 mg/1 ml pre-filled syringes	Not applicable	10 mg/100 µl	100 µl
Combination of Recombinant Human IL-10 Protein and TNF-α antagonist (Etanercept)	R&D Systems 217-IL-005/CF Pfizer	5 µg solution in vials 25 mg powder	12.5 µl IL-10 + 237.5 µl PBS + 0.75 mg/powder of pre-weighed Etanercept +250 µl sterile water	125 ng IL-10 + 0.15 mg Etanercept/ 100 µl	100 µl
TNF-α antagonist (Etanercept)	Pfizer	25 mg powder	0.75 mg/powder of pre-weighed Etanercept +500 µl sterile water	0.15 mg/100 µl	100 µl
Sterile water	Dechra	100 ml sterile water	Not applicable	0.1 ml/100 µl	100 µl

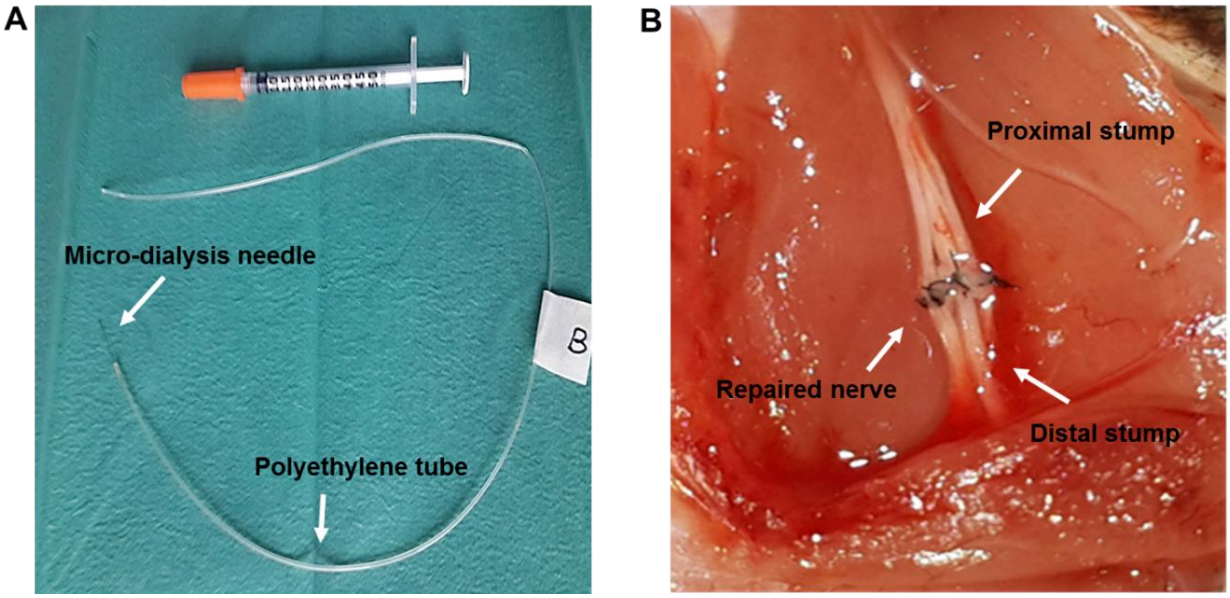

Figure 2.1: A: micro-dialysis needle attached to polyethylene tube and syringe for injection of agents. B: sciatic nerve repair with 9/0 monofilament polyamide sutures (ETHILON*) and immediate epineurial administration of treatment agent.

2.2.3 Sciatic nerve injury and repair model and administration of anti-inflammatory agent

Animals (Sprague Dawley rats [Males; 8 weeks old--weights 220 g–300 g] and C57 black-6 mice [Males; 8 weeks or older – weights 17-30 g]) were anaesthetised with a 2-3 % mixture of isoflurane (100 % w/w isoflurane liquid, IsoFlo®) and oxygen, delivered at a rate of 2 litres per minute. The animals were shaved in the area of the left thigh, and a 1-2 cm incision made along the lateral aspect of mid-thigh. Then, the left sciatic nerve was exposed and separated freely from the surrounding tissues. A slit was created in the epineurium and 40 µl of assigned agent (Table 2.1) injected under the epineurium. The sciatic nerve was sectioned transversely approximately 12 mm distal from the sciatic foramen with microscissors, and the proximal and distal sciatic nerve stumps immediately repaired with four 9/0 monofilament polyamide

(ETHILON*) epineurial suture knots (Figure 2.1B). Thereafter, the remaining volume of agent (60 µl) was administered intramuscularly around the nerve repair, and the surgical site closed in layers with vicryl suture material (6/0, ETHICON®). At the end of the surgical procedure each animal received a subcutaneous injection of buprenorphine hydrochloride (Vetergesic [0.05 mg/kg], Ceva). Animals were allowed to recover for either one week, following which, sciatic nerve tissue was harvested for immunohistochemical analysis alone (Chapter 3), or six weeks, following which animals were subjected to a series of non-recovery electrophysiological recordings (described below), and tissues extracted for immunohistochemical analysis (Chapters 4 and 5).

2.2.4 Sciatic nerve gap injury model

YFP-H mice (male or females [⩾8 weeks old – weights 17-30 g]) were anaesthetised with a 2-3 % mixture of isoflurane (100 % w/w isoflurane liquid, IsoFlo®) and oxygen, delivered at a rate of 2 litres per minute. Under the operating microscope, the area of the left mid-thigh was shaved, a 1-2 cm incision made along the mid-thigh, and the left sciatic nerve exposed and carefully dissected free from surrounding tissue. The distal end of the nerve was marked by making an epineurial cut with microscissors approximately 3 mm central to where it branches into the peroneal, tibial and sural nerves. The proximal end of the sciatic nerve was marked exactly 4 mm distal to the distal end to ensure consistency between the animals (Figure 2.2.A). Before sectioning the nerve, each nerve ending received 30 µl of treatment agent. A 5-minute lapse was allowed for the injected solution to diffuse into the nerve tissue and then a gap effect of 4 mm created to allow conduit tube insertion. The two sectioned nerve stumps were inserted approximately 0.5 mm into either end of the conduit tube and secured with an application of fibrin glue (Figure 2.2.B).

Following conduit implantation, the remaining 40 µl of treatment agent was injected into surrounding muscle tissues, and the wound closed in layers with vicryl suture (6/0, ETHICON®). A subcutaneous injection of buprenorphine hydrochloride (Vetergesic [0.05 mg/kg], Ceva) was administered at the end of the surgical procedure. Animals were allowed to recover for 5 weeks, during which time animals were assessed for locomotion function (gait assessment - described below). At the end of the recovery period animals underwent a series of non-recovery electrophysiological recordings (described below), after which tissues were extracted for immunohistochemical analysis and axonal tracing (Chapter 6).

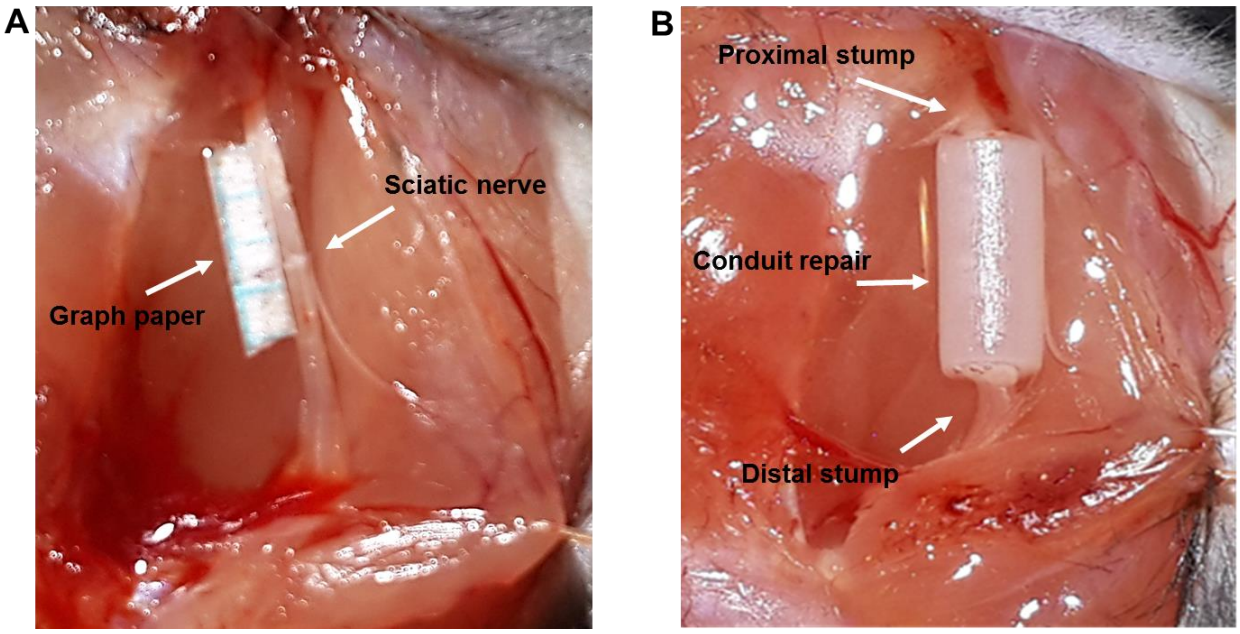

Figure 2.2: A: measurement of nerve segment with graph paper. B: nerve conduit repair in 4 mm gap defect of sciatic nerve.

2.2.5 Functional assessment of sciatic nerve regeneration

2.2.5.1 Gait assessment (Cat-Walk system)

In animals (YFP-H mice) receiving the nerve conduit implantation, locomotor function was evaluated prior to electrophysiological recordings (described below), using CatWalk system® (Noldus technology, Netherlands) and gait assessment. Described previously by Ngeow et al (2011b), the system incorporates software which helps to detect natural gait parameters including; paw print area and intensity which can be measured from each run an animal makes across the walking corridor (Deumens et al., 2007). The corridor system consists of a glass floor and a fluorescent tube which emits white light (Figure 2.3). Gait assessment was obtained from two runs conducted immediately before, and then 1, 2, 3, 4 and 5 weeks after implantation. The total surface areas and intensity of paw prints were sensed and recorded by a video camera attached beneath the walking glass plate (Deumens et al., 2007). Assessment of natural gait does have limitations due to variations in walking speed of the animals under the experimental condition (Ngeow et al., 2011b). Thus, to achieve accurate assessment, an average value of the two runs of each animal was counted.

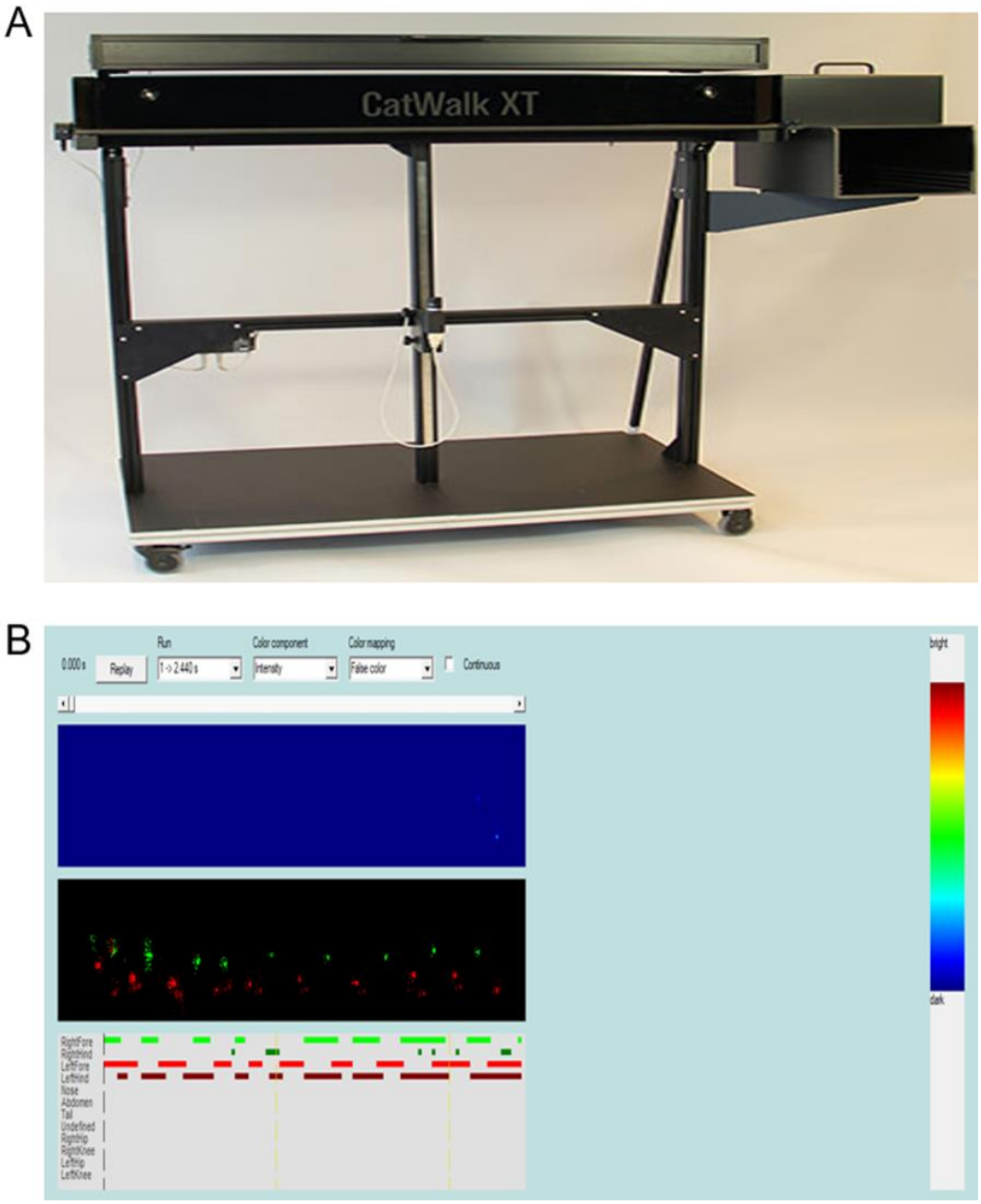

Figure 2.3: Illustration of CatWalk system® (Noldus technology, Netherlands). B: Examples of records of surface areas of paw prints each time the animal crosses the walkway. Diagram adapted from noldus technology, Netherlands (http://www.noldus.com/CatWalk-XT/specifications).

2.2.5.2 Electrophysiological recordings

Animals (YFP-H mice and C57 black-6 mice) were anaesthetised with an intraperitoneal (ip) injection of fluanisone (0.8 ml/kg) and midazolam (4 mg/kg). Here, the left sciatic nerve was exposed at the site of repair and released from the underlying tissues, and sectioned as far distally as possible. Proximally, the nerve was sectioned close to the sciatic foramen and raised by a pair of central recording electrodes of platinum wire (0.15 mm diameter). An evoked stimulation across the sciatic nerve was delivered from two pairs of distal and proximal electrodes each situated 2 mm distal and central to the repaired site. In the gap repair model, the stimulating electrodes were sited close to the conduit edges touching only the nerve tissues. The surrounding skin flaps were raised to create a pool filled with warm liquid paraffin. The ground electrode was positioned on the skin flap proximal to the stimulating and recording electrodes. Recording electrodes were connected to a computer where data was processed using Spike 2 software (version 5, Cambridge Electronic Design). An illustration of the electrophysiology recording set-up is shown in (Figure 2.4). The of compound action potential (CAP) from the proximal and distal segments was recorded from a 10 responses of stimulation along the sciatic nerve. As in previous study recording CAP, 10 Volts for 0.05 milliseconds is considered the maximum stimulus intensity which indicate the proportion of myelinated axons that successfully have crossed the repaired site (Atkins et al., 2007). The CAP ratio calculated between the responses evoked from proximal or distal to the repair (modulus with distal stimulation ÷ modulus with proximal stimulation). The CAP ratio gives an expression of the proportion of axons that have crossed the repair site.

Conduction velocities were also recorded after injury and repair by measuring the latency of the earliest component of the CAP evoked by stimulation distal to the

repair using the digital storage oscilloscope. This measurement of conduction velocities method was previously validated by Atkins et al. (2007) in comparing latencies of the regenerating axons after nerve repair.

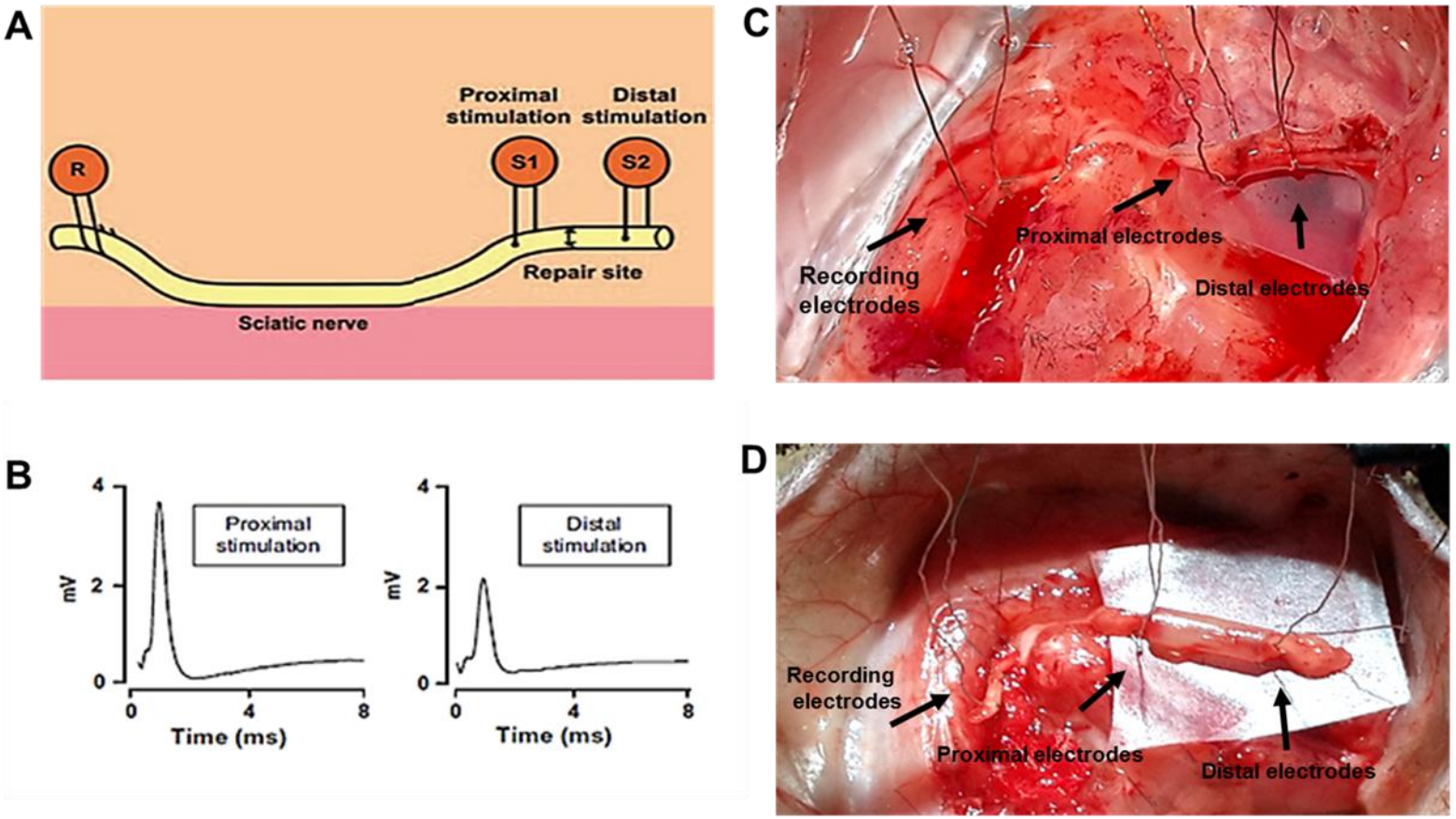

Figure 2.4: A: Diagram illustrates the arrangement of electrodes for the recording of compound action potentials. B: Examples of compound action potential recordings with electrical stimulation (proximal versus distal). C: Recording of compound action potential in direct nerve repair. D: Recording of compound action potential in nerve conduit repair. (Figure A and B reproduced with permission from John Wiley and Sons and Copyright Clearance Centre).

2.2.6 Tissue harvesting, processing and sectioning

Following one-week recovery (immunohistochemical analysis only) or electrophysiology recordings (Chapter 4), animals were perfusion-fixed and tissue harvested under non-recovery anaesthesia protocol. Animals were deeply anaesthetised with 0.5 ml of sodium pentobarbital (intraperitoneal injection, 20 % w/v, JML), and perfusion-fixed intracardially (via the left ventricle) under a surgical microscope, first with 0.2 M perfusion buffer (60 ml in mice and 750 ml in rats), followed by 4 % paraformaldehyde in 0.1 M phosphate buffer solution (PBS) (20 ml in mice and 750 ml in rats). The left and right sciatic nerves were harvested and a laminectomy performed to allow harvesting of the spinal cords. Tissues were immersed in 4 % paraformaldehyde for 4 hours and cryoprotected overnight in 30 % sucrose solution, both at 4 °C.

After completion of the electrophysiology recordings (Chapter 5), animals received a 0.5 ml (100 mg) intraperitoneal injection of sodium pentobarbital (20 % w/v) whilst under deep anaesthesia. Then the right and left sciatic nerves and spinal cord tissues were removed and fixed in 4 % paraformaldehyde for 24 hours, and cryoprotected overnight in 30 % sucrose solution, both at 4 °C. Following completion of the electrophysiological recordings in the YFP-H mice, the right and left sciatic nerves were fixed in situ with 4 % paraformaldehyde for 30 minutes and then tissues mounted directly onto slides and stored at 4 °C The spinal cords were harvested following laminectomy and processed as described above.

Before the nerves were frozen down, excessive connective tissues were removed. The sciatic nerves were orientated longitudinally on the cryostat chuck, with surgical repairs knots facing up, and embedded in Optimal cutting temperature compound medium (OCT; Thermo Scientific™). The meninges surrounding the spinal cords were

carefully removed and the cords dissected into three separate sections; cervical, thoracic and lumbosacral under a dissecting light microscope. The spinal cords were held in a vertical rostral (top) to caudal (bottom) position on the cryostat chuck, with the aid of a section of rubber tubing, which was filled with OCT medium. The sciatic nerves and spinal cords were frozen down to -50 °C freezing temperature using a cryostat freezing plate and stored in -80 °C freezer. Tissues were cut using a cryostat (CRYO-STAR HM 560 MV, Microm International, Germany) at optimal cutting temperature (-19-23 °C). The sciatic nerves were sectioned longitudinally at a thickness of 14 µm and collected serially onto Poly-D-lysine (PDL, SIGMA) coated slides (Figure 2.5). Three sections, without rolling or orientation distortion were collected per slide, and the slides left to air dry for 1 hour, before being stored at -80 °C, until required for immunohistochemical processing.

30 µm thick transverse spinal cord sections were cut from the lumbar region block. Representative L4 and L5 sections were identified under a light microscope and 12 sections per animal were collected into a 24-well plate filled with PBS (Figure 2.6). The sections were stored at 4 °C fridge before immunostaining.

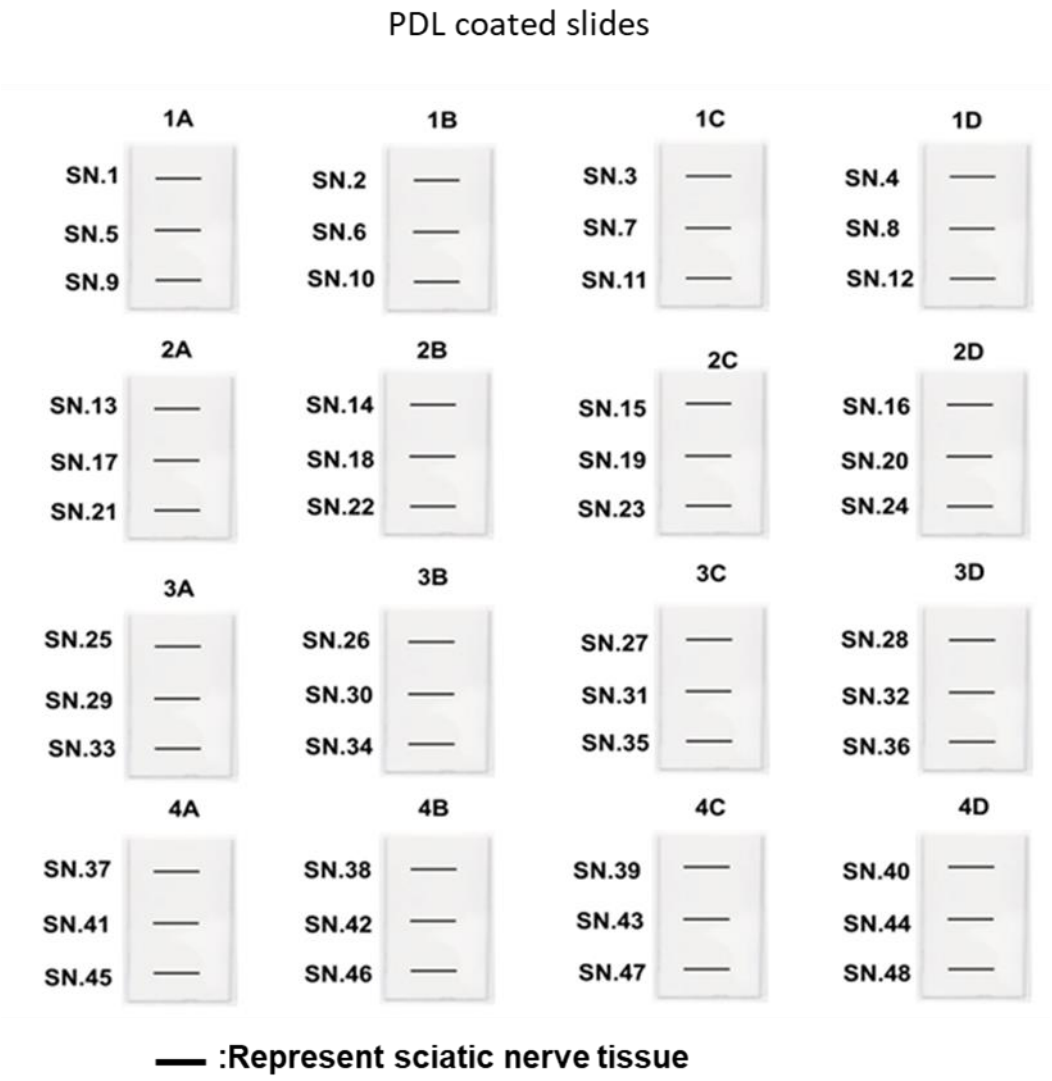

Figure 2.5: Serial collection of nerve tissue sections on PDL coated slides during sectioning of sciatic nerve. Sectioning of nerve tissue starts from SN.1 to SN.48. SN: nerve section number. For each nerve, 3 sections were taken across the width of the nerve for analysis. This serial collection of sciatic nerve tissues gives representative tissue sample of axons for immunostaining.

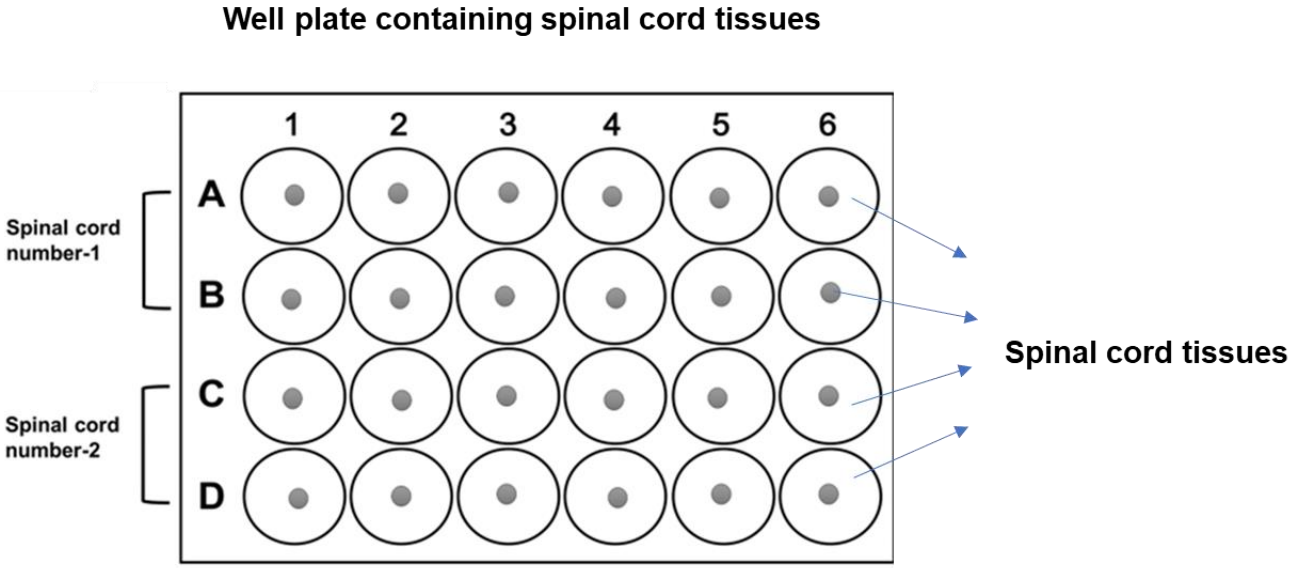

Figure 2.6: Spinal cords sections collected into well plate filled with PBS for immunostaining.

2.2.7 Immunohistochemistry

Indirect immunofluorescence immunohistochemistry was employed to label the sciatic nerve and spinal cord tissues for macrophages and glial cells

2.2.7.1 Antibody specificity and pre-absorption controls

The selection of primary and secondary antibodies for the study of macrophage and glial cells labelling was based on their use in previous immunocytochemical studies, and protocols developed and tested within the oral neuroscience group laboratory (Powis et al. 2012). The two types of controls conducted for the immunocytochemistry in this work were primary and secondary antibody controls. Pre-absorption of the primary antibodies used in these studies was carried out to assess the specificity of the primary antibody binding to the antigen. This procedure involved incubating with primary antibody with its specific blocking peptide for 24 hours, before its application in the standard immunohistochemical protocol, as described below. The specificity of the secondary antibody to the primary antibody was tested by omitting the primary antibodies from the protocol, and applying the secondary antibodies only.

Omission, and preabsorption of the CD68, IBA-1, and GFAP primary antibodies with their respective haptens (Tables 2.2 and 2.3), revealed no positive macrophage or glial immunofluorescent labelling in either the sciatic nerve or spinal cord tissues, confirming specificity of the antibodies employed in these studies (Figures 2.7-2.11).

Table 2.2: Pre-absorption volumes of primary antibodies and their respective peptides for macrophage labelling.

Antibody specifity **Rat sciatic nerve**	**Type**	**Total**	**Used**
Primary	Mouse Anti-rat CD68 (MCA341GA, BIO RAD)	0.1 mg/ ml (IgG concentration1.0 mg/ml)	1.5 µl (1:1500)
Secondary	Donkey Anti-mouse CY3 (715-165-150, Jackson Immuno-Research Inc)	0.5 mg/ml at 1.4 mg/ml)	4.5 µl (1:500)
Blocking peptide	mouse IgG1 negative control (MCA1209, BIO RAD)	0.1 mg/ ml	10 µg (100 µl)
Antibody specifity **Mouse sciatic nerve**	**Type**	**Total**	**Used**
Primary	Rat anti-mouse CD68 (MCA1957GA, BIO RAD)	0.1 mg/ ml (IgG concentration 0.5 mg/ml)	1.5 µl (1:1500)
Secondary	Goat Anti-Rat IgG CY3 (112-165-167, Jackson Immuno-Research Inc)	0.5 mg/ml at 1.4 mg/ml)	4.5 µl (1:500)
Blocking peptide	rat IgG2a negative control (MCA1212, BIO RAD)	0.1 mg/ ml	10 µg (100 µl)

Table 2.3: Pre-absorption volumes of primary antibodies and their respective peptides for glial cell labelling.

Antibody	**Type**	**Total**	**Used**
Primary	Goat polyclonal anti-IBA1 (ab5076)	100 µg at 0.5 mg/ml	0.48 µl (1:2500)
Secondary	Donkey anti-goat CY3 (705-165-147, Jackson Immuno-Research Inc)	1.5 mg/ml	2.4 µl (1:500)
Blocking peptide	Human IBA1 peptide (ab23067)	100 µg at 1 mg/ml	10 µg (10 µl)
Antibody	**Type**	**Total**	**Used**
Primary	Rabbit polyclonal anti-GFAP (ab7260)	50 µg at 0.5 mg/ml	0.6 µl (1:2000)
Secondary	Donkey anti-rabbit CY3 (711-165-152, Jackson Immuno-Research Inc)	1.4 mg/ml	2.4 µl (1:500)
Blocking peptide	Human GFAP peptide (ab48665)	100 µg at 1 mg/ml	10 µg (10 µl)

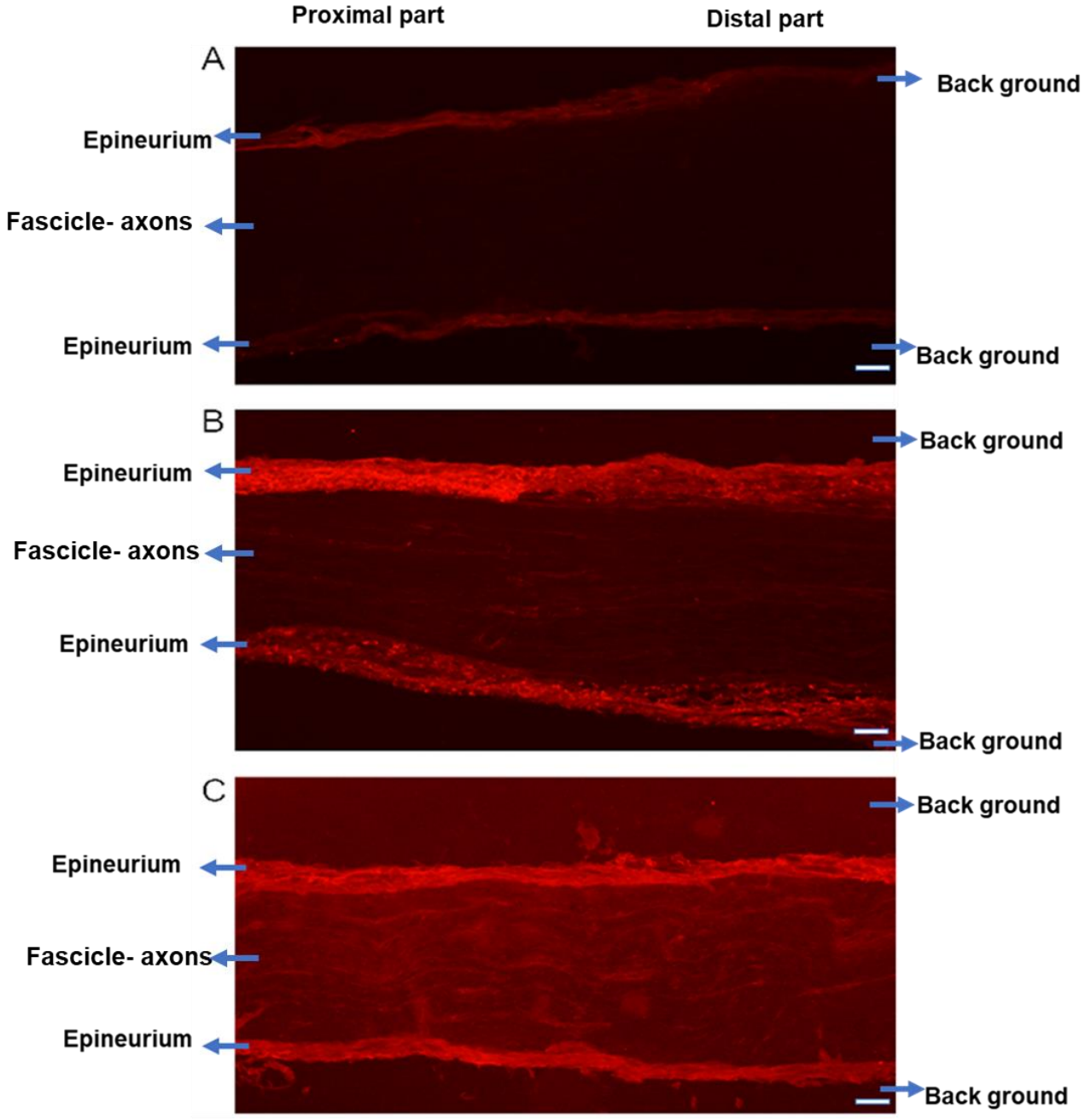

Figure 2.7: Microscopic images illustrating macrophage (CD68) antibody specificity and Immunofluorescent labelling in uninjured rat sciatic nerve seven days after sciatic nerve exposure. (A) Pre-absorption of primary antibody with blocking peptide shows negative macrophage staining. (B) Application of secondary antibody with omission of primary antibody shows negative macrophage staining. (C) Application of specific primary and secondary antibodies shows no macrophage staining. Scale bar= 100 µm.

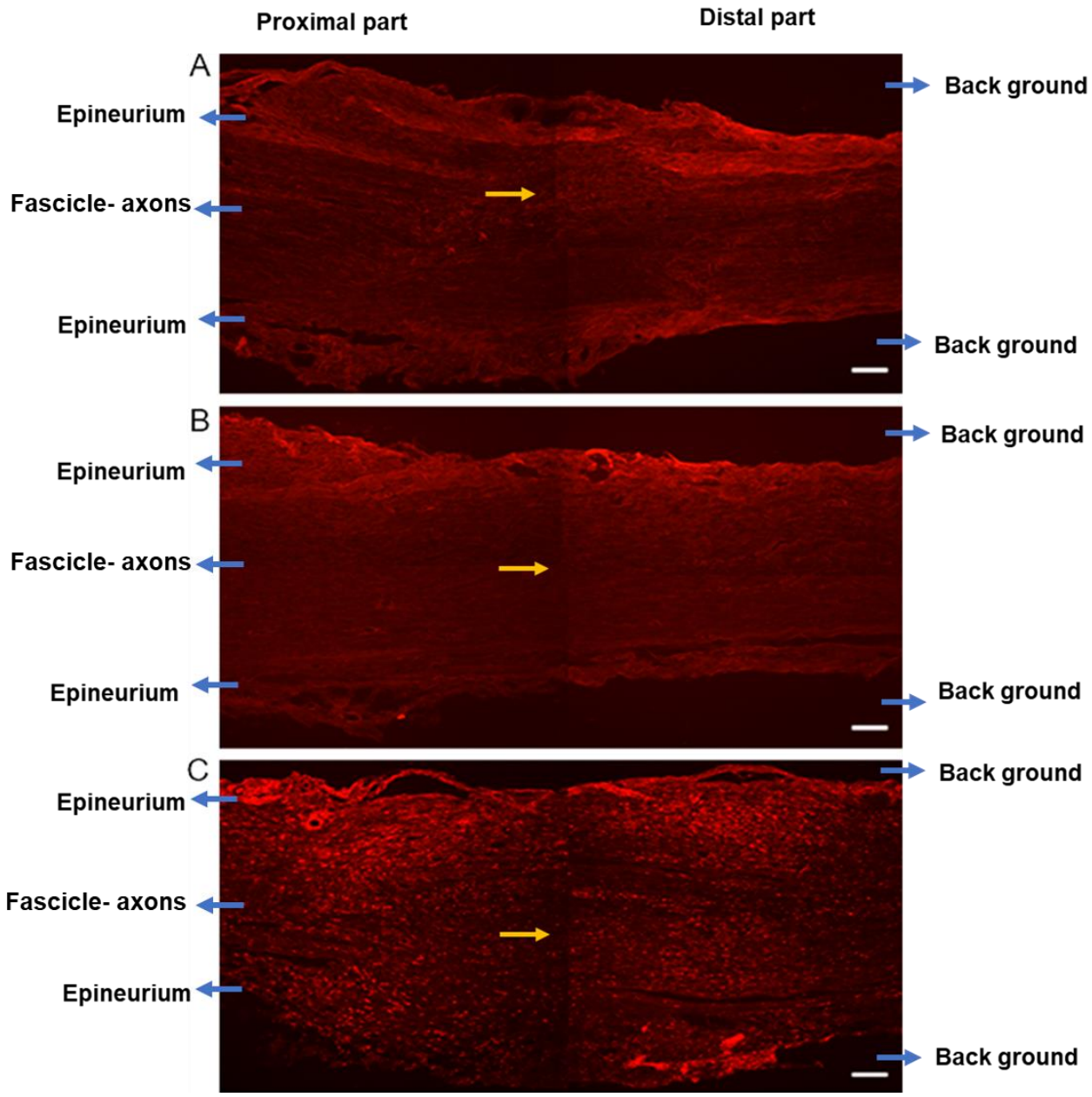

Figure 2.8: Microscopic images illustrating macrophage (CD68) antibody specificity and immunofluorescent labelling in rat sciatic nerve seven days after sciatic nerve injury and repair (yellow arrows: repaired site). The bright dots indicate active microphages. (A) Pre-absorption of primary antibody with blocking peptide shows negative macrophage staining. (B) Application of secondary antibody with omission of primary antibody shows negative macrophage staining. (C) Application of specific primary and secondary antibodies shows positive macrophage staining. Scale bar= 100 µm.

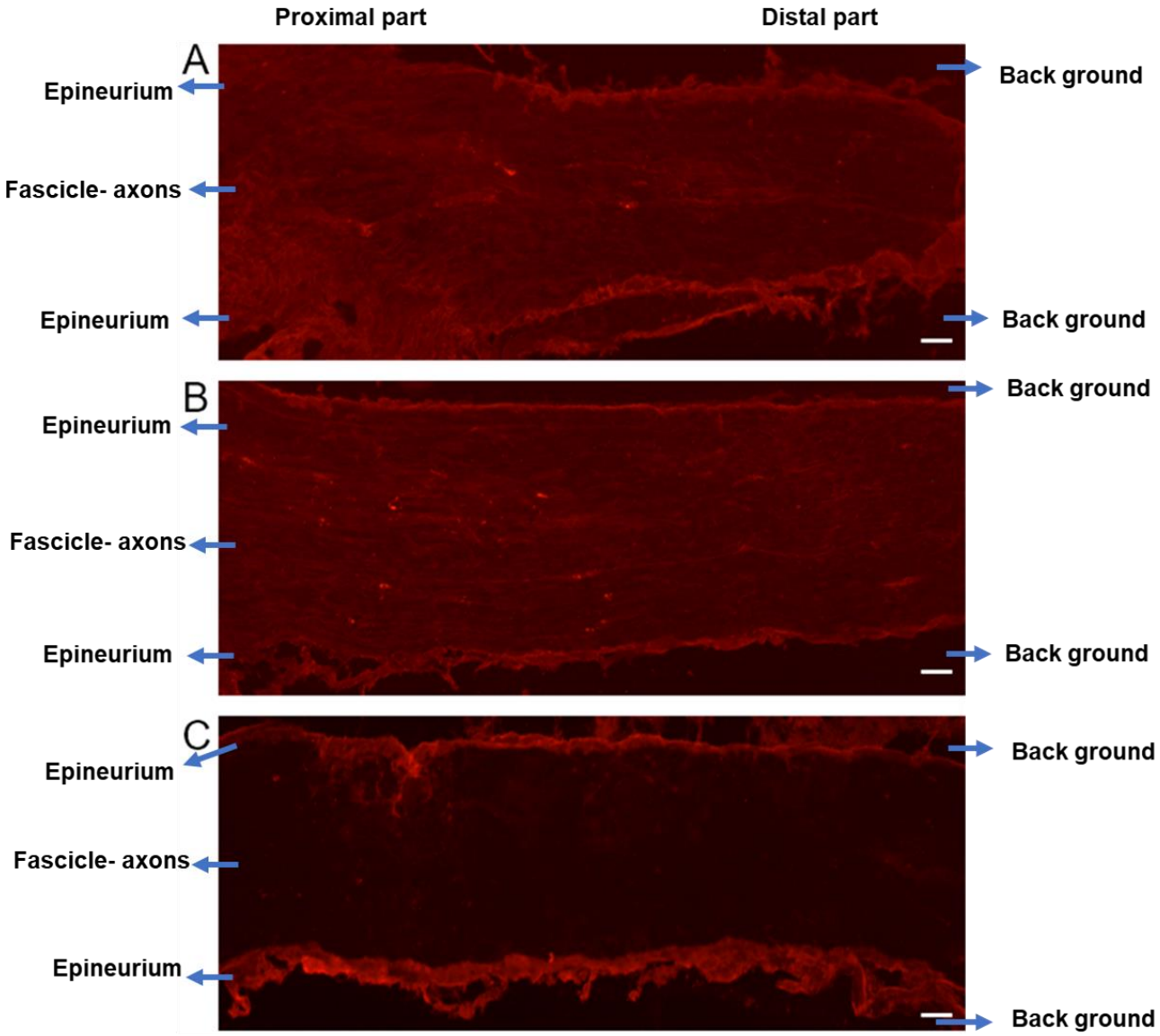

Figure 2.9: Microscopic images illustrating macrophage (CD68) antibody specificity and immunofluorescent labelling in uninjured mouse sciatic nerve. (A) Pre-absorption of primary antibody with blocking peptide shows negative macrophage staining. (B) Application of secondary antibody with omission of primary antibody shows negative macrophage staining. (C) Application of specific primary and secondary antibodies shows no macrophage staining. Scale bar= 100 µm.

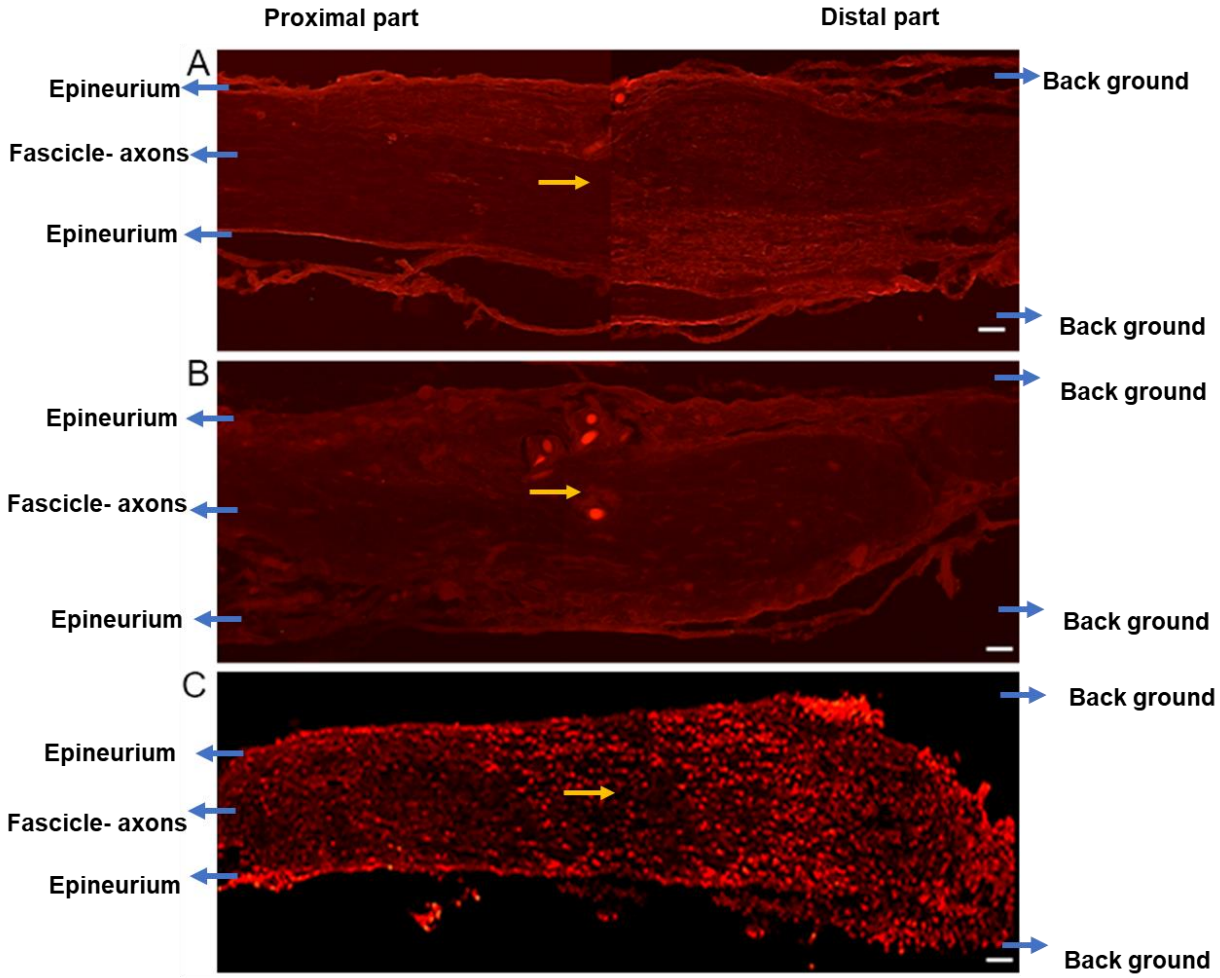

Figure 2.10: Microscopic images illustrating macrophage (CD68) antibody specificity and immunofluorescent labelling in mouse sciatic nerve six weeks after sciatic nerve injury and repair (yellow arrows: repaired site). The bright dots indicate active microphages. (A) Pre-absorption of primary antibody with blocking peptide shows negative macrophage staining. (B) Application of secondary antibody with omission of primary antibody shows negative macrophage staining. (C) Application of specific primary and secondary antibodies shows positive macrophage staining. Scale bar= 100 µm. (note: intense red dots in A and B images represent sutures materials).

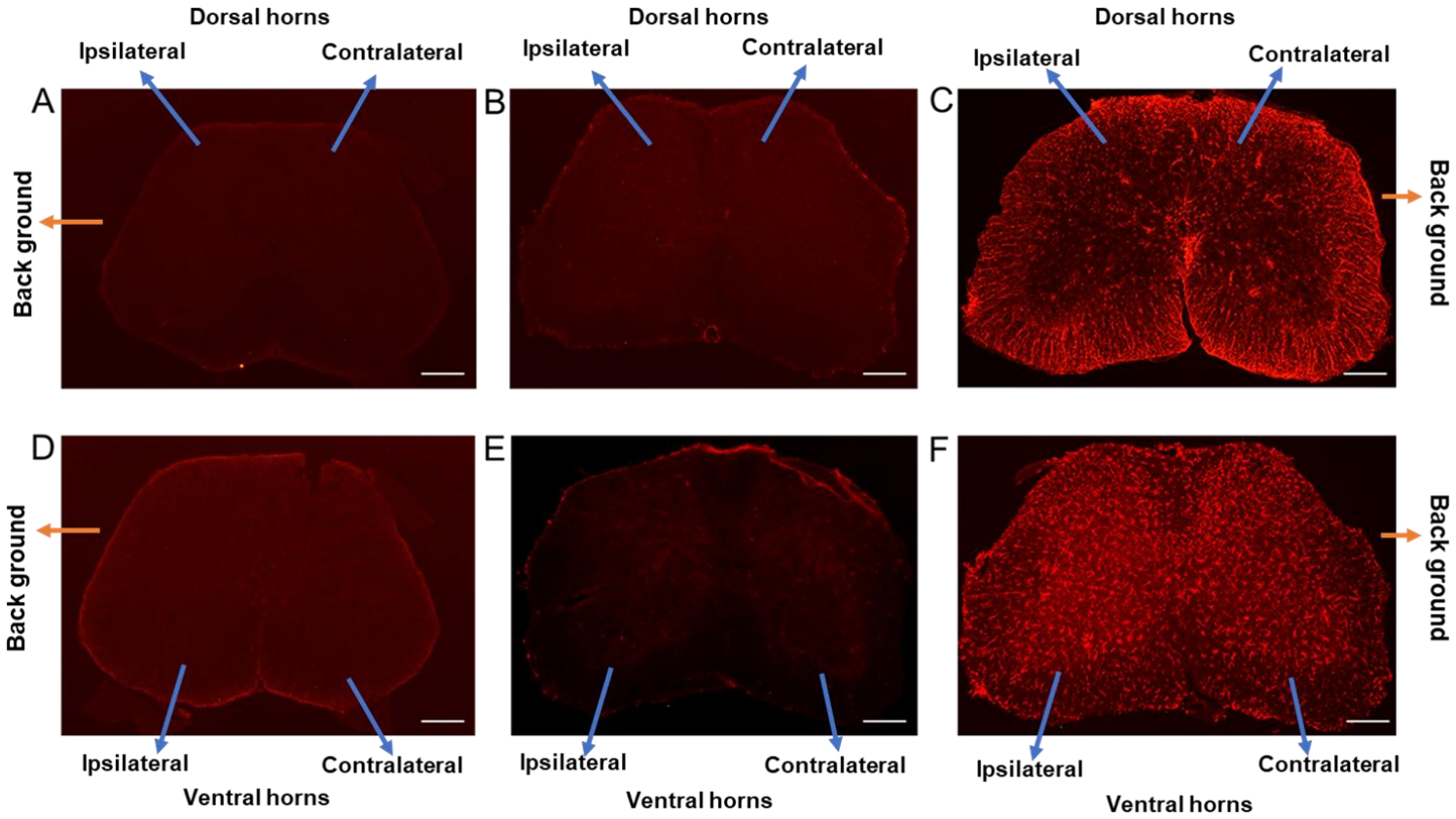

Figure 2.11: Microscopic images of spinal cords. Top: Astrocyte (GFAP) labelling in the L4 region of the mouse spinal cord. (A) Pre-absorption of primary antibody with blocking peptide shows negative astrocyte staining. (B) Application of secondary antibody with omission of primary antibody shows negative astrocyte staining. (C) Application of specific primary and secondary antibodies shows positive astrocyte staining. Bottom: Microglia (IBA-1) labelling in the L4 region of the mouse spinal cord. (D) Pre-absorption of primary antibody with blocking peptide shows negative microglia staining. (E) Application of secondary antibody with omission of primary antibody shows negative microglia staining. (F) Application of specific primary and secondary antibodies shows positive microglia staining. Scale bar= 25 µm. Blue arrows represent ipsilateral and contralateral horns to the site of nerve injury and repair.

2.2.7.2 Macrophage immunohistochemical labelling in the sciatic nerve

Sciatic nerve sections were stained for pan-macrophage marker CD68. The immunohistochemistry protocols applied for macrophages cell immunolabelling in the sciatic nerve for the rats and mice are illustrated in appendix D and E.

A set of three tissue slides (eg. slide set 1A, 2A, 3A – see Figure 2.5) per animal were taken out of the freezer and allowed to air dry for 1 hour, prior to immunohistochemical processing. The slides were placed in a glass staining trough and washed in phosphate buffered saline (PBS) containing 0.2 % Triton X-100, for 2 x 10 minutes at room temperature on a platform shaker. Immunostaining of the sciatic nerve tissues was achieved by inverting the slides and placing face down on a 24 well plate lid, and solutions applied and taken up through capillary action.

Each slide (a total of three sections) was blocked in 250 µl 20 % normal donkey (017-000-121, Jackson Immuno-Research Inc) or normal goat serum (S-1000, Vector Laboratories) diluted in 0.2 % PBS-T, in a moisture chamber for one hour at room temperature. Following tissue blocking, the sections were incubated with one of the primary antibodies mouse anti-rat CD68 (1:1500; MCA341GA; Serotec, Oxford, UK), or rat anti-mouse CD68 (1:1500; MCA1957GA; Serotec, UK) diluted in PBST and 5 % normal donkey serum, according to the animal species (listed in the Table 2.4), and placed in a moisture chamber overnight at 4 °C. Tissue sections were washed in PBS, 2 x 10 minutes, and either donkey anti-mouse CY3 (1:500; Jackson Immuno-Research, UK) or goat anti-rat CY3 secondary antibody (1:500; Jackson Immuno-Research, UK) applied for 90 minutes at room temperature, in a dark environment. Finally, slides were washed in PBS (2 x 10 minutes), mounted in vectashield mounting media (H-1000, Vector Laboratories) and cover-slipped.

2.2.7.3 Glial immunohistochemistry in the spinal cord

Spinal cord sections were stained for microglial marker IBA-1 and astrocyte marker GFAP. The immunohistochemistry protocols for microglial and astrocytes cells immune-labelling is illustrated in appendix F and G. Preparation of gelatine coated slides used in experiments is shown in appendix B.

Twelve sections per animal from the L4 region were selected for glial cell labelling. Spinal cord sections were stained using a free floating technique, carried out in a 24-well plate. Each tissue section per well plate, was blocked in 200 µl 10 % normal donkey serum (017-000-121, Jackson Immuno-Research Inc) in 0.2 % PBS-T, for one hour at room temperature on the platform shaker. Thereafter, IBA-1 goat polyclonal primary antibody (1:2500; Abcam ab5076) or GFAP rabbit polyclonal primary antibody (1:2000; ab7260 Abcam), in diluted in PBST and 5 % normal donkey serum was applied overnight at 4 °C. Following 2 x 10 minute washes in PBS, donkey anti-goat CY3 secondary antibody (1:500; Jackson Immuno-Research, UK) was applied to IBA-1 primary labelled sections and donkey anti- rabbit CY3 (1:500; Jackson Immuno-Research, UK) applied to GFAP primary labelled sections for two hours. The spinal cord tissues were finally washed in PBS 2 x 10 minutes, placed on gelatine coated slides, mounted with vectashield and cover-slipped.

2.2.8 Image acquisition and analysis of tissues

The processed sciatic nerve and spinal cord tissues were examined using a Zeiss Axioplan 2 fluorescence microscope (D-7082, Carl Zeiss, Germany) with Qimaging Retiga 1300R camera (MC 100, Carl Zeiss, Germany), fitted with filters to view fluorescent markers FITC (green fluorescence emitted at 490-500 nm maximum excitation wavelength) and Cy3 (red fluorescence emitted at 550-570 nm maximum

excitation wavelength). Fluorescent images were acquired using Image Pro-Plus software (Version 5; Media Cybernetics, Bethesda, MD), and immunofluorescent labelling analysed qualitatively and quantitatively.

Image processing of macrophage labelling in the sciatic nerve

Images of three sections of the injured sciatic nerve per animal were captured using the x10 objective, for qualitative and quantitative analysis of CD68 staining. The percentage area of positively stained tissue, 1.5 mm either side of the repair site, as represented by suture material, was included in the measured area of interest (Figure 2.12). To quantify the percentage area of macrophage CD68 labelling, Image-Pro Plus v.7 software was used. The area of interest highlighted by drawing green line to exclude epineurium. The levels of immunoreactivity of the cells were determined, by selecting thresholding of images to detect labelled structures and determine the percentage area fraction covered (Figure 2.13). Then, images brightness and contrast were adjusted to make the images similar to that observed in the fluorescent microscope. Each reading was taken three times, and the mean was taken.

Image processing of glial cell labelling in spinal cord

Images of three stained spinal cord sections per animal were captured using the x10 objective for qualitative analysis and x40 objective for quantitative analysis of astrocytes and microglial immunoreactivity in the lumbar spinal cord (L4 region). The percentage area of GFAP and IBA-1 labelling was measured as ratio in ipsilateral versus contralateral sides in the dorsal and ventral horns, per animal (Figure 2.14).

To quantify the percentage area of Iba-1 and GFAP labelling, Image-Pro Plus v.7 software was used. The percentage area of glial labelling calculated by selecting area of interest and then activation areas highlighted by pink, while the remaining areas

would be highlighted by yellow (Figure 2.15). The brightness and contrast of the images were adjusted to make the images similar to that observed in the fluorescent microscope. Each reading was taken three times, and the mean was taken.

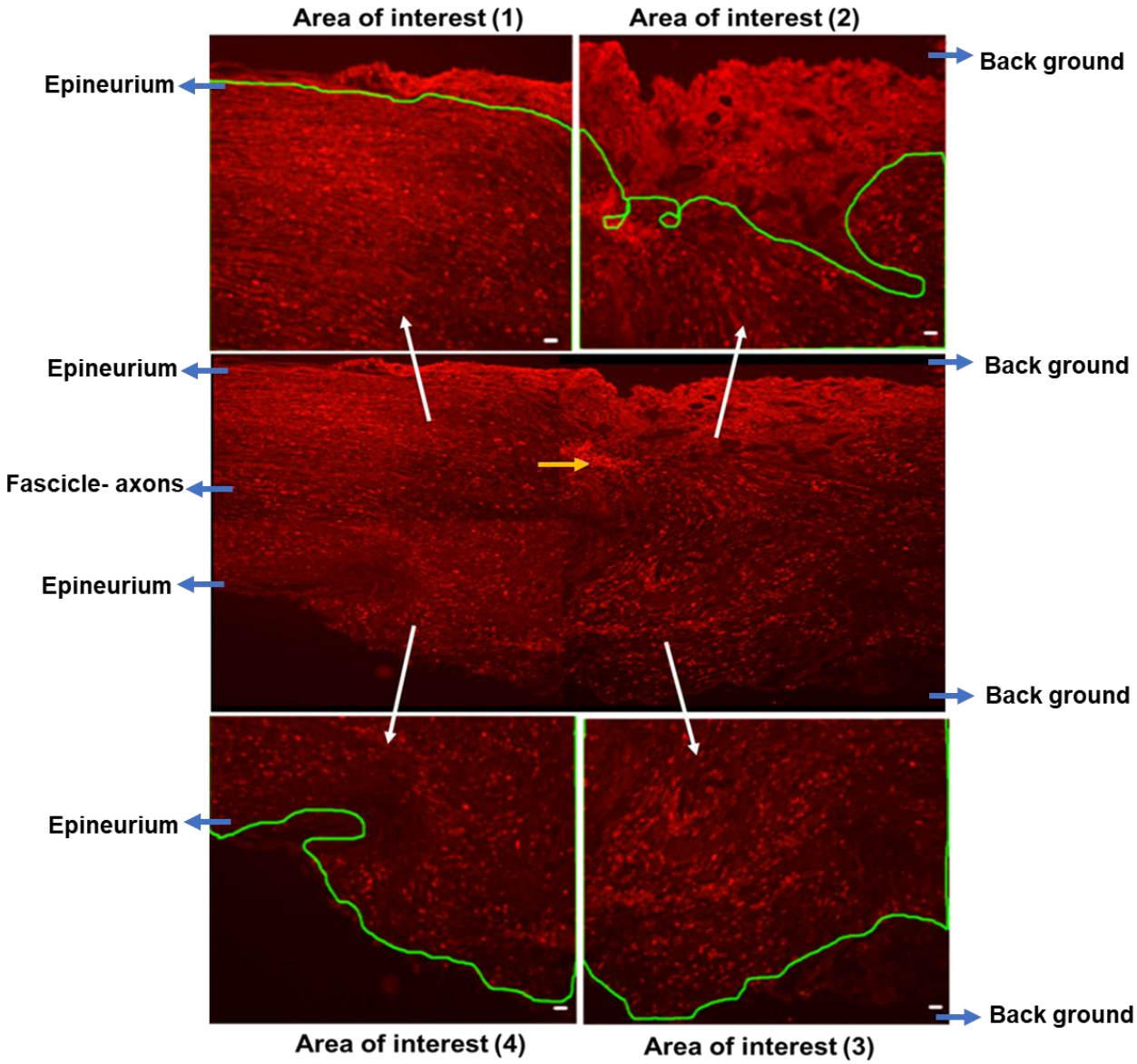

Figure 2.12: Microscopic images illustrating areas of interest measured and exclusion of epineurium, for quantitative analysis of percentage area of CD68 staining in sciatic nerve. The bright dots indicate active microphages. Yellow arrow indicated repaired site (suture materials). Scale bar= 100 μm.

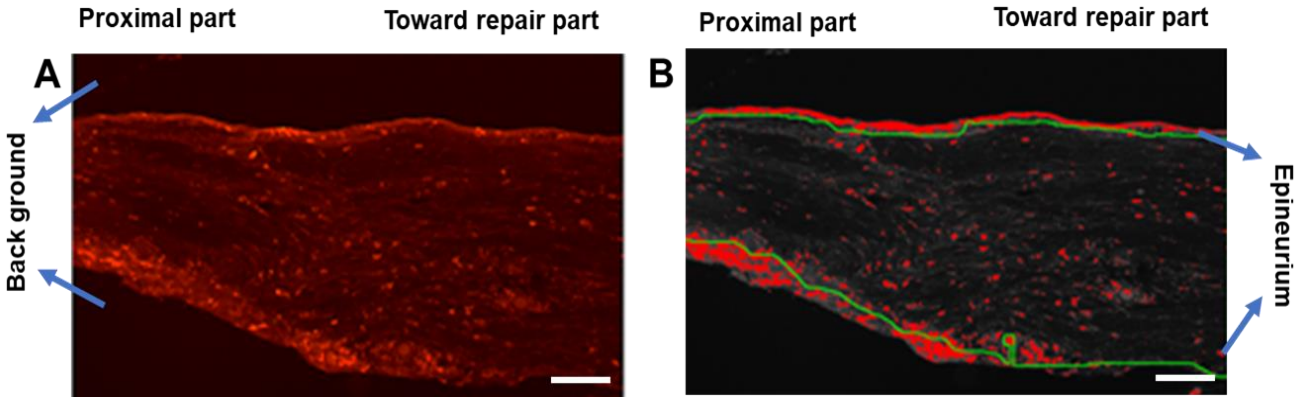

Figure 2.13: Analysis of a proximal part of the injured sciatic nerve and area of interest highlighted by drawing green line to exclude epineurium. A) The activation area (the bright dots). B) Highlighted activation area (area of interested by pink) and grey background area. The ratio of activation area (pink) to the selected area (grey) is calculated. Scale bar= 100 µm.

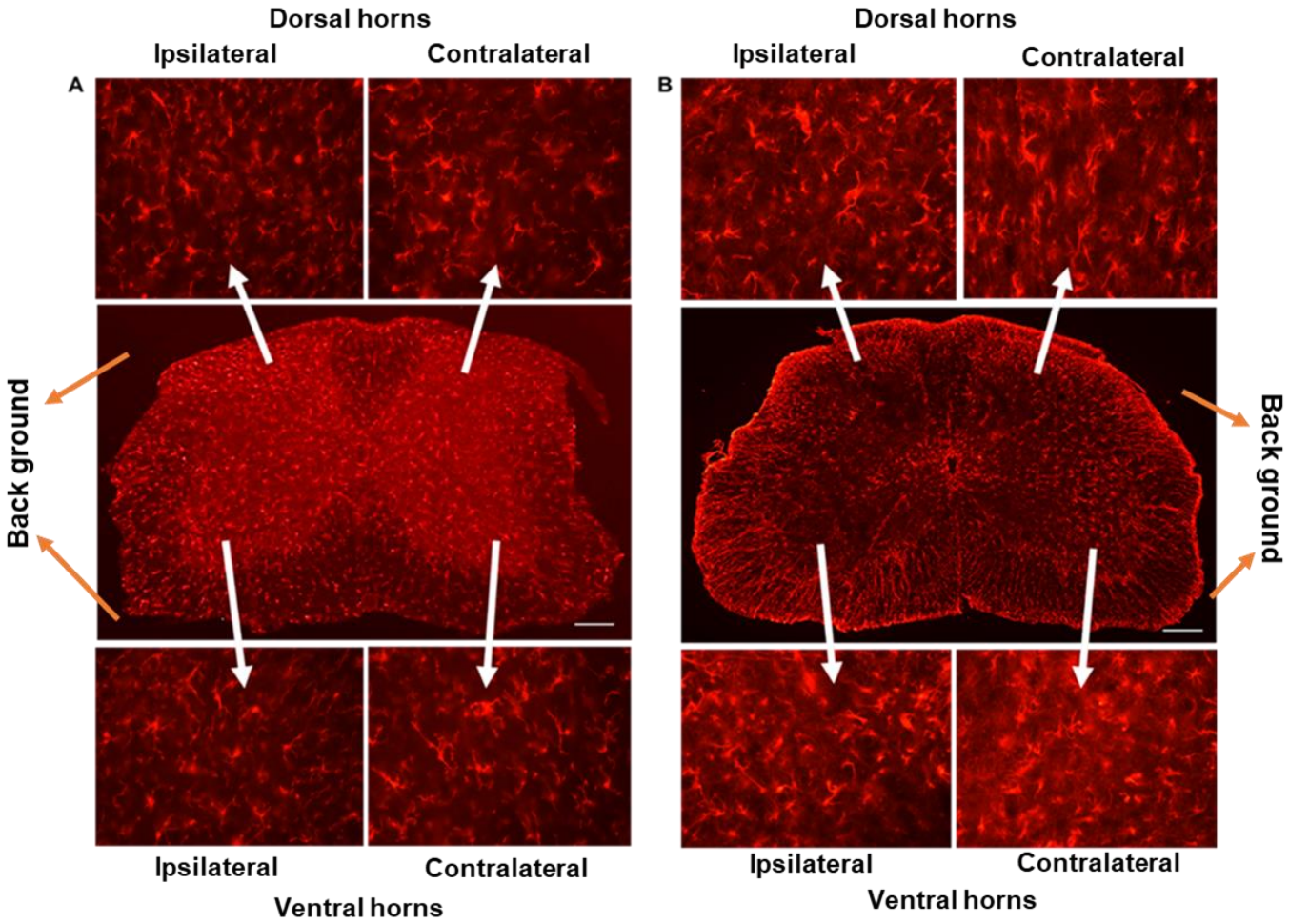

Figure 2.14: Microscopic images of spinal cord sections illustrating areas measured for quantitative analysis of percentage area of IBA-1 (A) and GFAP (B) glial cell labelling. white arrows indicated corresponding areas of interest and showing hypertrophied and amoeboid glial cells. Scale bar= 25 µm.

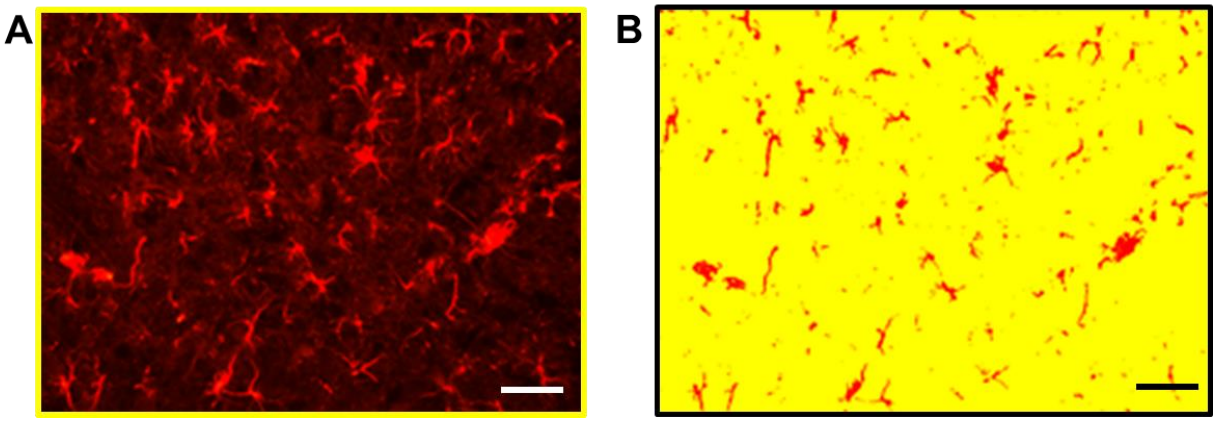

Figure 2.15: Analysis of a region of spinal cord. A) The activation area (the bright dots). B) Highlighted activation area (area of interested by pink) and background (yellow). The ratio of activation area (pink) to the entire picture (yellow) is calculated. Images showing hypertrophied and amoeboid glial cells. Scale bar = 25 µm.

2.2.9 Axon tracing

YFP-H mice were used for assessment of nerve regeneration following nerve injury and repair was based on a method described by Harding et al. (2014) and Pateman et al. (2015). YFP-H mice express a yellow fluorescent protein in their neurons which enables direct tracing of individual axons following nerve repair. The method measures sprouting index (SI), functional axon tracing and indicates the level of axon disruption across the conduit repair.

Images were captured by a laser scanning confocal microscope (Zeiss LSM510). Stacks of optical slices 10 µm thick were taken through the entire thickness of the nerve. Thereafter, for analysis the individual profile of each regenerating axons was reconstructed using Adobe Photoshop.

A reference point was determined by a line perpendicularly drawn across the nerve image starting at the interface of the proximal stump with the conduit repair (0.0 mm interval) (Figure 2.14). An additional point before the first interval was marked at -0.5 mm (uninjured region). Further intervals were determined on the nerve image from 0.0 mm to 4.0 mm.

The first parameter, sprouting Index was determined by counting the number of axons at each interval and dividing the axon number at -0.5 mm. An average value was used to minimise the estimation error.

Secondly, functional axon tracing was used to determine the percentage of axons that had successfully crossed the entire length of the conduit repair. A minimum of 75 % of the counted axons at each interval were traced in a backward direction either to the proximal stump or to the point of branching (Figure 2.15). Then, tracing was undertaken at all preceding intervals in turn to allow the percentage of axons from the

start interval represented at each interval to be calculated. Axons that successfully regenerated along entire conduit repair length were counted and the percentage of axons at all intervals was determined.

The third parameter is axon disruption pattern which has been correlated with low recovery of nerve function. Axons disruption primarily occurs shortly after the joining of the proximal stump conduit repair which was predetermined from the 0.0 mm to 1.5 mm intervals as described by Harding et al. (2014) and Pateman et al. (2015). Axons were typically traced across this region and their length measured to determine the average axon length as a proportion of the distance (i.e. 1.5 mm) (Figure 2.16).

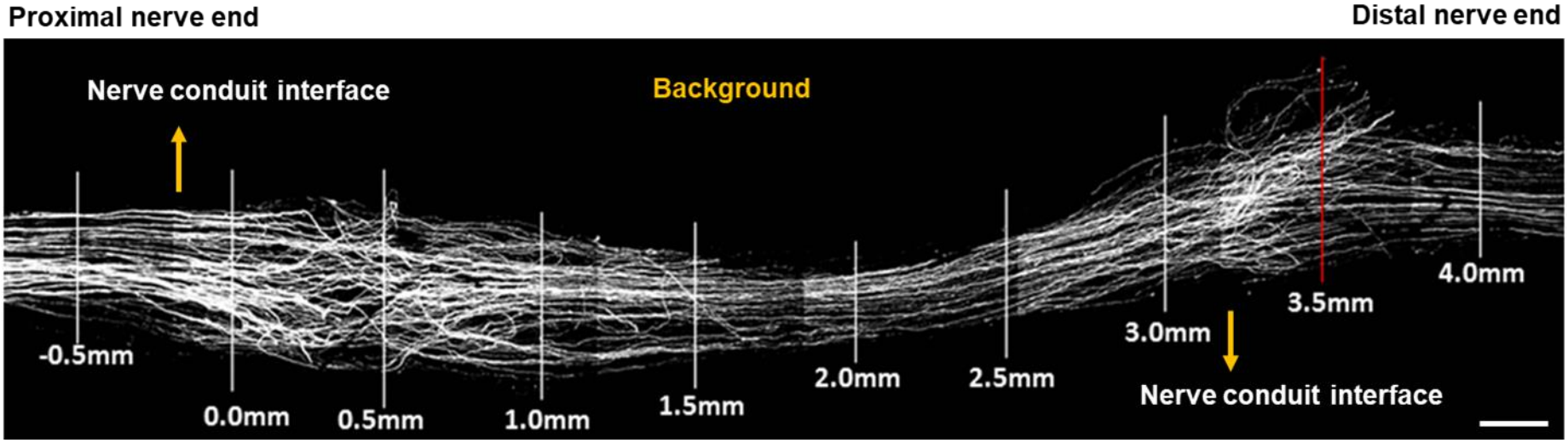

Figure 2.16: Confocal fluorescent microscopic image illustrates axons tracing from 4.0 mm interval position back to 0.0 mm. For sprouting index analysis, the images were marked at approximate 0.5 mm intervals originating from the point proximal nerve conduit interface to the point where axons had entered the distal nerve ending, with one additional interval marked at -0.5 mm prior to the first interval which represent uninjured axons. The number of axons at each interval were counted and the number of axons at each interval were divided by the number of axons counted at the -0.5 mm interval to give a sprouting index. Scale bar= 1.0 mm.

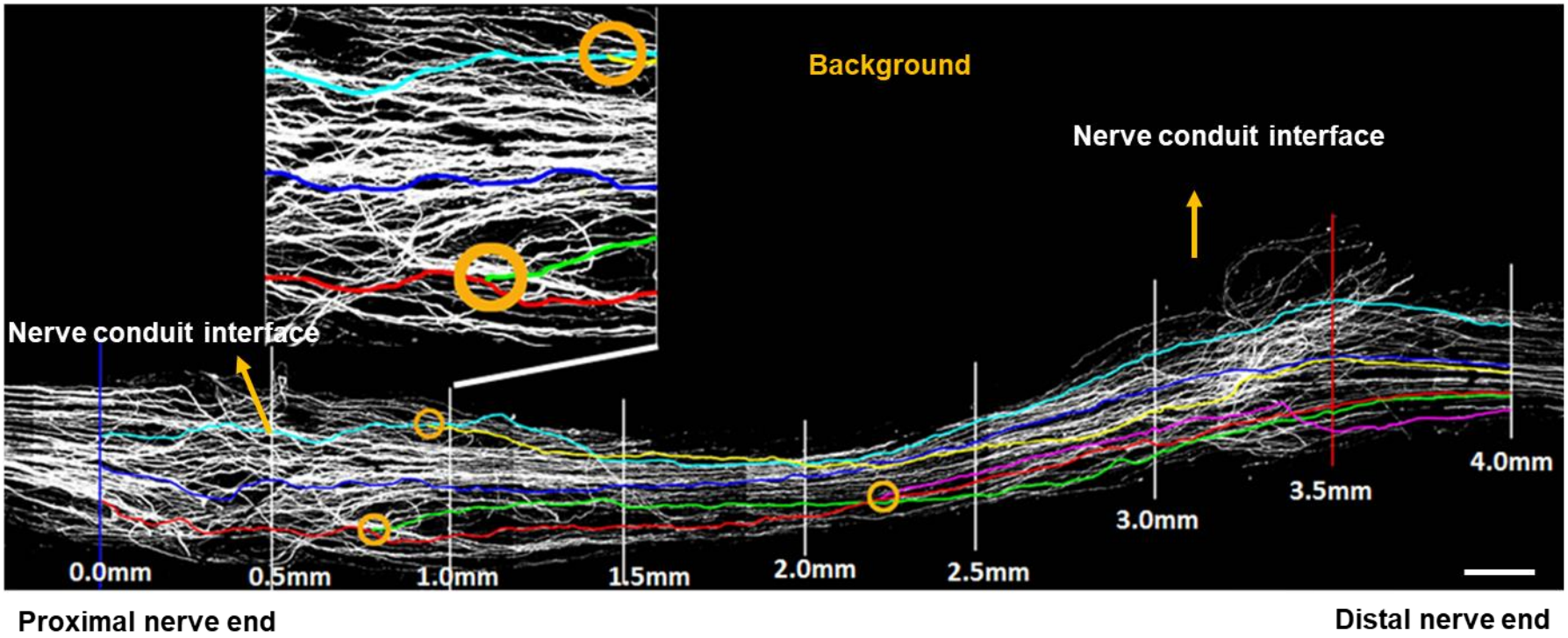

Figure 2.17: Confocal fluorescent microscopic image illustrates axon tracing from 4.0 mm intervals back to 0.0 mm to calculate percentage of axons crossed repair without branching or joining previously traced axons as highlighted with yellow circles. Axon tracing methods using Adobe Photoshop performed from the final interval back along the conduit repair to the first interval or a branch point with a previously traced axon, with a minimum of 75 % of the axons present traced. Scale bar= 1.0 mm.

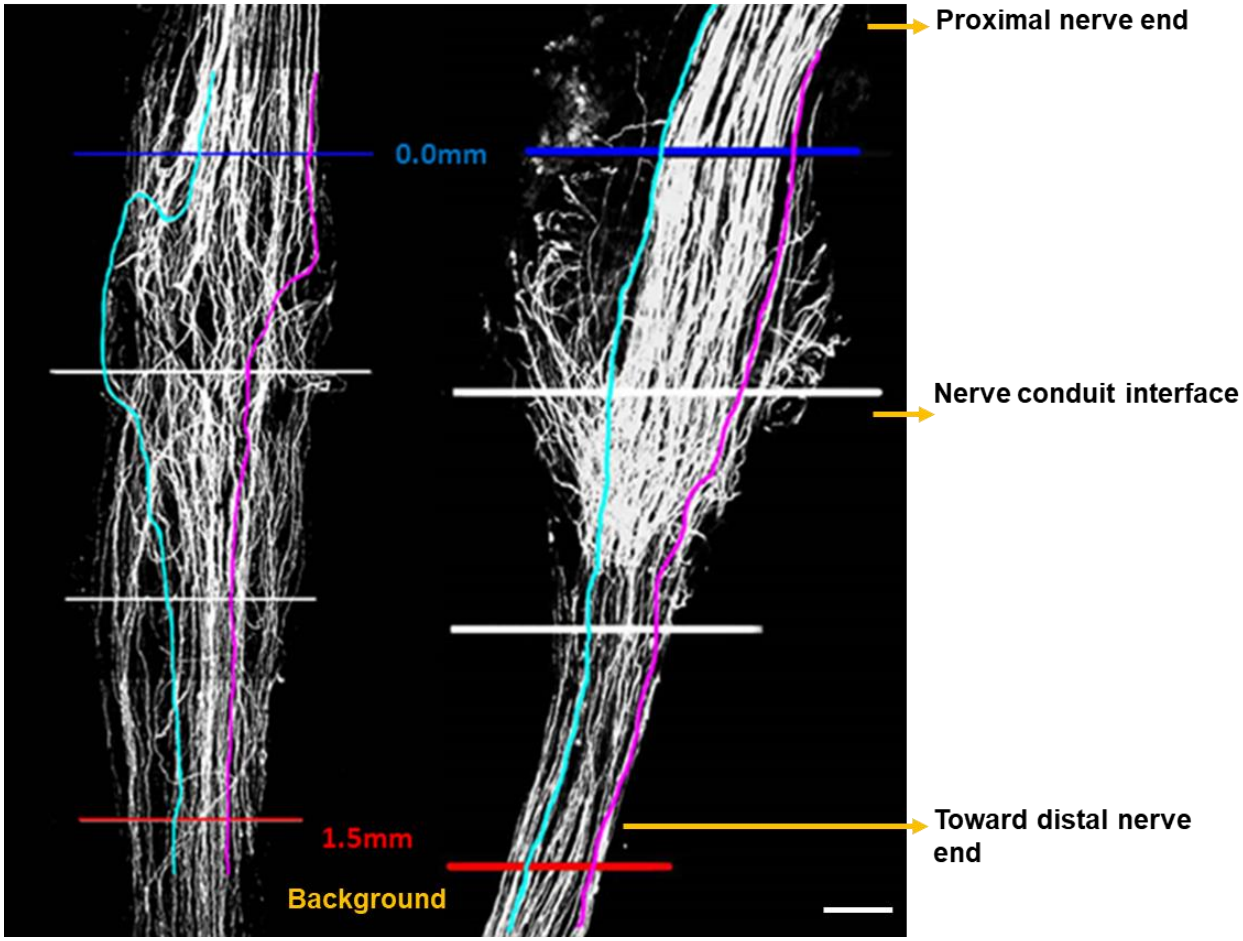

Figure 2.18: Confocal fluorescent microscopic image to determine an average increase in axon length (highlight axons disruption pattern). Traced axons from the 1.5 mm interval back to the 0.0 mm interval were measured and compared to the direct distance between intervals (An average increase in traced axon length between the 0.0 mm and 1.5 mm intervals was considered indicative of axon disruption between the central nerve end and conduit repair). Scale bar= 1.0 mm.

2.2.10 Poly-caprolactone conduit preparation, *in vitro* and *ex vivo* testing

Poly-caprolactone conduits used for this work were fabricated by Jonathan Field (PhD student) into 3-dimensional structures using microstereolithography in the laboratory of Dr. Fred Claeyssens at the University of Sheffield. Using microstereolithography conduits of 1 mm internal diameter, 250 µm wall thickness and 5 mm in length were manufactured for evaluation of axon regeneration in the sciatic nerve injury model in YFP- transgenic mice (Figure 2.17).

In vitro and *ex vivo* testing of Poly-caprolactone as a nerve guidance conduit were carried out by Dr. Christopher Pateman in the laboratory of Professor John Haycock at the University of Sheffield (Pateman et al., 2014). This revealed that cultured neuronal and DRG cells align along the topographical parallel channels which potentially enhances cellular adhesion and neurite outgrowth on the PCL surface. In addition, the grooves or channels act as a guide directing regeneration from the proximal toward the distal nerve end segment when used in vivo (Pateman et al., 2014).

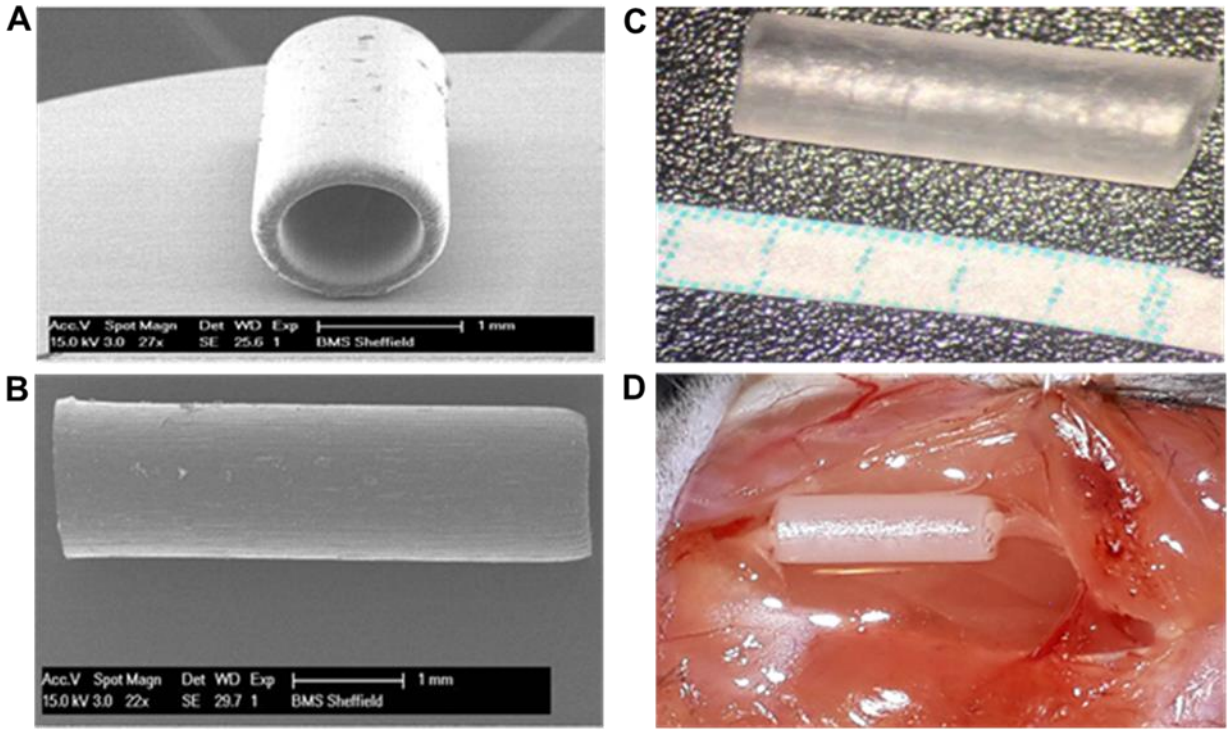

Figure 2.19: (A and B) Scanning electron microscopy images of PCL nerve guidance conduit. (C) An image of PCL nerve guidance conduit of 5 mm length. (D) Implantation of PCL nerve conduit for sciatic nerve in repair.

2.3 Sample size calculation

Calculation of sample sizes for this work was performed using Biomath online statistic package provided by division of Biomathematics/Biostatistics at Columbia University Medical Centre (http://www.biomath.info/power/index.html). Outcome measures considered in this research were based on results from previous experiments carried out in our laboratory (Ngeow et al., 2011b, and Pateman et al., 2015).

Sample size calculations were undertaken for different outcome measures using a power of 80 % and significance level (alpha) of 0.05 (two-tailed) and these measures are described below. The sample size chosen in Chapter 3 in the initial study was based on previous nerve injury and repair studies carried out by Atkins and colleagues (2006). Atkins et al. (2006) examined the hypothesis that the application of a scar-preventing agent to a nerve repair site would enhance function and regeneration of nerve axons fibres following administration of a scar reducing agent (TGF-b1 and TGF-b2) after repair. Out of 18 adult Sprague-Dawley rats, 6 animals acted as sham-control and the remaining 12 animals had their nerve sectioned and immediately repaired, with six receiving an anti-scarring agent. Data from this study revealed that the mean percentage of collagen fibres was not significantly different from that in the sham controls (3.45 %, p =0.15; Kruskal-Wallis multiple comparisons test), while CAP ratio was significantly reduced following administration of TGF-b1 and TGF-b2 (0.23, p =0.042). Sample size of studies in Chapters 4, 5 and 6 were calculated on standard deviations extracted from the initial and previous work in related studies (Ngeow et al., 2011b, and Pateman et al., 2015). Sample size calculation to detect significant differences between two groups for several parameters were measured using a power of 80% and significance level (alpha) of 0.05 (two-tailed).

The main parameters measured revealed the following information to determine the number of subjects to be studied;

A) Percentage of CD68 area staining at site of nerve injury and repair

The mean value of CD68 percentage area staining of two groups (for example; sterile water versus IL-1 cytokine antagonist) used from the initial study, were 22.6 % and 17.08 %. Using the mean standard deviation of 3.90 %, the difference of 5 % between the two treatments would be detected with groups of 9 animals (unpublished data from Chapter 3).

B) The extent of axon regeneration across the repaired site after nerve injury

The mean value of axon regeneration of 0.45 % and 0.29 % as shown by compound action potential ratio between two groups were extracted from previous work (Ngeow et al., 2011b). Using the mean standard deviation of 0.113 %, the difference of 0.16 % between the two treatments would be detected with groups of 9 animals.

c) Percentage of paw print areas following recovery of nerve injury and repair

The mean value of paw print areas of 0.74 % and 0.24 % as shown by gait analysis between two groups were taken from previous work (Ngeow et al., 2011b). Using the mean standard deviation of 0.353 %, the difference of 0.49 % between the two treatments would be detected with groups of 9 animals.

D) Extent of axon sprouting profile in nerve conduit guidance repair

The values of sprouting index (170.4 % vs 145.4 %), functional tracing (49.9 % vs 49.2 %) and axon disruption (21.5 % vs 11.4 %) between the two groups was shown by assessment of axon sprouting profile in nerve conduit repair in YFP-H mouse model (Pateman et al., 2015). Using the mean standard deviations of 17.67 %, 0.494 % and

7.14 %, the differences of 25 %, 0.69 % and 10 %, for sprouting index, functional axon tracing and axon disruption between the two treatments would be detected with groups of 9 animals.

Detectable differences with reasonable effect size would be achievable with sample sizes of 9 subjects, however, sample size in each treatment group is increased by 10 % to account for any attrition such as failed repairs or death of animals. Final adjusted sample size was 10 animals in each experimental group.

2.4 Statistical analysis

Statistical analysis was performed using GraphPad Prism7 (GraphPad Software, Inc, USA). In the initial study, multiple comparisons of immunohistochemical data between groups were performed using Dunn's-Kruskal-Wallis multiple comparisons test to the difference in mean percentage area of CD68 immunoreactivity in the sciatic nerve tissues of all experimental groups. Differences between groups were considered significant if $p \leq 0.05$. In Chapters 4,5 and 6, statistical comparisons in immunohistochemistry and electrophysiology recordings and the average axon length were performed using a two-tailed t-test. In addition, two-way repeated measures ANOVA was used for comparison between the groups to detect any difference in sprouting index and functional axon tracing and changes in gait parameters in Chapter 6. Quantitative data are expressed as mean ± SEM. Statistical significance between the groups was established if $p \leq 0.05$. Data in graphs are presented as mean ± SEM.

CHAPTER 3

Peripheral application of cytokines antagonist at the site of nerve injury and repair: preliminary immune-modulation response in peripheral nerve injury

3.1 Introduction

Nerve injury and repair often results in a functional recovery that is rarely satisfactory and often incomplete. Therefore, it is essential to understand the complex sequence of events and processes that follow nerve injury (Rodríguez et al., 2004; Stefano et al., 2013).

It is well documented that the inflammatory changes occurring in an injured peripheral nerve are regulated by the release of endogenous cytokines (Fregnan et al., 2012; Bastien and Lacroix, 2014), which are crucial to Wallerian degeneration (WD) and consequent neural regeneration. These include; IL-1 and TNF-α, cytokines and opposing anti-inflammatory cytokines such as IL-10. The regulation of these cytokines has been demonstrated to be vital to neuronal axon healing and the regeneration process (Fregnan et al., 2012; Bastien and Lacroix, 2014).

After peripheral nerve injury, pro-inflammatory cytokines are upregulated in the first phase of WD promoting the recruitment of macrophages and other immune cells. In addition, anti-inflammatory cytokines such as IL-10 are upregulated helping to reduce the initial inflammatory response (Taskinen, 2000; Gaudet et al., 2011). Consequently, anti-inflammatory cytokine action helps to accelerate the end of the degeneration stage and initiate the regeneration and healing phase to establish the recovery process of injured peripheral nerves.

It is generally agreed that cells such as Schwann cells and macrophages play a crucial part during Wallerian degeneration (Fregnan et al., 2012; Bastien and Lacroix, 2014). These cells clear degenerated material by phagocytosis and additionally, produce several cytokine mediators and neurotrophic factors that support nerve cell regeneration. It has been suggested that pro-inflammatory cytokines IL-1 and TNF-α,

are expressed as proactive proteins which are then split into their active form to regulate the immune inflammatory response by activation of networks of other cytokines and neurotrophic factors. Moreover, these pro-inflammatory cytokines produce their effects by acting on receptors that are expressed either on neurons or other neighbouring cells (Thacker et al., 2007; Fregnan et al., 2012; Bastien and Lacroix, 2014).

TNF-α acts on TNF-R1 and -R2 receptors which are both expressed on glial cells and neurons. After constriction nerve injury it was observed that, TNF-α expressed at an injury site played a significant role in the nerve degeneration and regeneration process by regulating the recruitment of macrophages, and subsequent production of inflammatory cytokines such as IL-1 (Sommer et al., 2001; George et al., 2005).

Several *in vivo* and *in vitro* studies have investigated the role of TNF-α following peripheral nerve injury. Knockout studies demonstrate that following sciatic nerve injury, mice lacking TNF-α protein displayed poorer functional nerve recovery, due to impaired cell infiltration and delayed myelin material clearance at the time of regeneration of damaged axons (Nadeau et al., 2011). Other studies have reported that TNF-α injections are associated with the development of neuropathic pain (Kato et al., 2009; Kato et al., 2010), and these *in vivo* studies revealed the direct effect of TNF-α antagonist (Etanercept) on attenuating pain-related behaviour in a dose-dependent regime after crush sciatic model of nerve injury. This highlights the critical role that TNF-α plays in direct chemoattraction of immune cells and the development of neuropathic pain following peripheral nerve injury.

IL-1 cytokine is an important pro-inflammatory cytokine that exists in two forms (IL-1 α and IL-1 β) with different biological effects at a cellular level (Fregnan et al., 2012;

Bastien and Lacroix, 2014). It is well documented, that after nerve injury, levels of IL-1 are rapidly upregulated by Schwann cells as they lose contact with their corresponding axons, and IL-1 upregulation is involved in the development of neuropathic pain following peripheral nerve injury (Sommer et al., 2001; Ren and Torres, 2009). IL-1 acts by binding to the IL-1 receptor accessory protein (IL-1 RAcP) of IL-1RI which has been proposed to stimulate surrounding glial cells and subsequently sensitize central neurones (Wolf et al., 2006; Bastien and, Lacroix, 2014). Therefore, it appears that IL-1 cytokine is a key mediator in the interaction between microglia and neurones, and blocking the action of its IL-1 receptor 1(IL-1R1) has been considered as a therapeutic approach in preventing development of neuropathic pain (Sommer et al., 2001; Ren and Torres, 2009).

Lastly, IL-10 a powerful anti-inflammatory cytokine, is produced by many different cell types including macrophages, T cells, mast cells and fibroblasts (Gaudet et al., 2011; Bastien and Lacroix, 2014). It has been observed that IL-10 plays a vital role in regulating production of the pro-inflammatory cytokines and subsequent downregulation of recruitment of immune cells following peripheral nerve injury (Gaudet et al., 2011; Bastien and Lacroix, 2014; Kwilasz et al., 2015). Several signalling pathways have been suggested to enhance or suppress IL-10 transcription which include MAPK and NFkB in immune cells. It is known that IL-10 acts through its 1L-10 receptor-1 (1L-10R1) that is expressed on the surface of immune cells, and as a result reduces the immune inflammatory response and resultant tissue damage. In addition, this anti-inflammatory cytokine is believed to exert a neuroprotective function centrally by decreasing glial cell activity and promoting neuronal cells survival after injury (Gaudet et al., 2011; Bastien and Lacroix, 2014; Kwilasz et al., 2015). After injury, it has been shown that expression of IL-10 is upregulated within a few hours

and peaks at 7 days, following macrophage infiltration at the site of injury (Taskinen et al., 2000). There is clear evidence that administration of IL-10 at the time of nerve repair reduced as fibrous tissue formation at the site of nerve injury and repair and, showed better regeneration in comparison to control groups (Atkins et al., 2007).

3.2 Aim and objectives

The aim of this study was to investigate the effects of novel pro-inflammatory cytokine interleukin-1 antagonist (Anakinra), and anti-inflammatory cytokine IL-10 and combination of TNF-α antagonist (Etanercept) and anti-inflammatory cytokine IL-10, on inflammatory reaction at the site of peripheral nerve injury, in order to establish their possible contribution to the reduction or prevention of neuropathic pain, and determine their potential effects on nerve regeneration.

3.3 Hypothesis

Application of anti-inflammatory agents at the time of nerve repair may reduce inflammation at the repair site and subsequently prevent development of neuropathic pain.

3.4 Materials and methods

Chapter 2 details the experimental materials, anaesthesia and methods employed in this series of experiments. A schematic overview of the experimental design of this study is shown in Figure 3.1.

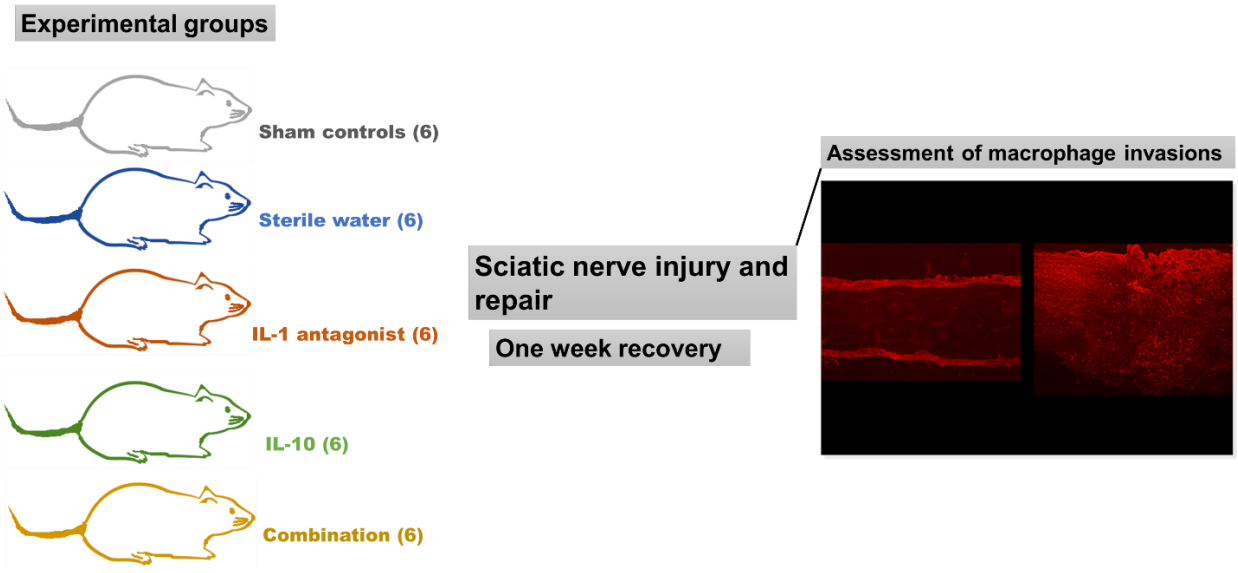

Figure 3.1: Illustration of the experimental design, investigating the effect of a range of anti-inflammatory cytokines in an *in vivo* model of sciatic nerve injury and repair.

Experimental groups

A total of thirty male Sprague Dawley rats (8 weeks old--weights 220 g–300 g) were used in this study. Animals are divided into five groups. In four groups, animals received sciatic nerve injury and repair and were randomly assigned different treatments: Interleukin-1 antagonist (n=6), Interleukin-10 treatment (n=6), combination treatment (IL-10 and TNF-α antagonist) (n=6) and sterile water (n=6). The fifth group of animals acted as sham controls and had their sciatic nerves exposed and dissected free (n=6). Preparation and concentration of treatment agents is detailed in Chapter 2, section 2.2.2.

Briefly, the animals were anaesthetized with 2-3 % isoflurane administrated at a rate of 2 litres per minute, and the left sciatic nerve exposed. 40 µl of assigned treatment agent was injected under the epineurium, and the nerve sectioned and immediately repaired. 60 µl of the remaining treatment agent was injected intramuscularly around the nerve repair, and the wound layers closed with 4/0 vicryl sutures. The animals received a subcutaneous injection of buprenorphine (0.05 mg/kg) and were left to recover for a period of seven days.

Following a recovery period of seven days, the animals were anaesthetised by intraperitoneal injection of 0.5 ml of sodium pentobarbital (20 % w/v) and perfusion-fixed intracardially. The left sciatic nerves were removed and post fixed in 4 % paraformaldehyde for 4 hours and stored overnight in 30 % sucrose overnight. The nerves were frozen down, sectioned longitudinally at a thickness of 14 µm and serially collected onto PDL coated slides. The sections were incubated with primary antibody raised in mouse against rat CD68, which was visualised with a fluorescent secondary antibody donkey anti-mouse CY3 (described in section 2.2.7.2).

Images of three non-overlapped nerve sections were captured using the x20 objective, and an area of interest traced and analysed 1.5 mm either side of the repair site, as previously described in Chapter 2.

To quantify the percentage area of macrophage CD68 labelling, the area of interest highlighted, and immunoreactivity of the cells were determined by selecting thresholding of images to detect labelled structures (See Chapter 2, section 2.2.8). Each reading was taken three times, and the mean was taken.

The investigator analysing the specimens was blinded to treatment received in order to avoid experimental bias.

Multiple comparisons of data between the experimental groups were performed using Dunn's-Kruskal-Wallis multiple comparisons test to compare the difference in mean percentage area of CD68 immunoreactivity in the sciatic nerve tissues of all experimental groups. Differences between groups were considered significant at $p < 0.05$. Statistical analysis was performed using Microsoft Excel 2010 and GraphPad Prism7 (GraphPad Software, Inc, USA).

3.5 Results

Qualitative Observations

The primary antibody specificity was tested and detailed in Chapter 2; section 2.2.7.1. The results confirmed that pre-absorption of mouse anti-rat CD68 with its respective antigen, and omitting it from the staining protocol, showed no positive CD68 labelling in the control and injured and repaired sciatic nerve tissue.

The width of the sciatic nerve in all injured animals appeared to be significantly greater than that in the sham-control group (Figure 3.2 and 3.3). Seven days following the

sciatic nerve transection and repair there was abundant positive CD68 macrophage labelling across the breadth of the injury site, particularly around the repair sutures, with less immunoreactivity evident either distal or proximal to the repaired site (Figure 3.2, A).

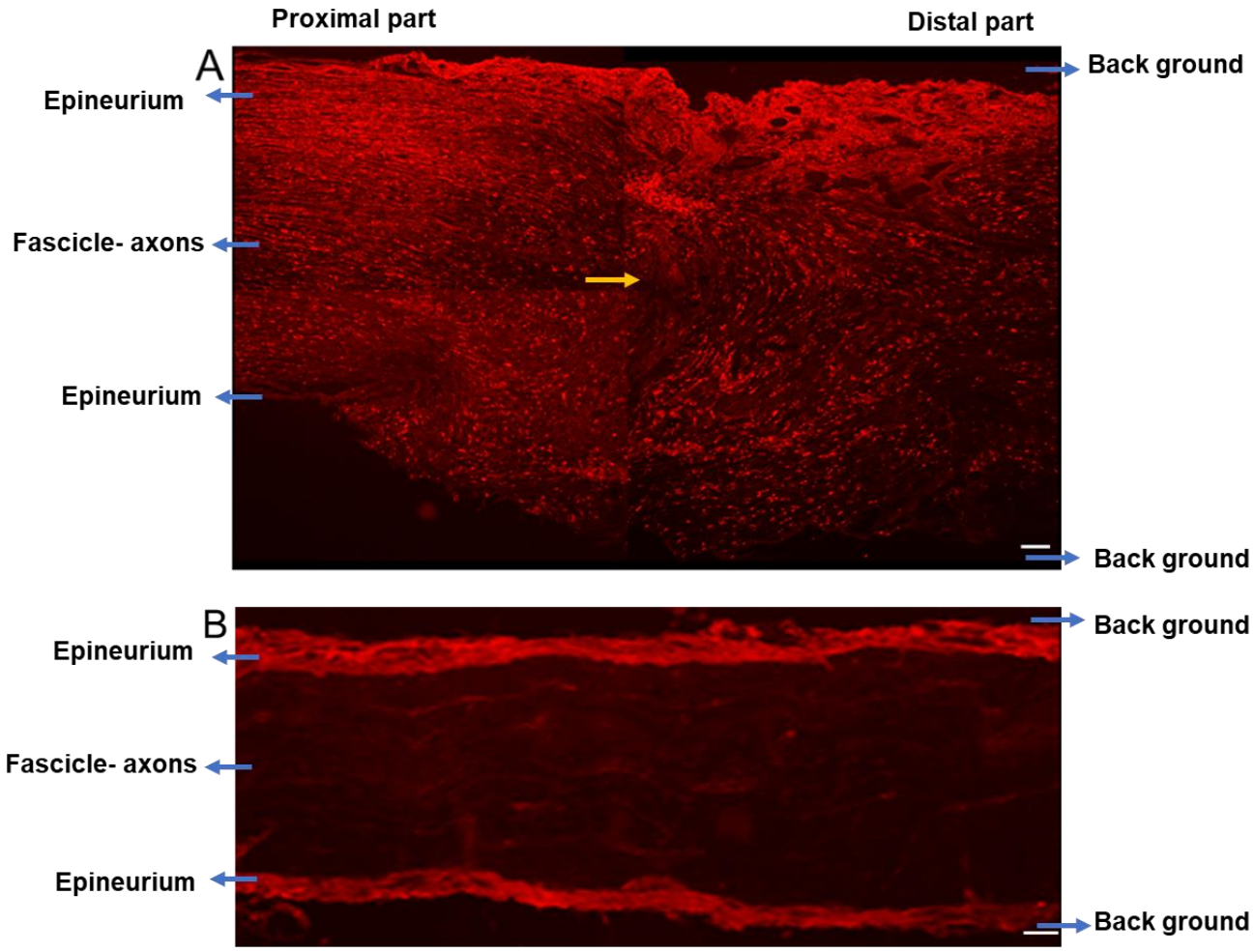

Figure 3.2: Immunofluorescent images illustrates macrophage infiltration and CD68 immunoreactivity in sciatic nerve following injury and repair. A: Montage of four images of an injured and repaired rat sciatic nerve (yellow arrow indicate repair site). B: Image of an uninjured rat sciatic nerve. Scale bar= 100 µm.

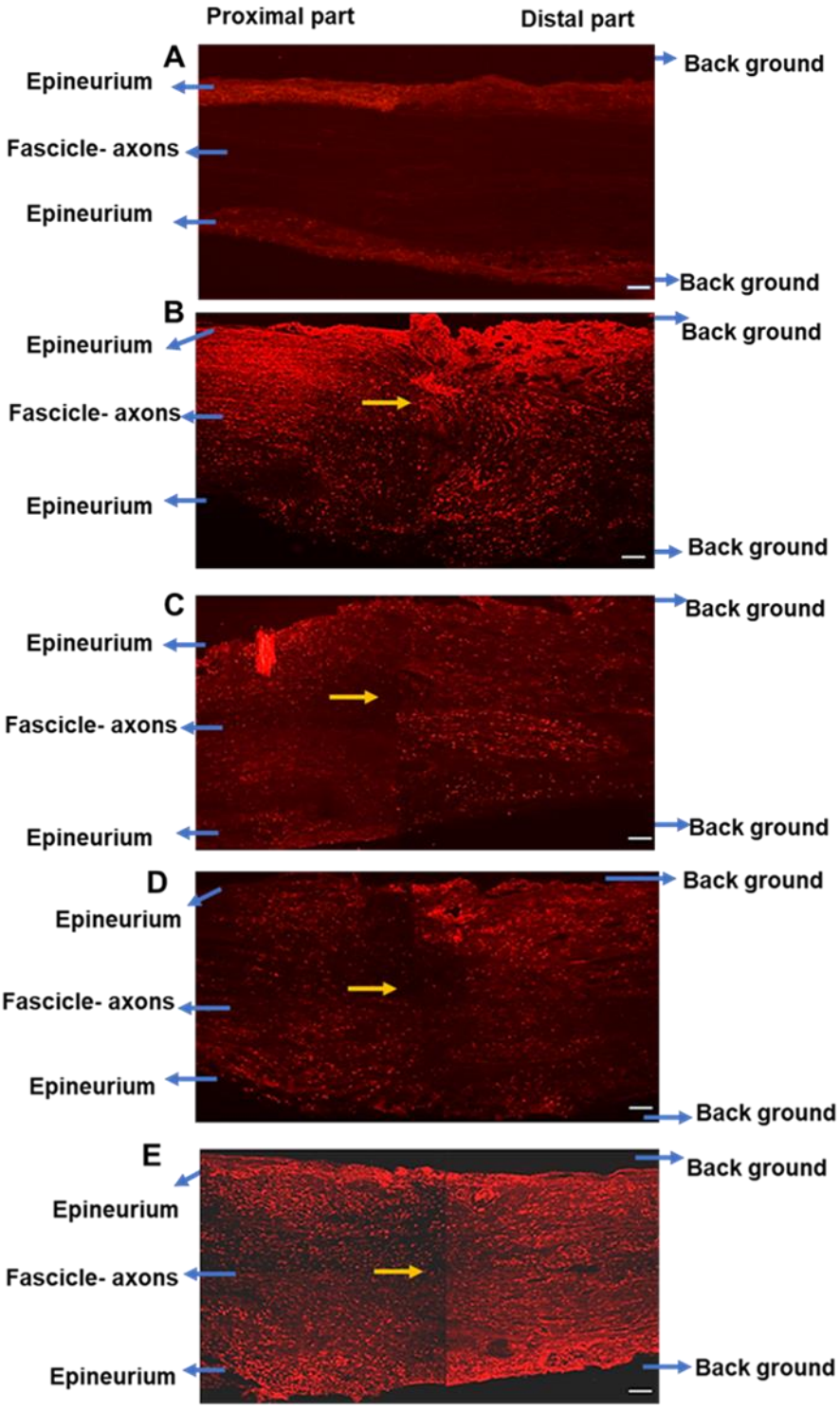

Figure 3.3: Immunofluorescent images illustrating macrophage infiltration and immunofluorescent CD68 expression in sciatic nerve, 7 days following peripheral nerve injury and repair, and following administration of different treatments (Bright dots indicate active microphages). A: Sham. B: sterile water. C: IL-1 antagonist. D: IL-10. E: Combination. Immunoreactive labelling for CD68 macrophage marker was observed in all repair groups (yellow arrows indicate repair site). Scale bar = 100 µm.

Quantitative Observations

Seven days following sciatic nerve injury and repair, immunoreactive labelling for CD68 macrophage marker was observed in all 5 groups of animals. Levels of CD68 labelling appeared low at the site of nerve injury and repair 7 days following application of IL-1 antagonist and IL-10 compared to the other groups (Figure 3.3). Quantitative analysis revealed that groups injected with sterile water (p=0.006; 22.6 (-19.17); Dunn's-Kruskal-Wallis multiple comparisons test) or combination treatment drugs (p=0.009; 22.08 (-18.58), Dunn's-Kruskal-Wallis multiple comparisons test), had a significant increase in macrophage expression at the injury site compared to the sham group (3.5) (Figure 3.4). However, following administration of IL-10 (p=0.990; 18.33 (-14.83); Dunn's-Kruskal-Wallis multiple comparisons test) or IL-1 antagonist (p=0.990; 17.08 (-13.58), Dunn's-Kruskal-Wallis multiple comparisons test), macrophage immunoreactivity at the site of repair was not significantly different to the sham group (Figure 3.4). Overall, the mean macrophage labelling following epineurial administration of IL-10 and IL-1 antagonist treatment were not different from the sham group, 7 days following nerve injury and repair.

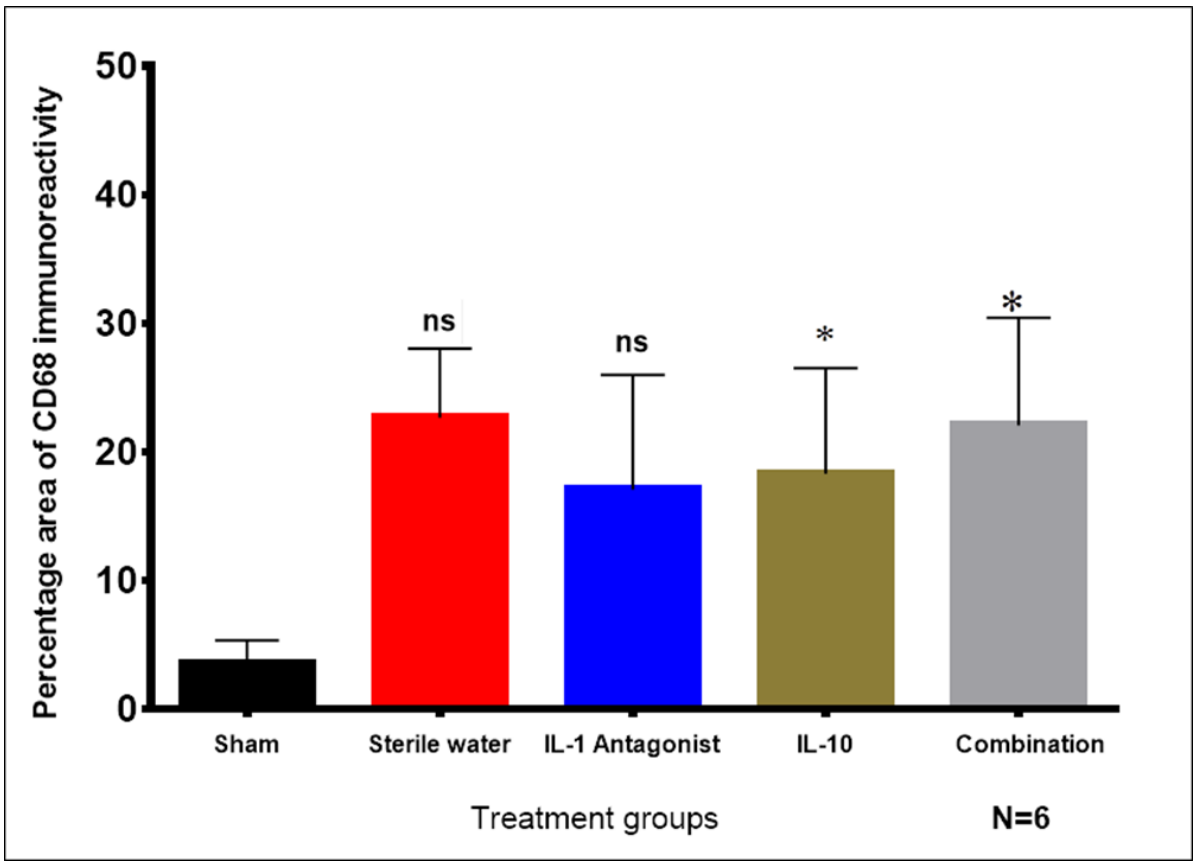

Figure 3.4: Percentage area of CD68 immunoreactivity in the sciatic nerve, 7 days following peripheral nerve injury and repair, and following administration of treatment. Data are expressed as the means. (*: $p<0.05$, ns: $p>0.05$).

3.6. Discussion

The study provided preliminary data on the effect of peripheral application of anti-inflammatory cytokines at the site of sciatic nerve injury and repair. Peripheral application of IL-1 antagonist (Anakinra) and anti-inflammatory IL-10 at the time of nerve injury and repair it was observed that macrophage reactivity was not different to the sham group, but in the sterile water and combination treatment groups macrophage reactivity was greater than the sham group. TNF-α antagonist has been investigated by Dr. Simon Atkins and Dr. Emma Bird in the oral neuroscience group at the University of Sheffield (Unpublished data). They studied the effect of TNF-α antagonist on the ectopic neural activity seven days after nerve injury and repair. So, TNF-α antagonist as single treatment was not included in this experiment.

The experiments demonstrated that although there was a demonstrable increase in the mean percentage area staining for macrophages in the IL-1 antagonist and IL-10 group it was not significantly different to the sham controls. However, the mean percentage area staining for macrophages was significantly higher in the sterile water and combination group. These findings suggest IL-1 cytokine antagonist and anti-inflammatory IL-10 may play a role in limiting macrophage recruitment in peripheral nerve injury. Furthermore, it would appear that a combination of IL-10 and TNF-α antagonist showed no significant reduction in the mean percentage area staining for macrophages. It also suggests IL-1 antagonist may be more effective at reducing macrophages numbers than TNF-α antagonist or IL-10 alone. This may indicate their possible contribution to the reduction or prevention of neuropathic pain, and potential effects on nerve regeneration.

The exact role these inflammatory mediators play in peripheral nerve injury is not completely understood, however there is ample evidence suggesting that their overall function may be involved in suppressing abnormal nociceptive signals primarily through the suppression of recruitment and activation of immune cells, as well as reduction of the effects of pro-inflammatory cytokines pooling at an injury site and in the CNS (Thacker et al., 2007; Gaudet et al., 2011; Bastien and Lacroix, 2014).

Following peripheral nerve injury, there is a slow process of degeneration initiated at severed segments of the peripheral nerve (Gaudet et al., 2011). Initially the distal segment swells and then later disintegration of their myelin sheet commences, with the proximal segment showing a reduction in diameter of nerve fibres (Johnson et al., 2005). The neuronal response to injury begins with a rapid division of Schwann cells which subsequently regulate degeneration and regeneration processes of severed neuronal axons by expression of neurotrophic molecules including nerve growth factor (NGF) and pro-inflammatory cytokines (Osbourne, 2007). After complete transection of the sciatic nerve, a severe inflammatory reaction ensues and promotes recruitment of immune inflammatory cells and proliferation of fibroblasts and scar tissue formation at the injury site (Thacker et al., 2007). Inflammatory cells including neutrophils and mast cells, infiltrate the site of nerve injury seven days' post injury and begin their phagocytosis and release of inflammatory mediators (Perkins and Tracey, 2000). These observations may explain, in part, the increase seen in the width of the sciatic nerve after injury, in our studies.

Following peripheral nerve injury, the recruitment of non-neuronal cells including macrophages, is considered to play an important part in the regeneration process of sectioned nerves (Gaudet et al., 2011). Macrophages enter the severed segments between days 4 to 7 after injury and clear the axon and myelin debris within two weeks

(Stoll and Müller, 1999). Our findings showed large numbers of macrophages invading the sciatic nerve as shown by positive CD68 marker immunofluorescent labelling which was marked across the injury site, particularly at the repair site.

In vivo studies have revealed that application of IL-1 antagonist, or neutralizing antibodies to TNF-α in a rodent sciatic nerve neuropathy model, attenuates pain-associated behaviours and this was confirmed by immunohistochemical analysis of macrophage immunoreactivity at site of nerve repair (Sommer et al., 1999; Schäfers et al., 2001). Data from this study showed that seven days following sciatic nerve injury and epineurial repair, and peripheral administration of IL-1 antagonist (Anakinra), CD68 macrophage labelling was not significantly different when compared to sham controls. This is consistent with previous immunohistochemical reports where reduced TNF immunoreactivity and macrophage infiltration was observed at the site of nerve injury following epineurial application of anti-IL-1R1 in a chronic constriction model of peripheral neuropathy (Sommer et al., 1999). Furthermore, in a mouse IL-1R1 knockout model, low levels of neutrophil and macrophage infiltration were associated with reduced pain-related behaviours and improved functional recovery of peripheral nerves (Nadeau et al., 2011).

Pro-inflammatory cytokines that are produced by immune cells 2-3 days following peripheral nerve injury, are responsible for the first stage of the healing process, inducing degeneration and clearing of debris at the site of injury. At this stage, these anti-inflammatory cytokine mediators are highly expressed by resident and infiltrating cells which regulate the inflammatory response following nerve damage. Peripheral administration of IL-10 immediately after nerve injury, has been reported to reduce macrophage activation and decreased production of inflammatory cytokines (Taskinen et al., 2000). In this experiment, IL-10 treated animals showed non-significant levels

of macrophages labelling when compared to sham nerves. In contrast, the effect of combined treatment of IL- 10 and TNF-α antagonist was insignificant, and it is possible that the dose of combination treatment was ineffective to reduce immune response at the site of nerve injury and repair. Although the current results showed short term downregulation of the immune inflammatory response at the site of peripheral nerve injury and repair, further research is necessary to investigate the long-lasting effects associated with cytokine-based therapy on functional regeneration and establish their role as neuropathic pain -targeted therapy in peripheral nerve injuries.

3.7 Summary

In summary, it is evident from the literature that the immune inflammatory cell response regulates pathways between the neurones at the levels of peripheral and central nervous system regions, by the production of inflammatory cytokines which are considered to play an important role in neuropathic pain development. Moreover, there is significant evidence that pro-inflammatory cytokines produced at a site of nerve injury may stimulate central sensitization and produce hyperalgesia due to increased ectopic neuronal activity, subsequently leading to the development of neuropathic pain (Ren and Torres, 2009). Therefore, selectively targeting peripheral cytokine signalling at the time of nerve repair, may influence signalling regulatory molecules that are responsible for initiation and maintenance of neuropathic pain.

CHAPTER 4

Interleukin-1 cytokine antagonist reduces the immune inflammatory response and promotes axon regeneration after peripheral nerve injury and repair

4.1 Introduction

Interleukin-1 cytokine is considered a key pro-inflammatory cytokine mediator which plays an important role in the axonal healing process after nerve injury. More specifically, IL-1 is considered a principal chemoattractant to macrophages at the site of nerve injury and involved in the regulation of nerve growth factor (NGF) synthesis, and so indirectly promotes axonal sprouting and growth (Brown et al., 1991; Burnett and Zager, 2004; Gaudet et al., 2011). Interleukin-1 cytokine exists in two forms; IL-1α, and IL-1β. As previously stated, IL-1α and IL-1β exhibit similar molecular structure and bind to IL-1R1, but induce different responses (Bastien and Lacroix, 2014).

The pro-inflammatory cytokine IL-1 acts by the binding to the IL-1 receptor accessory protein (IL-1acp) of IL-1RI to promote signal transductions which orchestrate the nociceptive signalling pathway after nerve injury, in both the spinal cord and peripheral nerves (Bastien and Lacroix, 2014). The recombinant form of IL-1RA (Anakinra) is widely used in the treatment of many inflammatory conditions, such as rheumatoid arthritis, and more recently recognized as a therapeutic approach in the treatment of neuropathic pain and promoting nerve regeneration after nerve injury (Richards and McMahon, 2013; Bastien and Lacroix, 2014).

Following peripheral nerve injury, IL-1 is believed to induce pain sensitivity and maintain this nociceptive response through the process of peripheral and central sensitization although these mechanisms are still not fully understood (Marchand et al., 2005; Wolf et al., 2006). Moreover, IL-1 cytokine antagonists have shown to induce central inhibition of mechanical allodynia and lower the pain threshold. As a consequence, this might reduce spontaneous ectopic firing and the development of abnormal behavioural symptoms such as hyperalgesia and allodynia (Sweitzer et al.,

2001; Sommer et al., 2001; Ren and Torres, 2009). Another possible suggestion regarding the initiation of central sensitization and neural plasticity is increased glial cell interactions with neural pain circuits secondary to an influx of pro-inflammatory cytokines such as IL-1 (Taves et al., 2013). The effect of recombinant IL-1 cytokine antagonist application reveals important mechanisms that are likely to suppress peripheral and central neurone sensitization involved in the initiation of neuropathic pain (Schäfers et al., 2001; Sommer et al., 2004; Wolf et al., 2006; Ren and Torres, 2009).

IL-1 is known to induce glial cell phenotypic changes following intrathecal injection, resulting in the expression of several inflammatory mediators which act in the recruitment and infiltration of immune cells (Mika et al., 2013). Additionally, activation of microglial and astrocytes in the dorsal and ventral horns of the spinal cord, in response to peripheral nerve damage has been observed several weeks following injury. This glial activation has been widely implicated in the development of neuropathic pain (Hansen and Malcangio, 2013, Mika et al., 2013). IL-1 released from activated microglia has been proposed to induce hyper excitability of dorsal horn neurones and activation of nearby glial-like cells and thus mediate nociceptive changes by modulation of the excitatory and inhibitory neurotransmissions processes through NMDA receptor activity in dorsal horn of the spinal cord (Zhang et al., 2008; Taves et al., 2013).

It has been shown that there is a positive correlation between increased recruitment of macrophages and functional recovery of axon following peripheral nerve injury (Brown et al., 1991; Nadeau et al., 2011). In several transgenic and knockout mice models, depletion of IL-1R1 and TNFR1 signalling was associated with reduced infiltration of macrophages as well as reduced mechanical hyperalgesia and

diminished functional recovery of peripheral nerves after injury (Brown et al., 1991; Nadeau et al., 2011). Therefore, targeting the entire IL-1 cytokine profile might be critical for axonal regeneration and reduce neuropathic pain.

Overall, there is substantial evidence that IL-1 plays a vital role in promoting axon growth and neurones excitability at the site of peripheral injury and in the spinal cord. Furthermore, IL-1's activation of immune cells provides a supplementary source for its continued production which could perhaps increase pain sensitivity.

4.2 Aim and objectives

The aim of this study was to investigate the effect of IL-1 cytokine antagonist on the inflammatory immune response and nerve regeneration, 6 weeks following peripheral nerve injury and repair. More specifically; to determine the effect of IL-1 cytokine antagonist on macrophage infiltration at the site of nerve injury and repair, and on glial activation in the dorsal and ventral horns of the spinal cord. In addition, to study the effect of IL-1 cytokine antagonist on axonal regeneration 6 weeks following peripheral nerve injury and repair.

4.3 Hypothesis

The application of IL-1 cytokine antagonist, peripherally at the site of nerve injury and repair will reduce immune cell reactivity, and spinal glial cell activation, thus potentially reducing neuropathic pain, and improve functional recovery.

4.4 Materials and methods

Chapter 2 details the experimental materials, anaesthesia and methods employed in this series of experiments. All treatments received by animals were randomised and

investigators performing the experiments and analysis of result were blinded. A schematic overview of the experimental design of this study is shown in Figure 4.1.

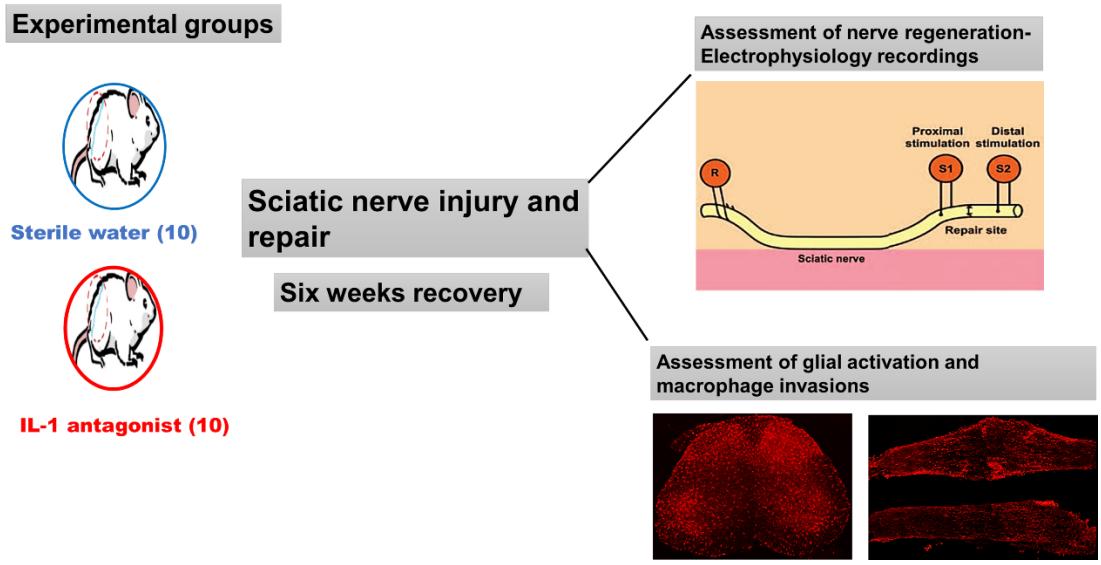

Figure 4.1: Illustration of the experiment design, investigating the effect of IL-1 antagonist in an *in vivo* model of sciatic nerve injury and repair.

Experimental groups

A total of 20 male C57 black-6 mice (8 weeks or older – weights 17-30 g) were used in this study. In the present work, a sample size calculation suggested that minor differences (5 %) in the extent of axon regeneration by electrophysiology recording and percentage area staining of macrophage marker, would be detected with a sample size of 10 animals in each group. Animals were randomly allocated to either treatment group IL-1 cytokine antagonist (n=10), or sterile water group (n=10). Preparation and concentration of IL-1 cytokine antagonist (10 mg/100 µl) is detailed in Chapter 2, section 2.2.2.

Briefly, the animals were anaesthetised with 2-3 % of isoflurane and oxygen (2 litres per minute), the left sciatic nerve exposed and 40 µl of treatment agent injected under the epineurium. The sciatic nerve was sectioned transversely and immediately repaired with four 9/0 monofilament polyamide (ETHILON*) epineurial suture knots (Figure 2.1B). Thereafter, the remaining 60 µl of treatment agent was injected intramuscularly around the nerve repair, and the wound closed in layers with vicryl suture material (6/0). Postoperative analgesia was maintained with a subcutaneous injection of single dose of opioid analgesic (0.05 mg/kg buprenorphine hydrochloride) and the animals were allowed to recover for a period of 6 weeks.

In this experiment additional sham group (n=10) from previous work in the Oral neuroscience group is included to explain difference between treatment groups under the investigation. Sterile water is considered as negative control and sham not included initially due to the ethical issue in accordance with the UK Home Office Animals (Scientific Procedure) Act 1986.

Functional assessment of nerve function recovery

Six weeks following sciatic nerve transection and repair, animals were anaesthetised with an intra-peritoneal injection of intravenous fluanisone (0.8 ml/kg) and midazolam (4 mg/kg). The left sciatic nerve was exposed and a pair of central recording electrodes applied to the nerve (platinum wire 0.15 mm diameter). An evoked stimulation across the sciatic nerve was delivered from two pairs of distal and proximal electrodes, each situated 2 mm either side of the repair site (Figure 2.4). Data was recorded and stored using Spike 2 software (version 5, Cambridge Electronic Design, UK). The CAP ratio calculated between the responses evoked from proximal or distal to the repair (modulus with distal stimulation ÷ modulus with proximal stimulation) were compared between the experimental groups, IL-1 cytokine antagonist and sterile water groups, from an average of 10 responses to stimulation along the sciatic nerve. In addition, conduction velocities were recorded by measuring the latency of the earliest component of the CAP evoked by stimulating the regenerated segment of the sciatic nerve. This recording would include both the proximal and the regenerated components of the nerve.

Tissue sectioning and immunohistochemistry analysis

Following completion of the electrophysiology recordings, animals received a 0.5 ml intraperitoneal injection of sodium pentobarbital (20 % w/v) and perfusion-fixed intracardially. The left sciatic nerves and spinal cord tissues were harvested, post fixed in 4 % paraformaldehyde for 4 hours and stored overnight in 30 % sucrose. The tissues were frozen down and sectioned as described previously (Chapter 2, section 2.2.6).

Staining and analysis of macrophage labelling in the sciatic nerve

Three slides (9 nerve sections) per animal were washed in phosphate buffered saline (PBS) containing 0.2 % Triton X-100, for 2 x 10 minutes, and then incubated overnight with a monoclonal antibody raised in rat against mouse CD68 (macrophage marker). Fluorescent macrophage labelling was visualised with goat anti-rat CY3 secondary antibody. For full details see Chapter 2, section 2.2.7.

Images of three sciatic nerve sections were captured using the x10 objective and the percentage area of CD68 positively stained tissue, 1.5 mm either side of the repair site, measured (Figure 2.12). To quantify the percentage area of macrophage CD68 labelling, the area of interest highlighted, and immunoreactivity of the cells were determined by selecting thresholding of images to detect labelled structures (See Chapter 2, section 2.2.8). Each reading was taken three times, and the mean was taken.

Staining and analysis of glial labelling in the spinal cord

Twelve sections from the L4 region were selected per animal and processed for fluorescent immunohistochemistry microglial (IBA-1) and astrocyte (GFAP) labelling. Free floating sections were blocked in in 200 µl 10 % normal donkey serum and incubated with a polyclonal antibody to IBA-1 raised in goat, or a polyclonal antibody to GFAP raised in rabbit, and respective secondary antibodies donkey anti-goat CY3 or donkey anti- rabbit CY3. For full details see Chapter 2, section 2.2.7.

Three images per animal, representative of dorsal and ventral horn regions, were captured at x5 objective for qualitative analysis and at x40 objective for quantitative analysis. Glial cell activation was interpreted by an increase in the number (proliferative changes) and complexity of the cells morphology (phenotypic alteration)

such as enlarged cell bodies and thicker processes in the dorsal and ventral spinal horns. The percentage area of glial labelling calculated by selecting area of interest and then activation areas highlighted by pink, while the remaining areas would be highlighted by yellow (See Chapter 2, section 2.2.8). Each reading was taken three times, and the mean was taken. The ratio of glial cell reactivity was determined by measuring and comparing the ratio of positive labelling between the ipsilateral and contralateral sides, in both the dorsal and ventral horn regions

Statistical comparisons were performed using t-test (Two-tailed). Quantitative data was expressed as mean values ± SEM. Differences between groups were considered significant at $p<0.05$. Statistical analysis was performed using Microsoft Excel 2010 and GraphPad Prism7 (GraphPad Software, Inc, USA).

4.5 RESULTS

4.5.1 Functional analysis

Following 6 weeks of recovery, electrophysiological studies were carried out to determine the efficacy of IL-1 cytokine antagonist on neuronal axon regeneration by recording a series of compound action potential after sciatic nerve injury and repair.

Compound action potentials (CAP)

CAPs were recorded from the sciatic nerve evoked by stimulation at the proximal and distal sides of the nerve repair using a stimulus of 10 Volts (Figure 4.2). In the uninjured sham group, the mean CAP ratio was 0.89 (SEM± 0.0793), indicating that higher compound action potentials were evoked by stimulation at the distal site.

The ratio of CAP from proximal and distal stimulation were compared between the experimental groups. The mean CAP ratio for the IL-1 cytokine antagonist group was

0.5950 (SEM ± 0.0656), while the mean CAP ratio for the sterile water group was 0.5338 (SEM ± 0.0766).

The CAP ratio in the IL-1 cytokine antagonist group was not statistically significantly different from the CAP ratio in the sterile water, 6 weeks following sciatic nerve injury and repair (p=0.550, two-tailed t-test) (Figure 4.3).

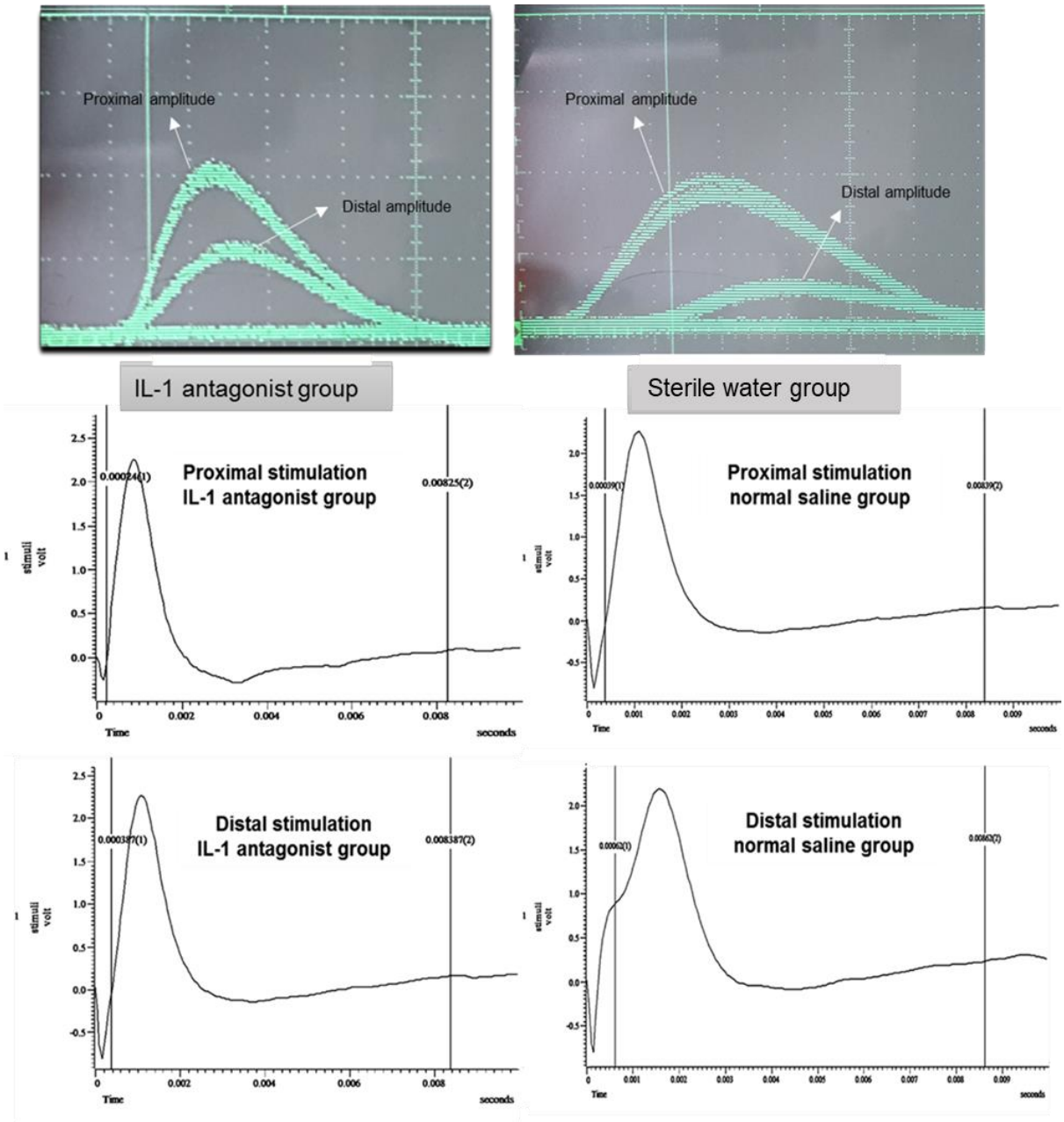

Figure 4.2: Calculation of CAP ratio as evoked by stimulation proximal and distal to the repair site, respectively.

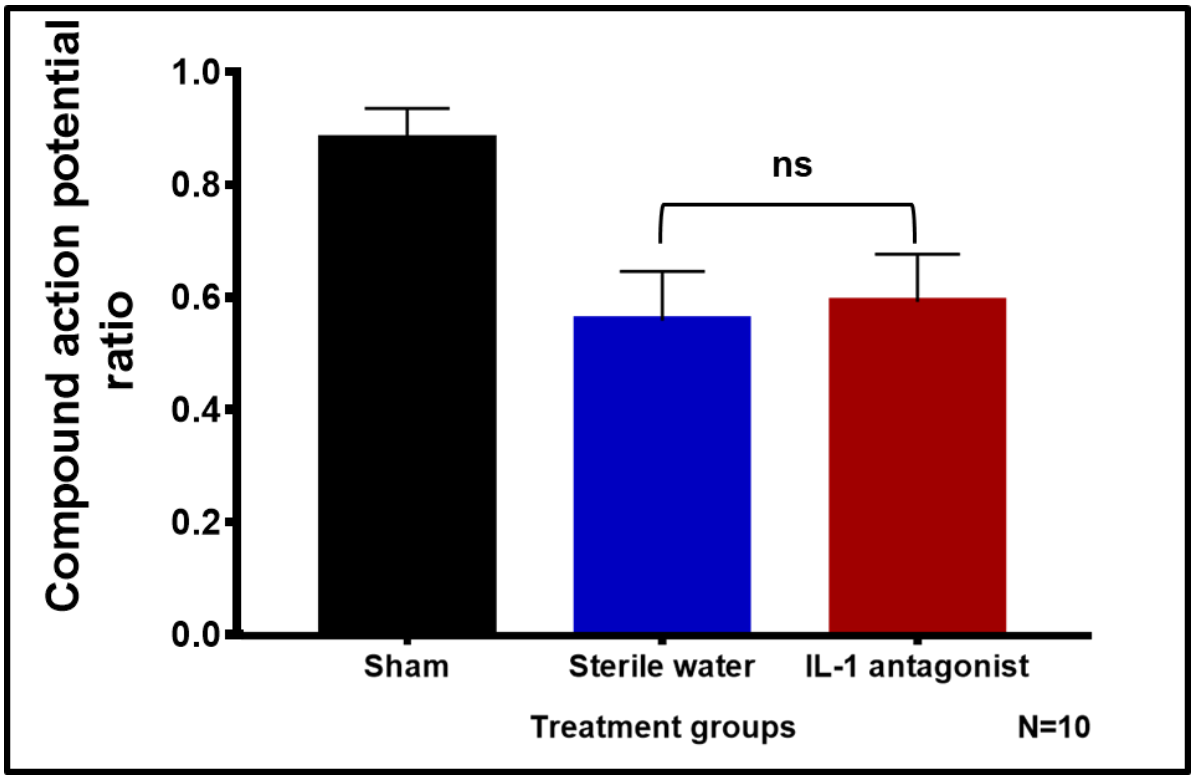

Figure 4.3: Comparison of mean compound action potential (CAP) amplitude ratios between experimental groups (Data expressed mean ± SEM; ns: $p>0.05$).

Conduction velocities

Assessment of the regeneration rates of repaired nerve fibres were compared by recording the conduction velocities six weeks after sciatic nerve injury and repair in both experimental groups (Figure 4.4).

Six weeks after recovery, the mean conduction velocities between the groups was not statistical significant differences (p=0.056, two-tailed t-test). The conduction velocity of the fastest axons in the sham controls was 53.3 m s-1 (SEM± 4.371). The conduction velocities were significantly slower in all the nerve repair groups. Although the conduction velocity was marginally higher in the IL-1 antagonist group when compared to the sterile water group, this was not statistical significant; 34.34 ms-1 (SEM ± 2.739) and 27.26 ms-1 (SEM ± 2.123) respectively.

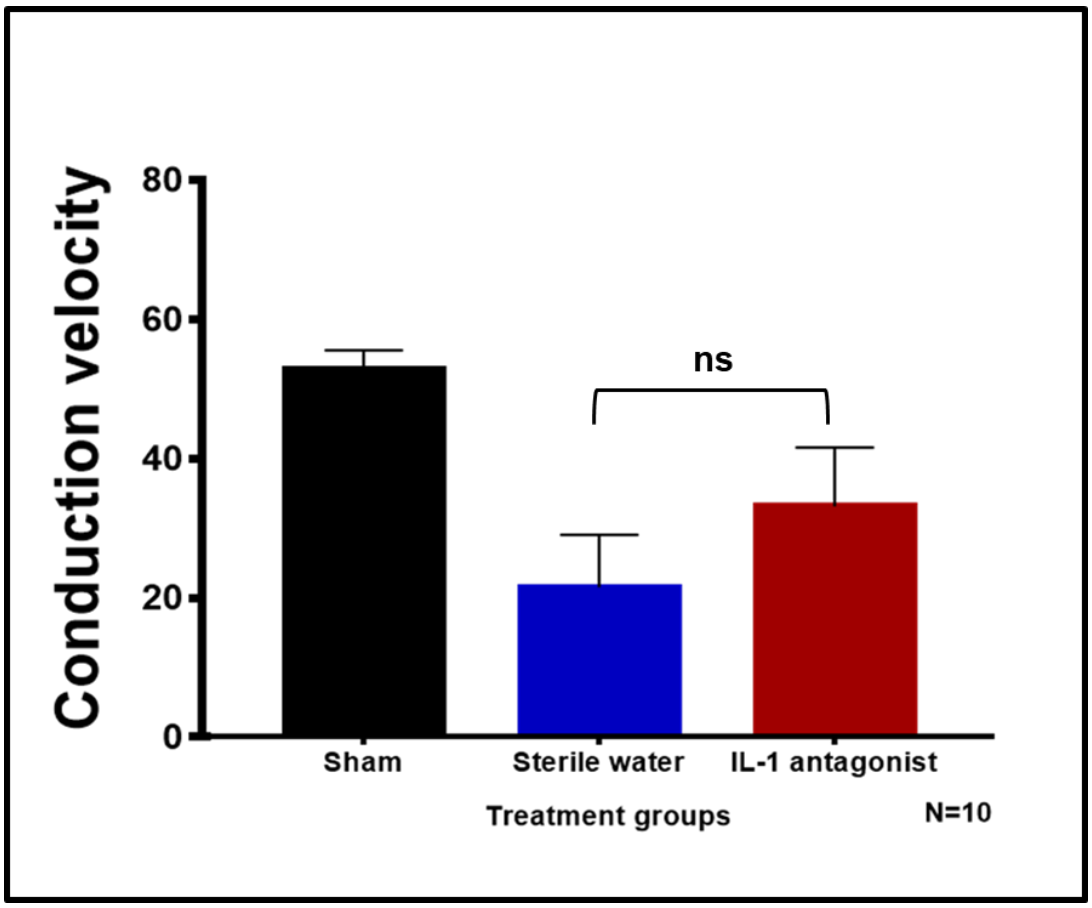

Figure 4.4: Mean conduction velocities of experimental groups (Data expressed mean ± SEM; ns: $p \geq 0.05$).

4.5.2 Immune cells fluorescent labelling

Immunohistochemical analysis was carried out to determine the effect of peripherally applied IL-1 cytokine antagonist, at the time of nerve repair, in a clinically relevant model of peripheral nerve injury and repair. Qualitative and quantitative assessment of expression of CD68 (macrophage marker), GFAP (astrocyte label) and IBA-1 (microglial marker) was carried out to determine the change in immune and glial cell response, at nerve injury site and in the dorsal and ventral horns of the spinal cord. The primary antibody specificity was tested and detailed in Chapter 2; section 2.2.7.1. The result of testing the primary antibody specificity in mouse sciatic nerve and spinal cord tissues is shown in Figures 2.9, 2.10 and 2.11.

CD68 macrophage labelling following sciatic nerve injury and repair

Qualitative Observations

Six weeks following sciatic nerve injury and repair CD68 macrophage labelling was present across the breadth of the injury site, in both experimental groups. Immunofluorescent labelling was particularly intense around the repair site and less immunoreactivity observed either distal or proximal to the repair site (Figure 4.5).

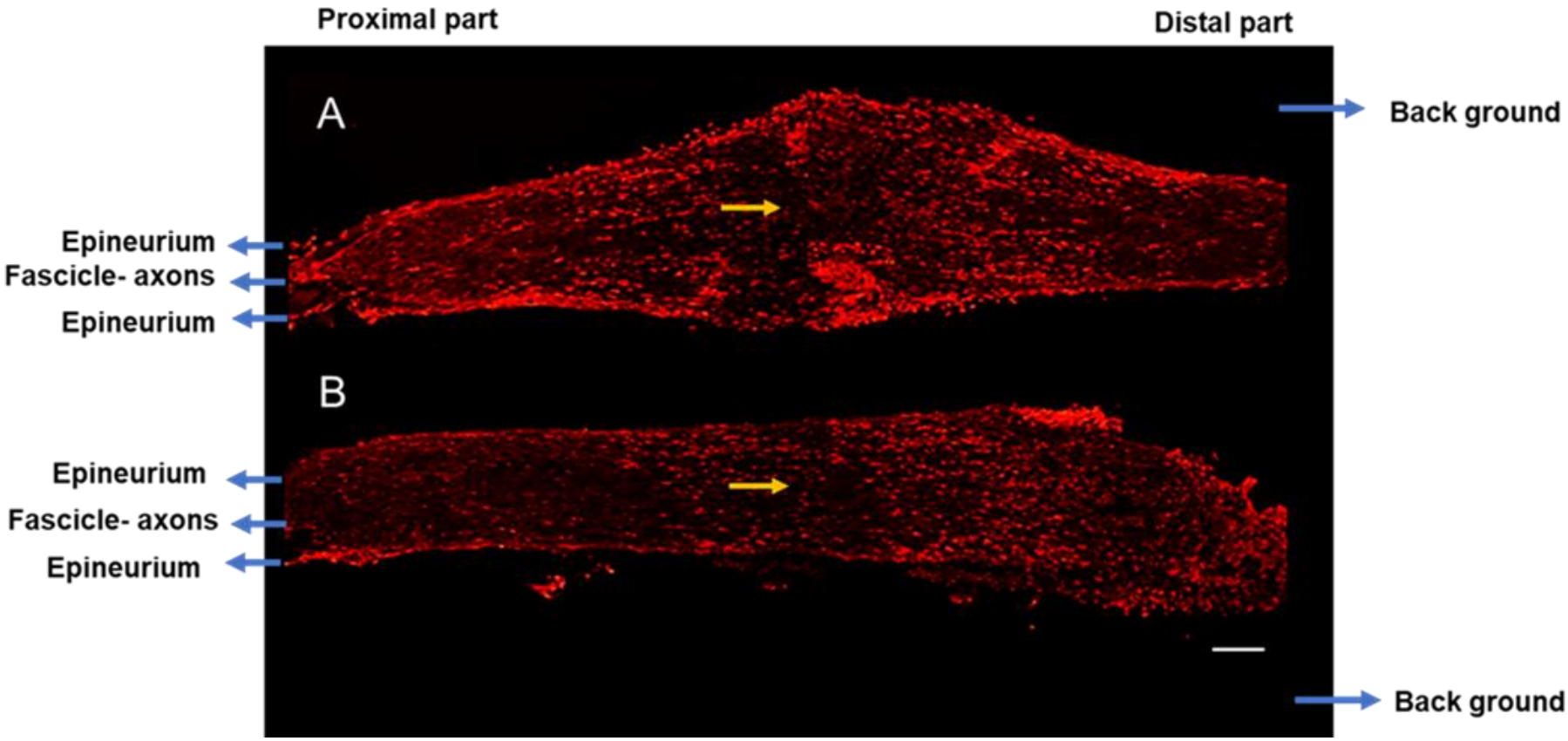

Figure 4.5: Immunofluorescent images illustrate macrophage infiltration and CD68 immunoreactivity in sciatic nerve 6 weeks following nerve injury and repair (yellow arrows: repaired site). A: Sterile water treatment group. B: IL-1 antagonist treatment. The bright dots indicate active microphages. Low macrophages immunoreactivity across the repair site in the IL-1 antagonist group when compared to the sterile water group. Scale bar= 100 µm.

Quantitative Observations

Six weeks following sciatic nerve injury and repair, there was a significant reduction in CD68 macrophage immunoreactivity at the site of nerve repair, in animals treated with IL-1 cytokine antagonist compared with the sterile water treatment group (p= 0.0268, two-tailed t-test) (Figure 4.6). The mean expression of macrophage labelling was statistically lower in the IL-1 cytokine antagonist treated C57- black-6 mice (21.96 ± 2.959) compared with those receiving sterile water (36.25 ± 5.193).

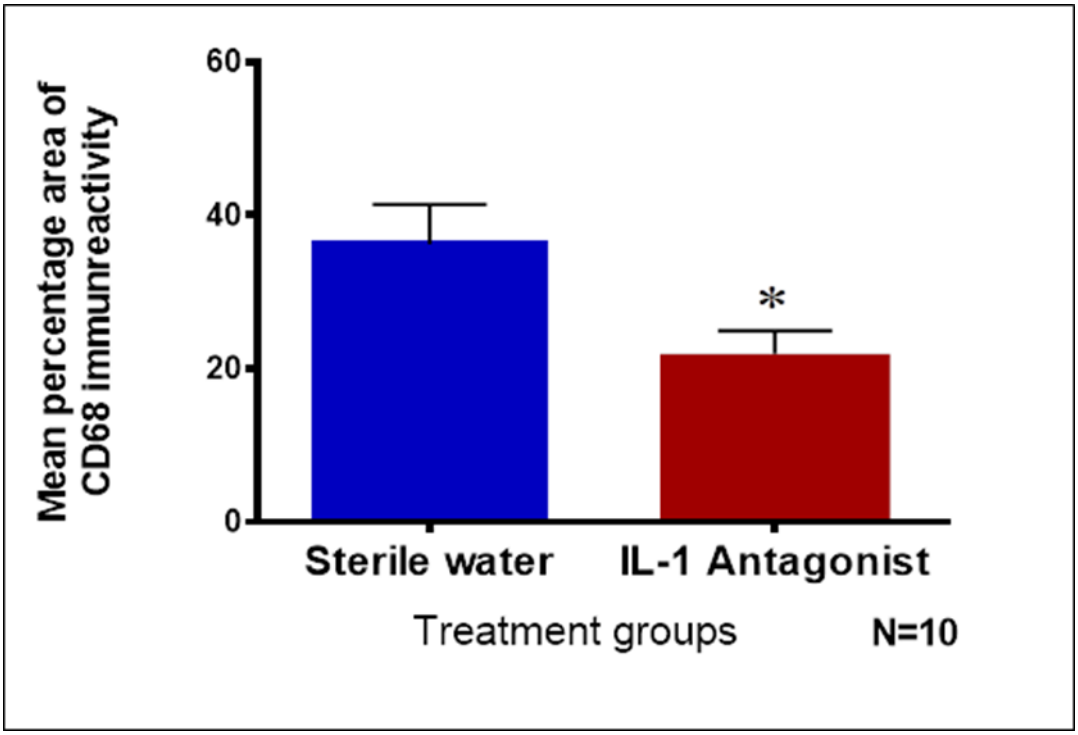

Figure 4.6: Quantification of CD68 macrophage labelling in the sciatic nerve six weeks following nerve injury and repair (Data expressed mean ± SEM; ∗: p <0.05).

IBA-1-microglia labelling following sciatic nerve injury and repair

Qualitative Observations

Qualitative analysis of the spinal cord sections revealed a similar pattern of distribution of IBA-1 microglia labelling in the two experimental groups; sterile water and IL-1 antagonist, six weeks following sciatic nerve injury and repair. Clusters of reactive microglial cells with long and branching processes were present, with high levels of IBA-1 present in the dorsal horns in both experimental groups (Figure 4.7). Furthermore, there appeared to be reduced activation of microglial cells in ventral horns in the IL-1 antagonist group (Figure 4.7).

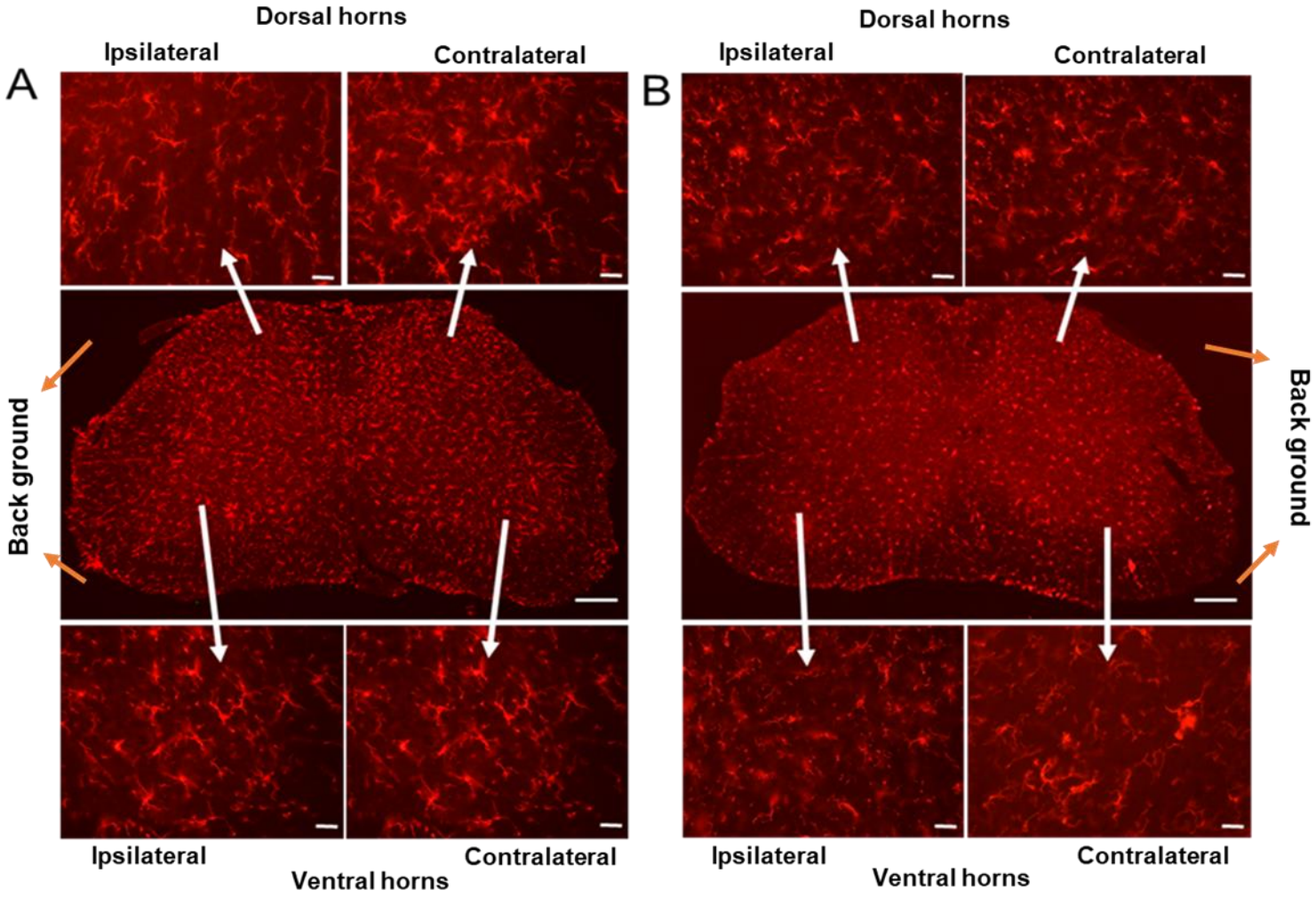

Figure 4.7: Immunofluorescent images of microglia (IBA-1) labelling in the spinal cord 6 weeks following nerve injury and repair. (A) Sterile water group. (B) IL-1 antagonist group. White arrows indicate corresponding areas of interest and showing hypertrophied and amoeboid active glial cells. Scale bar = 25 µm.

Quantitative Observations

Quantitative analysis revealed there was no significant statistical difference in the mean ratio of IBA-1 expression in ipsilateral versus contralateral sides in the dorsal horn region of the spinal cord (p= 0.780, two-tailed t-test), following treatment with IL-1 antagonist (1.453 ± 0.1004) when compared to animals treated with sterile water (1.416 ± 0.0804) (Figure 4.8).

However, there was a significant statistical difference in the mean ratio of microglia labelling in ipsilateral versus contralateral sides in the ventral horn region of the spinal cord (p= 0.022, two-tailed t-test), following treatment with IL-1 antagonist (1.229 ± 0.0737) compared to animals treated with sterile water (1.448 ± 0.0492) (Figure 4.8).

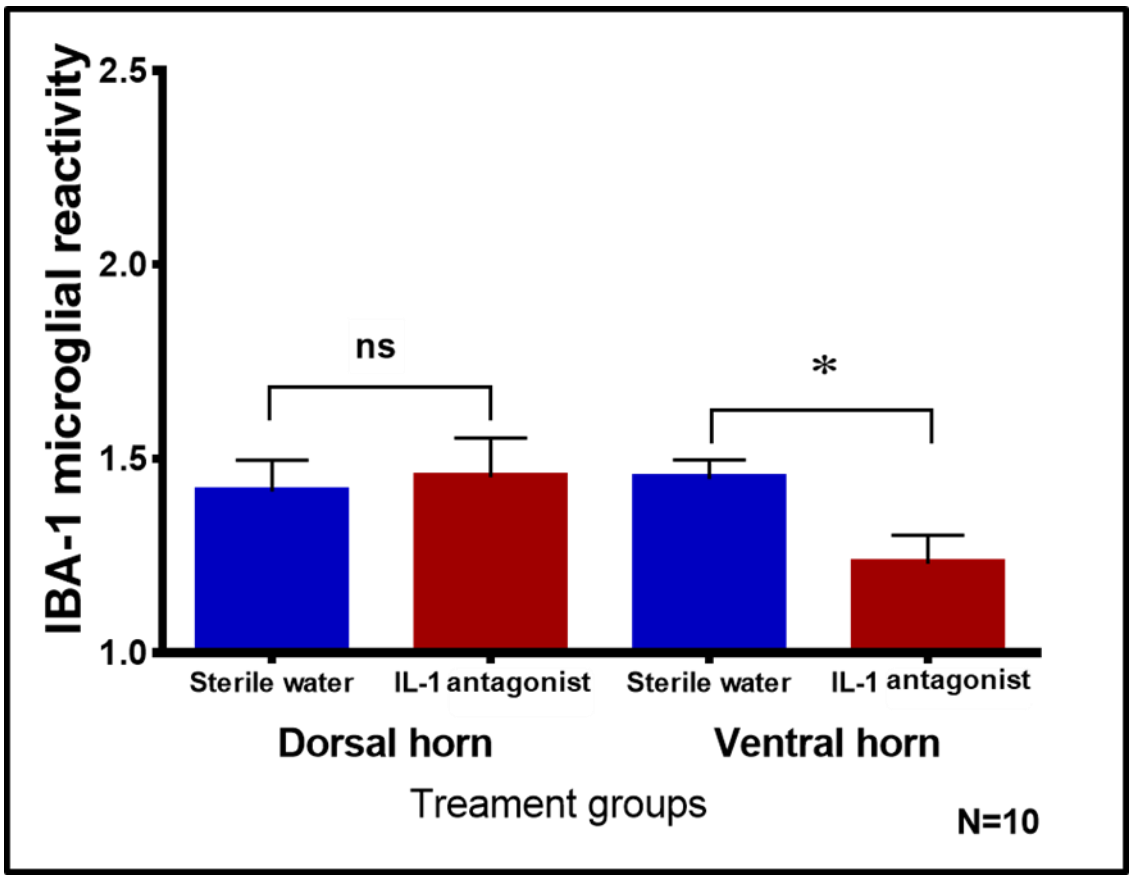

Figure 4.8: Quantification of the ratio of microglial activation (IBA-1 marker) in the ipsilateral and contralateral dorsal and ventral horns of the spinal cord, six weeks following peripheral nerve injury and repair. (Data expressed mean ± SEM; ∗: p <0.05, ns: p>0.05).

GFAP astrocyte labelling following sciatic nerve injury and repairs

Qualitative Observations

Six weeks following sciatic nerve injury and repair, there was a marked expression of astrocyte activation and morphological changes, as indicated by GFAP Immunofluorescent labelling, in the dorsal and ventral horns of the spinal cord (Figure 4.9). High levels of expression of astrocyte reactivity, with pronounced branching of processes was observed in dorsal horn regions in both experimental groups, which was accompanied by a reduced activation of astrocytes in the ventral horns (Figure 4.9).

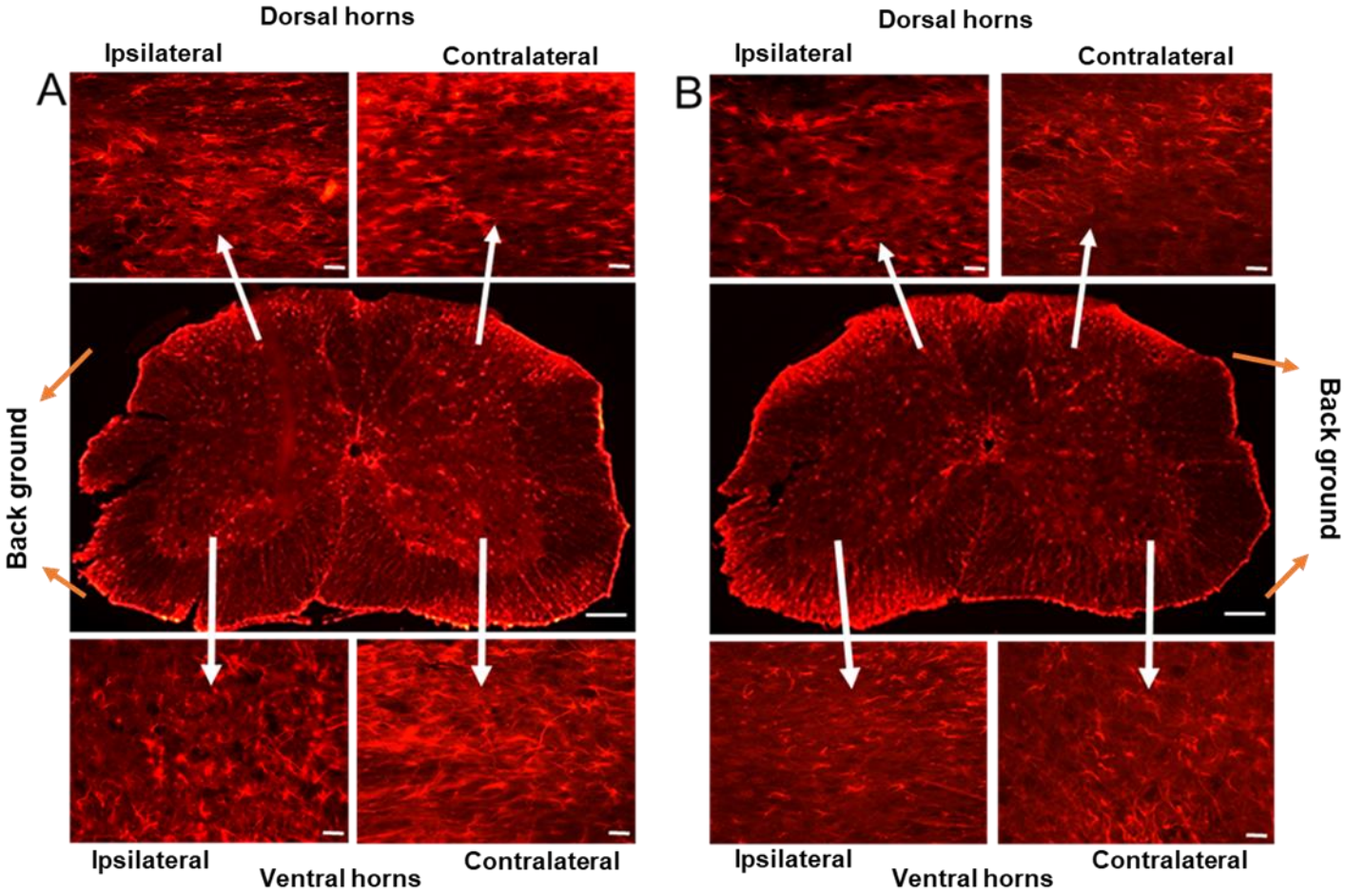

Figure 4.9: Immunofluorescent images of astrocytes (GFAP) labelling in the spinal cord 6 weeks following nerve injury and repair. (A) Sterile water group. (B) IL-1 antagonist group. White arrows indicate corresponding areas of interest and showing hypertrophied and amoeboid active glial cells. Scale bar = 25 µm.

Quantitative Observations

Six weeks following nerve injury and repair, quantitative analysis revealed no significant statistical difference in the mean ratio of astrocytes labelling using GFAP immune marker in ipsilateral versus contralateral sides in the dorsal horn region of the spinal cord (p= 0.139, two-tailed t-test), after treatment with IL-1 antagonist (1.313 ± 0.1251) as compared to animals treated with sterile water (1.555 ± 0.0958) (Figure 4.10).

Result of quantitative analysis also shows a statistical difference in the mean ratio of astrocytes cells labelling in ipsilateral versus contralateral sides in the ventral horn region of the spinal cord (p= 0.039, two-tailed t-test), following treatment with IL-1 antagonist (1.165 ± 0.0565) as compared to animals treated with sterile water (1.607 ± 0.1928) (Figure 4.10).

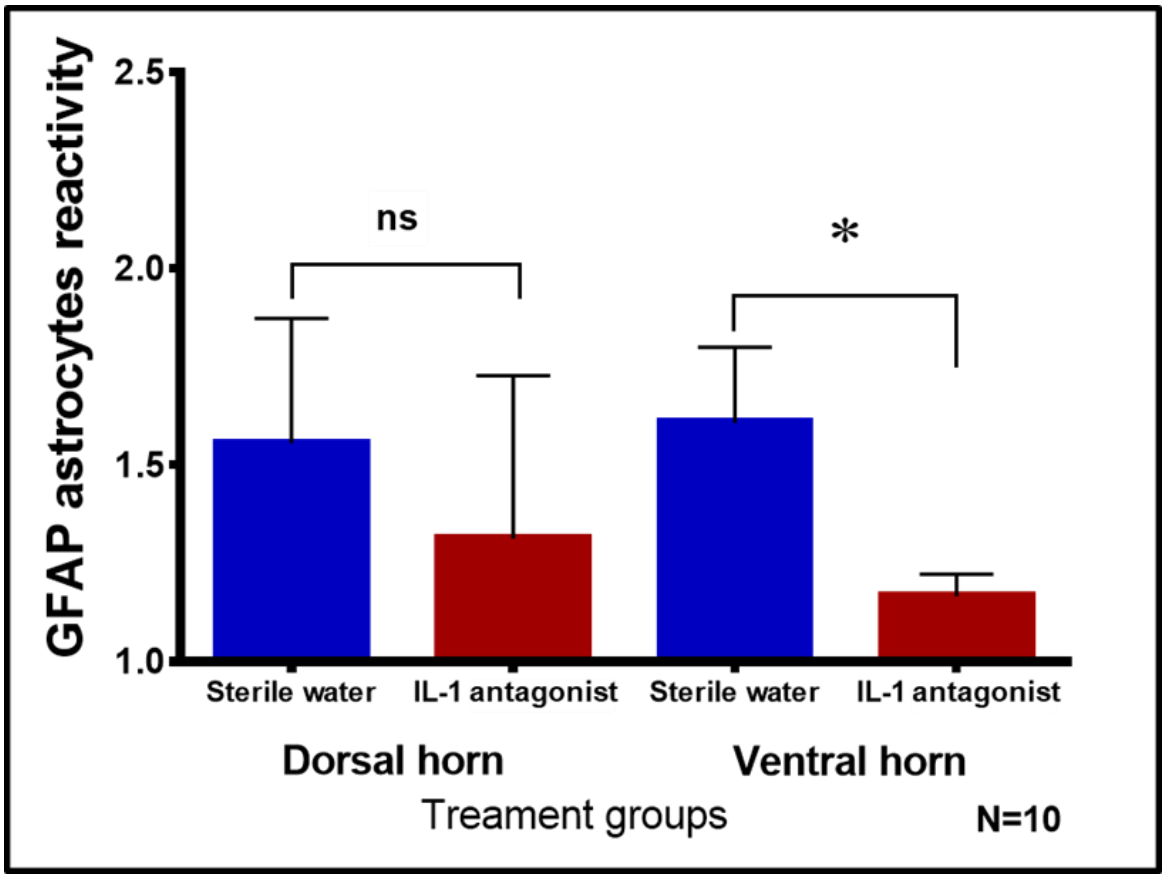

Figure 4.10: Quantification of the ratio of astrocyte activation (GFAP marker) in the ipsilateral and contralateral dorsal and ventral horns of the spinal cord, six weeks following peripheral nerve injury and repair. (Data expressed mean ± SEM; ∗: p <0.05, ns: p>0.05).

4.6 Discussion

Data from this study indicate an effect of IL-1 cytokine antagonist treatment at the time of peripheral nerve injury. Mice treated with IL-1 cytokine antagonist following peripheral nerve repair showed a significantly reduced immune cell reactivity at the injury site, and corresponding L4 ventral horn when compared to the sterile water group. Peripheral application of IL-1 antagonist reduced immune inflammatory response but did not significantly improve functional recovery as measured by CAP and conduction velocities in this experiment.

The degeneration process in a distal nerve segment is completed seven days after nerve injury, and the high levels of IL-1 activity seen in the degenerating segment, mediate axon disintegration, and are also likely to be associated with maintaining NGF synthesis at the site of nerve repair and macrophage infiltration (Ide, 1996, Navarro et al., 2007; Gaudet et al., 2011). Therefore, a therapeutic approach aimed at blocking IL-1 receptors may be more likely to succeed without interfering with the critical process of regeneration and achieve functional improvement if applied continually or in combination with other anti-inflammatory factors after nerve repair to enhance neuronal axons regeneration capability.

Recruitment of macrophages into severed nerve fibres at the site of injury is vital to the cellular events that follow nerve injury (Johnson et al., 2005, Gaudet et al., 2011). However, this involves various cell functions including; myelin material clearance and production of neurotrophic factors and cytokines. These cells usually infiltrate the site of nerve injury by 2 to 3 days, and contribute to the initial IL-1 production which is derived from other cells including Schwann cells. Previous studies show that, IL-1 activity is involved in the signalling pathway that mediates the inflammatory response,

which is responsible for repair mechanism in nerve tissues (Navarro et al., 2007; Gaudet et al., 2011). Hence, it may also have some positive effects on the process of nerve regeneration after nerve repair.

Peripheral nerve injury is associated with a rapid increase in IL-1 levels, which in turn induces NGF synthesis to promote axonal survival and out growth in the severed nerve segment (Brown et al., 1991). In our therapeutic approach studies, epineurial administration of IL-1 cytokine antagonist, down regulated the immune response but did not promote functional recovery after sciatic nerve injury. Although macrophage immunoreactivity was reduced at the site of nerve repair, the dose of IL-1 cytokine antagonist appears to be insufficient to promote axon regeneration, as indicated by low axonal regeneration potential. However, this may have been due to the possibility that the axons did not reach their maturation stage, low number of sprouting axons, or scar tissue formation. After severe nerve injury, axons can grow haphazardly to form a neuroma, which may result in some degree of irreversible blockage of electric nerve conductions distal to the site of nerve injury (Gunasekera et al., 2011).

Considering previous evidence on the correlation between severity of nerve injury, immune inflammatory activity and axonal response to injury, we investigated the effects of IL-1 signalling activity at the site of sciatic nerve injury and repair. When we blocked the IL-1RI activity with Anakinra in the periphery, the levels of immune cell reactivity was down regulated, proving its therapeutic efficacy as previously described in preclinical studies (Perkins and Tracey, 2000; Zuo et al., 2003, Thacker et al., 2007). Moreover, pre-treatment with IL-1 cytokine antagonist has been also shown to diminish onset of pain-related behaviours in peripheral nerve injury in rodents (Schäfers et al., 2001; Sweitzer et al., 2001; Sommer et al., 2004). Therefore, it is likely that the therapeutic regime we applied was partially effective in reducing the

persistent expression of IL-1 at the site of nerve injury, as indicated by decreased immune cell expression in peripheral nerves, six weeks after nerve repair. It is also reasonable to speculate that the Schwann cell myelination process is either impaired or delayed in severe injury which is known to regulate functional regeneration of axons during the regeneration process.

IL-1 cytokine is believed to be associated with early stages of peripheral nerve regeneration and in our experiment, Anakinra did not alter the levels of IL-1, but instead competed with its receptors. In our experiment no difference was recorded in CAP ratio and this may be due to scar tissue formation or that the IL-1 cytokine antagonist dose is suboptimal. While it was possible to obtain CAP of regenerating fibres, greater accuracy could possibly be obtained by direct measurement of electrical nerve fibres at different time intervals which could accurately predict functional recovery by reducing bias in regeneration contributed by different nerve fibres. In the comparisons between the uninjured sham controls and the nerve repair groups, the result showed that the CAPs were always smaller after repair. This might have resulted from a reduction in the number and/or size of regenerated axons in the distal stump.

Conduction velocity, conduction of nerve electricity, is a validated method to discriminate nerve fibre maturation, in which the heavily myelinated and largest diameter axons will conduct faster than those less myelinated with smaller diameter (Atkins et al., 2007). The conduction velocity of all of the repaired groups was significantly slower than for the sham uninjured at 6 weeks following nerve injury and repair.

Data from our study did not show difference in electric nerve conduction between the IL-1 cytokine antagonist and sterile water group, which may be due to Anakinra dose

or recovery time after nerve repair. Also, it is possible to speculate that axonal maturation occurred at a slow rate and this was shown by the similar conduction velocities ratio between the two groups. Moreover, severe nerve injury such as neurotmesis is another limiting factor of nerve fibre regeneration, due to formation of scar tissue and inappropriate guiding of the growth pathway. The rate of regeneration could be hindered after injury where the process of regeneration is slow and delayed, and Schwann cell tube lamina require greater time to establish the growth cone guidance signals to achieve or promote connection and healing.

In our investigation, epineurial administration of IL-1 antagonist reduced the immune inflammatory response but did not significantly improve functional recovery after sciatic nerve sectioning and repair. The effects of Anakinra did not significantly enhance regeneration in this experiment. However, the present therapeutic regime allows us to target the immune reaction and we found that mice receiving Anakinra at the time of nerve repair, showed lower levels of CD68 immune positive cells, 6 weeks following nerve injury and repair. Targeting IL-1 signals is considered one therapeutic approach in reducing pain due to its anti-inflammatory effects. On the other hand, Anakinra did not improve axons regeneration and this opposing outcome may be related to the degree and timing of inflammation, as severity of inflammation may reduce neural survival. Moreover, several studies reported that immediate and subsequent administration of IL-1 antagonist contributed to successful functional regeneration and survival (Schäfers et al., 2001; Sweitzer et al., 2001; Sommer et al., 2004). Therefore, it's important to control inflammation to ensure that it occurs in appropriate degree and at correct time and IL-1 may play an important role in this process in peripheral nerve injury.

In the spinal cord, the over expression of IL-1 cytokine induces activation and phenotypic changes of microglia and astrocytes (Mika et al., 2008; Mika et al., 2013, Pilat et al., 2015). It is well documented that injury to peripheral nerves is associated with phenotypic changes of glial cells in central sensory in the spinal cord (superficial and deep laminae I and II) (Eriksson et al.,1993; Taves et al., 2013). Previous studies using specific glial marker (OX-42) to highlight the response of glial cells in different sensory territories in response to peripheral nerve injuries, have revealed high levels of OX-42 pan-glial markers expression which indicate increased cell immunoreactivity. In addition, these studies reported that glial cells exhibited morphological changes similar to the qualitative results observed in the present experiment. These phenotypic changes include observable morphological features in this work highlighting the glial cells role in neurone excitability which trigger chronic pain behaviours following peripheral nerve injuries (Eriksson et al.,1993; Beggs et al., 2007; Taves et al., 2013).

It has been postulated that sensitization of spinal neurones contribute to glial activation, partly by receptor stimulation on neurones in the spinal cord which further activate microglial cell and promote production of pro-inflammatory cytokines, and these effects are blocked by pan-glial inhibitors such as interleukin-1 receptor antagonist and soluble tumour necrosis factor receptor antagonist (Mika et al., 2008; Mika et al., 2013; Pilat et al., 2015). However, our experiment showed reduced expression of glial markers in spinal ventral horns as opposed to the dorsal spinal region 6 weeks following epineurial injection of IL-1 antagonist at the time of sciatic nerve injury and repair. Since these markers mainly reflect the stages of their activation in response to continuous stimulus as a result of nerve injury, this would need further investigation at stages of nerve regeneration and different time periods after injury and repair.

4.7 Summary

Anakinra is recombinant human interleukin-1 receptor antagonist and its effectiveness has been described in many clinical trials in the treatment of chronic neuropathies. Furthermore, administration of IL-1 receptor antagonist has shown to reduce neuropathic pain in pre-clinical studies. In this experiment, epineurial injection of Anakinra did show reduced macrophage immunoreactivity, 6 weeks after sciatic nerve injury and repair. In addition, the dose regime may be ineffective in this experiment to have a compound effect on nerve regeneration and reducing pain markers simultaneously. However, Interleukin-1 receptor antagonist is unlikely to reduce pain behaviours as a single therapeutic approach. In such conditions, the use of either combination antibodies or continuous administration to compete with IL-1R1 activity, to reduce nerve apoptosis and promote axonal regeneration, along with blockage of inflammatory mediators to reduce nerve fibre nociception that leads to pain hypersensitivity and long- persisting pain state, may have greater effect.

Direct assessment of functional regeneration using electrophysiology to monitor the growth of axons after six weeks did not directly differentiate the rate of growth between the two experimental groups. Further experiments are required to test functional assessment of regenerating fibres at different time intervals along with different doses of Anakinra, and the consideration of continuous drug delivery approach at the site of nerve injury and repair. Finally, the dose of Anakinra administered epineural after nerve repair, appeared to show reduced inflammation locally as well as glial activation in the spinal cord. Hence this may be a potential therapeutic drug for reducing neuropathic pain following peripheral nerve injuries.

CHAPTER 5

Effect of combination of TNF-α antagonist and IL-10 on inflammation and neural regeneration in peripheral nerve injury

5.1 Introduction

Peripheral nerve recovery following severe nerve injury is never complete even when a nerve repair is achieved by direct anastomosis of nerve segments. This has been attributed to the disruption and subsequent disintegration of axon-Schwann cell unit (Rodríguez et al., 2004; Navarro et al., 2007; Li et al., 2014).

It has been shown that modulating the immune response at the axonal level following peripheral nerve injuries promote axon growth and improve functional regeneration after nerve repair (Thacker et al., 2007; Bastien and Lacroix, 2014; Wood and Mackinnon, 2015). Extensive evidence clearly demonstrates the contribution of immune cells in tissue damage and regeneration, and activation of cytokines in the development of neuropathic pain following nerve injury (Thacker et al., 2007; Bastien and Lacroix, 2014; Wood and Mackinnon, 2015). The effect of cytokine proteins, TNF-α and IL-10 has been discussed previously in Chapter 1, section 1.3.4 and 1.4.2. These cytokines have been shown to influence immune cell infiltration at the site of nerve injury and targeting these cytokines has been of much interest in nerve injury models. TNF-α and IL-10 cytokines are thought to contribute to the process of degeneration and regeneration by acting via different sets of specific Toll-like receptors (TLRs) expressed on various cell types including neurons (Thacker et al., 2007; Bastien and Lacroix, 2014).

TNF-α is an important pro-inflammatory cytokine which is expressed following peripheral nerve injury and believed to induce ectopic neuronal discharge and subsequently initiate neuropathic pain (George et al., 2005, Kato et al., 2009, Kato et al., 2010). Several studies have investigated the modulation of pro-inflammatory TNF-α cytokines following peripheral nerve injury and repair by using TNF-α antagonist

(Etanercept). It has been shown that local application of Etanercept at time of nerve repair is associated with reduced immunoreactivity of macrophages and this effect further suppressed pain related-behaviours. In addition, Etanercept enhanced the rate of growth and regeneration process of damaged neuronal axons (Kato et al., 2009; Kato et al., 2010).

The anti-inflammatory cytokine, IL-10 is greatly implicated in controlling the inflammatory immune response (Morris et al., 2014; Bastien and Lacroix, 2014; Kwilasz et al., 2015). IL-10 is also thought to be involved in neural regeneration by regulating other pro-inflammatory cytokines expression during process of degeneration of severed axons. Following peripheral nerve injury, IL-10 receptor activation leads to the inhibition of TNF-α and promotes release of endogenous anti-inflammatory mediators such as soluble TNFRs and IL-1 receptor antagonist (Wagner et al., 1998; Sakalidou et al., 2011). Because of its anti-inflammatory function, local application of IL-10 after nerve injury has been shown to reduce the inflammatory response and prevent development of neuropathic pain mediated by TNF-α expression (Wagner et al.,1998). Moreover, peripheral application of IL-10 at time of nerve repair has accelerated functional recovery and this was attributed to decreased amount of scar tissue formation at the site of nerve repair (Atkins et al., 2007; Sakalidou et al., 2011).

Hence, combination therapy of IL-10 and TNF-α antagonist (Etanercept) might achieve maximal effect in suppressing the process that initiates inflammatory response and thus reduces tissue damage. Furthermore, this creates a strong rational for testing this combination in enhancing functional nerve regeneration following peripheral nerve injuries. Synergistic effects of IL-10 and Etanercept have not previously been reported as a combination treatment in peripheral nerve injury.

However, previous reports of single therapy of either TNF-α antagonist and IL-10 have been criticized regarding the side effect and long-term bioavailability, respectively. This synergistic effect of drugs combination might provide better nerve regeneration and limit single drug inefficacy and dosing side effects of monotherapy use at time of nerve repair.

5.2 Aim and objectives

The aim of this study was to investigate the effect of combination of IL-10 and TNF-α antagonist on the inflammatory immune response and nerve regeneration, 6 weeks following peripheral nerve injury and repair. More specifically; to determine the effect of combination of IL-10 and TNF-α antagonist on macrophage infiltration at the site of nerve injury and repair, and on glial activation in the dorsal and ventral horns of the spinal cord. Furthermore, this study aimed to assess the effect of combination of IL-10 and TNF-α antagonist therapy on functional nerve regeneration 6 weeks following peripheral nerve injury and repair.

5.3 Hypothesis

Combined application of IL-10 and TNF-α antagonist, peripherally at the site of nerve injury and repair will reduce immune cell reactivity, and spinal glial cell activation, thus potentially reducing neuropathic pain, and improve functional recovery.

5.4 Materials and methods

Chapter 2 details the experimental materials, anaesthesia and methods employed in this series of experiments. All treatments received by animals were randomised and investigators performing the experiments and analysis of result were blinded. A schematic overview of the experimental design of this study is shown in Figure 5.1.

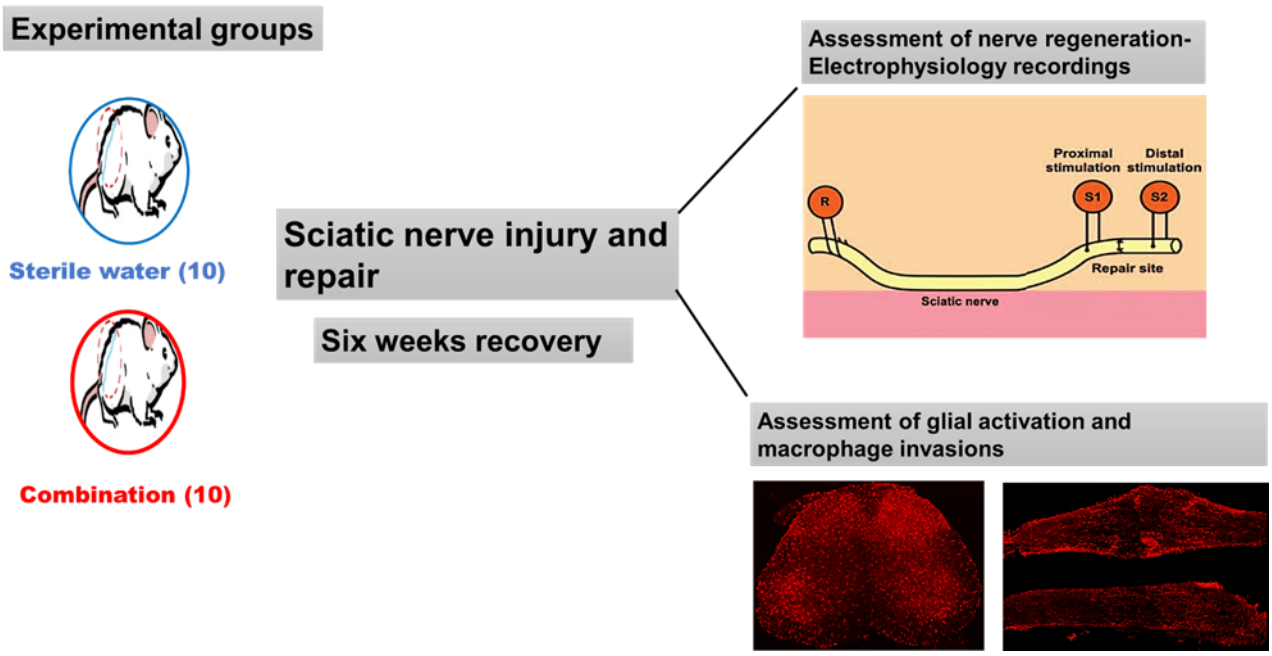

Figure 5.1: Illustration of the experimental design, investigating the effect of combined IL-10 + TNF-α therapy in an *in vivo* model of sciatic nerve injury and repair.

Experimental groups

A total of 20 male C57 black-6 mice (8 weeks or older – weights 17-30 g) were used in this study. In this study, a sample size calculation suggested that minor differences (5 %) in the extent of axon regeneration by electrophysiology recording and percentage area staining of macrophage marker can be detected with a sample size of 10 in each group. Animals were randomly allocated to either combined application of IL-10 and TNF-α antagonist (n=10) or sterile water group (n=10). Preparation and concentration of IL-10 (125 ng/100 µl) and TNF-α (0.15 mg/100 µl) antagonist is detailed in Chapter 2, section 2.2.2.

Briefly, the animals were anaesthetised with 2-3 % of isoflurane and oxygen (2 litres per minute). The left sciatic nerve was exposed, 40 µl of treatment agent injected under the epineurium, and the sciatic nerve sectioned transversely and immediately repaired with four 9/0 monofilament polyamide (ETHILON*) epineurial suture knots (Figure 2.1B). The remaining 60 µl of the treatment agent was injected intramuscularly around the nerve repair, and the wound closed in layers with vicryl suture material (6/0). Postoperative analgesia was maintained with a subcutaneous injection of single dose of opioid analgesic (0.05 mg/kg buprenorphine hydrochloride) and the animals were allowed to recover for a period of 6 weeks.

In this experiment additional sham group (n=10) from previous work in the Oral neuroscience group is included to explain difference between treatment groups under the investigation. Sterile water is considered as negative control and sham not included initially due to the ethical issue in accordance with the UK Home Office Animals (Scientific Procedure) Act 1986.

Functional assessment of nerve function recovery

Six weeks following sciatic nerve transection injury and repair, animals anaesthetised with an intra-peritoneal injection of intravenous fluanisone (0.8 ml/kg) and midazolam (4 mg/kg). The left sciatic nerve was exposed and a pair of central recording electrodes applied to the nerve (platinum wire 0.15 mm diameter). An evoked stimulation across the sciatic nerve was delivered from two pairs of distal and proximal electrodes, each situated 2 mm to the repaired site (Figure 2.4). Data was recorded and stored using Spike 2 software (version 5, Cambridge Electronic Design, UK). The CAP ratio calculated between the responses evoked from proximal or distal to the repair (modulus with distal stimulation ÷ modulus with proximal stimulation). were compared between the experimental groups, from an average of 10 responses to stimulation along the sciatic nerve. In addition, conduction velocities were recorded by measuring the latency of the earliest component of the CAP evoked by stimulating the regenerated segment of the sciatic nerve. This recording would include both the proximal and the regenerated components of the nerve.

Tissue sectioning and immunohistochemistry analysis

Following completion of the electrophysiological recordings, animals received a 0.5 ml (100 mg) intraperitoneal injection of sodium pentobarbital (20 % w/v) whilst under deep anaesthesia. Then the right and left sciatic nerves and spinal cord tissues were removed and fixed in 4 % paraformaldehyde for 24 hours, and cryoprotected overnight in 30 % sucrose solution, both at 4 °C. The tissues were frozen down and sectioned as described previously (Chapter 2, section 2.2.6).

Staining and analysis of macrophage labelling in the sciatic nerve

Three slides (9 nerve sections) per animal were washed in phosphate buffered saline (PBS) containing 0.2 % Triton X-100, for 2 x 10 minutes, and then incubated overnight with a monoclonal antibody raised in rat against mouse CD68 (macrophage marker). Fluorescent macrophage labelling was visualised with goat anti-rat CY3 secondary antibody. For full details see Chapter 2, section 2.2.7.

Images of three sciatic nerve sections were captured using the x10 objective, for qualitative and quantitative analysis of CD68 staining. The percentage area of positively stained tissue, 1.5 mm either side of the repair site, as represented by suture material, was included in the measured area of interest (Figure 2.12).

To quantify the percentage area of macrophage CD68 labelling, the area of interest highlighted, and immunoreactivity of the cells were determined by selecting thresholding of images to detect labelled structures (See Chapter 2, section 2.2.8). Each reading was taken three times, and the mean was taken.

Staining and analysis of glial cells in the spinal cord

Twelve sections from the L4 region were selected per animal and processed for free floating immunohistochemical processing for microglial marker (IBA-1) and astrocytes marker (GFAP) labelling. Sections were blocked in in 200 µl 10 % normal donkey serum and incubated with a polyclonal antibody to IBA-1 raised in goat, or a polyclonal antibody to GFAP raised in rabbit, and respective secondary antibodies donkey anti-goat CY3 or donkey anti- rabbit CY3. For full details see Chapter 2, section 2.2.7.

Three images per animal, representative of dorsal and ventral horn regions, were captured at x5 objective for qualitative analysis and at x40 objective for quantitative analysis. Glial cell activation was interpreted by an increase in the number

(proliferative changes) and complexity of the cells morphology (phenotypic alteration) such as enlarged cell bodies and thicker processes in the dorsal and ventral spinal horns. The percentage area of glial labelling calculated by selecting area of interest and then activation areas highlighted by pink, while the remaining areas would be highlighted by yellow (See Chapter 2, section 2.2.8). Each reading was taken three times, and the mean was taken.

The ratio of glial cell reactivity was determined by measuring and comparing the ratio of positive labelling between the ipsilateral and contralateral sides, in both the dorsal and ventral horn regions.

Statistical comparisons were performed using t-test (Two-tailed). Quantitative data was expressed as mean ± SEM and differences between groups were considered significant at $p<0.05$. Statistical analysis was performed using Microsoft Excel 2010 and GraphPad Prism7 (GraphPad Software, Inc, USA).

5.5 RESULTS

5.5.1 Functional analysis

Following 6 weeks of recovery, electrophysiological studies were carried out to determine the efficacy of combined application of IL-10 and TNF-α antagonist on neuronal axon regeneration by recording a series of CAP after sciatic nerve injury and repair.

Compound action potential (CAP)

Assessment of nerve function recovery was determined by recording CAP of nerve fibres proximal and distal to the site of nerve injury and repair six weeks following repair (Figure 5.2). In the uninjured sham group, the mean CAP ratio was 0.89 (SEM±

0.79), indicating that higher compound action potentials were evoked by stimulation at the distal site. Statistical analysis revealed that the combined treatment group had significant grater CAP ratio (0.525 [SEM± 0.05288] versus the sterile water group (0.2578 [SEM± 0.04633]; *p*= 0.001, two-tailed t-test) (Figure 5.3).

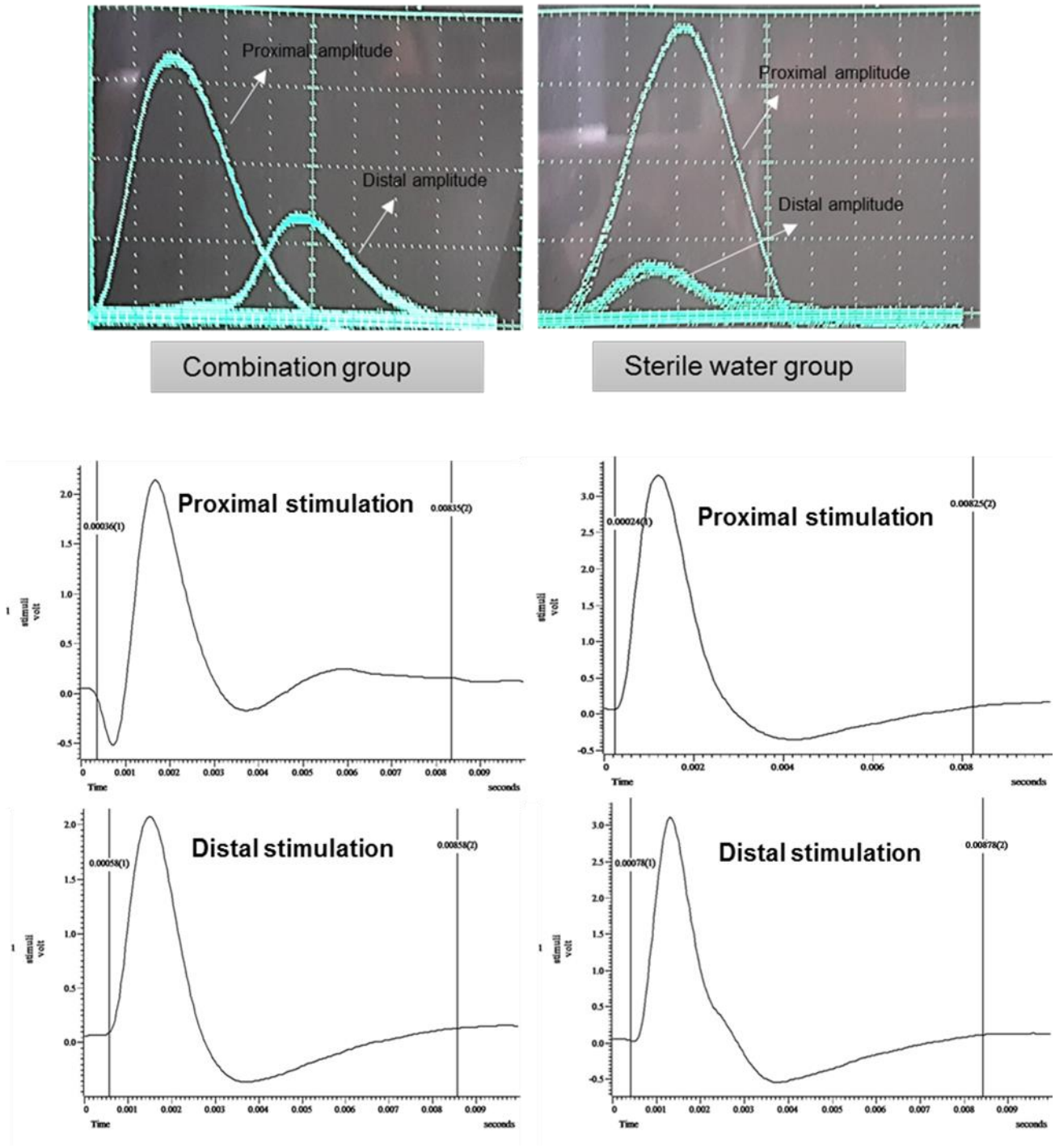

Figure 5.2: Calculation of CAP ratio as evoked by stimulation proximal and distal to the repair site, respectively.

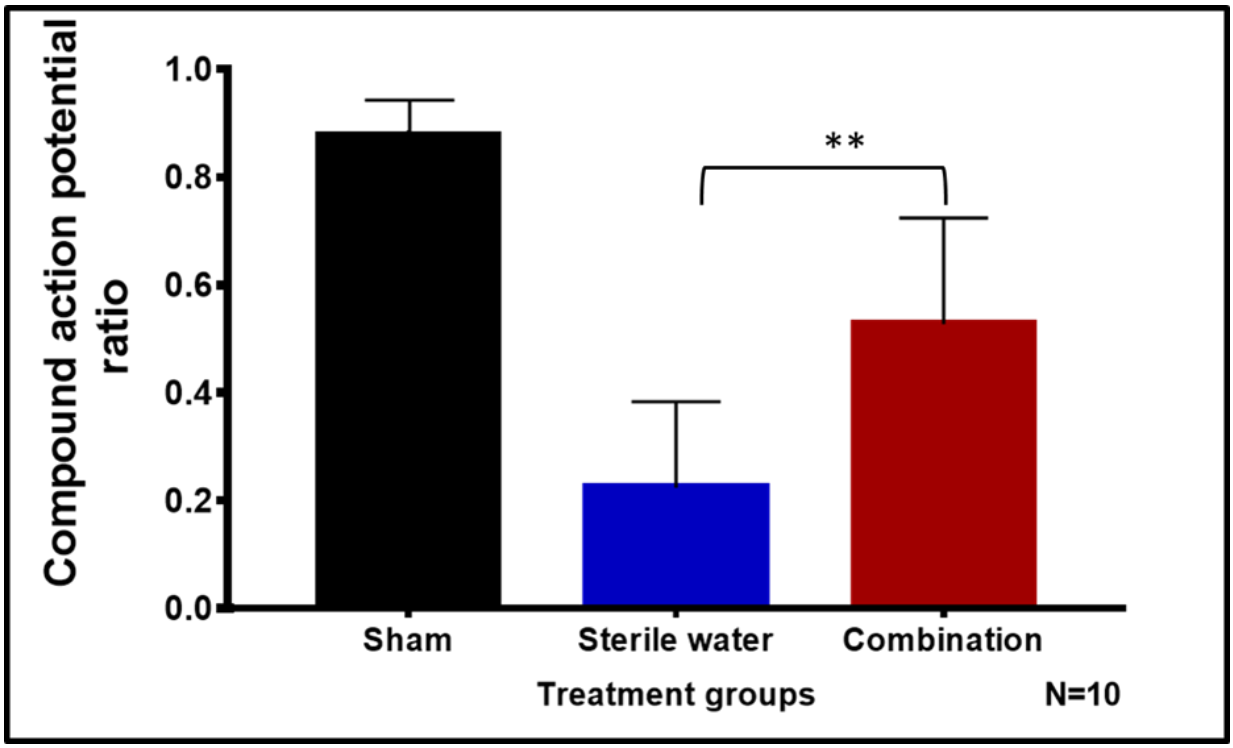

Figure 5.3: Comparison of mean compound action potential (CAP) amplitude ratios between experimental groups (Data expressed mean ± SEM; ** : p=0.001).

Conduction velocities

Six weeks following sciatic nerve injury and repair, no significant difference in distal conduction velocities were seen between the two experimental groups (p=0.599, two-tailed t-test). The conduction velocity of the fastest axons in the sham controls was 60.70 m s-1 (SEM± 3.529). The conduction velocities were significantly slower in all the nerve repair groups. The conduction velocities were slow in all experimental groups (Figure 5.4). The mean conduction velocity in the combination treated group was 28.3 ms-1 (SEM± 2.729), whereas in the sterile water group the mean conduction velocity was 26.41 ms-1 (SEM± 2.252).

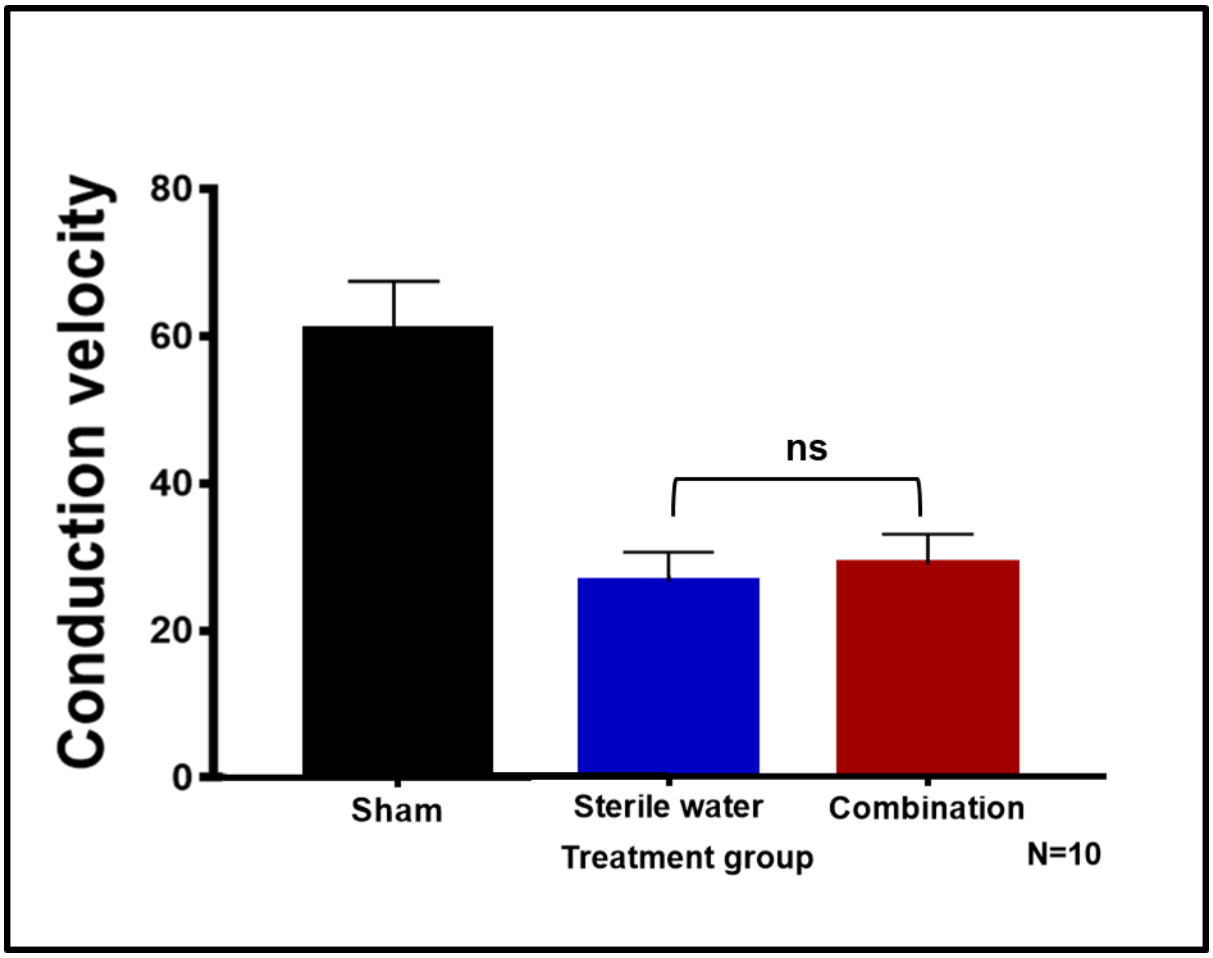

Figure 5.4: Mean conduction velocities of experimental groups (Data expressed mean ± SEM; ns: $p>0.05$).

5.5.2 Immune cells fluorescent labelling

Immunohistochemical analysis was carried out to determine the effect of peripherally applied combination treatment of IL-10 and TNF-α antagonist, at the time of nerve repair, in a clinically relevant model of peripheral nerve injury and repair. Qualitative and quantitative assessment of expression of CD68 (macrophage marker), GFAP (astrocyte label) and IBA-1 (microglial marker) was carried out to determine the change in immune and glial cell response, at the nerve injury site and in the dorsal and ventral horns of the spinal cord.

CD68 macrophage labelling following sciatic nerve injury and repair

Qualitative Observations

Six weeks following sciatic nerve injury and repair immunoreactivity for CD68 macrophage labelling was present in both groups of animals; combined treatment and sterile water. CD68 labelling was intense and highly expressed around the site of sciatic nerve repair, compared with less immunoreactivity observed either distal or proximal to the repaired site (Figure 5.5).

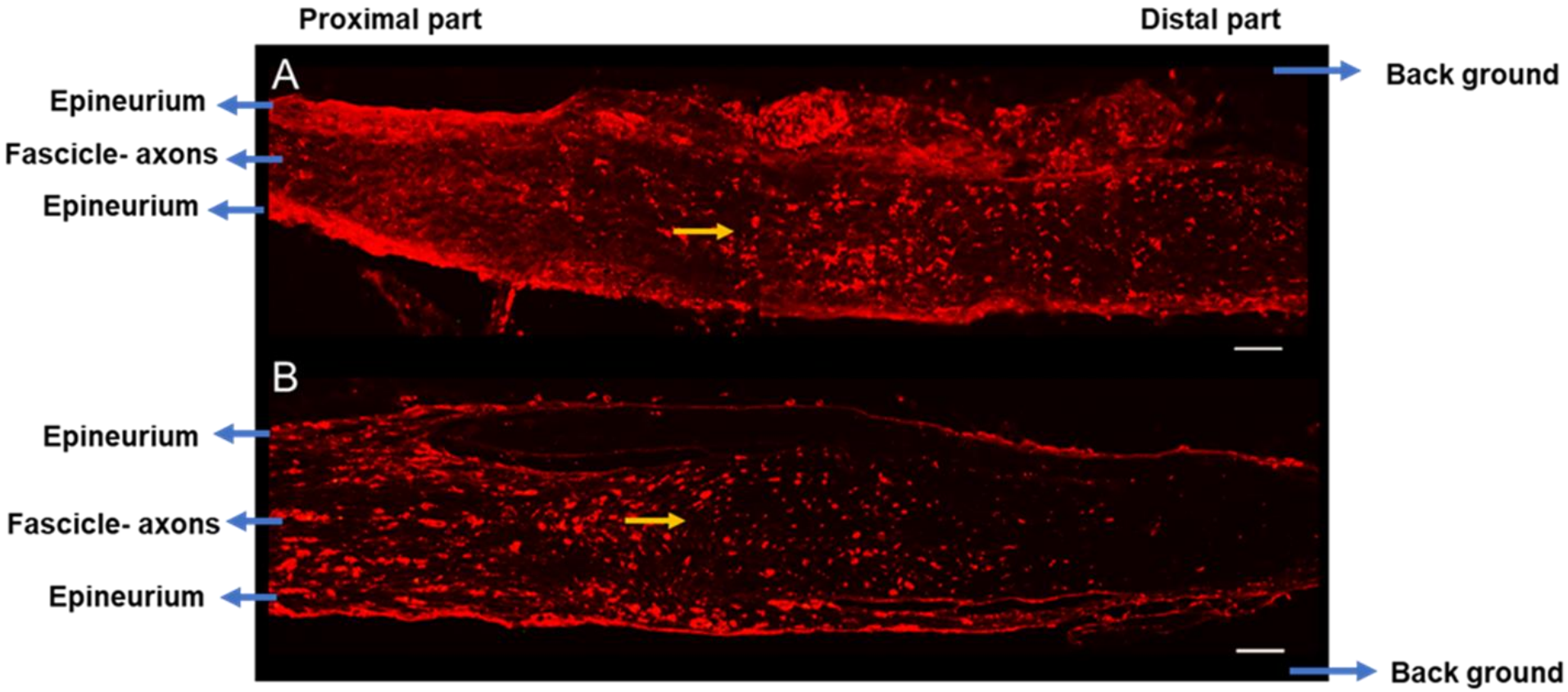

Figure 5.5: Immunofluorescent images illustrate macrophage infiltration and CD68 immunoreactivity in sciatic nerve 6 weeks following nerve injury and repair. (yellow arrows: repaired site). A: Combination treatment group. B: Sterile water group. The bright dots indicate active microphages. Low macrophages immunoreactivity across the repair site in the combination group when compared to the sterile water group. Scale bar= 100 µm.

Quantitative Observations

Quantitative image analysis of macrophage infiltration revealed a statistically significant difference in the levels of expression between the two experimental groups (p= 0.014, two-tailed t-test) (Figure 5.6). The mean percentage area of CD68 labelling following nerve repair and epineurial injection of combination agent was 16.12 (± 2.155) compared with those which received sterile water injection, where the mean percentage area of CD68 labelling was 27.78 (± 3.735).

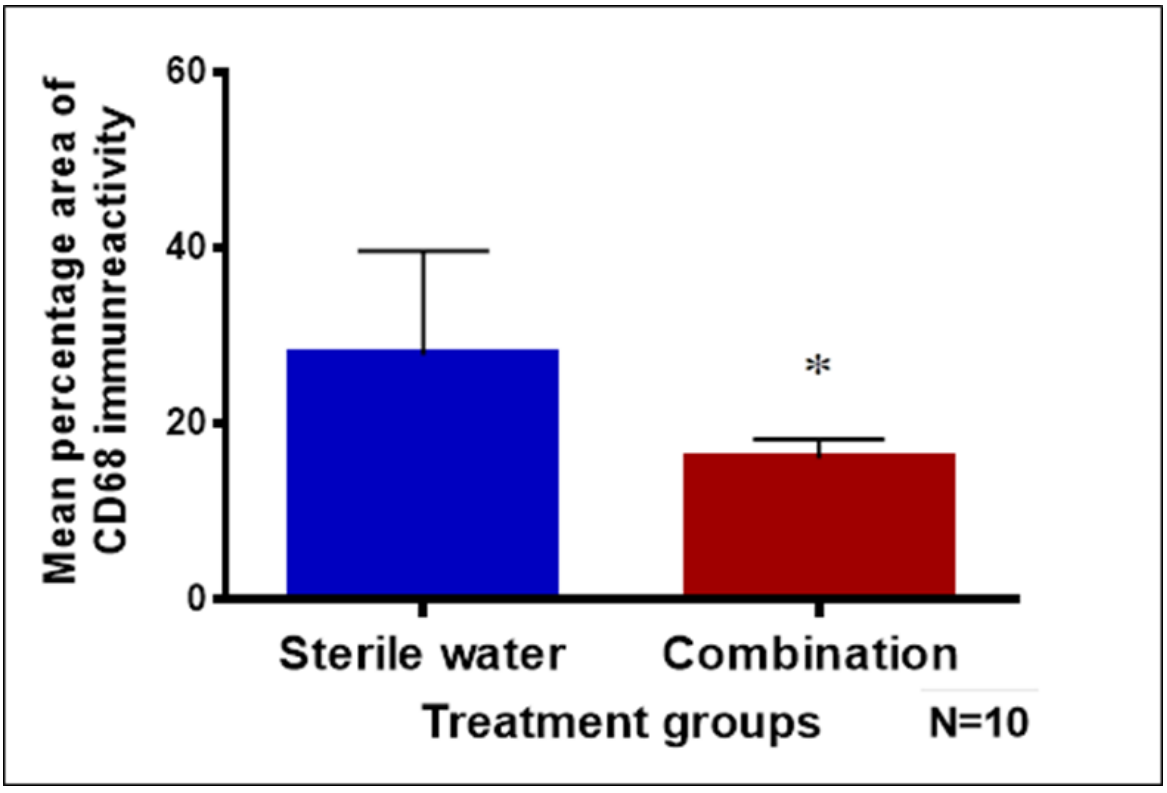

Figure 5.6: Quantification of CD68 macrophage labelling in the sciatic nerve six weeks following nerve injury and repair (Data expressed mean ± SEM; ∗: p <0.05).

IBA-1-microglia labelling following sciatic nerve injury and repair

Qualitative Observations

Qualitative analysis indicated that fluorescent IBA-1 microglia labelling was present in the dorsal and ventral horn regions of spinal cords taken from both experimental groups, and clusters of reactive microglial cells were present, exhibiting long and branching processes. Initial observations suggested that IBA-1 levels in the dorsal horns appeared to be higher in animals receiving sterile water compared with combined treatment agent, but IBA-1 labelling levels appears similar in the ventral horns in both experimental groups (Figure 5.7).

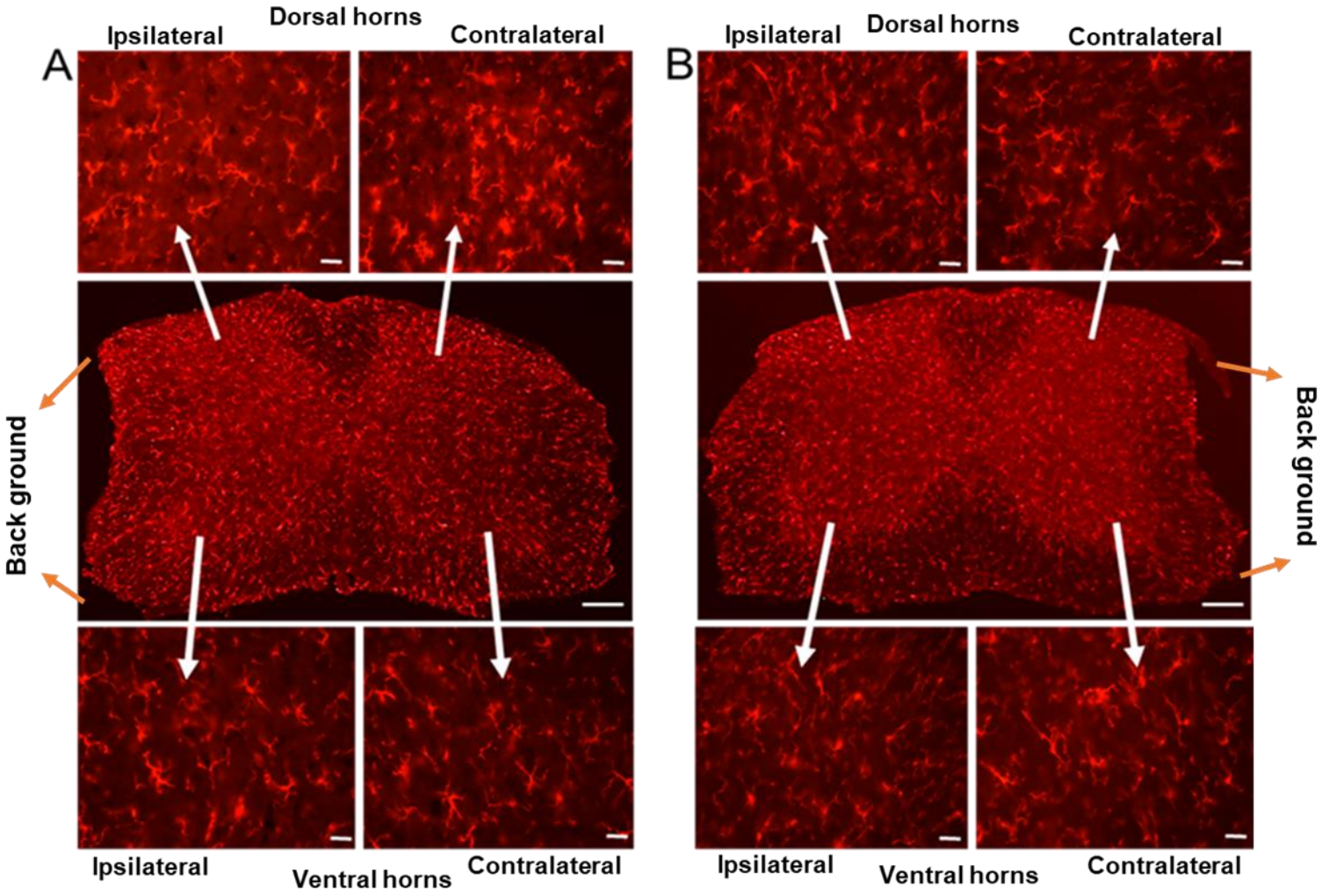

Figure 5.7: Immunofluorescent images of microglia (IBA-1) labelling in the spinal cord 6 weeks following nerve injury and repair. (A) Sterile water group. (B) Combination group. White arrows indicate corresponding areas of interest and showing hypertrophied and amoeboid active glial cells. Scale bar = 25 µm.

Quantitative Observations

Six weeks following nerve injury and repair, quantitative image analysis revealed a higher level of IBA-1 microglial activation in mice-treated with sterile water compared with those mice treated with combination agent of IL-10 and TNF-α antagonist, at the time of sciatic nerve repair. Statistical analysis revealed a significant difference in the mean ratio of IBA-1 microglial marker labelling in ipsilateral versus contralateral sides in the dorsal horn region of the spinal cord (p= 0.023, two-tailed t-test), following combined treatment (1.351 ± 0.1013) compared with sterile water treatment (1.966 ± 0.2276) (Figure 5.8).

There was no significant difference in the levels of IBA-1 microglial labelling in ipsilateral versus contralateral sides in the ventral horn of the spinal cord between the groups (p= 0.927, two-tailed t-test) (Figure 5.8). The ratio of IBA-1 positive cells in mice treated with combination agents was 1.542 (± 0.1815) compared with those treated with sterile water,1.561 (± 0.0961), six weeks after nerve injury and repair.

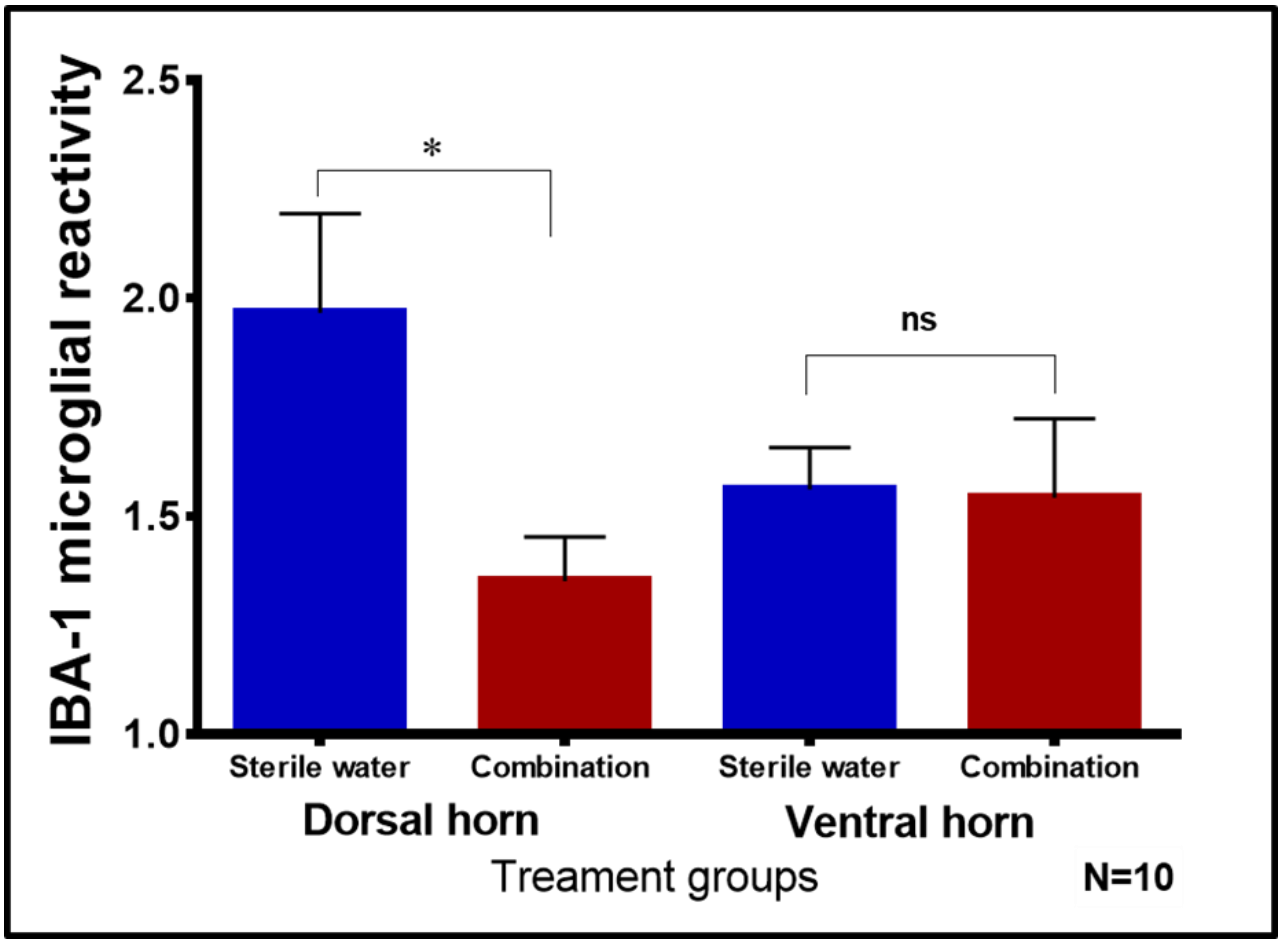

Figure 5.8: Quantification of ratio of microglial activation (IBA-1 marker) in ipsilateral versus contralateral dorsal and ventral horns six weeks following peripheral nerve injury and repair. (Data expressed mean ± SEM; ∗: p <0.05, *ns*: p>0.05).

GFAP astrocyte labelling following sciatic nerve injury and repairs

Qualitative Observations

A similar pattern of astrocyte (GFAP) activation and changes in morphology were observed in the spinal cord sections, as were seen in microglia (IBA-1) activation, six weeks following sciatic nerve injury and repair (Figure 5.9).

High levels of GFAP immunoreactivity with pronounced branching of astrocyte processes was observed in the dorsal horns of the sterile water group. This was accompanied by high GFAP labelling in ventral horns in both experimental groups (Figure 5.9).

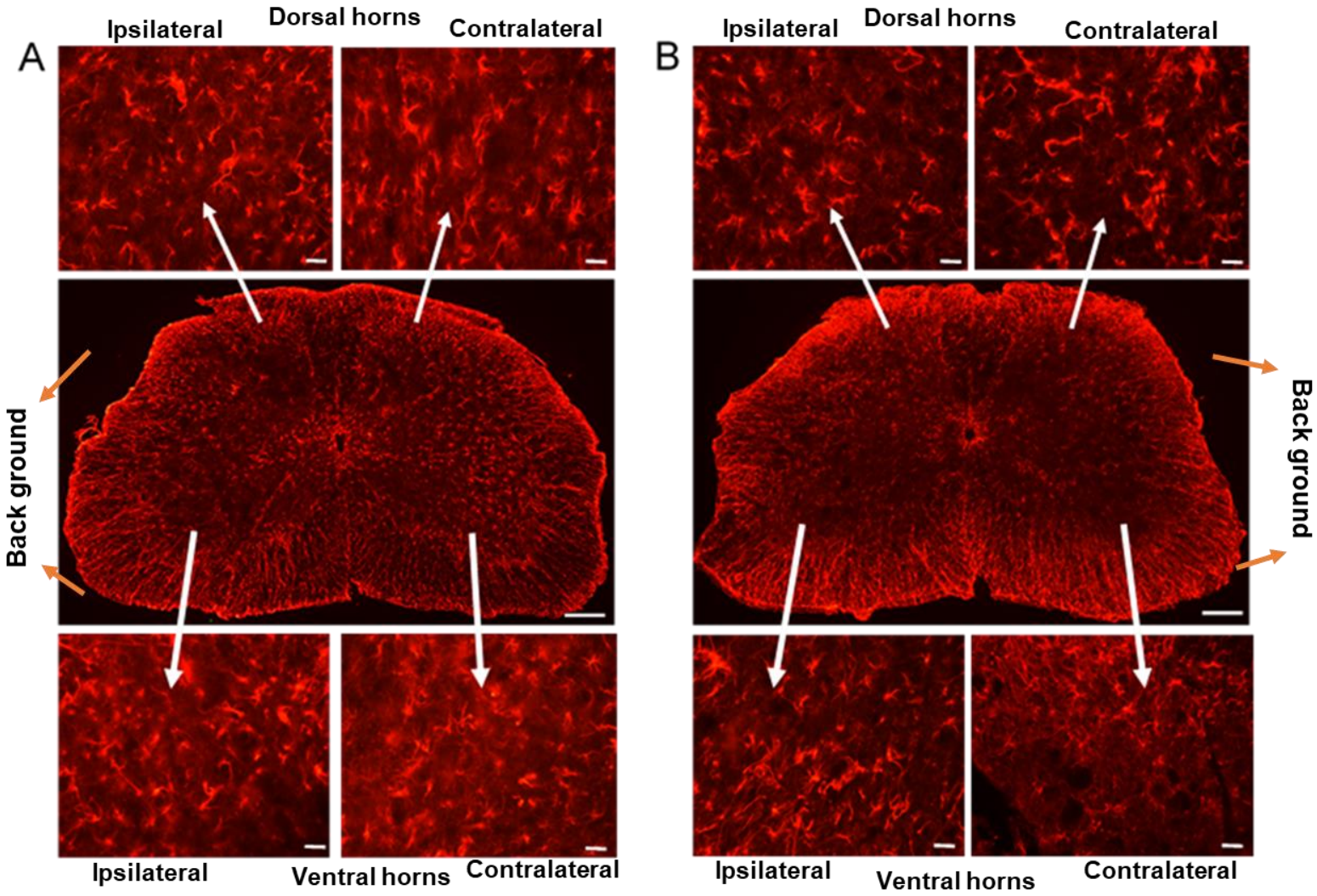

Figure 5.9: Immunofluorescent images of astrocytes (GFAP) labelling in the spinal cord 6 weeks following nerve injury and repair. (A) Sterile water group. (B) Combination group. White arrows indicate corresponding areas of interest and showing hypertrophied and amoeboid active glial cells. Scale bar = 25 µm.

Quantitative Observation

Quantitative analysis of astrocyte GFAP labelling, revealed a significant difference in levels of expression in ipsilateral versus contralateral sides in the dorsal horn region of the spinal cord (p= 0.022, two-tailed t-test) between the two treated groups, six weeks following of sciatic nerve injury and repair (Figure 5.10). The mean ratio of astrocyte labelling was lower in mice treated with combination agents (1.273 ± 0.06635) compared with mice treated with sterile water (1.572 ± 0.0997) at time of sciatic nerve repair.

In contrast, but similar to IBA-1 microglial labelling, there was no significant difference in astrocyte labelling in ipsilateral versus contralateral sides in the ventral horns between the two groups (p= 0.774, two-tailed t-test) (Figure 5.10). The mean ratio of astrocyte immunoreactivity in combination group was 1.451 (± 0.1582) compared with 1.389 (± 0.1427) in the sterile water group.

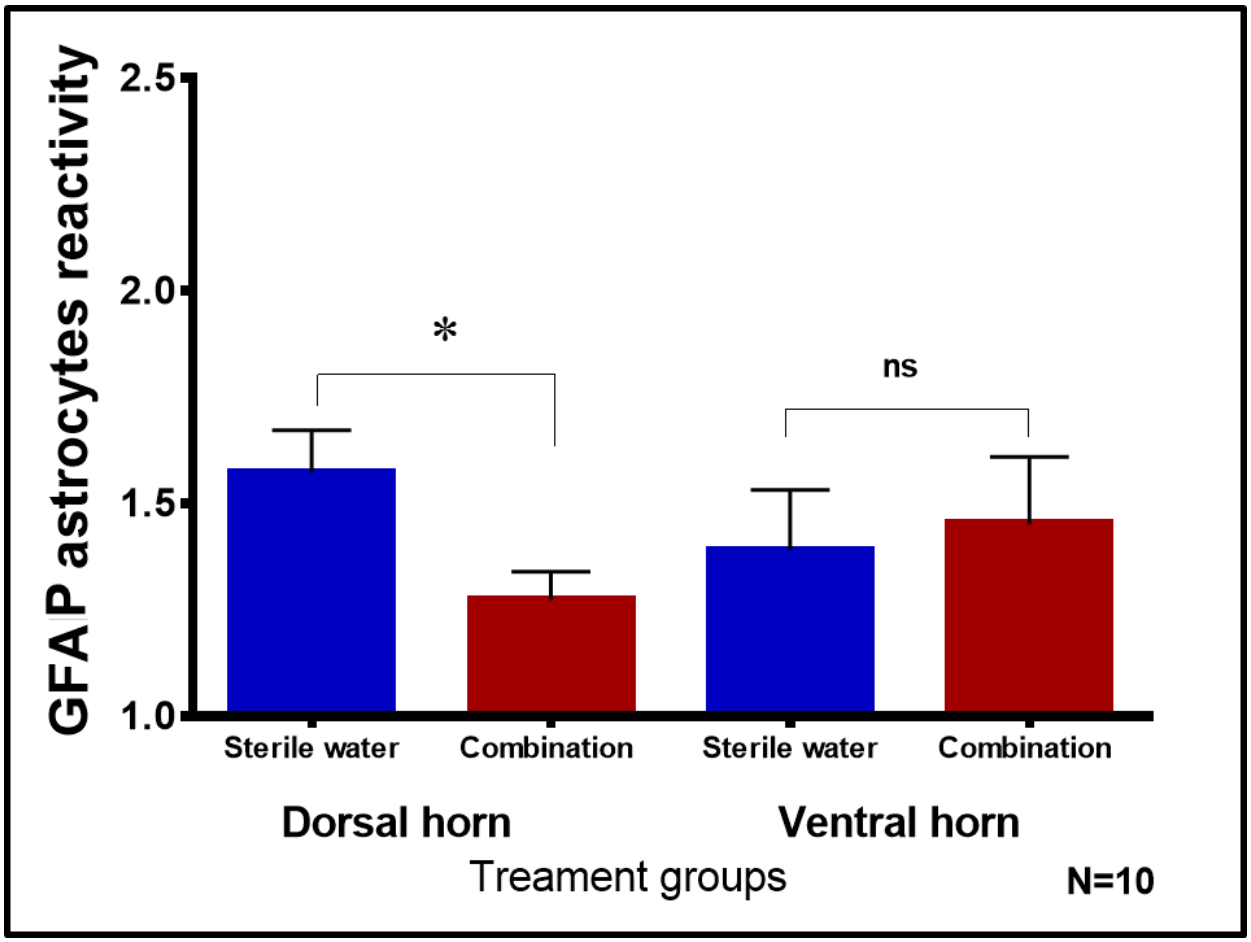

Figure 5.10: Quantification of ratio of astrocyte activation (GFAP marker) in ipsilateral versus contralateral dorsal and ventral horns six weeks following peripheral nerve injury and repair. (Data expressed mean ± SEM; ∗ : p <0.05, ns: p>0.05).

5.6 Discussion

These findings support the role of anti-inflammatory IL-10 cytokine and TNF-α antagonist as key modulators involved in the response to nerve injury. Administration of a combined treatment of IL-10 cytokine and TNF-α antagonist at time of nerve repair showed significantly improved nerve regeneration. Furthermore, a significant reduction in inflammatory markers at the site of nerve repair was seen, as was a decrease in glial activation in the dorsal horn of the spinal cord.

Electrophysiological analysis was chosen as a key evaluation of functional nerve regeneration in this sciatic nerve injury and repair model. The result showed that the CAP was always higher in the uninjured sham and the nerve repair groups, when compared the repair groups. This difference in the CAP might have resulted from a reduction in the number and/or size of regenerated axons in the distal stump after nerve injury and repair.

CAP ratio was significantly higher in combination treated animals compared with those in the sterile water group, suggesting a larger proportion of axons regenerated successfully across the repaired site (Ngeow et al., 2011b). It is possible combined application of IL-10 cytokine and TNF-α antagonist was effective in reducing fibrous tissue formation and subsequently improved nerve fibres regeneration, but histomorphometric analysis is essential to further assess this (Atkins et al., 2007; Sakalidou et al., 2011). However, assessment of conduction velocities did not show any difference in conduction speed between the experimental groups. Peripheral administration of combination therapy at time of nerve repair did not improve conduction speed and, moreover, it is more likely that axons matured at slow rates in both sensory and motor fibres within the sciatic nerve. This is consistent with previous studies that have reported enhanced recovery of nerve function, suppression of local

inflammation and reduction of scar tissue formation subsequently following application of either IL-10 cytokine or TNF-α antagonist, following peripheral nerve injury and repair (Atkins et al., 2007; Kato et al., 2010).

In our study, combined epineurial administration of IL-10 cytokine and TNF-α antagonist immediately after nerve repair reduced immune cell infiltration at the site of nerve injury and repair, compared with animals receiving sterile water treatment. The combination therapy appears to regulate the immune cell activity, which may possibly prevent development of neuropathic pain following peripheral nerve injury. Previous studies reported that local application of TNF-α antagonist Etanercept after sciatic nerve injury was associated with downregulation of inflammatory cytokines that mediate onset of neuropathic pain. Moreover, application of Etanercept was thought to support the rate of growth, and regeneration process of injured axons (Sommer et al., 2001; Kato et al., 2009; Kato et al., 2010).

It is well documented that IL-10 regulates production of pro-inflammatory cytokines, including TNF-α at the site of nerve injury, and subsequently suppresses sensitization and plasticity of neurons in the spinal cord (2014; Morris et al., 2014; Kwilasz et al., 2015). There is clear evidence that IL-10 functionally inhibits signalling pathways that contribute to immune cell chemotaxis and associated cellular events during Wallerian degeneration (Morris et al., 2014; Kwilasz et al., 2015). Here, combined therapy of IL-10 and TNF-α antagonist exerted a reduction of immune cell reactivity locally, and furthermore centrally in the spinal cord – indicated in our study, by reduced glial cell marker IBA-1 and GFAP immunoreactivity.

The precise role of pre-treatment of the injured peripheral nerve at the time of nerve repair with combination therapy has not previously been explored. However, the

current results suggest that combined epineurial application of IL-10 and TNF-α antagonist could suppress nociceptive pain signals largely through suppressing production of pro-inflammatory cytokines. In addition, this approach possibly reduces activation of immune cells at the injury site as well as in the sensory areas in the spinal dorsal horns regions.

The contribution of glial cells, microglia and astrocytes, to the development of neuropathic pain after nerve injury has largely been investigated using different glial inhibitors (interleukin-1 receptor antagonist and soluble tumour necrosis factor receptor antagonist) that were applied intrathecal at the site of spinal cord injury (Sweitzer et al., 2001; Mika et al., 2013). These inhibitors were shown to inhibit pain related mechanisms through reduced glial cell activation (Sweitzer et al., 2001; Zelenka et al., 2005; Kato et al., 2009; Hansen and Malcangio, 2013). However, these inhibitors reduced pain hypersensitivity immediately after nerve injury, but had no additive effect unless continuous application was delivered using special cutaneous pump for several weeks post injury. In our study, combined epineurial administration of IL-10 cytokine and TNF-α antagonist was the first to report and reduced glial cell activation shown by reduced IBA-1 and GFAP cell labelling in the dorsal horns of the spinal cord. It is possible that a combined IL-10 and TNF-α antagonist therapeutic approach interferes in the early stages of healing with signals that activate glial cells, and produces long lasting anti-inflammatory effects with a single injection that possibly suppresses pain related mechanisms, thus preventing the development of neuropathic pain.

5.7 Summary

The present study demonstrated that the effect of immediate combination therapy of IL-10 and TNF-α antagonist enhanced some aspects of nerve regeneration after nerve injury and repair. In addition, this therapeutic approach has resulted in a suppressed immune inflammatory response locally at the site of nerve injury, and centrally in the spinal dorsal horns. It should be highlighted that combined therapy of IL-10 and TNF-α antagonist appears to have a synergistic effect on the regeneration process without compromising immune cell function and subsequent healing process of the injured peripheral nerve. Although, the current combination therapy based method produced recognized long lasting anti-inflammatory effects, further research is necessary to optimise its therapeutic effect and tolerability, in the consideration for its targeted therapeutic approach in the management of neuropathic pain following peripheral nerve injury.

CHAPTER 6

Repair of peripheral nerve injury with gap defect using poly-carprolactone conduit and TNF-α antagonist

This study was undertaken in collaboration with my colleague Emad Albadawi (PhD student). I am grateful for his contribution in this study by carrying out conduit implantations and axon tracing techniques. Poly-caprolactone conduits used for this work were fabricated by Jonathan Field (PhD student) in the laboratory of Dr. Fred Claeyssens at the University of Sheffield.

6.1 Introduction

It has been long established that adequate restoration of function following peripheral nerve injury is clinically challenging. This is more apparent in nerve injuries where there is a 'gap deficit'. Poor outcome in repairing nerve tissue across a defect may be related to undue tension where there has been an attempt at direct surgical anastomosis of nerve stumps. Therefore, other treatment modalities have been advocated such as an autologous nerve graft where the nerve gap defect is too long and does not permit direct nerve repair. However, this type of repair is infrequently used due to restricted availability and morbidity associated with donor nerve tissue (Stefano et al., 2013). As a result, more work is being undertaken on developing novel biologically engineered tissues or materials that could functionally substitute nerve tissue (Johnson et al., 2005). Other challenges of neural tissue regeneration may be related to invasion of scar tissue, and limited angiogenesis and revascularization which are required to enhance neurogenesis and support axon regeneration (Johnson and Soucacos, 2008; Cattin et al., 2015).

During the reparation phase of a damaged peripheral nerve, the Schwann cell-basal lamina promote and guide axon growth, however, segmental nerve tissue loss has a detrimental effect of loss of axon growth potential and guidance across the gap defect. Therefore, nerve conduit guidance (NCG) provides an artificial means of guiding and supporting nerve growth, enhancing nerve regeneration and neurogenesis (Johnson and Soucacos, 2008; Chiono and Tonda-Turo 2015).

There are several types of NCG materials that have been used for repair of peripheral nerve injuries including biological (nerve autograft and autologous collagen) and synthetic (lactate polymer) nerve guides based on their ability to support axon growth

and prevent fibrous tissue invasion (Johnson et al., 2005; Johnson and Soucacos, 2008; Nan et al., 2012; Wood and Mackinnon, 2015).

Despite advancements in microsurgical replacement techniques, the misdirection of regenerating axons still provides a hindrance to fulfilling the aim of complete recovery of nerve function after nerve repair (Ichihara et al. 2008; Johnson and Soucacos 2008; Muheremu and Ao, 2015). In addition, it has been proposed that the NCG properties should support Schwann cells to migrate through the conduit without impeding the regeneration process. As a result, the NGC architecture should promote axonal regeneration in order to stimulate Schwann cells to migrate and enhance neuronal regeneration (Ichihara et al., 2008; Johnson and Soucacos, 2008; Muheremu and Ao, 2015). Several methods have been advocated to construct synthetic nerve conduit to replicate critical elements of regenerative environment during healing of damaged axons. Recently, Pateman et al (2015) developed microstereolithography method in the laboratory of Dr. Fred Claeyssens at the University of Sheffield. This method which is a new innovative 3D printing process that uses a laser source of A 405 nm. Briefly, the method involves object designing using optical laser beam, photosolidifcation of photocurable resin and finally custom conduit guidance printing (Pateman et al., 2015).

An overview of evidence available from experimental evaluation of poly-caprolactone (PCL) conduits in peripheral nerve repair, indicate that they are able to support axonal growth across a nerve defect and enhance nerve regeneration (Bertleff et al. 2005; R H Shin et al. 2009; Allodi et al. 2012).

Bertleff et al. (2005) compared the recovery of sensory function following traumatic hand injuries using a biodegradable PCL and repair a gap of 8 mm or more. Their study showed that recovery of sensation in the nerve conduit repair group was

considered at least as good as in the direct repair group and, thus PCL conduit is considered suitable for the repair of nerve gap defect up to 20 mm without tension.

Another study conducted by Shin et al. (2009) evaluated functional and histomorphological outcomes following conduit implantation of three synthetic materials (collagen, PCL and PGA) and nerve autograft in repairing a10 mm gap defect of sciatic nerve in a rodent model. After 12 weeks, there were no significant difference observed in compound muscle action potentials as shown by electromyographic measurements, and the percentage of axon counts between the autograft and synthetic conduit repairs. Furthermore, there were no differences in mean myelin thickness between the experimental groups. In addition, results showed that PCL and collagen conduits remained structurally stable with optimum results, whereas PGA conduits degraded quickly, and established that PCL conduits can be used to repair 10 mm sciatic nerve gap defect with better functional outcome similar to the autograft repair, as compared to other synthetic conduit guidance materials.

Several studies investigated nerve regeneration following repair of gap defects using either a biodegradable PCL conduit or an autologous nerve graft in rodent models (Den Dunnen et al., 1996; Reid et al., 2013). It has been reported that using a biodegradable PCL for repair is associated with faster nerve regeneration and is qualitatively better than using an autologous nerve graft (Den Dunnen et al., 1996). However, histomorphometric analysis did not show a significant difference in pattern and distribution of myelinated fibres between these two repair groups and results revealed similar numbers of axons in the distal stumps and equivalent re-innervation rate of end organ muscle and skin (Reid et al., 2013).

There is sufficient evidence that inflammatory cytokines such as TNF-α, produced by immune cells, have a detrimental effect on axonal regeneration, by upregulating the immune reaction following nerve injury (Gaudet et al., 2011; Bastien and Lacroix, 2014; Wood and Mackinnon, 2015). Although the precise effect of TNF-α is not completely understood, there is convincing evidence to support the fact that appropriate targeting of TNF-α receptors improves regeneration as well as nerve function and suppresses pain related behaviours (Liefner et al., 2000; Iwatsuki et al., 2013; Kato et al., 2010). Moreover, epineurial applications of TNF-α antagonist have been shown to inhibit immune cell activity and down regulate inflammation following peripheral nerve injury (Liefner et al., 2000; Iwatsuki et al., 2013; Kato et al., 2010).

6.2 Aim and objectives

The aim of this study was to investigate the effect of poly-carprolactone conduit and TNF-α antagonist (Etanercept) on the inflammatory immune response and nerve regeneration, 5 weeks following peripheral nerve injury and repair. More specifically; to determine the effect of TNF-α antagonist on glial activation in the dorsal and ventral horns of the spinal cord, and establish the effect of poly-carprolactone conduit and TNF-α antagonist (Etanercept) on axonal regeneration and gait movement, 5 weeks following peripheral nerve injury and repair.

6.3 Hypothesis

The implantation of PCL-based conduits with administration of TNF-α antagonist (Etanercept) peripherally at the site of nerve injury and repair will reduce the immune cell reactivity, and spinal glial cell activation, thus potentially reducing neuropathic pain, and improve functional recovery.

6.4 Materials and methods

Chapter 2 details the experimental materials, anaesthesia and methods employed in this series of experiments. All treatments received by animals were randomised and investigators performing the experiments and analysis of result were blinded. A schematic overview of the experimental design of this study is shown in Figure 6.1.

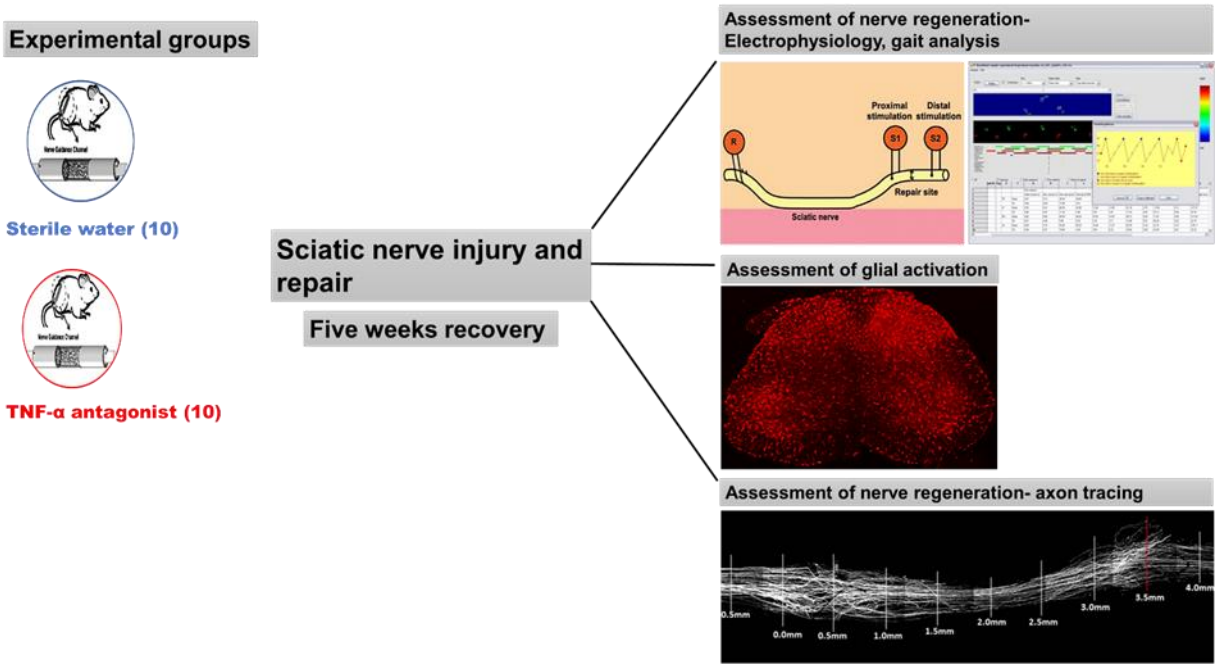

Figure 6.1: Illustration of the experimental design investigating the effect of poly-carprolactone conduit and TNF-α antagonist (Etanercept) on the inflammatory immune response and nerve regeneration in an *in vivo* model of sciatic nerve injury and repair.

Experimental groups

A total of 20 thy-YFP mice either male or females (≥8 weeks old– weights 17-30 g) were used in this study. For this study, a sample size calculation suggested that minor differences (5 %) in the extent of axon regeneration assessed by electrophysiological recording, functional axon tracing and gait analysis outcome can be detected with a sample size of 10 in each group. Animals were randomly allocated to either treatment groups: PCL conduit repair and Etanercept treatment (n=10) or PCL conduit repair with sterile water (n=10). Preparation and concentration of TNF-α (0.15 mg/100 µl) antagonist is detailed in Chapter 2, section 2.2.2.

Briefly, the animals were anaesthetised with 2-3 % of isoflurane and oxygen (2 L/min). The left sciatic nerve was exposed and 30 µl of treatment injected into either side of the segments (the proximal and distal) where the 4 mm defect would be created (see Chapter 2, section 2.2.4). A 5 mm PCL conduit was implanted and the two sectioned nerve stumps were inserted approximately 0.5 mm into either end of the conduit tube and secured with an application of fibrin glue (Figure 2.2). Following conduit implantation, the remaining 40 µl of the treatment agent was injected intramuscularly into surrounding muscle tissues, and the wound closed in layers with vicryl suture (6/0, ETHICON®). A subcutaneous injection of buprenorphine hydrochloride (Vetergesic [0.05 mg/kg], Ceva) was administered at the end of the surgical procedure, and animals allowed to recover for 5 weeks.

In this experiment additional sham group (n=10) from previous work in the Oral neuroscience group is included to explain difference between treatment groups under the investigation. Sterile water is considered as negative control and sham not

included initially due to the ethical issue in accordance with the UK Home Office Animals (Scientific Procedure) Act 1986.

Functional assessment of nerve function recovery

Gait analysis

As previously described in Chapter 2, section 2.2.5.1, gait assessment is acquired by use of CatWalk system that incorporates automated software analysis of natural gait parameters. Briefly, paw prints obtained from runs which were conducted immediately before (baseline) and then at weeks 1, 2, 3, 4 and 5 after nerve conduit repair. An average value of the two runs of each animal was counted

Electrophysiology

Electrophysiological recording is detailed in Chapter 2; section 2.2.5.1. For non-recovery electrophysiological recordings, animals anaesthetised with an intra-peritoneal (ip) injection of intravenous fluanisone (0.8 ml/kg) and midazolam (4 mg/kg). The sciatic nerve of left leg was exposed and a pair of central recording electrodes applied to the nerve (platinum wire 0.15 mm diameter). An evoked stimulation across the sciatic nerve was delivered from two pairs of distal and proximal electrodes, each sited close to the conduit edges touching only the nerve tissues. Data was recorded and stored using Spike 2 software and the CAP ratio calculated between the responses evoked from proximal or distal to the repair (modulus with distal stimulation ÷ modulus with proximal stimulation). were compared between the experimental groups, from an average of 10 responses to stimulation along the sciatic nerve. In addition, conduction velocities were recorded by measuring the latency of the earliest component of the CAP evoked by stimulating the regenerated segment of the sciatic

nerve. This recording would include both the proximal and the regenerated components of the nerve.

Axon tracing

Axon tracing measures the sprouting Index (SI), the number of individual axons that have crossed the defect and the level of axon disruption across the initial portion of the conduit repair. As previously stated (see Chapter 2, section 2.2.9), a reference line was drawn across the junction of central nerve segment and conduit edge and established as 0.0 mm interval and then subsequent intervals determined in forward direction at length of 0.5 mm up to 4.0 mm distal to the interface of axons and conduit edge.

The SI was determined by counting the number of axons at each interval and dividing by the axon number at the -0.5 mm interval (see Chapter 2, section 2.2.9). An average value was used to minimise the estimation error. Functional axon tracing is used to determine the percentage of axons that have successfully reached each interval across the nerve gap defect. Next axons were traced and the length measured from point 0.0 mm to 1.5 mm to determine the average axon length as proportion of the distance (i.e. 1.5 mm) (see Chapter 2, section 2.2.9).

Tissue sectioning and immunohistochemistry analysis

Following completion of the electrophysiology recordings, animals received a 0.5 ml intraperitoneal injection of sodium pentobarbital (20 % w/v) and the spinal cord tissues was removed and fixed in 4 % paraformaldehyde for 24 hours, and cryoprotected overnight in 30 % sucrose solution, both at 4°C. The spinal cords were frozen down and sectioned as previously described (Chapter 2, section 2.2.6).

Staining and analysis of glial cells in the spinal cord

Twelve sections from L4 region were selected per animal and stained for microglial marker (IBA-1) and astrocyte marker (GFAP) using free floating technique. Sections were blocked in in 200 µl 10 % normal donkey serum and incubated with a polyclonal antibody to IBA-1 raised in goat, or a polyclonal antibody to GFAP raised in rabbit, and respective secondary antibodies donkey anti-goat CY3 or donkey anti- rabbit CY3. Tissues were then mounted onto gelatine-coated slides and cover slipped with vectashield. For full details see Chapter 2, section 2.2.7.

Images of three immunostained sections, representative of dorsal and ventral horn regions, per animal, were captured at x40 objective for quantitative analysis and at x5 objective for qualitative analysis. Glial cell activation was interpreted by an increase in the number (proliferative changes) and complexity of the cells morphology (phenotypic alteration) such as enlarged cell bodies and thicker processes in the dorsal and ventral spinal horns.

The percentage area of glial labelling calculated by selecting area of interest and then activation areas highlighted by pink, while the remaining areas would be highlighted by yellow (See Chapter 2, section 2.2.8). Each reading was taken three times, and the mean was taken. The ratio of glial cell reactivity was determined by measuring and comparing the ratio of positive labelling between the ipsilateral and contralateral sides, in both the dorsal and ventral horn regions.

Statistical comparisons of CAP, conduction velocity and glial cell labelling were performed using t-test (Two-tailed). Quantitative data was expressed as mean ± SEM. Two-way repeated measures ANOVA was used for comparison between the groups to detect any difference in sprouting index and functional axon tracing and gait

parameters. Differences between groups were considered significant at $p<0.05$. Statistical analysis was performed using Microsoft Excel 2010 and GraphPad Prism7 (GraphPad Software, Inc, USA).

6.5 RESULTS

Five weeks following conduit implantation, the sciatic nerve had regenerated through the conduit in 8 out of 20 mice (four in each group). The remaining 12 mice where their nerves had failed to regenerate due to technical failure as conduit become separated from either the proximal or the distal end were excluded from further analysis.

6.5.1 Functional analysis

6.5.1.1 Gait analysis of paw print intensity and total paw print area

Analysis of changes in gait movement is considered an effective method to analyse function after peripheral nerve repair, and is assessed by measuring paw print intensity and surface area.

Paw print intensity

Immediately after the nerve injury and repair there was dramatic drop of the left paw print intensity in both groups. The TNF-α antagonist group had 60 % of the preoperative paw print intensity after one week (Figure 6.2), whilst the sterile water had 50 % of preoperative paw print intensity at this time point, although this difference was not statistically significant ($p= 0.999$, two-way repeated measures ANOVA). The results obtained at weeks 2 and 3 showed that there was a significant difference between the left paw print intensity in the TNF-α antagonist group when compared to the sterile water group (week 2, $p= 0.0333$; week 3, $p= 0.0372$, two-way repeated

measures ANOVA). In the TNF-α antagonist group, the left paw print intensity had recovered to 70 % of the preoperative value at week 2 and week 3 in comparison to the sterile water group where intensity remained at 50 % of preoperative values. Furthermore, the TNF-α antagonist group showed reduction in function at week 4 and 5, but remained slightly above the sterile water group (week 4, p=0.999; week 5, p=0.999, two-way repeated measures ANOVA).

However, the print intensity of the right paw (uninjured side) were reduced compared to preoperative value, and become indistinguishable from week 1 as no significant differences was registered between the experimental groups during the study (week1, p=0.877; week 2, p=0.998; week3, p=0.999; week 4, p=0.789; week 5, p=0.939, two-way repeated measures ANOVA) (Figure 6.3).

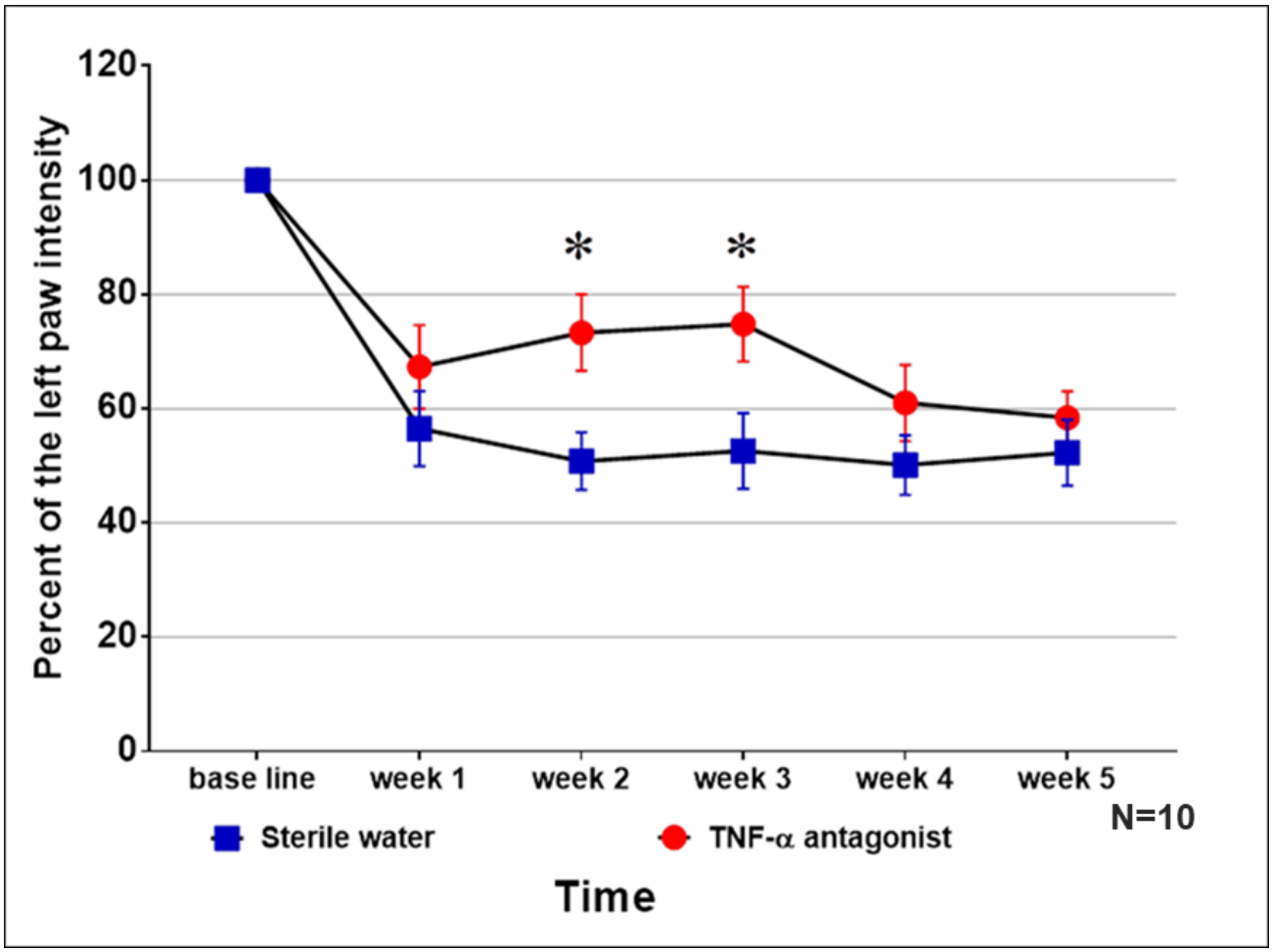

Figure 6.2: The mean intensity of the left paw print as a percentage of the preoperative value (100 %) for each group at each time point of function assessment. $*$: p <0.05).

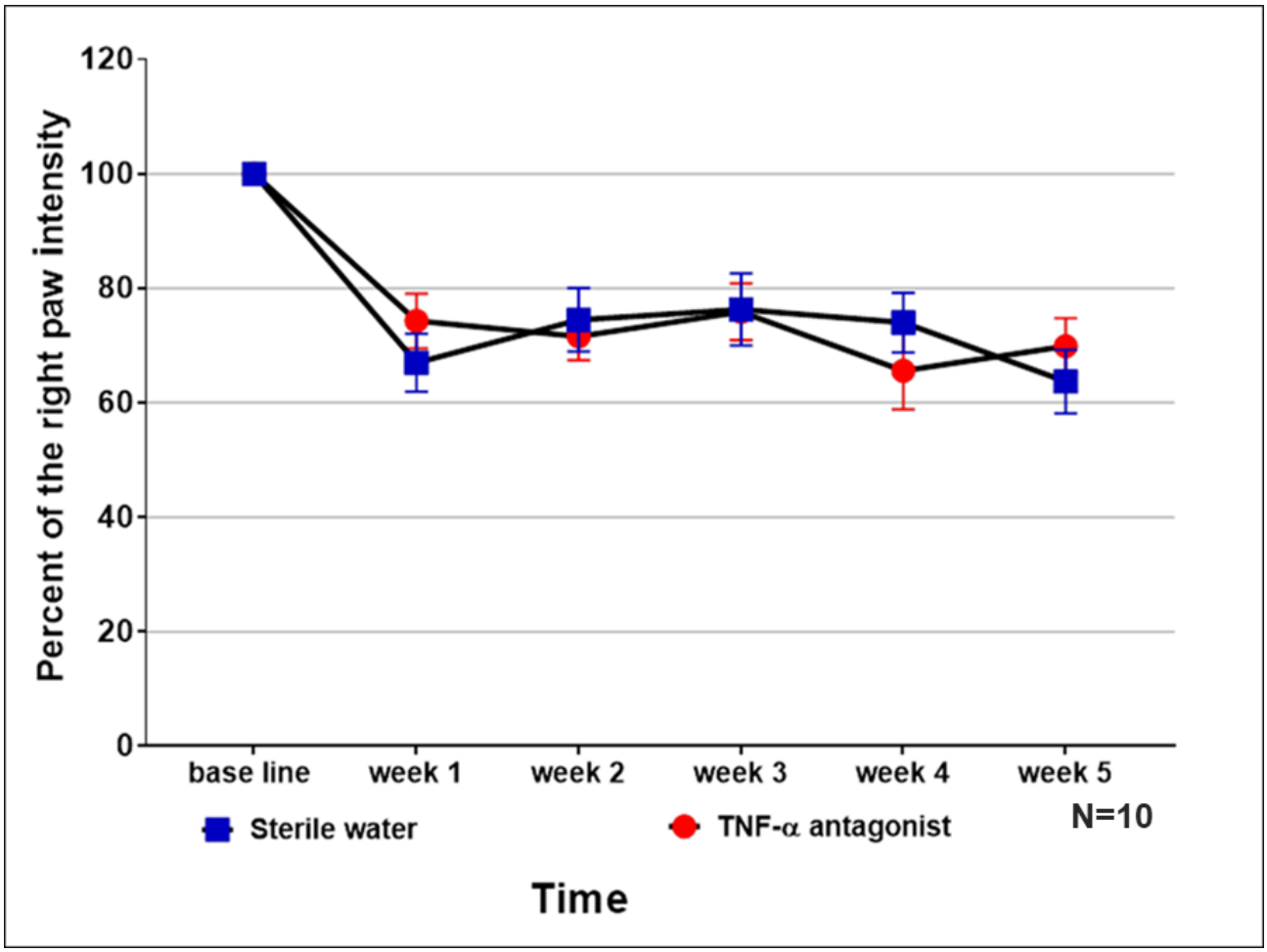

Figure 6.3: The mean intensity of right paw print as a percentage of the preoperative value (100 %) for each group at each time point of function assessment.

Total paw print area

The percentages of total print area of the left paw (injured side) were negatively affected in both groups when compared to baseline values (Figure 6.4). At week 1 and week 2 assessment, the TNF-α antagonist group had 60 % of preoperative value of total paw print area, and the sterile water had 40 % of preoperative value of total paw print area this time point, but not significant (week 1, p= 0.139; week 2, p=0.166, two- way repeated measures ANOVA). However, the value of total print area of the left paw was significantly different between the experimental groups at week 3 assessment (p= 0.0252, two-way repeated measures ANOVA) and analysis shows that the TNF-α antagonist repair group had a significantly greater left paw print area as compared to the sterile water group. Moreover, changes in gait function as shown by variation in values of total paw print area at weeks 4 and week 5 showed no significant difference between groups at these time points (week 4, p= 0.1612; week 5, p= 0.4972, two-way repeated measures ANOVA).

The values of total print area of the right paw (uninjured side) were reduced as compared to the preoperative values in both groups at week 1 assessment (Figure 6.5). By week 2 of gait assessment the TNF-α antagonist had a total paw print area slightly greater than the sterile water group but this was not statistically significant (p= 0.742, two-way repeated measures ANOVA). Once more, there were transient changes in gait function for the rest of assessment period at week 3,4 and 5 and results did not reveal any difference between treatment groups (p= 0.999, two-way repeated measures ANOVA).

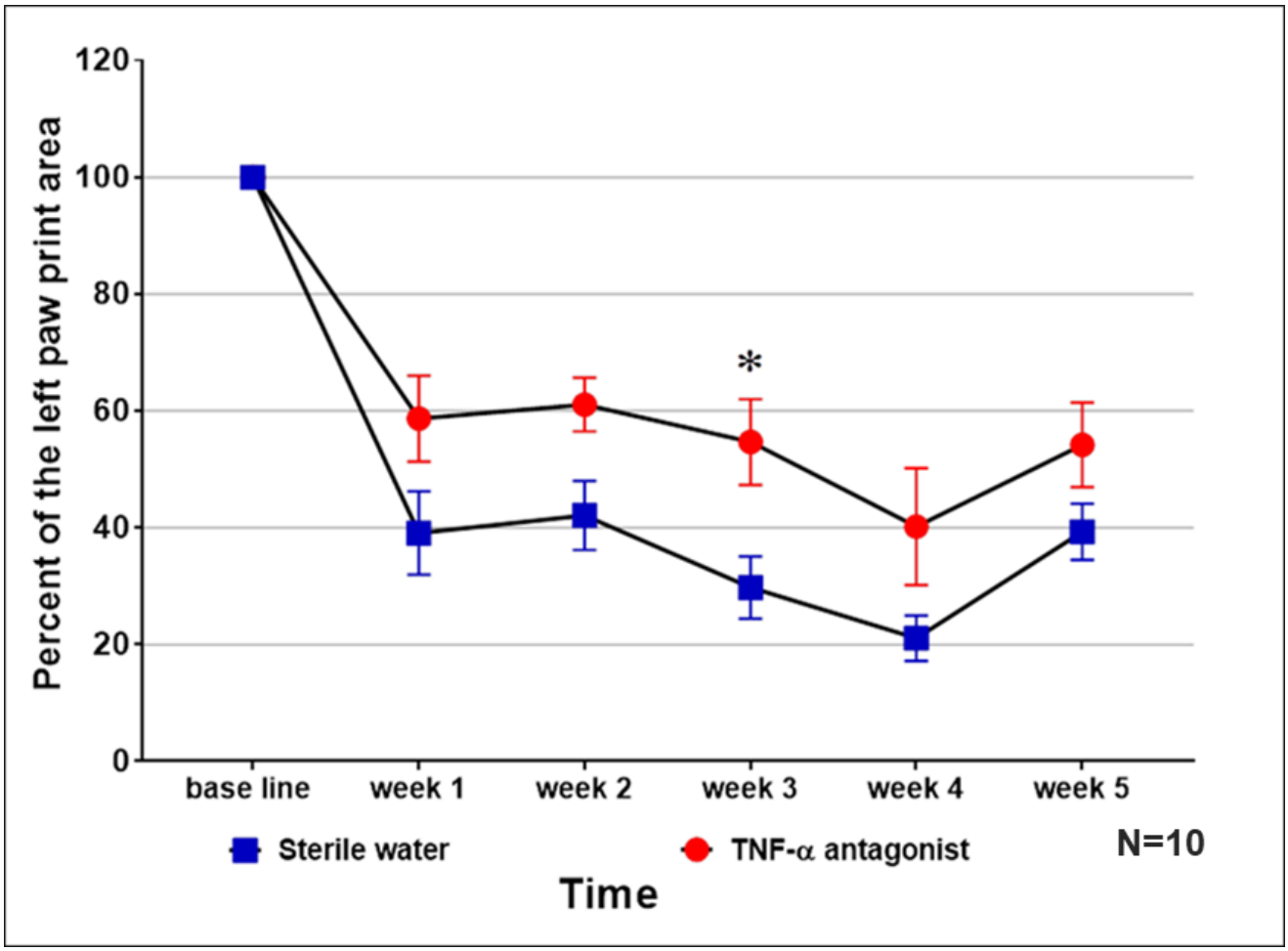

Figure 6.4: The mean total area of left paw print as a percentage of the preoperative value (100 %) for each group at each time point of function assessment. ＊: p <0.05).

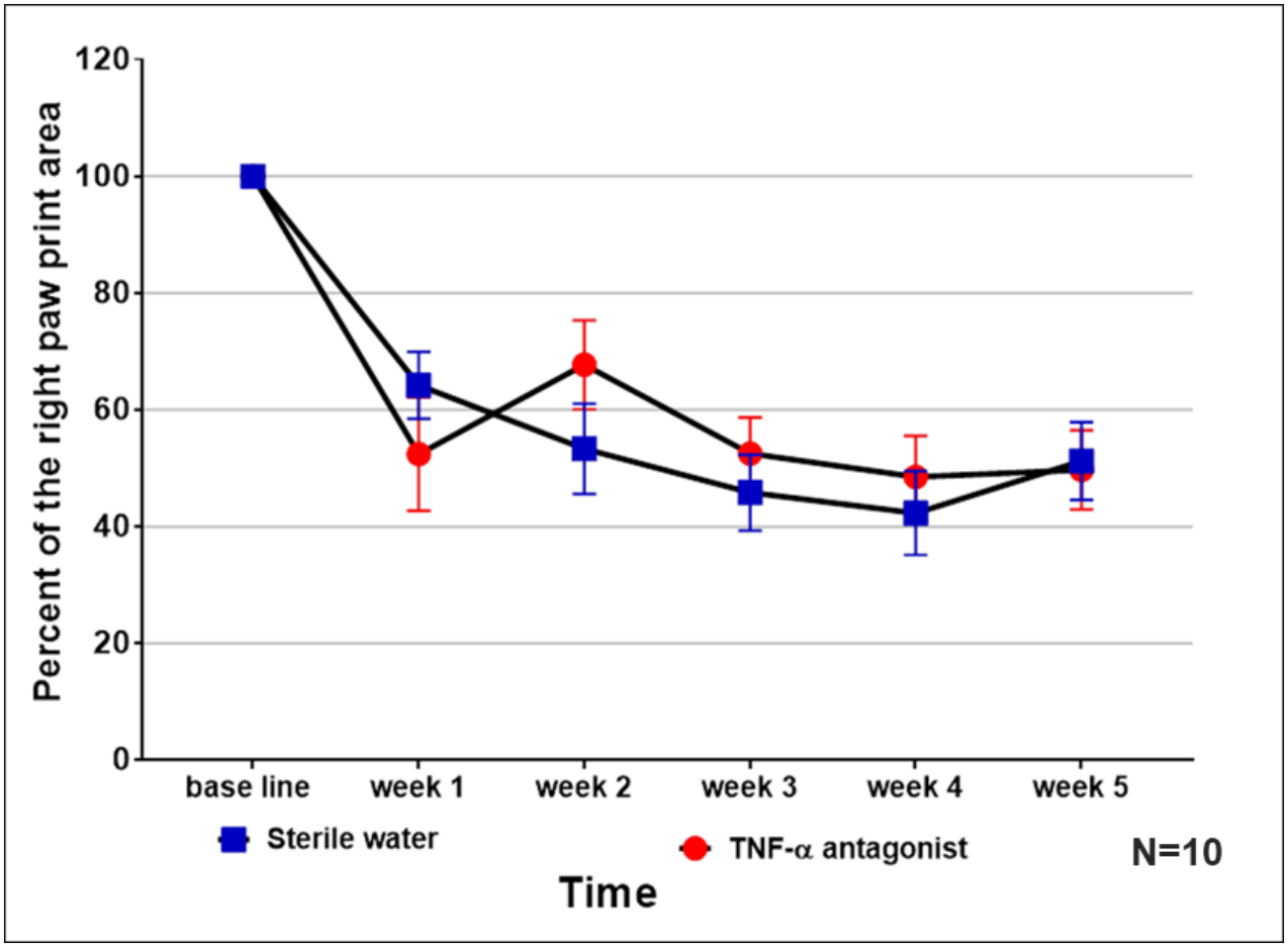

Figure 6.5: The mean total area of the right paw print as a percentage of the preoperative value (100 %) for each group at each time point of function assessment.

6.5.1.2 Electrophysiology analysis

Following 5 weeks of recovery, electrophysiological studies were carried out to determine the efficacy of poly-carprolactone conduit and TNF-α antagonist (Etanercept) on neuronal axon regeneration by recording a series of a compound action potential after sciatic nerve injury and repair.

Compound action potentials (CAP)

The CAP ratio in the uninjured sham group was 0.89 (SEM± 0.79), indicating that higher compound action potentials were evoked by stimulation at the distal site. The ratio of CAP from the proximal and distal segment was compared between the experimental groups and whilst data show some indication of better regeneration of nerve fibres in animals receiving TNF-α antagonist treatment, compared with receiving sterile water, the results were not statistically significant (p=0.313, two-tailed t-test) (Figure 6.6). In the TNF-α antagonist group, the mean CAP ratio was 0.4895 (SEM± 0.1371), while the mean CAP ratio for the sterile water group was 0.311 (SEM± 0.104) (Figure 6.7).

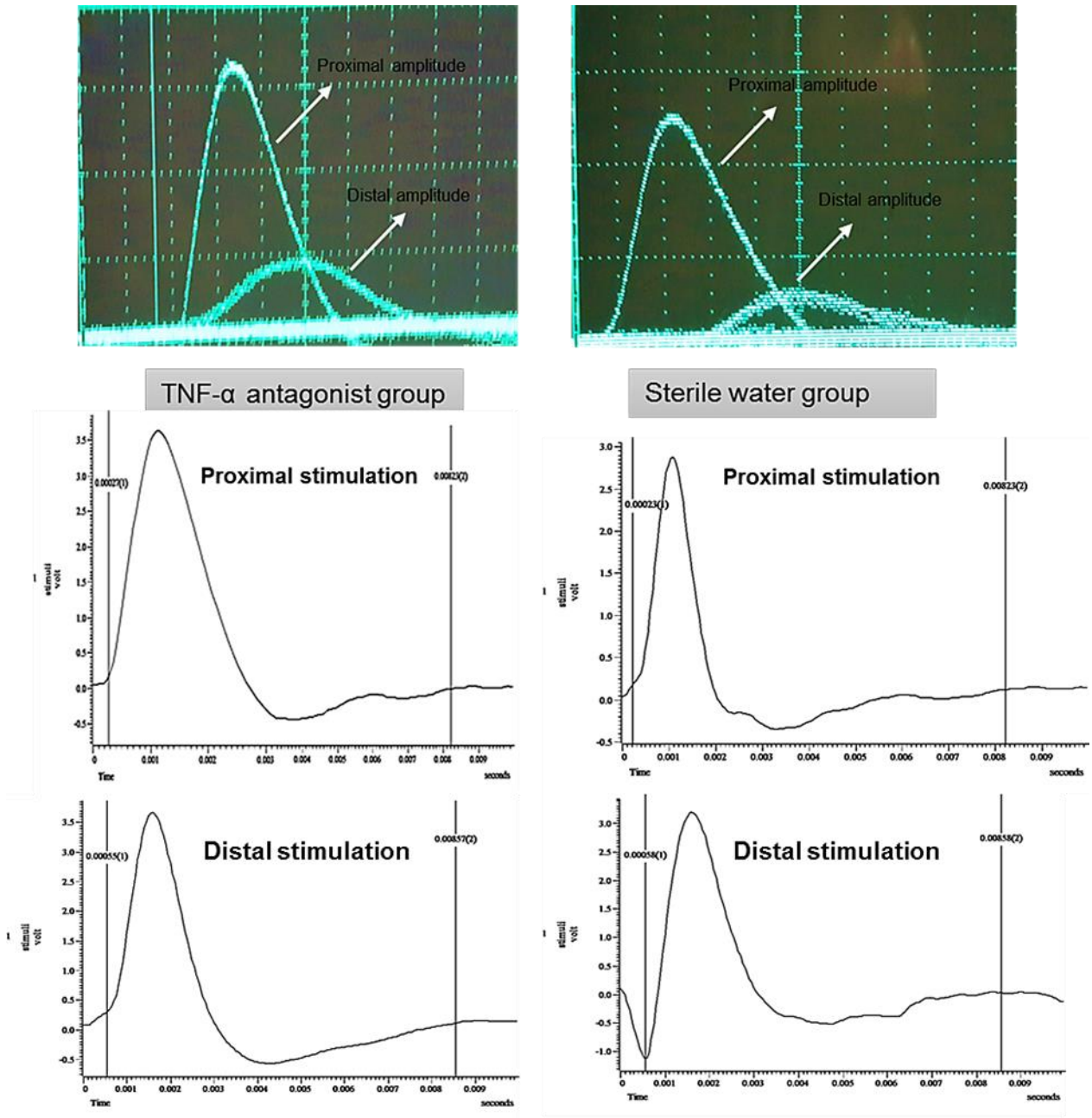

Figure 6.6: Calculation of CAP ratio as evoked by stimulation proximal and distal to the repair site, respectively.

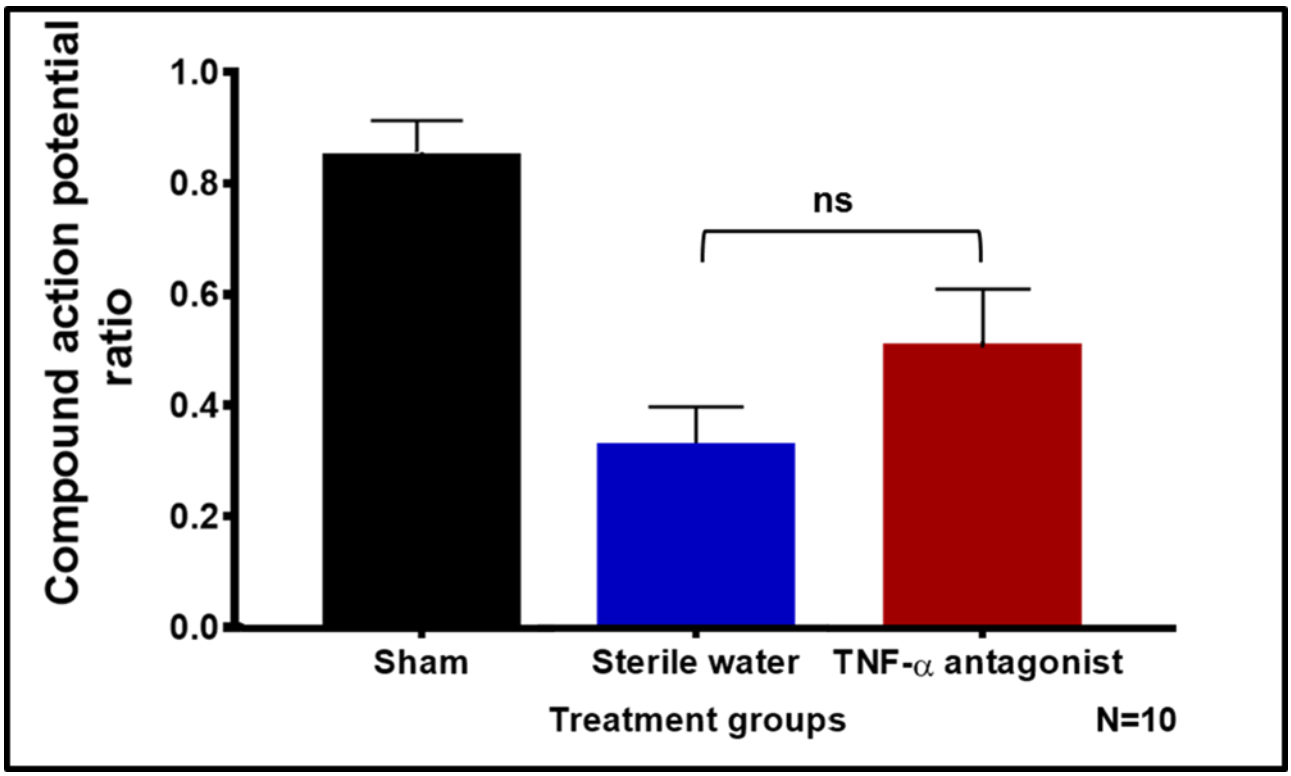

Figure 6.7: Comparison of mean compound action potential (CAP) amplitude ratios between experimental groups (Data expressed mean ± SEM; ns: $p>0.05$).

Conduction velocities

The conduction velocity of the fastest axons in the sham controls was 60.70 m s-1 (SEM± 3.529). The conduction velocities were significantly slower in all the nerve repair groups. The results revealed no significant difference in the conduction velocities attained by stimulating distal nerve fibres in both groups (p= 0.777, two-tailed t-test) (Figure 6.8). The mean conduction velocities in the sterile water group were 14.1 ms^{-1} (SEM± 2.896), whereas in the TNF-α antagonist group the mean conduction velocities were 15.5 ms^{-1} (SEM± 3.931).

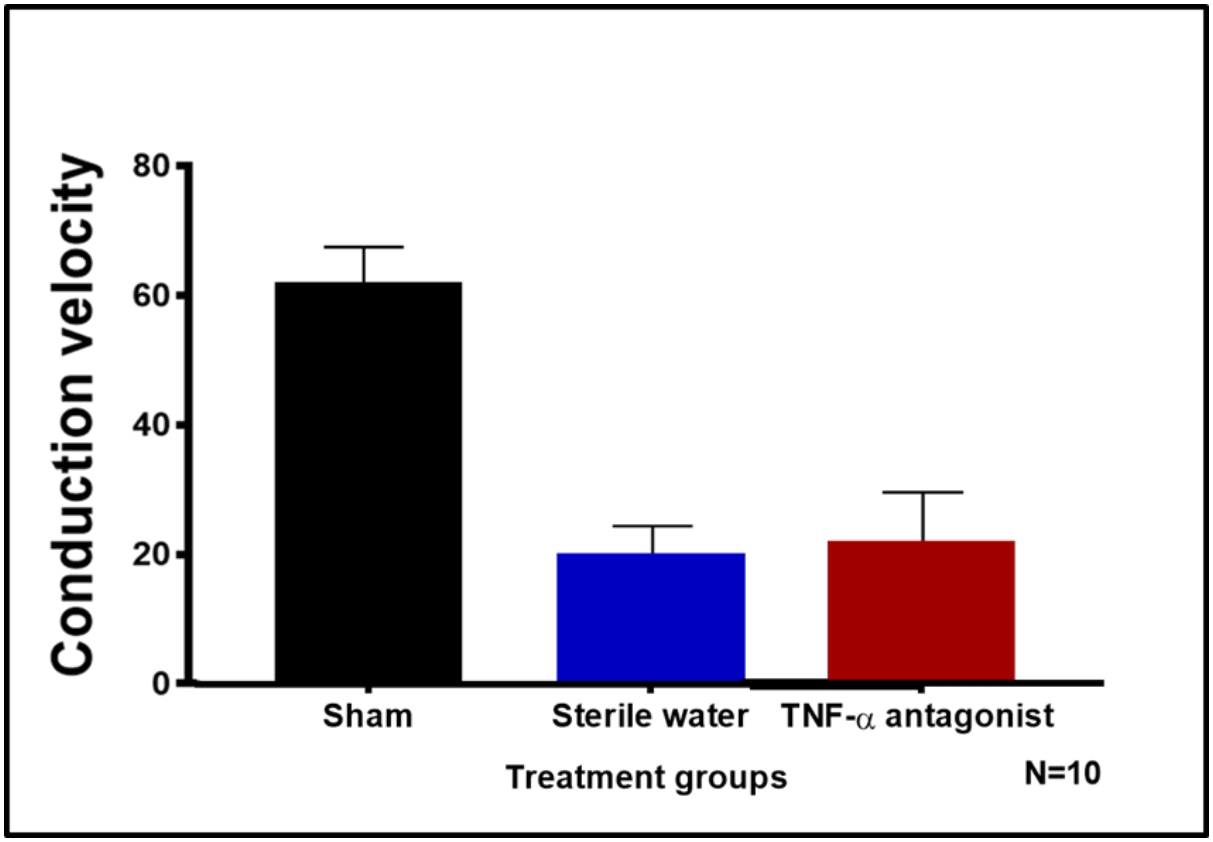

Figure 6.8: Mean conduction velocities of experimental groups, 5 weeks following conduit implantation (Data expressed mean ± SEM; ns: p>0.05).

6.5.1.3 Axon tracing

Five weeks following sciatic nerve repair, only 8 out of 20 mice (four in each group) their nerves successfully regenerated as the conduits did not dislodge or separate from the proximal or distal never end and the remaining were excluded from further analysis.

Qualitative Observations

Morphological assessment of axonal regeneration across a 4 mm gap following 5 weeks of PCL nerve conduit repair of sciatic nerve showed a difference in the pattern of axon growth between the groups. More, specifically, axonal sprouting was more organized in the TNF-α antagonist group as compared to the sterile water group at the start of axonal regeneration within the conduit (0.0 mm interval) (Figure 6.9). Thereafter, as axons enter the conduit and progressed towards the distal nerve segment they showed more uniform pattern of regeneration through the conduit after 5 weeks of nerve injury and repair in all experimental groups.

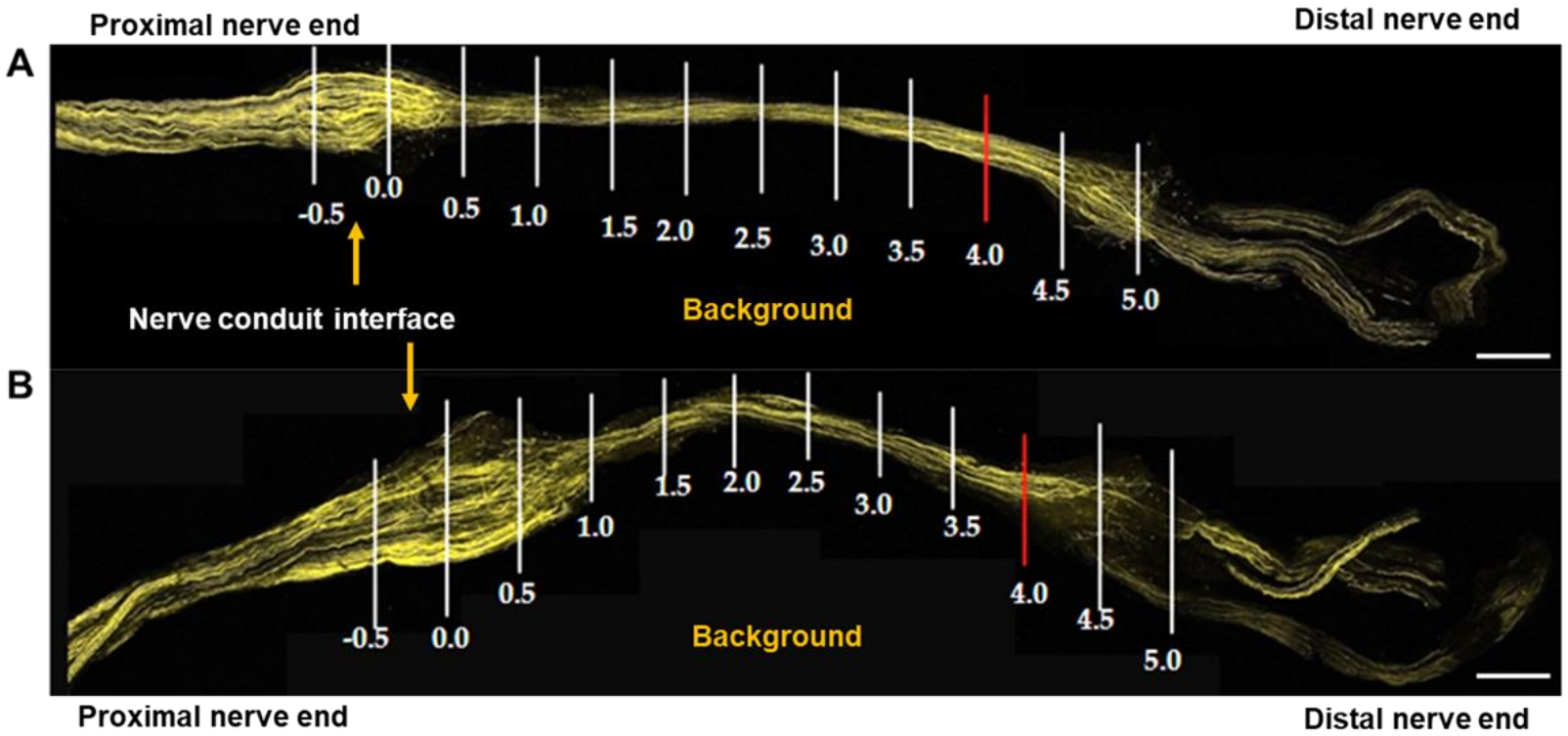

Figure 6.9: Confocal fluorescent microscopic images of Thy-1-YFP-H nerve conduit repair with intervals marked from 4.0 mm interval position back to 0.0 mm (start) interval. (A) TNF-α antagonist group. (B) Sterile water group. In all of the repair groups, there is an area of disrupted axons shown around the proximal nerve ending-conduit interface, with axons then becoming more organised once had crossed the conduit and entered the distal nerve stump. TNF-α antagonist group typically appeared to have less axon sprouting at the join between proximal nerve end and conduit than the sterile water repairs. In the sterile water group axons typically were disrupted and disorganised upon regenerating out from the proximal transected segment, whilst in the TNF-α antagonist group axons regenerating through the PCL conduits tended to be more densely arranged than axons with greater organisation pattern. Scale bar= 1.0 mm.

Quantitative Observations

Sprouting index

The results obtained show that at 0.5 mm, axonal sprouting was significantly less in the TNF-α antagonist group (p=0.010, two-way repeated measures ANOVA) (Figure 6.10). The sprouting index was lower in the TNF-α antagonist group compared to the sterile water group at 0.5 mm interval into the conduit (41 % versus 69 %).

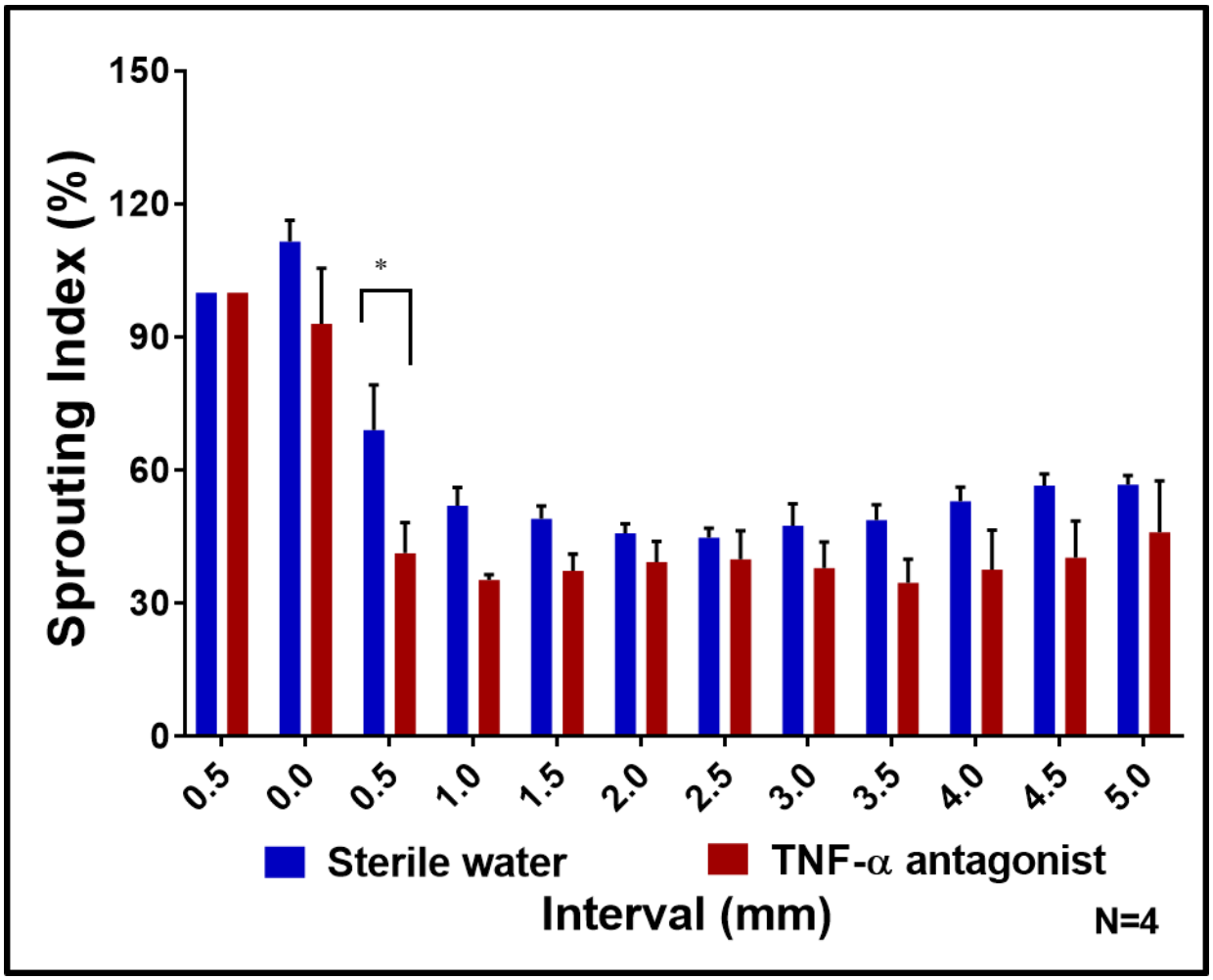

Figure 6.10: Sprouting index values for each 0.5 mm interval. Data expressed mean ± SEM; * : p <0.05).

Functional axon tracing

Regenerated axons were traced across the repair site to determine the proportion of axons that had successfully regenerated across the distal nerve segment (4.5 mm interval) through the conduit 5 weeks after nerve injury and repair (Figure 6.11). When comparing the proportion of regenerated axons, the results showed that 30 % of axons in the TNF-α antagonist group, compared to 24 % of axons in the sterile water group, reached the last distal point at interval 4.5 mm, but this was not statistically significant (p=0.999, two-way repeated measures ANOVA). Furthermore, comparing overall axon proportions from the 0.0 mm interval, almost 60-70 % of axons in the TNF-α antagonist and the sterile water groups failed to regenerate across the repaired site.

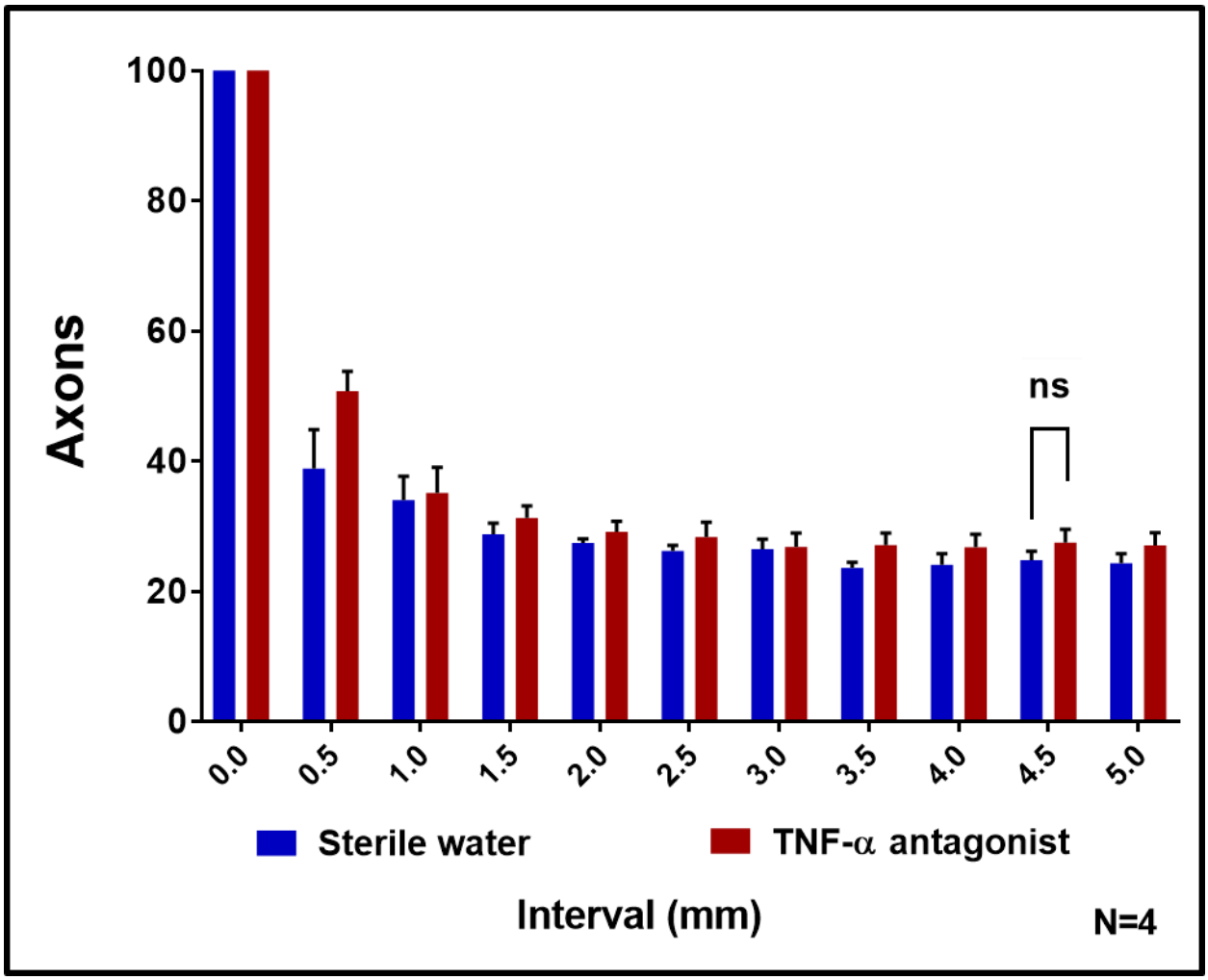

Figure 6.11: Percentages of axons that successfully had reached the distal segment from the repair start point (0.0 mm interval) (Data expressed mean ± SEM; ns: $p>0.05$).

Axon disruption

Axonal disruption mostly occurs shortly after joining of the proximal stump with the conduit repair and predetermined between 0.0 mm and 1.5 mm intervals as described in Chapter 2, section 2.2.9. When comparing the length of regenerated axons across repair site between 0.0 mm and 1.5 mm intervals there was significant reduction in the level of axonal disruption in the TNF-α antagonist group as compared to the sterile water group (7.288 [SEM±0.656] versus 12.36 [SEM±1.981]; p=0.039, two-tailed t-test) (Figure 6.12).

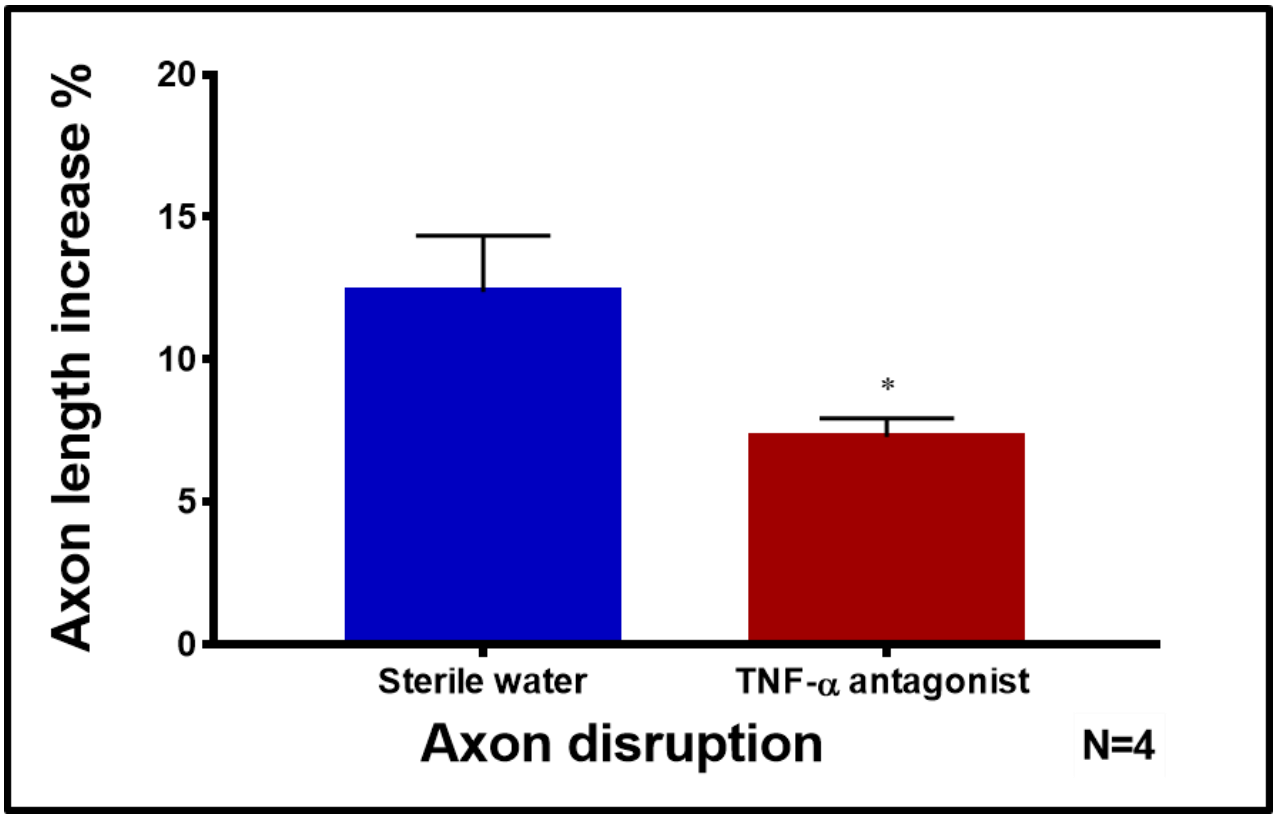

Figure 6.12: Axon disruption across the initial 1.5 mm of nerve conduit repair (Data expressed mean ± SEM; * : p <0.05).

6.5.2 Immune cells fluorescent labelling

The qualitative and quantitative assessment of immune cell expression of IBA-1 (microglial marker) and GFAP (astrocyte label) was carried out to determine the change in immune cell response, in the dorsal and ventral horns of the spinal cord.

IBA-1-microglia labelling following sciatic nerve injury and repair

Qualitative Observations

Five weeks following sciatic nerve injury and repair, and conduit implantation, clusters of IBA-1 immunofluorescent reactive microglial cells with long and branching processes were observed in the dorsal horns of animals receiving sterile water treatment (Figure 6.13). This was accompanied by dense microglial activation in ventral horns in both experimental groups (Figure 6.13).

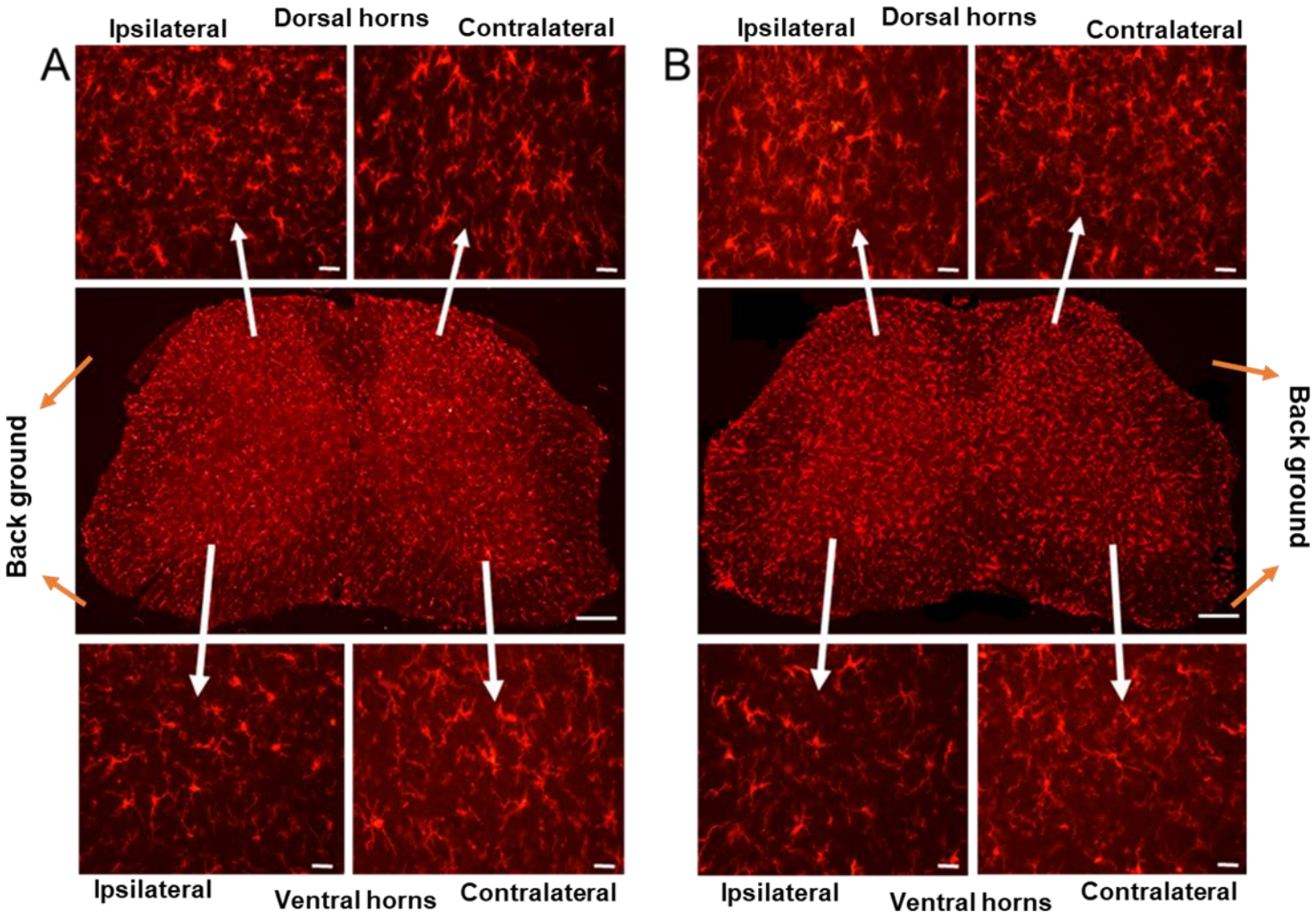

Figure 6.13: Immunofluorescent images of microglia (IBA-1) labelling in the spinal cord, 5 weeks following conduit implantation. (A) Sterile water group. (B) TNF-α antagonist group. White arrows indicate corresponding areas of interest and showing hypertrophied and amoeboid active glial cells. Scale bar = 25 µm.

Quantitative Observations

Five weeks following nerve injury and conduit implantation and repair, statistical analysis revealed a significant difference in IBA-1 microglial marker labelling in ipsilateral versus contralateral sides in the dorsal horns between the two experimental groups (p= 0.030, two-tailed t-test) (Figure 6.14). The mean ratio of IBA-1 fluorescent labelling in ipsilateral and contralateral sides in the dorsal horn after five weeks of injury in the TNF-α antagonist group was 1.28 (SEM± 0.0697), compared with those treated with sterile water,1.505 (SEM± 0.0388).

The quantitative analysis of IBA-1 microglial labelling in the ventral horn of the spinal cord did not show any difference between the groups (p= 0.866, two-tailed t-test) (Figure 6.14). The mean ratio of IBA-1 positive cells in ipsilateral versus contralateral sides in the ventral horns in mice treated with TNF-α antagonist was 1.32 (SEM± 0.0393) whereas those treated with sterile water was 1.333 (SEM± 0.0590).

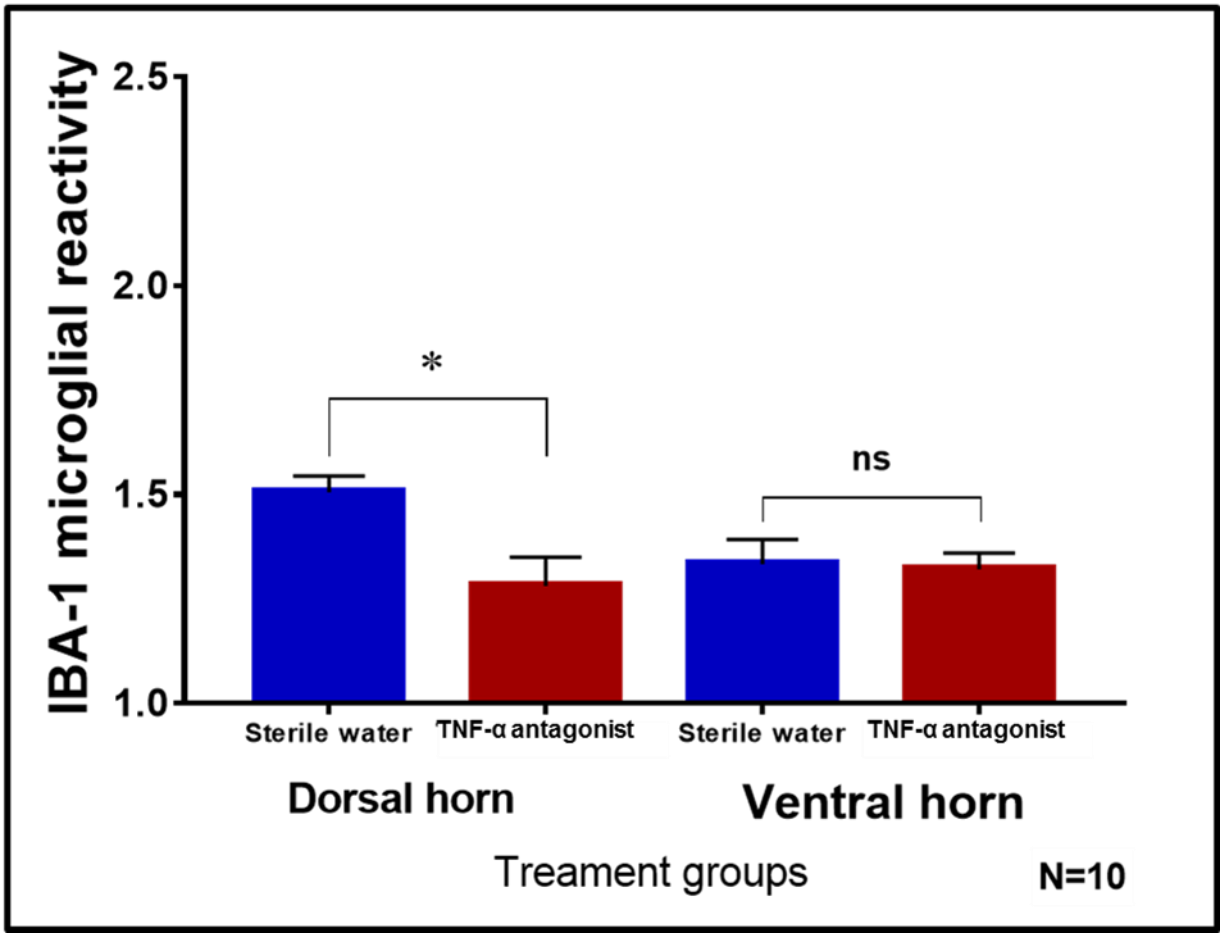

Figure 6.14: Quantification of ratio of microglial activation (IBA-1 marker) in ipsilateral versus contralateral dorsal and ventral horns five weeks following peripheral nerve injury and conduit implantation. (Data expressed mean ± SEM; ∗: p <0.05, ns: p>0.05).

GFAP astrocyte labelling following sciatic nerve injury and repairs

Qualitative Observations

Astrocyte activation and morphological changes observed in the spinal cord sections, five weeks following nerve injury and conduit implantation, were similar to changes seen in microglia activation (Figure 6.15).

Qualitative analysis of the spinal cord sections in the lumbar-4 region, showed high levels of immunofluorescent astrocyte labelling, with pronounced branching of processes, in dorsal horns in the sterile water group. Moreover, there was also high GFAP labelling in the ventral horns in both experimental groups (Figure 6.15).

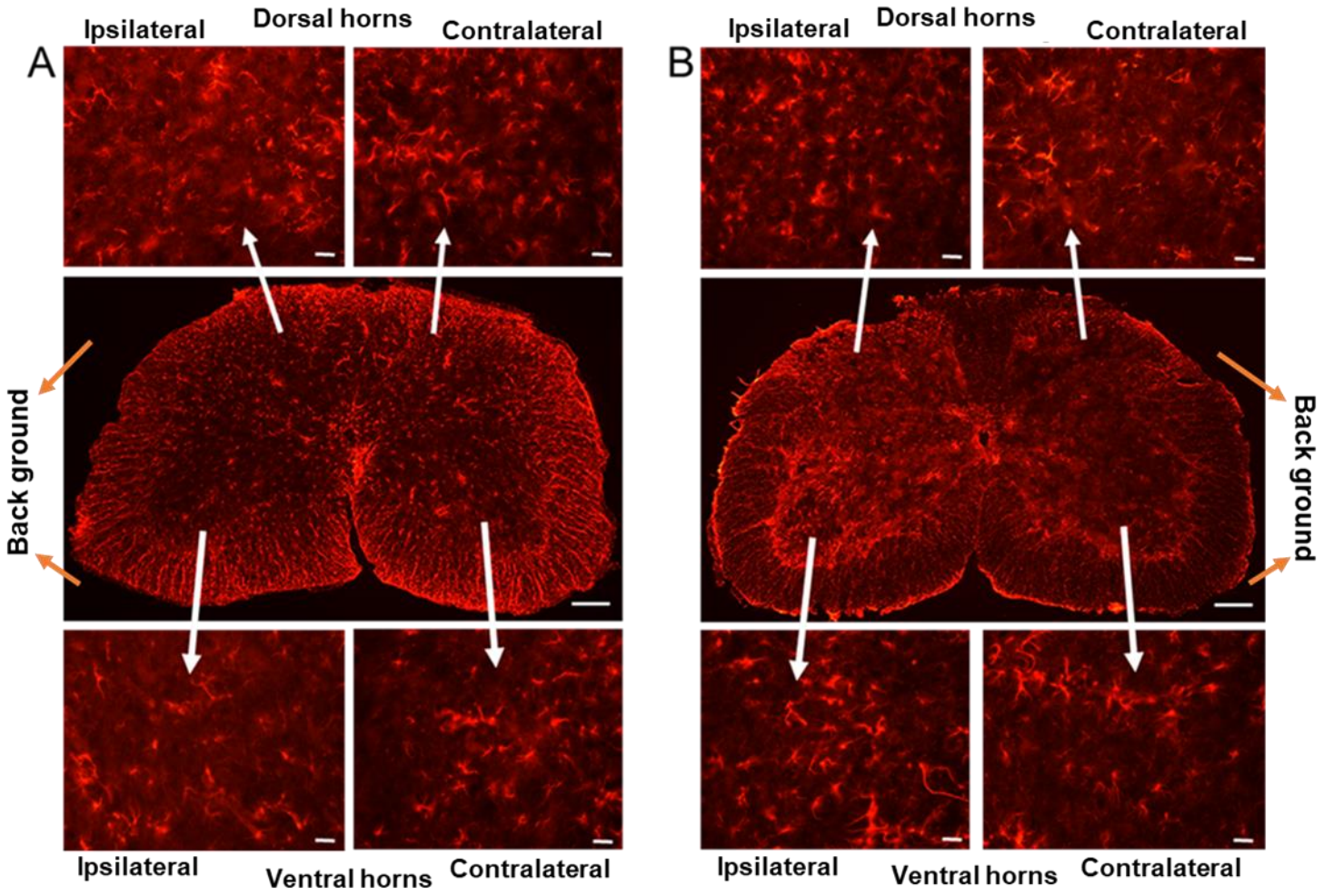

Figure 6.15: Immunofluorescent images of astrocyte (GFAP) labelling in the spinal cord, 5 weeks following conduit implantation. (A) Sterile water group. (B) TNF-α antagonist. White arrows indicate corresponding areas of interest and showing hypertrophied and amoeboid active glial cells. Scale bar = 25 µm.

Quantitative Observation

Quantitative analysis of GFAP astrocyte labelling in the L4 region of the spinal cord, revealed a significant difference in the ratio of expression in ipsilateral versus contralateral sides in the ventral horns between the two treated groups, five weeks following sciatic nerve injury and conduit implantation (p= 0.022, two-tailed t-test) (Figure 6.16).

The mean ratio of astrocyte labelling was lower in dorsal horns of mice treated with TNF-α antagonist 1.218 (SEM± 0.0666) compared with mice treated with sterile water (1.465 [SEM± 0.0457]) at time of sciatic nerve repair. In contrast, there was no significant difference in the ratio of astrocytes labelling in ipsilateral versus contralateral sides in the ventral horns between the two groups (p= 0.389, two-tailed t-test) (Figure 6.16). The mean ratio of astrocyte immunoreactivity in the TNF-α antagonist group was 1.163 (SEM± 0.0466) compared with mice treated with sterile water at time of nerve repair the cell labelling was 1.23 (SEM± 0.0559).

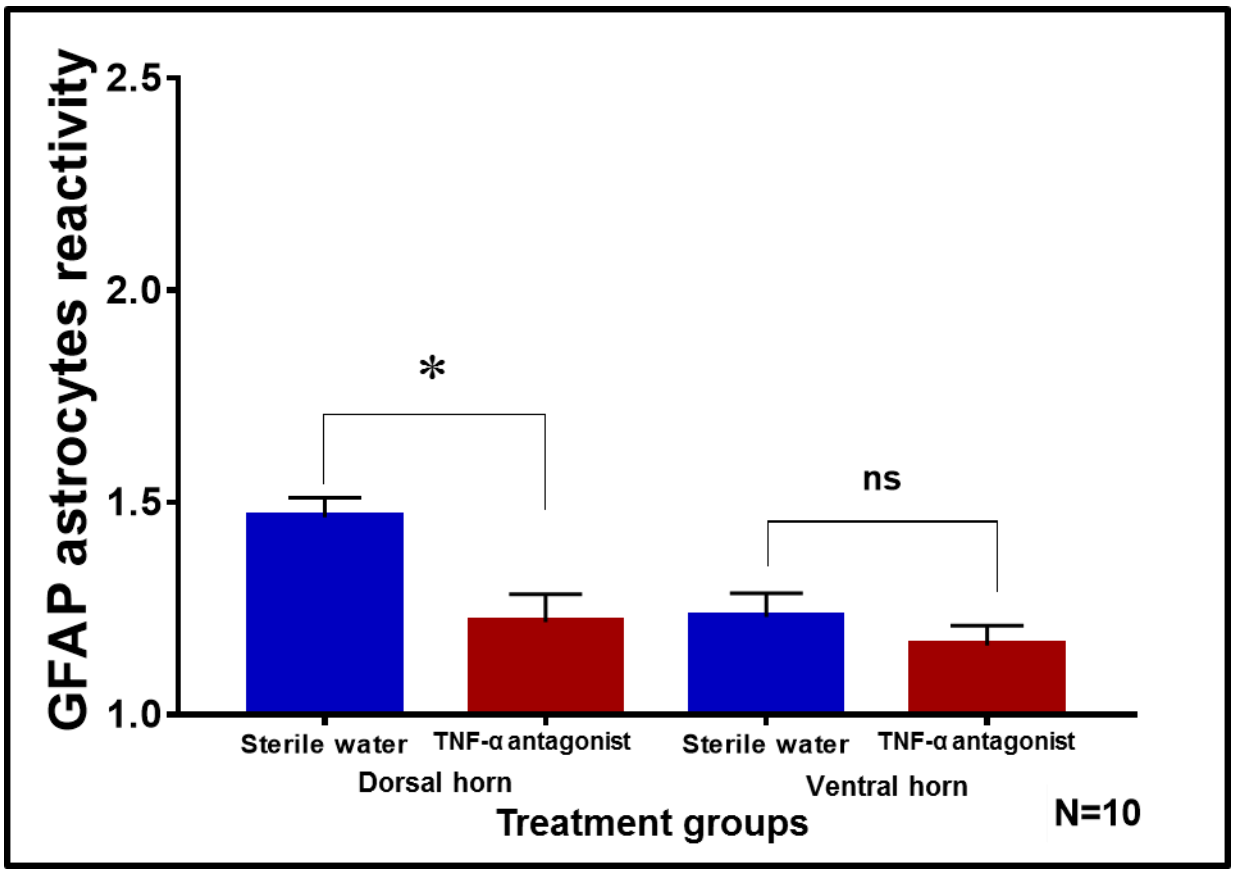

Figure 6.16: Quantification of ratio of astrocyte activation (GFAP marker) in ipsilateral versus contralateral dorsal and ventral horns five weeks following peripheral nerve injury and conduit implantation. (Data expressed mean ± SEM; ∗: p <0.05, ns: p>0.05).

6.6 Discussion

This study demonstrated that sciatic nerve repair with a poly-carprolactone (PCL) conduit and TNF-α antagonist (administrated at the time of repair) resulted in a demonstrable increase in CAP ratio, compared with PCL conduit repair and sterile water, however these results were not significant. In addition, there were improvements in gait movements, axonal regeneration, and the axons appeared to have less disrupted growth. Furthermore, there was a significant reduction in glial markers, centrally, in the spinal cord. Five weeks following sciatic nerve repair, only 8 out of 20 mice (four in each group) their nerves successfully regenerated as the conduits did not dislodge or separate from the proximal or distal nerve end and the remaining were excluded from further analysis.

Gait analysis is increasingly used as another a means of evaluating functional nerve recovery in rodent models of peripheral nerve injury and repair (Deumens et al., 2007; Deumens et al., 2010; Ngeow et al., 2011b). In this study, the assessment of gait function showed a similar pattern of functional recovery across the experimental groups during the study period. In addition, analysis of gait movements (intensity and total paw print area) revealed a sharp decline one week after conduit implantation compared to baseline values, which was followed by some improvement, when treated with TNF-α antagonist. However, improvements in gait movement were significantly evident in intensity and total paw print area at week 2 and 3 week after nerve injury and repair. This improvement possibly due to the effect of TNF-α antagonist on the axon regeneration rate at early time following nerve injury and repair. This effect was also reported by Ngeow et al (2011) following epineurial injection of Mannose-6-Phosphate after sciatic nerve repair in mice.

In general, the pattern of nerve function recovery was consistent with those expected as a consequence of nerve injury, and as previously reported by Ngeow et al (2011b). Ngeow et al (2011b) described gait analysis of gait movements using the catwalk system to assess motor and sensory recovery 12 weeks following sciatic nerve injury and repair in mice. Their study showed a sharp decline in paw print area up to 3 weeks after nerve injury and repair and limited improvement was observed over the study period. In our experiment the recovery period was five weeks and this showed an immediate a drop of gait function one week after nerve injury and repair. However, significant improvement were recorded at weeks 2 and 3, but a decline in function was seen again during the reminder of the study period at weeks 4 and 5. The decline in gait function in this experiment as well as those reported by Ngeow et al (2011b) may be due to development of some degree of neuropathic pain which prevented animals from using their injured paw. Analysis of gait function parameters such as intensity and total paw print area is highly sensitive and potentially valuable for assessment of nerve regeneration as a measurement of functional recovery of peripheral nerve after injury.

Five weeks following nerve conduit repair and administration of TNF-α antagonist, a greater CAP ratio was observed, but was not significant. In the comparisons between the uninjured sham controls and the nerve repair groups, the result showed that the CAPs were always smaller after repair. This might have resulted from a reduction in the number and/or size of regenerated axons in the distal stump.

A similar finding was observed following epineurial injection of IL-1 cytokine antagonist 6 weeks after nerve injury and repair (Chapter 4). The results did show a better CAP ratio, which was not significant, and it is possible that axons had similar regeneration rate. Although the experiment recorded the CAP following nerve injury and repair, it

may be possible that the TNF-α antagonist dose was not optimal to enhance regeneration of the repaired nerves. The conduction velocity of all of the repaired groups was significantly slower than for the sham uninjured at 5 weeks following nerve injury and repair. In addition, conduction velocities showed reduced propagation of electrically evoked action potentials which may be due to axons having regenerated at a slow rate.

A few studies have reported the use of axon tracing to evaluate functional regeneration after nerve injury and repair. Axon tracing assesses sprouting Index (SI), the number of individual axons successfully crossed the defect and the level of axon disruption across the initial portion of the conduit repair (Harding et al., 2014; Pateman et al., 2015), which was adopted for this study. In our experiment sprouting index were high at 0.0 mm interval and thereafter began to fall to their lowest values at intervals 4.0 mm and 4.5 mm, indicating a similar pattern of axonal regeneration through the conduit as axons reached the distal nerve end, in both groups. In mice receiving TNF-α antagonist treatment, there was a reduced axon disruption possibly indicating a better recovery of nerve function with less scar tissue formation. In addition, axons regenerating through the PCL conduit appeared to have more organized growth as opposed to the sterile water group. These observations possibly related to a reduction in scarring. A similar result to Pateman et al. (2015), their study showed less disrupted axon growth following both poly-ethylene glycol (PEG) conduit implantation as compared to nerve graft repair. In addition, their study did not show any difference in axon SI or unique axon tracing and they speculated this attributed to the conduit biocompatibility and internal structural support between nerve segments.

It has been proposed that the development of neuropathic pain after nerve injury is associated with sensitization of spinal neurones, partly by glial activation and

production of pro-inflammatory cytokines which stimulate neurones in the spinal cord, and these effects are blocked by pan-glial inhibitors (interleukin-1 receptor antagonist and soluble tumour necrosis factor receptor antagonist) that were applied intrathecal at the site of spinal cord injury (Sweitzer et al., 2001; Mika et al., 2008; Mika et al., 2013; Pilat et al., 2015). These inhibitors were shown to inhibit pain related mechanisms through targeting molecules critical for glial cell activation in peripheral nerve injury, including c-JUN and p38 MAPK pathways (Sweitzer et al., 2001; Zelenka et al., 2005; Kato et al., 2009; Hansen and Malcangio, 2013).

In our study, epineurial injection of TNF-α antagonist at the time of conduit implantation was associated with downregulated glial cells immunoreactivity as well as reduced glial cells labelling of their respective markers in the dorsal regions of the spinal cord. This was also observed following epineurial injection of TNF-α antagonist and possibly related to the synergistic effect of the treatment applied on the immune inflammatory response. However, epineurial injection of IL-1 antagonist did show reduced glial cells immunoreactivity in the ventral horns of the spinal cord and it is not clear whether the this related to the early effect of treatment or the dose was suboptimal to abolish glial cells activation after 6 weeks of nerve injury and repair. In agreement with others, the current observation shows that TNF-α antagonist therapeutic approach interferes in the early stages with signals that activate glial cells, and produces long lasting anti-inflammatory effects with a single injection that possibly suppresses pain related mechanisms, thus preventing the development of neuropathic pain.

6.7 Summary

Data from this study demonstrated that the use of PCL nerve conduit with administration of TNF-α antagonist promoted more organized growth pattern of

regenerated axons. In addition, it showed early improvements in functional recovery as well as reduced glial markers in the dorsal spinal horns five weeks after of nerve injury and conduit implantation.

CHAPTER 7

General discussion

7.1 Introduction

The aim of this chapter is to discuss the results described in previous sections. In addition, it will also highlight consideration of assessment methods and any potential future work. Finally, this section will draw the conclusion of the key findings from the work contained within this thesis.

7.2 The effect of cytokines therapy on inflammatory response

Macrophage immunoreactivity in peripheral nerve injury

The IL-1 antagonist, TNF-α antagonist and the anti-inflammatory cytokine IL-10 demonstrated variable effects on the abundance of macrophage immunoreactivity seven days and six weeks following sciatic nerve injury and repair.

An epineurial injection of IL-10 and IL-1 cytokine antagonist reduced macrophages immunoreactivity at the site of nerve injury and repair which was not significantly different when compared to the sham group (see Chapter 3). In contrast, the combination of IL-10 and TNF-α antagonist was associated with an increased expression of CD68 macrophage labelling as compared to the sham group, seven days following sciatic nerve injury and repair (see chapter 3). Although this was a short term follow up, the effect of combined treatment of IL- 10 and TNF-α antagonist was expected to down regulate macrophage immunoreactivity, but this was not observed in this experiment. However, it may be possible that the dose used for the combination of IL- 10 and TNF-α antagonist was not optimal to reduce macrophage immunoreactivity at the site of nerve injury and repair.

In Chapter 4 and 5, the results showed that both IL-1 cytokine antagonist and a combination of IL-10 and TNF-α antagonist applied at the time of nerve repair significantly reduced macrophage immunoreactivity as seen by macrophage labelling,

6 weeks following nerve injury and repair (see chapter 4 and 5). Previous studies reported that injection of either IL-1 or TNF-α antagonist contributed to reduction of pain related behaviours and subsequent successful functional nerve regeneration (Schäfers et al., 2001; Sweitzer et al., 2001; Sommer et al., 2004). This effect was thought to be contributed to by downregulating macrophage immunoreactivity and controlling the degree of immune inflammatory response at appropriate time following nerve injury and repair.

There is also clear evidence that the anti-inflammatory cytokine IL-10 regulates the production of pro-inflammatory cytokines and the combined treatment of IL-10 and TNF-α antagonist possibly exerts a synergistic effect on reducing macrophage immunoreactivity (Gaudet et al., 2011; Morris et al., 2014). Although this was opposing to the effect shown at short term follow up, this needs further work to explore anti-inflammatory effect of this therapeutic approach by investigating different therapeutic dose at different recovery periods of time following nerve repair.

Glial activation in peripheral nerve injury

Peripheral injection of IL-1 cytokine antagonist and combination treatment of IL-10 and TNF-α antagonist all showed significant reduction in microglial and astrocytes activation as well as diminished glial cells labelling of its respective immune marker in the dorsal and ventral horns of the spinal cord. Similar to previous studies, nerve injury induced dense activation and phenotypic changes of microglia and astrocytes and increased expression of their respective immune markers (Mika et al., 2008; Mika et al., 2013, Pilat et al., 2015).

Six weeks following epineurial administration of IL-1 cytokine antagonist reduced glial cell immunoreactivity was seen in the ventral horns, but not in the dorsal horns of the

spinal cord (see chapter 4). This may reflect different stages of glial cells activation in response to continuous stimulus as a result of nerve injury, and this would need further exploring.

The combined effect of IL-10 and TNF-α antagonist on immune response has not previously been explored (see Chapter 5). However, this therapeutic approach possibly exerted beneficial effect by downregulating glial cells reactivity as shown by less IBA-1 and GFAP cells labelling in the dorsal horns of the spinal cord. Previous studies have investigated the role of glial cells, microglia and astrocyte, using different glial inhibitors (Sweitzer et al., 2001; Mika et al., 2008; Mika et al., 2013). These studies showed that intrathecal administration of glial inhibitors such as interleukin-1 receptor antagonist and soluble tumour necrosis factor receptor antagonist at the site of spinal cord injury diminished pain-related behaviours. Our experiment first to record the effect of peripheral application of combined treatment of IL-10 and TNF-α antagonist at the site of nerve injury and repair (see chapter 5). In agreement with these studies, it is possible the effect contributed by downregulating glial cells activation and produced long lasting anti-inflammatory effect following peripheral nerve injury and repair.

These findings provide supplementary evidence that the key cytokines molecules of IL-1, TNF-α and anti-inflammatory IL-10 influence the regenerative process and subsequent functional recovery of injured and repaired peripheral nerves.

7.3 The effect of cytokines therapy on nerve regeneration

Electrophysiological analysis

The electrophysiological recordings did not show improvement in nerve regeneration as shown by low compound action potential (CAP) and conduction velocity following

epineurial injections of either TNF-α antagonist or IL-1 cytokine antagonist 5 or 6 weeks after nerve injury and repair (see Chapter 4 and 6). These measures remained low and intraneural scaring at the repair site may have influenced this outcome. It is also possible that the dose used in these studies was not optimal to enhance regeneration of the repaired nerves. This needs further investigation, including different doses at different recording and recovery periods for assessment of nerve regeneration.

There is clear evidence that anti-inflammatory IL-10 cytokine can overcome scar tissue formation and this intervention eventually improved functional nerve regeneration by significant remodelling of collagen fibres formation. By considering results from Atkins et al., work (2007), a significant correlation was noted between the degree of scarring and improvement in CAP ratio which predicted that a low level of scar formation was associated with better regeneration of repaired nerves. The result supports the observation following combined epineurial administration of IL-10 and TNF-α antagonist at time of nerve repair. This was possibly associated with low propensity for scarring by acting as anti-scarring agents and possibly reduced endogenous constrain to regenerating axons. Certainly, it is possible that scar remodelling improved the recovery of nerve action potential propagation which has contributed to the difference between the groups at six weeks post injury and repair. Besides, the efficiency of optimal administration of IL-1 and TNF-α antagonist suggest that a single dose was useful to suppress the inflammation, but was also associated with some improvement in nerve regeneration. It is seemed likely that the dose of these agents was less optimal and may be that an insufficient concentration contributed to the outcome.

Gait function analysis

The pattern of recovery of paw prints in the last experiment was consistent with previous studies in nerve injuries and repairs described by Ngeow et al. (2011b).

The recovery of gait function in this experiment showed limited improvement, with the TNF-α antagonist group only reaching to 58 % of the preoperative value at week 5 after nerve repair. However, epineurial injection of TNF-α antagonist at the time of nerve conduit repair did show a significant difference in paw print intensities at the earlier time point, particularly at week 2 and in the total paw print area values at week 3 postoperatively when compared to the sterile water treatment. In this respect, this may have occurred due to early the effect of TNF-α antagonist which possibly increased the rate of axon regeneration following nerve injury and repair. Although, the recovery period in our experiment was shorter (5 weeks), assessment of gait function using the catwalk system was similar to those seen by Ngeow et al. (2011b) and the limited improvements was attributed to the lack of motivation or increased anxiety level of the animals due to the development of some degree of neuropathic pain following sciatic nerve injury and repair. Moreover, it has also been claimed that the walking speed affect gait parameters in the dynamic and stance phase (Ngeow et al., 2011b). Taken together, these results suggest that the analysis of paw print variables using the catwalk system is important and can provide more useful outcome measures of functional recovery of sensory and motor nerve fibres.

Axon tracing

Axon tracing is based on measuring the sprouting Index, the number of individual axons that have crossed the defect and the level of axon disruption across the initial portion of the conduit repair.

The results only showed a significant difference in the axon count and sprouting index that occurred at the start of axon regeneration in mice treated with TNF-α antagonist when compared to those treated with sterile water, 5 weeks following nerve injury and repair. However, the lowest sprouting index level was observed at the 0.5 mm interval following nerve conduit repair with TNF-α antagonist treatment when compared to the sterile water group. The difference observed may be related to a reduction in scar tissue and this could have contributed to the reduced level of axon disruption, but this was not confirmed histologically. The production of scar tissue may be influenced by the early effects of the TNF-α antagonist. Moreover, no further difference was observed in the axons proportion as they extended toward the distal segment of the repair as shown by the axon tracing either after epineurial injection of TNF-α antagonist or sterile water treatment, and this indicates that a low proportion of axons crossed the full defect. In our experiment (see Chapter 6), peripheral application of TNF-α antagonist at the time of repair was associated with reduced axon disruption when compared to the sterile water treatment and this could indicate a better recovery of nerve function with less scar tissue formation. In a study conducted by Pateman et al. (2015) axon length analysis was used to indicate axonal disruption at the early stage of regeneration. They demonstrated mice that had received poly-ethylene glycol (PEG) conduit implantation had less disrupted axon growth when compared to nerve graft repair.

7.4 Methodological consideration

Several methods have been described in the literature that are considered as objective and quantitatively measure the extent of nerve regeneration, and these includes electrophysiological recordings, axon tracing, functional gait analysis, and immunohistochemistry studies of immune cells activity and their related markers.

Besides, these methods allowed for a wide assessment of nerve function and assessed variable parameters that could correlate to one another to show improvements in nerve function.

Electrophysiology recordings

Electrophysiological recordings of evoked nerve action potentials provide an objective measures of nerve integrity and this method has been frequently used for assessment of nerve regeneration following nerve injuries in preclinical research (Atkins et al., 2007; Ngeow et al., 2011a). Although sensory function is the most studied outcome measure in preclinical research, this work recorded evoked CAP following stimulation of successfully regenerated fibres across the repair. The nerve was stimulated on either side of the repair site with electrical pulses of maximum recommended intensity that provoke a nerve response. Thereafter, CAP ratio allowed comparisons between the groups to reduce interpretation bias of only recording distal segment stimulation. The conduction velocity of regenerated fibres is determined by measuring the latency of the early part of CAP of nerve fibres population which is responsible for the majority of fast firing response during stimulation of the distal nerve segment.

Gait analysis

Assessment of gait dynamics are considered sensitive and quantitatively reliable for evaluation of return of both sensory and motor function in rodent following successful regeneration of nerve fibres after injury and repair (Deumens et al., 2007; Ngeow et al., 2011b). The method of gait analysis is based on the measurements of paw prints obtained during the stance phase in which the hind limb contacts the walkway screen glass which is considered sensitive measure of assessment of nerve regeneration. However, gait analysis has been disputed because the data obtained cannot be

correlated with other outcome measures (Deumens et al., 2007; Ngeow et al., 2011b). Additionally, the accuracy of gait analysis has been challenged because the paw print parameters are affected by the animals walking speed. As a result, to reduce variability of interpretation, an average values of paw print parameters were taken to achieve a representative paw print reading from each experimental group.

Axon tracing

This method is considered essential to complement the outcome measures of the electrophysiological recordings and gait analysis (Sabatier et al., 2008; Harding et al., 2014; Pateman et al., 2015). Although this method is valuable, it is demanding as there are species dependent variations in axons numbers from one nerve to another due to the inherent variability in anatomical component or axon numbers within the nerve trunk. It has also been criticized as being more time consuming to perform and subjective in its interpretation, because no formal functional assessment can be conducted (Sabatier et al., 2008; Harding et al., 2014; Pateman et al., 2015). Although this method is still evolving it has potential to reduce inaccuracies associated with computerized system analysis. Besides, this method provides a more rapid assessment of results and accurate interpretation of sample morphology which will present more reliable and reproducible findings.

Immunochemistry analysis

Immunochemistry is considered valuable for the assessment of expression levels of immune cells markers at the site of nerve injury and centrally in the spinal cord. In addition, assessment of macrophage immunoreactivity and glial activation can contribute to the assessment of nerve recovery and regeneration as these cells and their respective markers are upregulated in the injury related response of damaged

axons during degeneration and the healing process following peripheral nerve injury (Eriksson et al., 1993; Taves et al., 2013). However, for accurate experimentation of primary and secondary antibody labelling appropriate negative controls were performed for this work and incorporated into the relevant staining protocol to count for variation in results between the experimental groups (Chapter 2; section 2.2.6.1). In addition, accurate analysis of sections need appropriate and consistent selection of tissues to render the sample more representative in order to reduce bias during interpretations.

7.5 Future perspectives

Comprehensive investigation of nerve regeneration in peripheral nerve injuries

Driven by the observed results in this work further study is essential to assess potential nerve regeneration following application of different novel cytokines agents. It is also vital to apply different dosage concentration and timings to assess obstacles to recovery of nerve function using histomorphometric and functional methods.

Gait analysis is considered an objective measure and likely to be subject to excess variability between gait movement parameters. However, precise quantification of functional loss using several paw print parameters such as percentage of toe spread and paw angle to measure functional recovery and to understand adaptive activity associated with gait movement, will enable more accurate assessments to monitor functional recovery.

Nerve conduit repair improvement

Future in vitro and in vivo experiments will be valuable to assess any potential improvements in the PCL conduit model as an alternative means for repairing damaged peripheral nerves. It would also sensible to increase the number of

experimental subjects along with the use of several outcome measures over different recovery periods to fully investigate peripheral nerve regeneration. The next important step is to use different method such as histomorphometric, and immunohistochemistry to investigate the comprehensive profile of immune cells activity as well as assess recovery of nerve function.

7.6 Conclusion

Recovery of peripheral nerve function is limited, and the outcome is usually associated with significant morbidity following nerve injury. Hence, novel therapeutic agents, including IL-1 antagonist, and TNF-α antagonist and anti-inflammatory IL-10 cytokine represent new treatment modalities that have shown considerable promise for improving nerve regeneration capacity. Moreover, combining different therapeutic agents to attain complementary molecular targeting approaches following suitable repair strategies in peripheral nerve injuries has shown some promise. This line of experimental research could provide new insight into the clinical benefit through the development of successful therapeutic strategies to prevent neuropathic pain development, enhance nerve fibre regeneration and improve functional recovery following peripheral nerve injury.

References

De Albornoz, P.M. et al. (2011) Non-surgical therapies for peripheral nerve injury. British Medical Bulletin, 100(100), pp.73-100.

De Bock, M. et al. (1843) The dual face of connexin-based astroglial Ca2+ communication: a key player in brain physiology and a prime target in pathology. Biochimica et Biophysica Acta (BBA)-Molecular Cell Research, 1843(10), pp.2211-2232.

Aldskogius, H. and Kozlova, E.N., 1998. Central neuron–glial and glial–glial interactions following axon injury. Progress in neurobiology, 55(1), pp.1-26.

Alhassani, A.A. and AlGhamdi, A.S.T., 2010. Inferior alveolar nerve injury in implant dentistry: diagnosis, causes, prevention, and management. Journal of Oral Implantology, 36(5), pp.401-407.

Allodi, I. et al. (2012) Specificity of peripheral nerve regeneration: interactions at the axon level. Progress in neurobiology, 98(1), pp.16-37.

Atkins, S. et al. (2007) Interleukin-10 reduces scarring and enhances regeneration at a site of sciatic nerve repair. Journal of the Peripheral Nervous System, 12(4), pp.269-276.

Atkins, S. et al. (2006) The effect of antibodies to TGF-β1 and TGF-β2 at a site of sciatic nerve repair. Journal of the Peripheral Nervous System, 11(4), pp.286-293.

Bastien, D. and Lacroix, S. (2014) Cytokine pathways regulating glial and leukocyte function after spinal cord and peripheral nerve injury. Experimental neurology, 258, pp.62-77.

Bagheri, S.C. et al. (2009) Microsurgical repair of peripheral trigeminal nerve injuries from maxillofacial trauma. Journal of Oral and Maxillofacial Surgery, 67(9), pp.1791-1799.

Bagheri, S.C. et al. (2010) Microsurgical repair of the peripheral trigeminal nerve after mandibular sagittal split ramus osteotomy. Journal of Oral and Maxillofacial Surgery, 68(11), pp.2770-2782.

Beggs, S. and Salter, M.W. (2007) Stereological and somatotopic analysis of the spinal microglial response to peripheral nerve injury. Brain, behavior, and immunity, 21(5), pp.624-633.

Bertleff, M.J. et al. (2005) A prospective clinical evaluation of biodegradable neurolac nerve guides for sensory nerve repair in the hand. Journal of Hand Surgery, 30(3), pp.513-518.

Bird, E.V. et al. (2013) Correlation of Nav1. 8 and Nav1. 9 sodium channel expression with neuropathic pain in human subjects with lingual nerve neuromas. Molecular pain, 9(1), p.52.

Biomath online statistic package, division of biomathematics/biostatistics at Columbia University Medical Centre. [online] Available at: http://biomath.info/power/index.html [Accessed: 10 February 2015].

Brown, M.C. et al. (1991) Macrophage dependence of peripheral sensory nerve regeneration: possible involvement of nerve growth factor. Neuron, 6(3), pp.359-370.

Burnett, M.G. and Zager, E.L. (2004) Pathophysiology of peripheral nerve injury: a brief review. Neurosurgical focus, 16(5), pp.1-7.

Campbell, W.W. (2008) Evaluation and management of peripheral nerve injury. Clinical neurophysiology, 119(9), pp.1951-1965.

Cattin, A.L. et al. (2015) Macrophage-induced blood vessels guide Schwann cell-mediated regeneration of peripheral nerves. Cell, 162(5), pp.1127-1139.

Chhabra, A. et al. (2014) Peripheral nerve injury grading simplified on MR neurography: as referenced to Seddon and Sunderland classifications. The Indian journal of radiology & imaging, 24(3), p.217.

Ciaramitaro, P. et al. (2010) Traumatic peripheral nerve injuries: epidemiological findings, neuropathic pain and quality of life in 158 patients. Journal of the Peripheral Nervous System, 15(2), pp.120-127.

Chiono, V. and Tonda-Turo, C. (2015) Trends in the design of nerve guidance channels in peripheral nerve tissue engineering. Progress in neurobiology, 131, pp.87-104.

Colella, G. et al. (2007) Neurosensory disturbance of the inferior alveolar nerve after bilateral sagittal split osteotomy: a systematic review. Journal of oral and maxillofacial surgery, 65(9), pp.1707-1715.

Craven, J., 2010. Anatomy of the cranial nerves. Anaesthesia & Intensive Care Medicine, 11(12), pp.529-534.

Crossman, A.R. and Neary, D. (2015) Neuroanatomy: an illustrated colour text Fifth edit., Edinburgh, Scotland: Churchill Livingstone; p:32-34,103-115.

Dahlin, L.B. (2008) (ii) Nerve injuries. Current Orthopaedics, 22(1), pp.9-16.

Decosterd, I. and Woolf, C.J. (2000) Spared nerve injury: an animal model of persistent peripheral neuropathic pain. Pain, 87(2), pp.149-158.

Deumens, R. et al. (2007) The CatWalk gait analysis in assessment of both dynamic and static gait changes after adult rat sciatic nerve resection. Journal of neuroscience methods, 164(1), pp.120-130.

Deumens, R. et al. (2010) Repairing injured peripheral nerves: bridging the gap. Progress in neurobiology, 92(3), pp.245-276.

Dib-Hajj, S.D. et al. (2010) Sodium channels in normal and pathological pain. Annual review of neuroscience, 33, pp.325-347.

Dinarello, C.A. (1988) Biology of interleukin 1. The FASEB Journal, official publication of the Federation of American Societies for Experimental Biology 2(2), pp.108-115.

Djouhri, L. et al. (2012) Partial nerve injury induces electrophysiological changes in conducting (uninjured) nociceptive and nonnociceptive DRG neurons: Possible relationships to aspects of peripheral neuropathic pain and paresthesias. PAIN®, 153(9), pp.1824-1836.

Den Dunnen, W.F.A. et al. (1996) Poly (DL-lactide-ϵ-caprolactone) nerve guides perform better than autologous nerve grafts. Microsurgery, 17(7), pp.348-357.

de Waal Malefyt, R. Et al. (1992) Interleukin-10. Current opinion in immunology, 4(3), pp.314-320.

Eser, F. et al. (2009) Etiological factors of traumatic peripheral nerve injuries. Neurology India, 57(4), p.434.

Eriksson, N.P. et al. (1993) A quantitative analysis of the microglial cell reaction in central primary sensory projection territories following peripheral nerve injury in the adult rat. Experimental brain research, 96(1), pp.19-27.

Evans, G.R. (2001) Peripheral nerve injury: a review and approach to tissue engineered constructs. The Anatomical Record, 263(4), pp.396-404.

Fawcett, J.W. and Keynes, R.J. (1990) Peripheral nerve regeneration. Annual review of neuroscience, 13(1), pp.43-60.

Ferguson, M.W. and O'Kane, S. (2004) Scar–free healing: from embryonic mechanisms to adult therapeutic intervention. Philosophical Transactions of the Royal Society B: Biological Sciences, 359(1445), pp.839-850.

Fitzgerald, M.J.T. et al. (2012) Clinical neuroanatomy and neuroscience. In Clinical neuroanatomy and neuroscience. Edinburgh, Scotland: Saunders Elsevier, p. 70.

Flores, A.J. et al. (2000) Anatomy and physiology of peripheral nerve injury and repair. American journal of orthopedics, 29(3), pp.167-178.

Foltán, R. et al. (2008) Mechanism of traumatic neuroma development. Medical hypotheses, 71(4), pp.572-576.

Fu, S.Y. and Gordon, T. (1997) The cellular and molecular basis of peripheral nerve regeneration. Molecular neurobiology, 14(1-2), pp.67-116.

Fukuoka, H. et al. (1994) Cutaneous hyperalgesia induced by peripheral injection of interleukin-1β in the rat. Brain research, 657(1-2), pp.133-140.

Gaudet, A.D. et al. (2011) Wallerian degeneration: gaining perspective on inflammatory events after peripheral nerve injury. Journal of neuroinflammation, 8(1), p.110.

Galiano, M. et al. (2001) Interleukin-6 (IL6) and cellular response to facial nerve injury: effects on lymphocyte recruitment, early microglial activation and axonal outgrowth in IL6-deficient mice. European Journal of Neuroscience, 14(2), pp.327-341.

George, A. et al. (2005) Tumor necrosis factor receptor 1 and 2 proteins are differentially regulated during Wallerian degeneration of mouse sciatic nerve. Experimental neurology, 192(1), pp.163-166.

George, A. et al. (2004) Wallerian degeneration after crush injury of rat sciatic nerve increases endo-and epineurial tumor necrosis factor-alpha protein. Neuroscience letters, 372(3), pp.215-219.

Grafstein, B. (1975) The nerve cell body response to axotomy. Experimental Neurology, 48(3), pp.32-51.

Grötz, K.A. et al. (1998) Treatment of injuries to the inferior alveolar nerve after endodontic procedures. Clinical oral investigations, 2(2), pp.73-76.

Gunasekera, S.M. et al. (2011) Proximal axonal changes after peripheral nerve injury in man. Muscle & nerve, 43(3), pp.425-431.

Haas, D.A. (2006) Articaine and paresthesia: epidemiological studies. The Journal of the American College of Dentists, 73(3), pp.5-10.

Hall, S. (2001) Nerve repair: a neurobiologist's view. Journal of hand surgery, 26(2), pp.129-136.

Hansen, R.R. and Malcangio, M. (2013) Astrocytes—multitaskers in chronic pain. European journal of pharmacology, 716(1-3), pp.120-128.

Harding, A.J. et al. (2014) Mannose-6-phosphate facilitates early peripheral nerve regeneration in thy-1-YFP-H mice. Neuroscience, 279, pp.23-32.

Hillerup, S. et al. (2011) Concentration-dependent neurotoxicity of articaine: an electrophysiological and stereological study of the rat sciatic nerve. Anesthesia & Analgesia, 112(6), pp.1330-1338.

Hillerup, S. and Jensen, R. (2006) Nerve injury caused by mandibular block analgesia. International journal of oral and maxillofacial surgery, 35(5), pp.437-443.

Hogan, Q.H. (2008) Pathophysiology of peripheral nerve injury during regional anesthesia. Regional anesthesia and pain medicine, 33(5), pp.435-441.

Hospital Episode Statistics, Admitted Patient Care - England, 2014-15. [online] Available at: http://content.digital.nhs.uk/hes [Accessed: 24 November 2016].

Ide, C., 1996. Peripheral nerve regeneration. Neuroscience research, 25(2), pp.101-121.

Ichihara, S. et al. (2008) Artificial nerve tubes and their application for repair of peripheral nerve injury: an update of current concepts. Injury, 39, pp.29-39.

Iwatsuki, K. et al. (2013) Targeting anti-inflammatory treatment can ameliorate injury-induced neuropathic pain. PLoS One (Public Library of Science), 8(2), p. e57721.

Johnson, E.O. and Soucacos, P.N. (2008) Nerve repair: experimental and clinical evaluation of biodegradable artificial nerve guides. Injury, 39(3), pp.30-36.

Johnson, E.O. et al. (2005) Regeneration and repair of peripheral nerves. Injury, 36(4), pp. S24-S29.

Juodzbalys, G. et al. (2013) Inferior alveolar nerve injury associated with implant surgery. Clinical oral implants research, 24(2), pp.183-190.

Kato, K. et al. (2009) Distribution and tumor necrosis factor-alpha isoform binding specificity of locally administered etanercept into injured and uninjured rat sciatic nerve. Neuroscience, 160(2), pp.492-500.

Kato, K. et al. (2010) Immediate anti-tumor necrosis factor-α (etanercept) therapy enhances axonal regeneration after sciatic nerve crush. Journal of neuroscience research, 88(2), pp.360-368.

Kelleher, J.H. et al. (2017) Neurotrophic factors and their inhibitors in chronic pain treatment. Neurobiology of disease, 97, pp.127-138.

Kerns, J.M. (2008) The microstructure of peripheral nerves. Techniques in Regional Anaesthesia & Pain Management, 12(3), pp.127-133.

Köbbert, C. and Thanos, S. (2000) Topographic representation of the sciatic nerve motor neurons in the spinal cord of the adult rat correlates to region-specific activation patterns of microglia. Journal of neurocytology, 29(4), pp.271-283.

Korompilias, A.V. et al. (1999) Interleukin-1 beta promotes functional recovery of crushed peripheral nerve. Journal of orthopaedic research, 17(5), pp.714-719.

Kouyoumdjian, J.A. (2006) Peripheral nerve injuries: a retrospective survey of 456 cases. Muscle & nerve, 34(6), pp.785-788.

Kurosinski, P. and Götz, J. (2002) Glial cells under physiologic and pathologic conditions. Archives of neurology, 59(10), pp.1524-1528.

Kwilasz, A.J. et al. (2015) The therapeutic potential of interleukin-10 in neuroimmune diseases. Neuropharmacology, 96, pp.55-69.

Li, R. et al. (2014) Peripheral nerve injuries treatment: a systematic review. Cell biochemistry and biophysics, 68(3), pp.449-454.

Liefner, M. et al. (2000) The role of TNF-α during Wallerian degeneration. Journal of neuroimmunology, 108(1), pp.147-152.

Liu, M. and Wood, J.N. (2011) The roles of sodium channels in nociception: implications for mechanisms of neuropathic pain. Pain medicine, 12(s3).

Lloyd, T.E. (2012) Axonal transport disruption in peripheral nerve disease. Journal of the Peripheral Nervous System, 17(s3), pp.46-51.

Marchand, F. et al. (2005) Role of the immune system in chronic pain. Nature Reviews Neuroscience, 6(7), p.521.

Martins, R.S. et al. (2013) Traumatic injuries of peripheral nerves: a review with emphasis on surgical indication. Arquivos de neuro-psiquiatria, 71(10), pp.811-814.

Meyer, M. et al. (1992) Enhanced synthesis of brain-derived neurotrophic factor in the lesioned peripheral nerve: different mechanisms are responsible for the regulation of BDNF and NGF mRNA. The Journal of cell biology, 119(1), pp.45-54.

Mika, J. et al. (2008) Interleukin-1alpha has antiallodynic and antihyperalgesic activities in a rat neuropathic pain model. Pain, 138(3), pp.587-597.

Mika, J. et al. (2013) Importance of glial activation in neuropathic pain. European journal of pharmacology, 716(1-3), pp.106-119.

Moalem, G., Xu, K. and Yu, L. (2004) T lymphocytes play a role in neuropathic pain following peripheral nerve injury in rats. Neuroscience, 129(3), pp.767-777.

Mohanna, P.N. et al. (2003) A composite poly-hydroxybutyrate–glial growth factor conduit for long nerve gap repairs. Journal of anatomy, 203(6), pp.553-565.

Morris, M.W. et al. (2014) Modulation of the inflammatory response by increasing fetal wound size or interleukin-10 overexpression determines wound phenotype and scar formation. Wound Repair and Regeneration, 22(3), pp.406-414.

Muheremu, A. and Ao, Q. (2015) Past, present, and future of nerve conduits in the treatment of peripheral nerve injury. BioMed research international, 2015.

Myers, R.R. et al. (2006) The role of neuroinflammation in neuropathic pain: mechanisms and therapeutic targets. Drug discovery today, 11(1-2), pp.8-20.

Nadeau, S. et al. (2011) Functional recovery after peripheral nerve injury is dependent on the pro-inflammatory cytokines IL-1β and TNF: implications for neuropathic pain. Journal of Neuroscience, 31(35), pp.12533-12542.

Nan, J. et al. (2012) Use of nerve conduits for peripheral nerve injury repair: A Web of Science-based literature analysis. Neural regeneration research, 7(35), p.2826.

Nath, R.K. et al. (1998) Antibody to transforming growth factor beta reduces collagen production in injured peripheral nerve. Plastic and reconstructive surgery, 102(4), pp.1100-6.

Navarro, X. et al. (2007) Neural plasticity after peripheral nerve injury and regeneration. Progress in neurobiology, 82(4), pp.163-201.

Ngeow, W.C. et al. (2011a) Histomorphometric changes in repaired mouse sciatic nerves are unaffected by the application of a scar-reducing agent. Journal of anatomy, 219(5), pp.638-645.

Ngeow, W.C. et al. (2011b) The effect of Mannose-6-Phosphate on recovery after sciatic nerve repair. Brain research, 1394, pp.40-48.

O'Kane, S. and Ferguson, M.W. (1997) Transforming growth factor βs and wound healing. The international journal of biochemistry & cell biology, 29(1), pp.63-78.

Osbourne, A. (2007) Peripheral nerve injury and repair. Tsmj, 8, pp.29-33.

Pateman, CJ. et al. (2014) 3d micro-printing of nerve guides for peripheral nerve repair [poster 81]. Switzerland. European Cells and Materials Vol. 28. Suppl. 4, 2014.

Availablefrom:http://www.ecmconferences.org/abstracts/2014/Collection6/tces2014.html [accessed 11 November 2016].

Pateman, C.J. et al. (2015) Nerve guides manufactured from photocurable polymers to aid peripheral nerve repair. Biomaterials, 49, pp.77-89.

Perkins, N.M. and Tracey, D.J. (2000) Hyperalgesia due to nerve injury: role of neutrophils. Neuroscience, 101(3), pp.745-757.

Pilat, D. et al. (2015) IL-1 receptor antagonist improves morphine and buprenorphine efficacy in a rat neuropathic pain model. European journal of pharmacology, 764, pp.240-248.

Pogrel, M.A. (2011) Long-term outcome of trigeminal nerve injuries related to dental treatment. Journal of Oral and Maxillofacial Surgery, 69(9), pp.2284-2288.

Powis. R. A. et al. (2012) Etanercept application to the site of sciatic nerve repair reduces glial activation in the spinal cord following peripheral nerve injury in the rat. MSc Research Project submitted to the University of Sheffield (unpublished).

Redett, R. et al. (2005) Peripheral pathways regulate motoneuron collateral dynamics. Journal of Neuroscience, 25(41), pp.9406-9412.

Reid, A.J. et al. (2013) Long term peripheral nerve regeneration using a novel PCL nerve conduit. Neuroscience letters, 544, pp.125-130.

Renton, T. and Yilmaz, Z. (2012) Managing iatrogenic trigeminal nerve injury: a case series and review of the literature. International journal of oral and maxillofacial surgery, 41(5), pp.629-637.

Richards, N. and McMahon, S.B. (2013) Targeting novel peripheral mediators for the treatment of chronic pain. British journal of anaesthesia, 111(1), pp.46-51.

Rigaud, M.et al. (2008) Species and strain differences in rodent sciatic nerve anatomy: implications for studies of neuropathic pain. Pain, 136(1-2), pp.188-201.

Robinson, L.R. (2000) Traumatic injury to peripheral nerves. Muscle & nerve, 23(6), pp.863-873.

Robinson, P.P. et al. (2000) A prospective, quantitative study on the clinical outcome of lingual nerve repair. British Journal of Oral and Maxillofacial Surgery, 38(4), pp.255-263.

Rodríguez, F.J. et al. (2004) Regeneration and functional recovery following peripheral nerve injury. Drug Discovery Today: Disease Models, 1(2), pp.177-185.

Rosen, E. (2014) Nerve injury during endodontic surgical procedures. In Complications in endodontic surgery (pp. 137-151). Springer, Berlin, Heidelberg.

Rosen, E. (2017) The diagnosis and management of nerve injury during endodontic treatment. Evidence-Based Endodontics, 2(1), p.7.

Ruangsri, S. et al. (2011) Relationship of axonal voltage-gated sodium channel 1.8 (NaV1. 8) mRNA accumulation to sciatic nerve injury-induced painful neuropathy in rats. Journal of Biological Chemistry, 286(46), pp.39836-39847.

Sabatier, M.J. et al. (2008) Treadmill training promotes axon regeneration in injured peripheral nerves. Experimental neurology, 211(2), pp.489-493.

Sakalidou, M. et al. (2011) Interleukin-10 and regeneration in an end-to-side nerve repair model of the rat. Journal of the Peripheral Nervous System, 16(4), pp.334-340.

Sandstedt, P. and Sörensen, S. (1995) Neurosensory disturbances of the trigeminal nerve: a long-term follow-up of traumatic injuries. Journal of oral and maxillofacial surgery, 53(5), pp.498-505.

Schäfers, M. et al. (2001) Combined epineurial therapy with neutralizing antibodies to tumor necrosis factor-alpha and interleukin-1 receptor has an additive effect in reducing neuropathic pain in mice. Neuroscience letters, 310(2-3), pp.113-116.

Scholz, J. and Woolf, C.J. (2007) The neuropathic pain triad: neurons, immune cells and glia. Nature neuroscience, 10(11), p.1361.

Seiler, J.G. and Payne, S.H. (1999) Treatment of peripheral nerve injuries: surgeons' perspective. Journal of Hand Therapy, 12(2), pp.135-140.

Shen, K.F. et al. (2013) Interleukin-10 down-regulates voltage gated sodium channels in rat dorsal root ganglion neurons. Experimental neurology, 247, pp.466-475.

Shin, R.H. et al. (2009) Treatment of a segmental nerve defect in the rat with use of bioabsorbable synthetic nerve conduits: a comparison of commercially available conduits. JBJS, 91(9), pp.2194-2204.

Sommer, C. et al. (2001) Etanercept reduces hyperalgesia in experimental painful neuropathy. Journal of the peripheral nervous system, 6(2), pp.67-72.

Sommer, C. et al. (1999) Neutralizing antibodies to interleukin 1-receptor reduce pain associated behavior in mice with experimental neuropathy. Neuroscience letters, 270(1), pp.25-28.

Sommer, C. and Kress, M. (2004) Recent findings on how proinflammatory cytokines cause pain: peripheral mechanisms in inflammatory and neuropathic hyperalgesia. Neuroscience letters, 361(1-3), pp.184-187.

De Stefano, M.E. et al. (2013) Therapeutic approaches enhancing peripheral nerve regeneration. Advances in Bioscience and Biotechnology, 4(06), p.53.

Stoll, G. and Müller, H.W. (1999) Nerve injury, axonal degeneration and neural regeneration: basic insights. Brain pathology, 9(2), pp.313-325.

Sunderland, S.S. (1990) The anatomy and physiology of nerve injury. Muscle & nerve, 13(9), pp.771-784.

Suzuki, R. et al. (2004) Descending facilitatory control of mechanically evoked responses is enhanced in deep dorsal horn neurones following peripheral nerve injury. Brain research, 1019(1-2), pp.68-76.

Svendsen, O. et al. (2005) Intramuscular injection of hypertonic saline: in vitro and in vivo muscle tissue toxicity and spinal neurone c ‐ fos expression. Basic & clinical pharmacology & toxicology, 97(1), pp.52-57.

Sweitzer, S. et al. (2001) Intrathecal interleukin-1 receptor antagonist in combination with soluble tumor necrosis factor receptor exhibits an anti-allodynic action in a rat model of neuropathic pain. Neuroscience, 103(2), pp.529-539.

Taskinen, H.S. et al. (2000) Peripheral nerve injury induces endoneurial expression of IFN-γ, IL-10 and TNF-α mRNA. Journal of neuroimmunology, 102(1), pp.17-25.

Taves, S. et al. (2013) Microglia and spinal cord synaptic plasticity in persistent pain. Neural plasticity, 2013.

Thacker, M.A. et al. (2007) Pathophysiology of peripheral neuropathic pain: immune cells and molecules. Anesthesia & Analgesia, 105(3), pp.838-847.

Tofaris, G.K. et al. (2002.) Denervated Schwann cells attract macrophages by secretion of leukemia inhibitory factor (LIF) and monocyte chemoattractant protein-1 in a process regulated by interleukin-6 and LIF. Journal of Neuroscience, 22(15), pp.6696-6703.

Topp, K.S. and Boyd, B.S. (2012) Peripheral nerve: from the microscopic functional unit of the axon to the biomechanically loaded macroscopic structure. Journal of Hand Therapy, 25(2), pp.142-152.

Tsantoulas, C. et al. (2012) Sensory neuron downregulation of the Kv9. 1 potassium channel subunit mediates neuropathic pain following nerve injury. Journal of Neuroscience, 32(48), pp.17502-17513.

Urtikova, N. et al. (2012) Antinociceptive effect of peripheral serotonin 5-HT2B receptor activation on neuropathic pain. Pain, 153(6), pp.1320-1331.

Vidal, P.M. et al. (2013) The role of “anti-inflammatory” cytokines in axon regeneration. Cytokine & growth factor reviews, 24(1), pp.1-12.

de Waal Malefyt, R. Et al. (1992) Interleukin-10. Current opinion in immunology, 4(3), pp.314-320.

Wagner, R. et al. (1998) Anti-inflammatory interleukin-10 therapy in CCI neuropathy decreases thermal hyperalgesia, macrophage recruitment, and endoneurial TNF-α expression. Pain, 74(1), pp.35-42.

Watson, C. et al. (2009) The Spinal Cord: A Christopher and Dana Reeve Foundation Text and Atlas by Charles Watson, George Paxinos and Gülgün Kayalıoğlu. Anatomy, 3(1); p:3-6,37-48, 64-80.

Winkelstein, B.A. et al. (2001) Nerve injury proximal or distal to the DRG induces similar spinal glial activation and selective cytokine expression but differential behavioral responses to pharmacologic treatment. Journal of Comparative Neurology, 439(2), pp.127-139.

White, J.P. et al. (2011) Extracellular signal-regulated kinases in pain of peripheral origin. European journal of pharmacology, 650(1), pp.8-17.

Wolf, G. et al. (2006) Genetic impairment of interleukin-1 signaling attenuates neuropathic pain, autotomy, and spontaneous ectopic neuronal activity, following nerve injury in mice. Pain, 120(3), pp.315-324.

Wojtkiewicz, D.M. et al. (2015) Social impact of peripheral nerve injuries. Hand, 10(2), pp.161-167.

Wood, M.D. and Mackinnon, S.E. (2015) Pathways regulating modality-specific axonal regeneration in peripheral nerve. Experimental neurology, 265, pp.171-175.

Yapp, K.E. et al. (2011) Articaine: a review of the literature. British dental journal, 210(7), p.323.

Zhang, R.X. et al. (2008) Interleukin 1β facilitates bone cancer pain in rats by enhancing NMDA receptor NR-1 subunit phosphorylation. Neuroscience, 154(4), pp.1533-1538.

Zuniga, J.R. and Radwan, A.M. (2013) Classification of Nerve Injuries. In Trigeminal Nerve Injuries (pp. 17-25). Springer, Berlin, Heidelberg.

Zuo, Y. et al. (2003) Inflammation and hyperalgesia induced by nerve injury in the rat: a key role of mast cells. Pain, 105(3), pp.467-479.

Appendices

The following appendices contains laboratories related techniques including slide preparation, tissue cutting and immunostaining technique which were used in this research experiments.

APPENDIX A

Preparation of Poly-D-lycine hydrobromide (P1149, 10mg vial PDL, SIGMA) slides used in the experiments.

Preparation steps:
- Dilute 10 mg vial to 1 mg/ml (i.e. add 100ml of distilled water in to the vial) - Aliquot 250 µl samples and freeze at -80 °C - Use 250 µl of PDL to coat approximately 33 slides (7 µl/slide) - Coating of slides done one day before tissue sectioning and use within a week. - Put a mark on top left corner frosted section of the slide to identify which side of the slide is coated - Use a 10 µl Gilsen pipette to put a 7 µl of PDL drop nearest to the frosted end of the slide - with another slide at 45^{o} angle, spread the PDL solution toward frosted end of the slide and then toward the other end to ensure that slide is completely coated in PDL solution - leave slide to dry for a minimum of 15 minutes at room temperature, then place slide box and refrigerate

APPENDIX B

Preparation of gelatine coated slides used in free-floating sections technique**.**

Preparation steps: gelatine coated slides used in experiments
- Heat 600 ml of distilled water to approximately 50 ° C in a flask
- Add 4 g of gelatine (purified grade-100 bloom) into the flask
- Stir solution until gelatine dissolved
- Add 0.3 mg of chrome alum
- Filter solution
- Dip slides into solution while warm
- Leave slide to dry for a minimum of 15 minutes at room temperature
- Store slide at room temperature in slide box

APPENDIX C

Preparations of most commonly used solutions in the experiments.

Solutions	Volume	Solutions preparation
Phosphate Buffered Saline (PBS)	1litre	- Weigh 8.8 g of Sodium Chloride (NaCl) + 0.2 g of Potassium Chloride (KCl) - Add salts to 950 ml of distilled water (2H2O) - Add 50 ml of 0.2 M phosphate buffer - Stir until the salts dissolve
Phosphate Buffered Saline (PBST; 0.2 % Triton)	1 litre	- Weigh 8.8 g of Sodium Chloride (NaCl) + 0.2 g of Potassium Chloride (KCl) - Add salts to 950 ml of distilled water (2H2O) - Add 50 ml of 0.2 M phosphate buffer and 2 ml Triton - Stir until the salts dissolve
0.2 M Phosphate Buffer	1 litre	- Solution A: add 59.28 g of 0.2 M sodium hydrogen phosphate (NaH_2PO_4) to 1.9 litre of distilled water (2H2O) - Solution B: add 23 g of disodium hydrogen phosphate (0.2M HN_2PO_4) to 8.1 litre of distilled water - Add solution A to Solution B. (pH 7.4)
30 % Sucrose Solution	100 Millilitres	- Add 30 g of sucrose to buffer and 50 ml of distilled water (2H2O) in a flask. - Add 50 ml of 0.2 M phosphate - Stir until the solution become clear - Store the solution in the 4° C fridge
NaCl: Sodium Chloride; **KCl**: Potassium Chloride; **2H2O**: Distilled water; **PBS**: Phosphate Buffered Saline; **PBST**: Phosphate Buffered Saline Triton; **NaH2PO4.2H2O**: sodium hydrogen phosphate; **HN2PO4**: disodium hydrogen phosphate; **1N NaOH**: sodium hydroxide		

Solutions	Volume	Solutions preparation
4 % Paraformaldehyde	1litre	- Heat 400 ml of distilled water to approximately 80 °C in a flask - Add 40 g of paraformaldehyde powder to the water - Add 15 drops of sodium hydroxide (1N NaOH) and stir until the solution become clear - Cover the flask with cling film and cool down in bucket of ice water to approximately 15 °C - Add 500 ml 0.2 M Phosphate Buffer to the solution - Top up the solution to 1litre with distilled water - Filter the solution to attain 4 % Paraformaldehyde - Store the solution in the 4 °C fridge
Sodium hydroxide **(1N NaOH)**	100 Milliliters	-Dissolve 4.5 g NaOH in 100 mL distilled water -Add drops of saturated barium hydroxide solution until a precipitate is formed. -Allow for complete precipitation and filter the solution.
Perfusion buffer solution	1litre	-Weigh 8 g of Sodium Chloride (NaCl) + 0.25 g of Potassium Chloride (KCl) + 0.5 g Sodium bicarbonate (NaHCO3) - Add salts to 950 ml distilled water - Add 50 ml of 0.2 M phosphate buffer and 2 ml Triton -Stir until the salts dissolve and store the solution in the 4 °C fridge
NaCl: Sodium Chloride; **KCl**: Potassium Chloride; **PBS**: Phosphate Buffered Saline; **PBST**: Phosphate Buffered Saline Triton; **NaH2PO4.2H2O**: sodium hydrogen phosphate; **HN2PO4**: disodium hydrogen phosphate; **1N NaOH**: sodium hydroxide		

APPENDIX D

Primary and secondary antibodies staining protocols for rat sciatic nerve tissues (three slides per animal)

Protocol steps for Primary antibody Mouse Anti- Rat CD 68	
1	Tissue out of the freezer and allow to air dry for 1 hour
2	Tissue slides wash with PBS triton 2 times X 10 minutes @ room temperature on the shaker
3	Block tissue slides with normal donkey serum (NDS 20 %) for 1 hour @ room temperature on the bench - 9 slides @ 250 µl per slide = 2250 µl total volume - 2250 µl= 450 µl NDS+ 1800 µl PBST - dry slides from the step 2 and apply 250 µl to each slide of NDS 20 % - place the slides in plastic container with moistened tissue and cover it for 1 hour @ the bench.
4	Primary antibody Mouse Anti- Rat CD 68 @ 1:1500dilution 2250 µl total volume: 1.5 µl Mouse Anti- Rat CD 68+ 2248.5 µl NDS 5 % ↓ 2250 µl total [112.5 µl NDS + 2137.5 µl PBST] - dry slides from step 3 and apply 250 µl to each slide - place the slides in the plastic container and leave them overnight @ 4 °C Fridge.

Protocol steps for secondary antibody Donkey Anti- Mouse CY3	
1	Tissue slides out of the fridge (4°C)
2	Wash slides with PBS2 times X 10 minutes @ room temperature on the shaker
3	Secondary antibody Donkey Anti- Mouse CY3 @ 1:500 dilutions (work in dark environment) - 2250 µl= 4.5 µl dx CY3 + 2245.5 µl NDS 1.5 % ↓ 2250 µl total [33.75 µl NDS+ 2216.25 µl PBS] - dry slides from step 3 and apply 250 µl to each slide - place the slides in the plastic container and cover with box in dark environment for 90 minutes.
4	Wash slides with PBS2 times X 10 minutes @ room temperature on the shaker
5	Dry slides and then Cover slides and store @ 4°C fridge.

APPENDIX E

Primary and secondary antibodies staining protocols for mouse sciatic nerve tissues (three slides per animal).

Protocol steps for Primary antibody Rat Anti- Mouse CD 68	
1	Tissue out of the freezer and allow to air dry for 1 hour
2	Tissue slides wash with PBS triton 2 times X 10 minutes @ room temperature on the shaker
3	Block tissue slides with normal donkey serum (NGS 20 %) for 1 hour @ room temperature on the bench - 9 slides @ 250 µl per slide = 2250 µl total volume - 2250 µl= 450 µl NGS+ 1800 µl PBST - dry slides from the step 2 and apply 250 µl to each slide of NGS 20 % - place the slides in plastic container with moistened tissue and cover it for 1 hour @ the bench.
4	Primary antibody Rat Anti- Mouse CD 68 @ 1:1500dilution 2250 µl total volume: 1.5 µl Rat Anti- Mouse CD 68+ 2248.5 µl NGS 5 % ↓ 2250 µl total [112.5 µl NGS + 2137.5 µl PBST] - dry slides from step3 and apply 250 µl to each slide - place the slides in the plastic container and leave them overnight @ 4 °C Fridge.

Protocol steps for secondary antibody Goat Anti- Rat CY3	
1	Tissue slides out of the fridge (4 °C)
2	Wash slides with PBS2 times X 10 minutes @ room temperature on the shaker
3	Secondary antibody Goat Anti- Rat CY3 @ 1:500 dilution (work in dark environment) - 2250 µl= 4.5 µl dx CY3 + 2245.5 µl NGS 1.5 % ↓ 2250 µl total [33.75 µl NGS+ 2216.25 µl PBS] - dry slides from step 3 and apply 250 µl to each slide - place the slides in the plastic container and cover with box in dark environment for 90 minutes.
4	Wash slides with PBS2 times X 10 minutes @ room temperature on the shaker
5	Dry slides and then Cover slides and store @ 4 °C fridge.

APPENDIX F

Microglial labelling protocols for mouse spinal cords (six spinal cord tissues per animal).

	Protocol steps for primary antibody IBA-1 goat polyclonal microglial marker
1	spinal cord sections out of the fridge (4°C)
	Wash tissues with PBS one-time X 10 minutes in well plate @ room temperature on the shaker
2	Wash tissues with PBST 2 times X 10 minutes in well plate @ room temperature on the shaker
3	Block tissue in PBST 10 % NDS @ 200 µl per space for 1 hour on platform shaker - 6 spaces @ 200 µl = 1200 µl total volume
4	Apply primary antibody IBA-1 goat polyclonal @ 1:2500 dilution and leave it overnight in the fridge (4 °C) -1200 µl total volume: 0.48 µl Iba-1 goat + 1199.52 PBST NDS 5 % ↓ 1200 µl [60 µl NDS + 1140 µl PBST]

	Protocol steps for secondary antibody Donkey anti-goat CY3
1	spinal cord sections out of the fridge (4 °C)
2	Wash tissues with PBS 2 times X 10 minutes in well plate @ room temperature on the shaker
3	Apply secondary antibody Donkey anti-goat CY3 @ 1:500 dilution for 2 hours in dark environment - 1200 µl total volume: 2.4 µl Donkey anti-goat CY3 + 1197.6 PBST NDS 2 % ↓ 1200 µl [24 µl NDS + 1176 µl PBST]
4	Wash tissues with PBS one-time X 10 minutes in well plate @ room temperature on the shaker
5	Fill box of PBS and mount section in the orientation order on gelatine coated slides (free floating technique)
6	Cover slip slides with vectashield and store in the fridge (4 °C)

APPENDIX G

Astrocytes labelling protocols for mouse spinal cords (six spinal cord tissues per animal).

Protocol steps for primary antibody GFAP Astrocytes Marker	
1	spinal cord sections out of the fridge (4 °C)
	Wash tissues with PBS one-time X 10 minutes in well plate @ room temperature on the shaker
2	Wash tissues with PBST 2 times X 10 minutes in well plate @ room temperature on the shaker
3	Block tissue in PBST 10 % NDS @ 200 µl per space for 1 hour on platform shaker - 6 spaces @ 200 µl = 1200 µl total volume
4	Apply primary antibody GFAP rabbit polyclonal @ 1:2000 dilution and leave it overnight in the fridge (4 °C) -1200 µl total volume: 0.6 µl GFAP rabbit polyclonal + 1199.52 PBST NDS 5 % ↓ 1200 µl [60 µl NDS + 1140 µl PBST]

Protocol steps for secondary antibody Donkey anti-rabbit CY3	
1	spinal cord sections out of the fridge (4 °C)
2	Wash tissues with PBS 2 times X 10 minutes in well plate @ room temperature on the shaker
3	Apply secondary antibody Donkey anti-rabbit CY3 @ 1:500 dilution for 2 hours in dark environment - 1200 µl total volume: 2.4 µl Donkey anti-rabbit CY3 + 1197.6 PBST NDS 2 % ↓ 1200 µl [24 µl NDS + 1176 µl PBST]
4	Wash tissues with PBS one-time X 10 minutes in well plate @ room temperature on the shaker
5	Fill box of PBS and mount section in the orientation order on gelatine coated slides (free floating technique)
6	Cover slip slides with vectashield and store in the fridge (4 °C)